

Titre: Computational biomechanics of the human spine in static lifting tasks
Title: tasks

Auteur: Navid Arjmand
Author:

Date: 2006

Type: Mémoire ou thèse / Dissertation or Thesis

Référence: Arjmand, N. (2006). Computational biomechanics of the human spine in static lifting tasks [Thèse de doctorat, École Polytechnique de Montréal]. PolyPublie.
Citation: <https://publications.polymtl.ca/7788/>

Document en libre accès dans PolyPublie

Open Access document in PolyPublie

URL de PolyPublie: <https://publications.polymtl.ca/7788/>
PolyPublie URL:

Directeurs de recherche: Aboulfazl Shirazi-Adl
Advisors:

Programme: Non spécifié
Program:

UNIVERSITÉ DE MONTRÉAL

**COMPUTATIONAL BIOMECHANICS OF THE HUMAN
SPINE IN STATIC LIFTING TASKS**

**NAVID ARJMAND
DÉPARTEMENT DE GÉNIE MÉCANIQUE
ÉCOLE POLYTECHNIQUE DE MONTRÉAL**

**THÈSE PRÉSENTÉE EN VUE DE L'OBTENTION
DU DIPLÔME DE PHILOSOPHIAE DOCTOR
(GÉNIE MÉCANIQUE)
OCTOBER 2006**



Library and
Archives Canada

Published Heritage
Branch

395 Wellington Street
Ottawa ON K1A 0N4
Canada

Bibliothèque et
Archives Canada

Direction du
Patrimoine de l'édition

395, rue Wellington
Ottawa ON K1A 0N4
Canada

Your file *Votre référence*
ISBN: 978-0-494-24536-1

Our file *Notre référence*
ISBN: 978-0-494-24536-1

NOTICE:

The author has granted a non-exclusive license allowing Library and Archives Canada to reproduce, publish, archive, preserve, conserve, communicate to the public by telecommunication or on the Internet, loan, distribute and sell theses worldwide, for commercial or non-commercial purposes, in microform, paper, electronic and/or any other formats.

The author retains copyright ownership and moral rights in this thesis. Neither the thesis nor substantial extracts from it may be printed or otherwise reproduced without the author's permission.

In compliance with the Canadian Privacy Act some supporting forms may have been removed from this thesis.

While these forms may be included in the document page count, their removal does not represent any loss of content from the thesis.

AVIS:

L'auteur a accordé une licence non exclusive permettant à la Bibliothèque et Archives Canada de reproduire, publier, archiver, sauvegarder, conserver, transmettre au public par télécommunication ou par l'Internet, prêter, distribuer et vendre des thèses partout dans le monde, à des fins commerciales ou autres, sur support microforme, papier, électronique et/ou autres formats.

L'auteur conserve la propriété du droit d'auteur et des droits moraux qui protège cette thèse. Ni la thèse ni des extraits substantiels de celle-ci ne doivent être imprimés ou autrement reproduits sans son autorisation.

Conformément à la loi canadienne sur la protection de la vie privée, quelques formulaires secondaires ont été enlevés de cette thèse.

Bien que ces formulaires aient inclus dans la pagination, il n'y aura aucun contenu manquant.

**
Canada

UNIVERSITÉ DE MONTRÉAL

ÉCOLE POLYTECHNIQUE DE MONTRÉAL

Cette thèse intitulée:

**COMPUTATIONAL BIOMECHANICS OF THE HUMAN
SPINE IN STATIC LIFTING TASKS**

**présentée par: ARJMAND Navid
en vue de l'obtention du diplôme de: Philosophiae Doctor
a été dûment acceptée par le jury d'examen constitué de:**

M. YAHIA L'Hocine, Ph.D., président

M. SHIRAZI-ADL Aboulfazl, Ph.D., membre et directeur de recherche

M. GAGNON Denis, Ph.D., membre

M. LAKIS Aouni A., Ph.D., membre

Dedicated to my wife Maryam

Acknowledgments

I express my warmest thanks to:

Prof. Shirazi-Adl, for his friendly and stimulating supervision and support, patience, and timely advice throughout the course of this work, for being of invaluable help during the period leading to my thesis and in all submitted papers for publication during the course of my PhD.

Prof. M. Parnianpour for his contributions in paper 6.

Dr. M. El-Rich for fruitful discussions with regard to the model and the methodology.

Mr. B. Bazrgari for continuous discussions as well as his contributions in paper 5.

Dr. A. Mitnitski for collection and subsequent partial analyses of *in vivo* data.

Ms. M. Trottier for helpful discussions concerning the data processing of experiments as well as assistance in translation process of “Résumé”.

Ms. D. Mokhbi-Soukane for her help in translation process of “Condensé en Français”.

Prof. P. Mathieu for his valuable discussions on the analyses of measured data.

All present and former graduate students of the section mécanique appliquée with whom I had constructive discussions and lived in a pleasant environment.

My parents, sister, and brothers for their unconditional support and love through the years.

Finally, and most of all, my wife, Maryam, for her constant devotion, support, endurance, and for all her love during the whole course of our stay in Montréal.

The financial supports from the NSERC (Canada) and the IRSST (Québec) are gratefully acknowledged.

Résumé

Depuis que les charges et les déplacements excessifs sont identifiés comme des causes majeures des blessures de la colonne vertébrale soient d'ordre récréatif ou industriel, la connaissance des charges imposées sur les différents tissus spinaux est essentielle pour le développement effectif de programmes de prévention et de traitement. La limitation au niveau des méthodes de mesures *in vivo* a obligé les chercheurs à se tourner vers des techniques de modélisation biomécanique. Les études *in vitro* démontrent que la colonne seule (sans l'apport des muscles) subit le flambement sous l'application de faibles charges de compression (~20 N) suggérant que des analyses de stabilité mécanique de même que d'équilibre sont nécessaires pour étudier la tolérance limite de la colonne.

Les charges imposées sur la colonne s'estiment par des calculs de moments d'équilibre, à l'aide d'un diagramme de corps libre, considérant différentes charges: celles externes (comprenant la gravité) et internes produites par les muscles et les tissus passifs. Le problème majeur relié à ce type d'analyse est que le nombre de forces musculaires inconnues dépasse largement celui des équations d'équilibre. Deux approches peuvent contourner cette situation d'inégalité: des modèles utilisant soit l'optimisation soit les signaux d'électromyographie ('EMG-assisted'). Une limitation importante dans ces modèles est que les muscles et les charges imposées s'estiment en considérant les conditions d'équilibre seulement sur une section au lieu de l'entièreté de la colonne. Cette réduction à une seule section engendre une violation des lois de l'équilibre dans les autres sections non considérées. En outre, aucune des études préalables n'a considéré les forces de contact entre les muscles thoraciques et la colonne: cette simplification peut engendrer une prédiction erronée de la modélisation du tronc durant la phase de grande flexion.

Récemment, une nouvelle approche a été développée par notre groupe: des valeurs cinématiques de la colonne mesurées expérimentalement sont appliquées sur un

modèle numérique d'éléments finis non linéaires afin d'évaluer les forces musculaires et les charges internes ainsi que la stabilité. Cette approche a pour avantage de contraindre la cinématique de la colonne qui a été mesurée *in vivo* sous des charges externes et des forces musculaires. À chaque niveau de la colonne vertébrale une cinématique particulière est appliquée (rotation et/ou translation) ce qui génère une (ou plusieurs) équation(s) d'équilibre additionnelle(s) entre les forces musculaires inconnues et les charges externes: réduisant ainsi la redondance des équations d'équilibre. Lorsque le nombre d'équations d'équilibre égale celui des forces musculaires inconnues, le système d'équations devient déterminé et peut être résolu mathématiquement. Une telle approche satisfait les conditions d'équilibre selon toutes les directions et pour l'ensemble des niveaux de la colonne et entraîne une réponse cinématique en concordance avec les forces externes, les forces musculaires et la résistance des tissus passifs. À ce jour, l'application de cette approche se limite pour des tâches de levage statique en position debout.

Dans la présente étude, cette approche sert à calculer les forces musculaires et les charges internes à différents niveaux de la colonne de même que la stabilité de celle-ci dans des tâches de levage dans lesquelles des flexions antérieures dans le plan sagittal du tronc sont réalisées. Il est bien reconnu dans la littérature que ces tâches sont des causes majeures de blessures lombaires. La cinématique de la colonne, la rotation du pelvis et la position d'une charge externe ont été enregistrés lors du protocole expérimental chez 15 sujets mâles sains. Des électrodes bipolaires de surface ont été placées symétriquement de chaque côté de la colonne afin de recueillir le signal EMG des muscles superficiels. Différentes postures (position debout, flexion du tronc de $\sim 40^\circ$ ainsi que de $\sim 65^\circ$) en combinaison avec des postures lombaires variées (cyphotique, lordotique et libre) ont été considérées et ce sous l'application ou non d'une charge externe de 180 N posées dans les mains.

Un modèle symétrique de la colonne (selon l'axe sagittal) au niveau T1-S1 considérant 56 muscles a été développé. Les propriétés mécaniques non linéaires et dépendantes de la direction des segments T12-S1 sont représentées par des éléments poutres déformables. Le poids du membre supérieur de 387 N est distribué sur la colonne plus 180 N en sus dans les mains selon le cas considéré. La cinématique mesurée est appliquée sur le modèle pour obtenir les moments de réaction à chaque niveau de la colonne. Un algorithme d'optimisation s'ajoute à chaque niveau afin de distribuer ces moments entre les muscles, selon leur implication, et permet de résoudre le problème de redondance. Huit fonctions d'optimisation ont été considérées afin de déterminer celle la plus fiable. La stabilité du système a été étudiée sous différentes postures et charges à l'aide d'éléments uni axiaux possédant des rigidités variables afin de représenter les muscles ($K=qF/l$). De plus, les rôles de la pression intra abdominale (PIA) et de la posture lombaire ont été investiguées pour leur effet sur la répartition des charges et la stabilisation de la colonne.

Les prédictions du modèle sont qualitativement validées par les mesures des signaux EMG et les valeurs de pression intra discale. Lors que le tronc est fléchi de 65°, les forces de compression axiale et de cisaillement antéropostérieur au niveau critique de L5-S1 atteignent 2 026 et 598 N (sans charge externe) et 3 247 et 869 N (avec la charge de 180 N) respectivement. Dans cette posture, les forces musculaires des érecteurs du rachis représentent 716 et 1 140 N (sans et avec la charge externe) démontrant une augmentation de 1 332% (comparativement à 50 N) sans charge externe et de 149 % (comparativement à 458 N) en chargement versus la position debout. Des risques élevés de blessures aux tissus actifs/passifs lors d'activités de levage impliquant une flexion antérieure du tronc devient alors évident. L'effet des différentes fonctions d'optimisation sur ces valeurs relatives est minimal. En position fléchie, le risque de blessures spinales dues à l'instabilité se révèle une considération moins importante qu'en position debout. Par exemple, la valeur q requise pour maintenir la stabilité en position debout lorsque la charge externe est appliquée de chaque côté correspond à 17 ce qui

redevient nulle lorsque le tronc est fléchie de 40° ou 65°. Lors de ces dernières tâches, les forces musculaires de même que la rigidité de la colonne de part les tissus passifs se révèlent assez importantes pour stabiliser la colonne.

La posture lordotique, en comparaison à celle cyphotique, diminue le moment de flexion tout en accroissant l'implication musculaire des extenseurs, de la compression axiale, de la force de cisaillement au niveau de L5-S1 et la stabilité spinale (légèrement). En considérant les forces musculaires et les charges spinales, les résultats de cette étude supportent le choix d'une posture avec une légère flexion lors des tâches de levage statiques. En position debout, le rôle de déchargement de la PIA disparaît avec un niveau bas de coactivité des muscles abdominaux (RA: 0.5%, OE: 1%, OI: 2%) introduit dans le modèle tandis que son rôle stabilisateur se renforce avec l'élévation de la coactivité abdominale. En position fléchie, le rôle de déchargement de la PIA disparaît seulement avec un niveau élevé de coactivité abdominale (4 fois plus important que le niveau bas) tandis que son rôle stabilisateur diminue avec la hausse de la coactivité abdominale. Les rôles de déchargement et stabilisateur de la PIA sont d'abord spécifiques aux tâches et à la posture.

Dans les positions fléchies, lorsque les lignes d'action des muscles thoraciques sont considérées non linéaires (en courbes et en ne permettant pas aucune réduction de leurs bras de levier par rapport à la position initiale), les forces musculaires et les compressions axiales dans tous les niveaux spinaux diminuent considérablement en comparaison à l'application de lignes d'action linéaire. Lorsque l'on permet une réduction du bras de levier de 10% de sa valeur initiale durant la flexion, les forces musculaires et de compression axiale augmentent dans tous les niveaux spinaux. La considération de géométrie précise (non linéaire en courbe) pour les muscles et de leurs bras de levier de manière physiologiquement réaliste est essentielle afin d'obtenir des résultats acceptables. Le modèle et la méthodologie présentés dans cette étude, assurent les conditions d'équilibre dans toutes les directions et pour l'ensemble des niveaux de la

colonne et entraînent une réponse pour la cinématique spinale en concordance avec les forces externes, les forces musculaires et la résistance des tissus passifs avec des propriétés non linéaires.

Abstract

Since mechanical overload and/or overuse are known as major causes of recreational and occupational injuries to the spine, knowledge of spinal tissue loads is essential for design of effective prevention and treatment programs. Infeasibility of experimental methods to measure these loads has persuaded researchers towards the use of biomechanical modeling techniques. *In vitro* studies show that the spine devoid of muscles buckles under small loads (~20 N) suggesting that both mechanical stability and equilibrium analyses are needed to investigate the safe load tolerance limits of the spine.

Spinal loads are estimated by satisfying moment equilibrium, in a free-body-diagram of the spine, between external/gravity and internal loads produced by muscles and the passive spine. The major problem is that the number of unknown muscle forces is much larger than that of equilibrium equations. Two approaches have commonly been employed to tackle this redundant problem; optimization and EMG-assisted. A major shortcoming in these models is that muscle and spinal loads are estimated by considering equilibrium conditions only at a single cross section rather than along the entire length of the spine; a simplification that results in violation of equilibrium at remaining levels. Besides, none of previous studies has considered wrapping contact force between trunk muscles and the spine, which could yield erroneous predictions during trunk flexion.

A novel Kinematics-based approach in which the measured kinematics of the spine are prescribed in a nonlinear finite element model to evaluate muscle/spinal loads and stability in upright standing postures has, recently, been developed by our group. An advantage of this approach is in prescribing the *in vivo* kinematics data that constrain the spinal deformation under external loading and muscle exertions. Each prescribed kinematics generates an additional equilibrium equation between unknown muscle forces and external loads; thus decreasing the degree of redundancy. If the number of equilibrium equations at a spinal level reaches that of unknown muscle forces, the problem is solved deterministically. Such approach satisfies the equilibrium conditions

in all directions along the entire length of the spine and yields spinal postures in full accordance with external loads, muscle forces, and passive tissues. To date, application of this method has been limited to static lifting tasks in upright standing postures.

In the current work, the Kinematics-based approach was applied to compute muscle and spinal loads at different spinal levels as well as system stability in static lifting activities involving forward flexion of trunk. Such lifting activities have been indicated as major causes of injuries to the lumbar spine. Posture, pelvic tilt, and load location were recorded in an *in vivo* study on 15 healthy male volunteers. Surface EMG electrodes were placed symmetrically to record the activity of superficial muscle groups. Upright standing and forward flexion ($\sim 40^\circ$ and 65°) postures with different lumbar postures (kyphotic, lordotic, and free) with or without 180 N in hands were considered.

A sagittally-symmetric model of the T1-S1 spine with 56 muscle fascicles was used. The nonlinear and direction-dependent mechanical properties of T12-S1 segments were represented by deformable beams. The upper-body gravity load of 387 N was distributed along the spine in addition to a 180 N applied in hands. The measured kinematics were prescribed in the model yielding required moments at all spinal levels that when coupled with an optimization algorithm allowed for the solution of the redundant system. Effect of eight optimization cost functions on predictions was studied. The system stability was investigated under given postures and loads with muscles replaced by uniaxial elements with different stiffness ($K=qF/l$). Role of intra-abdominal pressure (IAP) and lumbar posture on loading and stabilizing the spine was also studied.

Predictions were validated by comparison with measured EMG and intra discal pressure. When flexing forward by 65° , compression and shear forces in the critical L5-S1 disc reached 2026 and 598 N (no load in hands) and 3247 and 869 N (180 N in hands), respectively. In this posture, force in erector spinae was 716 and 1140 N without and with 180 N in hands, respectively. This shows increases of 1332% (from 50 N) and

of 149% (from 458 N) compared to the upright posture without and with 180 N held in front, respectively. High risk of injury to active/passive tissues in lifting activities involving trunk flexion, hence, becomes evident. The effect of different optimization cost functions on these relative effects was minimal. In flexed postures, risk of injury to the spine due to instability was of lesser concern compared to the upright postures. For instance, the required q value to maintain stability in upright posture when lifting 180 N on sides was 17 that decreased to zero when trunk flexed by 40° or 65°. In such tasks, due to great muscle forces and passive lumbar stiffness the spine was sufficiently stable.

Compared to the kyphotic postures, the lordotic postures increased extensor muscle activities, compression and shear forces at the L5-S1 disc, and (slightly) the spinal stability while decreasing segmental flexion moments. Considering muscle and spinal loads, results support free style posture with slight flexion as the posture of choice in static lifting. In the upright posture, the unloading role of IAP faded away as low level of abdominal coactivities (RA: 0.5%, EO: 1%, IO: 2%) was introduced in the model while its stabilizing role continued to improve as abdominal coactivity increased. In flexed postures, the unloading role of IAP disappeared with high level of abdominal coactivities (4-fold of low level) while its stabilizing role deteriorated as abdominal coactivities increased. The IAP unloading/stabilizing roles are posture and task specific.

Compared to the case in which linear line of actions were considered for thoracic muscles, muscle forces and spinal compression at all levels substantially decreased as these muscles took curved paths while not allowing any reduction in their lever arm from upright posture. Allowing for a 10% reduction in these lever arms during flexion increased muscle and compression forces at all levels. Consideration of thoracic muscles with curved paths and realistic lever arms is essential. The presented model and methodology guarantees satisfaction of the equilibrium equations in all directions along the entire length of the spine while yielding spinal postures in full accordance with external/gravity loads, muscle forces, and passive tissues with nonlinear properties.

Condensé en Français

Introduction

Tant au niveau de la prédominance que des coûts reliés, les troubles lombaires sont reconnus comme les plus significatifs parmi les différents troubles musculosquelettiques (Praemer et al., 1992; Webster et Snook, 1994). Selon le consensus général, les causes majeures des blessures de la colonne vertébrale sont la surcharge mécanique des tissus excédant leurs seuils de l'endommagement. La connaissance adéquate des charges imposées sur les tissus spinaux est donc essentielle pour le développement effectif de programmes de prévention et de traitement. Cependant, les charges spinales ne peuvent pas être mesurées directement. Les estimations indirectes, comme celles basées sur la pression intradiscale, présentent également un lot de difficultés important en raison des coûts et des considérations éthiques. Les chercheurs ont ainsi opté pour l'utilisation de techniques de modélisation biomécanique.

En compensant les moments de charges externes dans des tâches de levage, les muscles de tronc, en raison de leur petit bras de levier par rapport à celui des charges externes, exercent des forces considérablement plus importantes que les charges externes sur la colonne vertébrale. La prédiction exacte des forces musculaires est donc critique pour une estimation adéquate des charges spinales. Les études *in vitro* démontrent que la colonne sans l'apport des muscles subit le flambement sous l'application de faibles charges (~20 N) (Lucas and Bresler; Shirazi-Adl and Parnianpour, 1996) suggérant que des analyses de stabilité mécanique de même que d'équilibre sont nécessaires pour étudier la tolérance limite de la colonne pour sa sécurité.

Les charges spinales sont estimées en appliquant les conditions d'équilibre entre les charges externes/gravité/inertie et internes produites par les muscles et les tissus passifs de la colonne vertébrale. Le problème majeur est que les équations d'équilibre ne peuvent pas être résolues mathématiquement puisque le nombre des forces inconnues de

muscles est plus grand que le nombre d'équations d'équilibre disponibles. Deux approches bien-reconnues ont été souvent utilisées pour s'attaquer à ce problème; l'assistance par les signaux d'électromyographie ('EMG-assisted') et l'optimisation. Cette dernière fournit une solution mathématique du problème en optimisant une fonction de coût (par exemple la minimisation de somme de tensions des muscles) en satisfaisant les conditions d'équilibre. 'EMG-assisted', utilise les signaux d'EMG pour estimer les forces musculaires en supposant une relation entre l'activité EMG de muscles et leurs forces.

Une importante lacune des modèles biomécaniques, anciens et présents, de la colonne vertébrale est que les forces musculaires et les charges spinale sont estimées en considérant les conditions d'équilibre sur une seule section (généralement sur le disque le plus bas comme L5-S1) plutôt que de les considérer le long de l'entièrre colonne; une simplification qui s'ensuit dans la violation d'équilibre aux niveaux restants. Les modèles simples d'éléments finis de la colonne vertébrale avec l'optimisation ou les algorithmes d'EMG ont été développés pour obvier à cette lacune (Cholewicki et McGill, 1996; Stokes et Gardner-Morse 1995). Par contre, ces modèles souffrent de la représentation inadéquate de non linéarités et de propriétés passives de la colonne vertébrale. Pour une meilleure fiabilité des résultats, la considération adéquate des propriétés matérielles non linéaires des segments lombaires avec des propriétés qui dépendent de la direction et de la charge s'avère importante.

Aucune des études précédentes n'a considéré la force de contact entre les muscles qui enveloppent la colonne vertébrale et cette dernière pendant les tâches de flexion du tronc. Une telle hypothèse pourrait engendrer une erreur importante dans les charges spinale estimées spécialement dans les charges de cisaillement antéropostérieures. En plus, le rôle de la pression intra abdominale (PIA) et son interaction avec les activités abdominales n'ont pas été souvent correctement modélisé (Cholewicki et Reeves, 2004; Daggfeldt et Thorstensson, 2004). L'incapacité de déterminer précisément les forces

musculaires, les charges spinales et la stabilité de la colonne vertébrale est un obstacle critique dans le développement de directives ergonomiques pour le design de tâches plus sécuritaires.

L'Approche basée sur la cinématique ('Kinematics-based approach')

Récemment, une nouvelle approche a été développée par notre groupe de recherche: des valeurs cinématiques de la colonne mesurées expérimentalement sont appliquées sur un modèle d'éléments finis non linéaire afin d'évaluer les forces musculaires et les charges spinales ainsi que la stabilité de la colonne vertébrale (El-Rich et d'autres., 2004; El-Rich et Shirazi-Adl, 2005). Cette approche a pour avantage d'appliquer la cinématique de la colonne, mesurée *in vivo*, pour contraindre la déformation de celle-ci sous des charges externes et des forces musculaires. En plus, à chaque niveau, une cinématique particulière (rotation et/ou translation) est appliquée sur chacune des vertèbres ce qui génère une équation d'équilibre additionnelle entre les forces musculaires inconnues et les charges externes à ce niveau; réduisant ainsi la redondance des équations d'équilibre. Si le nombre d'équations d'équilibre à un niveau spinal particulier atteint celui des forces de muscle inconnues, le problème est résolu mathématiquement. Une telle approche satisfait non seulement les équations d'équilibre selon toutes les directions et pour l'ensemble des niveaux de la colonne, mais aussi entraîne une réponse pour la cinématique spinale en concordance avec les forces externes, les forces musculaires et la résistance des tissus passifs. À ce jour, l'application de cette approche se limite aux tâches de levage statique en position debout.

Dans la présente étude, cette approche a été appliquée pour calculer les forces musculaires et les charges spinales à différents niveaux spinaux ainsi que la stabilité du système dans des tâches qui sont reconnues comme étant les causes les plus importantes des blessures de la colonne vertébrale lombaire: les tâches de levage statiques impliquant la flexion du tronc. La posture de la colonne, la rotation du pelvis et la position de la charge externe ont été enregistrées lors du protocole expérimental chez 15

sujets mâles sains. Des électrodes bipolaires de EMG ont été placées symétriquement de chaque côté de la colonne afin de recueillir les activités des muscles superficiels. Différentes postures (position debout, flexion du tronc de $\sim 40^\circ$ ainsi que de $\sim 65^\circ$) en combinaison avec des différentes postures lombaires (cyphotique, lordotique et libre) ont été considérées et ce avec ou sans l'application d'une charge externe de 180 N tenue dans les mains.

Un modèle symétrique de la colonne, (selon l'axe sagittal) au niveau T1-S1 avec 46 fascicules musculaires locaux et 10 globaux, est utilisé. Les propriétés mécaniques non linéaires et dépendantes de la direction du segment T12-S1 sont représentées par des éléments déformables de poutre. Un poids de 387 N du corps supérieur, est distribué excentriquement sur la colonne, auquel s'ajoute 180 N appliquée dans les mains. La cinématique mesurée est appliquée sur le modèle pour obtenir les moments de réaction à chaque niveau de la colonne. Un algorithme d'optimisation s'ajoute afin de distribuer ces moments entre les muscles, selon leur implication, et permet de résoudre le problème de redondance. Par la suite, la marge de stabilité du système a été étudiée sous les postures et les charges données où les muscles sont remplacés par des éléments uniaxiaux avec différents paramètres de rigidité ($K=qF/I$).

Pour étudier l'effet de rigidité passive de la colonne vertébrale sur les charges spinales et la stabilité, les analyses ont été réalisées en diminuant la rigidité de flexion de la colonne vertébrale jusqu'à 30 %, chose qui peut se produire en raison d'une blessure au système passif. L'effet des changements dans la posture lombaire (i.e., cyphotique, lordotique et le style libre) sur les charges spinales et la stabilité pendant le levage statique a été également étudié. Les résultats d'une telle étude servent à recommander la posture lombaire la plus sécuritaire en termes de réduction des charges spinales ou de l'amélioration de la stabilité spinale.

L'effet de huit différentes fonctions d'optimisation linéaires et non linéaires sur les prédictions a été étudié. Quatre critères non linéaire (Σ stress³, Σ stress², Σ force² et la fatigue des muscles) et quatre linéaires (Σ stress, Σ force, la compression axiale et la méthode linéaire-double) ont été considérés. Cette étude avait pour but d'examiner jusqu'à quel point le choix de la fonction d'optimisation utilisée pourrait influencer les forces musculaires prédites, les charges spinales et la stabilité du système. Elle pourrait identifier la fonction qui prédit les forces musculaires en accord qualitatif avec l'activité EMG de muscles de tronc mesurés dans l'étude *in vivo* sous la même posture et le même chargement considéré dans le modèle.

Pour évaluer le rôle de la PIA dans le déchargement et la stabilisation de la colonne vertébrale pendant les tâches de levage, quatre niveaux de coactivité des muscles abdominaux ont été considérés: nulle, bas (0.5 % dans RA, 1 % dans OE, 2 % dans OI), modéré (augmentation de 2 fois par rapport au niveau bas) et haut (augmentation de 4 fois par rapport au niveau bas). Ces niveaux de coactivité ont été appliqués simultanément avec une augmentation dans PIA de 0 kPa à 4 kPa en soulevant une charge de 180 N en position debout et de 0 kPa à 9 kPa en soulevant la même charge dans les flexions de tronc de 40 ° et 65 °.

Dans cette étude, une approche originale a été développée pour la simulation nécessaire du phénomène d'emballage des muscles d'extenseur autour des vertèbres en tenant compte des forces de contact entre les muscles et la colonne vertébrale. Elle a aussi pour but d'investiguer les effets probables d'emballage des muscles d'extenseur globaux et de la réduction ultérieure de leur bras de levier sur les forces de muscle calculées, les charges spinales et la stabilité de système dans des tâches de levage.

Finalement, une étude quantitative a été réalisée pour évaluer jusqu'à quel point les forces musculaires et les charges spinales ainsi que les exigences d'équilibre aux différents niveaux sont influencées par les résultats des modèles du diagramme du corps

libre ('single level free body diagram', SLFBD) dans lesquels les forces musculaires et les charges spinales sont calculées en satisfaisant l'équilibre à un seul niveau de la colonne vertébrale; pour ce faire, deux tâches symétriques isométriques sont considérées (la position debout et fléchi de 65°). Les résultats de notre modèle d'éléments finis qui satisfait la condition d'équilibre à tous les niveaux sont comparés à ceux obtenus par les modèles de SLFBD. Puisque les moments externes, le bras de levier de muscles et le nombre des muscles qui traversent chaque niveau changent d'un niveau à un autre, on pourrait s'attendre à ce que les modèles de SLFBD violent grossièrement l'équilibre aux niveaux restants.

Résultats

Les résultats du modèle sont validés par les mesures du signal EMG et les valeurs de pression intradiscale. Lorsque le tronc est fléchi de ~65° sans charge dans les mains, les forces de compression axiale et de cisaillement antéropostérieure au niveau critique de L5-S1 atteignent 2026 N et 598 N respectivement, comparé à seulement 570 N et 190 N en position debout. Dans la posture fléchie de 65°, en soulevant 180 N dans les mains, les valeurs prédites pour la compression axiale et les forces de cisaillement dans le niveau critique de disque L5-S1 ont atteint 3247 N et 869 N, respectivement. Dans cette posture, les forces musculaires des érecteurs du rachis représentent 716 et 1140 N (sans et avec la charge externe) démontrant une augmentation de 1332% (comparativement à 50 N sans charge externe) et de 149 % (comparativement à 458 N avec charge) en position debout. Des risques élevés de blessures aux tissus actifs/passifs lors des activités de levage impliquant une flexion antérieure du tronc devient alors évidents, suggérant ainsi la vulnérabilité de ces muscles à la fatigue dans les conditions répétitives ou soutenues semblables. L'impact de différentes fonctions d'optimisation sur ces effets relatifs est minimal puisque les variations dans la compression axiale prédite et les forces de cisaillement ne dépassent pas 11 % et 9 % respectivement, pour différentes fonctions d'optimisation non linéaires dont les prédictions correspondent aux données EMG. Nos conclusions confirment les suggestions avancées par les études

épidémiologiques précédentes qui reconnaissent les tâches de levage comme étant le facteur de risque le mieux documenté pour les troubles lombaires.

Les résultats de la présente étude, cependant, montrent que dans les tâches de levage avec la flexion du tronc, le risque de blessure à la colonne vertébrale en raison de l'instabilité du système est inférieur au risque de blessure causé par des forces musculaires élevées et des charges spinales. Par exemple, la valeur de q nécessaire pour maintenir la stabilité dans la position debout en soulevant 180 N dans les mains était d'environ 17 qui a diminué jusqu'à zéro lorsque le tronc fléchi par 40° ou 65°. Dans de telles tâches, en raison de grandes forces musculaires et d'une rigidité lombaire passive, la colonne vertébrale est suffisamment stable surtout en portant la charge dans les mains. Une blessure au système passif de la colonne vertébrale qui a été simulée en diminuant la rigidité de celui-ci, aura d'une part entraîné une augmentation compensatrice substantielle des forces musculaires actives qui auront augmenté les charges spinales et, donc, le risque de blessure et de fatigue. D'autre part, elle aura détérioré la stabilité du système qui pourrait à son tour causer une activation musculaire supplémentaire plus importante.

Les modifications dans la posture lombaire durant les tâches de levage ont provoqué des changements significatifs dans les forces musculaires et les charges spinales. Les valeurs maximales pour la compression axiale et les forces de cisaillement sont produites au niveau du disque L5-S1 et sont plus élevées dans la posture lordotique que dans la posture cyphotique. Les forces de cisaillement ont diminué considérablement de 23-36 % tandis que les forces de compression ont diminué seulement de 2-14 % lorsqu'on passe d'une posture lordotique à une posture cyphotique. Comparées aux postures cyphotiques, les postures lordotiques ont augmenté la composante active des forces musculaires, la compression axiale, les forces de cisaillement au niveau L5-S1 et légèrement la marge de stabilité spinale mais ont également diminué la composante passive des forces musculaires et les moments de

flexion segmentaires. En considérant les charges spinales et les forces musculaires (actives et passives), la présente étude soutient la posture de style libre ou une posture avec flexion modérée comme étant la posture de choix dans les tâches statiques de levage.

Toutes les prédictions, sans tenir compte de la fonction d'optimisation, ont satisfait la cinétique, la cinématique et les conditions de stabilité le long de la colonne vertébrale. Les activités musculaires correspondant qualitativement aux données d'EMG mesurées ont été prédites par quatre critères (Σ stress³, Σ stress², fatigue et la méthode linéaire-double). Les critères de minimisation de fatigue et linéaires-doubles sont inadéquats puisqu'ils associent de plus grandes forces dans les plus grands muscles sans considérer leurs bras de levier. La fonction de Σ stress² ou de Σ stress³ a été trouvée plus adéquate dans la production des résultats plausibles comparables avec les données EMG et la pression intradiscale. Presque la même marge de stabilité a été calculée dans ces quatre fonctions d'optimisation.

Pour toutes les tâches de levage quelque soit la posture considérée, une augmentation de PIA a déchargé et stabilisé la colonne vertébrale lorsqu'aucune coactivité n'a été considérée dans les muscles abdominaux. En position debout, le rôle du déchargement de PIA a disparu même en présence du bas niveau de coactivité abdominale tandis que son rôle de stabilisation continue à s'améliorer lorsque la coactivité abdominale a augmenté. En position fléchie, le rôle du déchargement de PIA a disparu seulement avec le haut niveau de coactivité abdominale tandis que son rôle de stabilisation s'est détérioré quand la coactivité abdominale a augmenté. Les rôles du déchargement et de la stabilisation de PIA sont d'abord spécifiques aux tâches et à la posture. Nos résultats démontrent qu'il est extrêmement important de considérer la coactivité abdominale et la PIA ensemble dans un modèle biomécanique.

Comparées au cas dans lequel les lignes linéaires d'action ont été considérées pour les muscles thoraciques, les forces musculaires et la compression spinale à tous les niveaux ont considérablement diminué lorsque les muscles d'extenseur ont pris des sentiers courbés et ne permettent aucune réduction de leur bras de levier par rapport à la position debout. Le fait de tenir compte d'une réduction de 10% de ces bras de levier pendant la flexion a augmenté les forces musculaires et les forces de compression à tous les niveaux. La considération de muscles d'extenseur globaux avec les trajectoires courbées et les bras de levier réalistes est importante dans l'analyse biomécanique des tâches de levage.

Les résultats démontrent que l'équilibre doit être satisfait simultanément à tous les niveaux spinaux puisque les modèles SLFBD produisent des estimations qui ont énormément changé dépendamment du niveau de coupe dans la DCL. De surcroît, l'équilibre de moment a grossièrement été enfreint aux niveaux restants avec l'erreur augmentant dans les tâches plus exigeantes. La comparaison entre les résultats prédits par notre modèle d'élément fini avec les modèles de SLFBD, sans tenir compte de la méthode utilisée pour s'attaquer à la surabondance, montre que les différences dans la force de compression axiale calculée aux différents niveaux sont restées <9 % étant beaucoup plus basses que celles calculées pour les forces de cisaillement et les forces musculaires. Autrement dit, la force de compression axiale a l'air d'être moins sensible aux manques dans les modèles de SLFBD. Pour cette raison et en raison de l'aisance des applications de modèle de SLFBD, on peut soutenir que de tels modèles de SLFBD pourraient être réalisés avec l'objectif spécifique d'estimer seulement des charges de compression, mais pas les forces de cisaillement et les forces musculaires.

Conclusion

En conclusion, la colonne vertébrale et ses systèmes passifs-actifs deviennent beaucoup plus vulnérables à la blessure pendant des tâches de levage impliquant la flexion du tronc en raison des forces musculaires et des charges spinales trop élevées. La

stabilité du tronc reste, pourtant, d'une inquiétude moins importante dans les tâches de flexion. La prise de posture lordotique aggraverait même ces conditions en termes d'augmentation des charges spinales et forces musculaires; suggérant qu'un levage avec une posture lombaire fléchie impliquerait moins de risque de blessure. La PIA joue un rôle dans le déchargement et la stabilisation de la colonne vertébrale pendant les tâches de levage; un rôle qui cependant reste spécifique aux tâches et à la posture. Ces prédictions sont obtenues à partir d'un modèle d'élément fini non linéaire détaillé de la colonne vertébrale dans lequel les données *in vivo* cinématiques ont été appliquées pour s'attaquer au problème de surabondance.

Table of Contents

Dedication.....	iv
Acknowledgments.....	v
Résumé.....	vi
Abstract.....	xi
Condensé en Français.....	xiv
Table of Contents.....	xxiv
List of Tables.....	xxx
List of Figures.....	xxxiii
List of Annexes.....	xli
CHAPTER 1 INTRODUCTION.....	1
1.1 Low Back Disorder (LBD).....	1
1.2 Biomechanical Models of the Human Spine.....	2
1.3 Biomechanical Models of the Spine and the Kinetic Redundancy.....	3
1.4 Single-Equivalent Approach.....	5
1.5 Optimization-Based Approach.....	6
1.6 EMG-Assisted Approach.....	8
1.7 Kinematics-driven approach.....	10
1.8 Spinal Stability.....	10
1.9 Lifting Techniques.....	13
1.10 Intra-Abdominal Pressure (IAP).....	15
1.11 Geometry of Trunk Thoracic Extensor Muscles.....	18
1.12 Free Body Diagram-based Model of the Spine.....	19
1.13 Finite Element Models of the Spine and the Kinematics-Based Approach....	20
CHAPTER 2 OBJECTIVES AND THESIS ORGANIZATION.....	23

2.1 Application of the Kinematics-Based Approach for Lifting Tasks Involving Forward Trunk Flexion.....	23
2.2 Addressing the Controversial Issue of Lifting Techniques Using the Kinematics-Based Approach.....	23
2.3 Effect of Optimization Cost Function Used in the Kinematics-Based Approach on Predictions.....	24
2.4 Addressing the Controversial role of Intra-Abdominal Pressure (IAP) in Unloading and Stabilizing the Spine during Lifting Tasks.....	26
2.5 A Novel Approach for Proper Simulation of Wrapping of Trunk Thoracic Extensor Muscles around Vertebra.....	26
2.6 The Importance of Satisfaction of Equilibrium Conditions At All Spinal Levels and Not Only At One Single Level of the Spine on Model Predictions.....	27
2.7 Thesis Organization.....	27
2.8 List of Publications.....	28

CHAPTER 3 MODEL AND *IN VIVO* STUDIES ON HUMAN TRUNK LOAD PARTITIONING AND STABILITY IN ISOMETRIC FORWARD FLEXIONS (First Article)..... 29

3.1 ABSTRACT.....	30
3.2 INTRODUCTION.....	31
3.3 METHODS.....	33
3.4 RESULTS.....	36
3.5 DISCUSSION.....	37
3.6 ACKNOWLEDGEMENTS.....	44
3.7 REFERENCES	44

CHAPTER 4 BIOMECHANICS OF CHANGES IN LUMBAR POSTURE IN STATIC LIFTING (Second Article)..... 68

4.1 ABSTRACT.....	69
4.2 INTRODUCTION.....	70

4.3 MATERIALS AND METHODS.....	72
4.4 RESULTS.....	76
4.5 DISCUSSION.....	78
4.6 ACKNOWLEDGEMENT.....	84
4.7 REFERENCES.....	84
CHAPTER 5 SENSITIVITY OF KINEMATICS-BASED MODEL PREDICTIONS TO OPTIMIZATION CRITERIA IN STATIC LIFTING TASKS (Third Article).....	107
5.1 ABSTRACT	108
5.2 INTRODUCTION.....	109
5.3 METHODS.....	111
5.4 RESULTS.....	116
5.5 DISCUSSION.....	117
5.6 ACKNOWLEDGMENT.....	124
5.7 REFERENCES.....	124
CHAPTER 6 ROLE OF INTRA-ABDOMINAL PRESSURE IN UNLOADING AND STABILIZATION OF THE HUMAN SPINE DURING STATIC LIFTING TASKS (Forth Article).....	139
6.1 ABSTRACT.....	140
6.2 INTRODUCTION.....	141
6.3 METHODS	143
6.4 RESULTS.....	147
6.5 DISCUSSION.....	148
6.6. CONCLUSION.....	155
6.7 ACKNOWLEDGEMENT.....	155
6.8 REFERENCES.....	156

CHAPTER 7 WRAPPING OF TRUNK THORACIC EXTENSOR MUSCLES INFLUENCES MUSCLE FORCES AND SPINAL LOADS IN LIFTING TASKS (Fifth Article).....	169
7.1 ABSTRACT.....	170
7.2 INTRODUCTION.....	171
7.3 METHODS.....	173
7.4. RESULTS.....	176
7.5 DISCUSSION.....	177
7.6 ACKNOWLEDGEMENT.....	180
7.7 REFERENCES.....	181
CHAPTER 8 TRUNK BIOMECHANICAL MODELS BASED ON EQUILIBRIUM AT A SINGLE-LEVEL VIOLATE EQUILIBRIUM AT OTHER LEVELS (Sixth Article).....	191
8.1 ABSTRACT.....	192
8.2 INTRODUCTION.....	193
8.3 METHOD.....	195
8.4 RESULTS.....	199
8.5 DISCUSSION.....	200
8.6 ACKNOWLEDGEMENT.....	204
8.7 REFERENCES.....	204
CHAPTER 9 DISCUSSIONS AND CONCLUSIONS.....	215
9.1 Overview.....	215
9.2 Finite Element Model.....	216
9.2.1 Verifications of the Passive Spine Model.....	216
9.2.2 Model Loadings.....	218
9.2.3 Boundary Conditions.....	221
9.3 Muscles.....	221

9.3.1 Muscle Anatomy.....	221
9.3.2 Passive Property of Muscles.....	222
9.4 Optimization Algorithm.....	222
9.5 Model Validations	223
9.6 Methodological Issues (Limitations).....	229
9.6.1 Experimental Study.....	229
9.6.2 Model Study.....	230
9.7 Advantages of the Current Work.....	237
9.8 Comparisons and implications	240
9.8.1 Flexion Posture versus Upright Posture and the Effect of Load.....	240
9.8.2 Comparison with Tolerant Limits.....	242
9.8.3 Comparisons for Erector Spinae Force in Upright Posture.....	243
9.8.4 Comparisons for Erector Spinae Force in Flexed Posture.....	245
9.8.5 Comparisons for Predicted Spinal Compression and IDP.....	245
9.8.6 Comparisons for Predicted Local Muscle Forces.....	246
9.9 Conclusions.....	247
9.9.1 Stabilizing Action of the Passive Spine.....	248
9.9.2 Lumbar Posture (Lordotic vs. Kyphotic) During Lifting.....	249
9.9.3 Intra-Abdominal Pressure (IAP).....	250
9.9.4 Consideration of Muscle Wrapping Phenomenon.....	251
9.10 Concluding Remarks	251
9.11 Future Studies.....	252
9.11.1 Dynamics Lifting Task.....	252
9.11.2 Relative Contribution of Individual Muscles to the Spinal Stability...	252
9.11.3 Simulation of the Flexion-Relaxation During Full Trunk Flexion.....	252
9.11.4 Simulation of Asymmetric Tasks.....	253
9.11.5 Application of the Kinematics-based Approach to the Cervical Spine..	254

References	255
Annexes	275

List of Tables

Table 3.1 Mean measured, prescribed thorax and pelvis rotations from the neutral standing posture as well as prescribed lumber rotations in the FE model assuming relative rotations of 8% at T12-L1, 13% at L1-L2, 16% at L2-L3, 23% at L3-L4, 26% at L4-L5, and 14% at L5-S1 level for both flexion postures of ~40° and 65° (based on reported <i>in vivo</i> kinematics measurements).....	53
Table 3.2 Physiological cross sectional areas (PCSA, mm ²) and initial length (in brackets, mm) for muscles on each side of the spine at different insertion levels. ICpl: Iliocostalis Lumborum pars lumborum, ICpt: Iliocostalis Lumborum pars thoracic, IP: Iliopsoas, LGpl: Longissimus Thoracis pars lumborum, LGpt: Longissimus Thoracis pars thoracic, MF: Multifidus, QL: Quadratus Lumborum, IO: Internal Oblique, EO: External Oblique, and RA: Rectus Abdominus.....	54
Table 3.3 Internal loads in passive ligamentous spine at various levels for neutral standing and flexed postures ± 180 N in hands.....	55
Table 4.1 Physiological cross sectional area (PCSA, mm ²) and initial length (in brackets, mm) for muscles on each side of the spine at different insertion levels. ICPL: Iliocostalis Lumborum pars lumborum, ICPT: Iliocostalis Lumborum pars thoracic, IP: Iliopsoas, LGPL: Longissimus Thoracis pars lumborum, LGPT: Longissimus Thoracis pars thoracic, MF: Multifidus, QL: Quadratus Lumborum, IO: Internal Oblique, EO: External Oblique, and RA: Rectus Abdominus.....	93
Table 4.2 Three-way analysis of variance for repeated measures for trunk muscle EMG activities during lifting tasks (values with statistical significance at p<0.05 are highlighted). ICPT: Iliocostalis Lumborum Pars Thoracic, LGPT: Longissimus Thoracis Pars Thoracic, MF: Multifidus, EO: External Oblique, and RA: Rectus Abdominus...	94
Table 4.3 Predicted total (Ft), passive (Fp), and active (Fa=Ft - Fp: listed for global muscles) muscle forces at different segmental levels for various tasks (N). LGPT: Longissimus Thoracis Pars Thoracic, ICPT: Iliocostalis Lumborum Pars Thoracic, IP: Iliopsoas, LGPL: Longissimus Thoracis Pars Lumborum, ICPL: Iliocostalis Lumborum Pars Lumborum, MF: Multifidus, QL: Quadratus Lumborum.....	95

Table 4.4 Predicted internal loads in passive ligamentous spine at various levels for static lifting tasks \pm 180 N in hands for different lumbar postures.....	97
Table 5.1 Physiological cross sectional area (PCSA, mm ²) and initial length (in brackets, mm) of muscles on each side of the spine at different insertion levels. ICPL: Iliocostalis Lumborum pars lumborum, IP: Iliopsoas, LGPL: Longissimus Thoracis pars lumborum, MF: Multifidus, QL: Quadratus Lumborum, RA: Rectus Abdominus, EO: External Oblique, IO: Internal Oblique, ICPT: Iliocostalis Lumborum pars thoracic, and LGPT: Longissimus Thoracis pars thoracic.....	131
Table 5.2 Predicted total force in global muscles (ICPT and LGPT) for different cost functions and tasks (each side of the spine, N).....	132
Table 5.3 Tukey's post hoc tests preceded by three-way analysis of variance (ANOVA) to determine significant differences in predicted axial compression based on eight different cost functions during lifting tasks (statistical significance at $p < 0.05$ is highlighted).....	133
Table 5.4 Predicted critical muscle stiffness coefficient (q) based on different cost functions used in simulation of various lifting tasks.....	133
Table 5.5 Spinal loads and global muscle (ICPT and LGPT) forces predicted based on cost function of sum of cubed muscle stresses using two optimization strategies; (1) with and (2) without the muscle passive force components considered also as unknowns in optimization.....	134
Table 6.1 Characteristics considered for the application of IAP in the model.....	163
Table 6.2 Physiological cross sectional area (PCSA, mm ²) and initial length (in parentheses, mm) for muscles on each side of the spine at different insertion levels. ICPL: Iliocostalis Lumborum pars lumborum, ICPT: Iliocostalis Lumborum pars thoracic, IP: Iliopsoas, LGPL: Longissimus Thoracis pars lumborum, LGPT: Longissimus Thoracis pars thoracic, MF: Multifidus, QL: Quadratus Lumborum, IO: Internal Oblique, EO: External Oblique, and RA: Rectus Abdominus.....	163
Table 6.3 Three levels of abdominal muscle coactivities and the generated force/flexor moment.....	164

Table 7.1 Spinal loads including axial compression, anterior-posterior shear force, and passive moment for different lifting tasks and lumbar postures without and with (no reduction or 10% reduction in lever arm) wrapping of global muscles.....	184
Table 7.2 Wrapping contact forces at various vertebral levels for different lifting tasks and lumbar postures without and with (no reduction or 10% reduction in lever arm) wrapping of global muscles.....	185
Table 8.1A Predicted muscle forces under flexed posture using KD approach as well as SLFBD models at different disc levels from L5-S1 through T12-L1 (forces in Iliopsoas muscles are zero in all SLFBD models and are not shown for the KD model).....	207
Table 8.1B Predicted muscle forces under upright posture using KD approach as well as SLFBD models at different disc levels from L5-S1 through T12-L1 (forces in Iliopsoas muscles are zero in all SLFBD models and are not shown for the KD model).....	208
Table 8.2 Predicted local spinal loads in both loading cases using KD model as well as SLFBD models cut at different disc levels from L5-S1 through T12-L1.....	209
Table 9.1 Predicted local and global muscle forces on each side based on two different proportions considered to partition total lumbar rotation between lumbar vertebrae.	217
Table 9.2 Predicted spinal loads based on two different proportions considered to partition total lumbar rotation between lumbar vertebrae.....	218
Table 9.3 Predicted spinal loads while neglecting translational degrees-of- freedom (DOF) at vertebral joints compared to our reference case for lifting of 180 N with trunk flexion of 65° while considering wrapping of global muscles.....	239

List of Figures

Fig. 1.1 Free-body diagram for calculating spinal and muscle loads at a typical lumbar disc during lifting.....	4
Fig. 1.2 Stoop (left) versus squat (right) lift.....	14
Fig. 1.3 Kyphotic (left) versus lordotic (right) lift during a squat lift.....	14
Fig. 1.4 Free-body diagram for calculating spinal and muscle loads on a lumbar disc during lifting while taking account for the IAP force.....	16
Fig. 3.1 Sagittal profile of the FE model at $\sim 40^\circ$ flexion prescribed based on measurements. Positions of distributed gravity loads (total of ~ 387 N: 256 N anteriorly at T1-L5 levels for the torso, 58.5 N for the head/neck at 1 cm anterior to T1, and 72.2 N for arms/shoulder at 3 cm posterior to T2-T4) and concentrated 180 N held in front via a barbell are shown. The external load is applied on the T4 at a location based on mean of measured data.....	56
Fig. 3.2 Representation of global and local musculatures in the sagittal and frontal planes used in the FE model. Only fascicles at one side have been shown. ICpl: Iliocostalis Lumborum pars lumborum, ICpt: Iliocostalis Lumborum pars thoracic, IP: Iliopsoas, LGpl: Longissimus Thoracis pars lumborum, LGpt: Longissimus Thoracis pars thoracic, MF: Multifidus, QL: Quadratus Lumborum, IO: Internal Oblique, EO: External oblique, and RA: Rectus Abdominus.....	57
Fig. 3.3 Flow-chart for the application of the kinematics-based approach and determination/validation of trunk muscle forces, internal loads as well as stability margin of the spine. The moments required for the prescribed rotations were fed into a separate algorithm that calculated muscle forces at each level. Axial compression and horizontal shear penalties of these muscle forces were then fed back into the finite element model as additional updated external loads. This iterative approach was continued at each load step till convergence was reached.....	58
Fig. 3.4A <i>In vivo</i> measured normalized EMG activity (mean \pm S.D.) of extensor muscles in standing and flexed postures as a function of load carried symmetrically in hands. IC: Iliocostalis, LG: Longissimus, and MF: Multifidus. * Significant change in EMG	

activity compared to that of standing posture due to flexion under identical load in hands (as explicitly shown for LG). + Significant change in EMG activity compared to that of 0 N due to load magnitude under identical postures (as explicitly shown for IC muscle).	59
Fig. 3.4B <i>In vivo</i> measured normalized EMG activity (mean \pm S.D.) of abdominal muscles in standing and flexed postures as a function of load carried symmetrically in hands. EO: External oblique, and RA: Rectus Abdominus. * Significant change in EMG activity compared to that of standing posture due to flexion under identical load in hands (as explicitly shown for EO muscles). No significant change in EMG activity compared to that of 0 N due to load magnitude under identical postures was observed.....	60
Fig. 3.5 Mean measured kinematics along with deformed finite element model in standing and flexed postures without load in hands.....	61
Fig. 3.6 Calculated trunk muscle forces in different fascicles, on each side, for flexed postures with and without load of 180N in hands. Global muscle forces in standing postures have also been shown.....	62
Fig. 3.7A Variation of computed T1 sagittal translation with the muscle stiffness coefficient, q , for different postures with and without load of 180 N in hands using linear perturbation analysis at deformed configurations due to 1 N horizontal force at the T1 (in agreement with nonlinear analyses). The smallest q in each case is the critical value below which the system becomes unstable.....	63
Fig. 3.7B Variation of computed T1 sagittal translation with the muscle stiffness coefficient, q , for the case with $\sim 40^\circ$ flexion and 180 N load in hands (while altering the flexion stiffness of passive ligamentous spine by up to $\pm 30\%$) using linear perturbation analysis at deformed configurations due to 1 N horizontal force at the T1 (in agreement with nonlinear analyses).....	64
Fig. 3.8 Measured (<i>in vivo</i>) and computed intradiscal pressure values at the L4-L5 disc under different loads and postures. Values have been normalized to their respective values in the neutral standing posture.....	65

Fig. 3.9 Comparison of measured normalized EMG activity with computed muscle forces normalized to their respective maximum active force ($0.6 \times \text{PCSA}$, Table 2) for global muscles in flexed postures with and without load of 180 N in hands..... 66

Fig. 3.10 Relative contribution of trunk muscles (passive and active) and of passive motion segments (ligamentous spine) to counterbalance the total moment of external/gravity loads (indicated by *) for flexed postures with or without load of 180 N in hands..... 67

Fig. 4.1 The FE model as well as representation of global and local musculatures in the sagittal and frontal planes used in the model. Only fascicles on one side have been shown. ICPL: Iliocostalis Lumborum pars lumborum, ICPT: Iliocostalis Lumborum pars thoracic, IP: Iliopsoas, LGPL: Longissimus Thoracis pars lumborum, LGPT: Longissimus Thoracis pars thoracic, MF: Multifidus, QL: Quadratus Lumborum, IO: Internal Oblique, EO: External oblique, and RA: Rectus Abdominus..... 98

Fig. 4.2 Nonlinear stiffness properties of motion segments at different levels; axial compression force-axial strain on the left and flexion moment-curvature under large compression preloads (~ 2700 N) on the right..... 99

Fig. 4.3 Flow-chart for the application of the Kinematics-based approach and determination of trunk muscle forces, internal loads and stability margin of the spine. The moments required for the prescribed rotations were used in a separate algorithm to calculate muscle forces at each level. Axial compression and horizontal shear force components (i.e., penalties) of these muscle forces were then considered in the finite element model as additional updated external loads. This iterative approach was continued at each load step till convergence was reached..... 100

Fig. 4.4 *In vivo* measured (mean \pm SD) pelvic and torso rotations for different lifting tasks and postures. Mean rotation values as prescribed in the FE model for various cases as well as significant p-levels are also listed. *F: free, L: lordotic, K: kyphotic..... 101

Fig. 4.5 *In vivo* measured normalized EMG activity (mean \pm SD) of extensor and abdominal muscles for different lifting tasks. The predicted normalized force in extensor muscles is also shown. ICPT: Iliocostalis Lumborum Pars Thoracic, LGPT: Longissimus

Thoracis Pars Thoracic, EO: External Oblique, and RA: Rectus Abdominus. *F: free, L: lordotic, K: kyphotic.....	102
Fig. 4.6 Variation of the critical muscle stiffness coefficient, q , with lumbar posture for two flexed tasks (~ 40 and 65°) without external load in hands.....	103
Fig. 4.7 Relative contribution of trunk muscles (passive and active) and of passive motion segments (ligamentous spine) to offset the net total moment of external/gravity loads at the S1 level for different tasks and lumbar postures. *F: free, L: lordotic, K: kyphotic.....	104
Fig. 4.8 Axial compression and anterior shear force components acting on the L4-L5 and L5-S1disc mid-height planes presented separately due to gravity, global muscle and local muscle forces in static flexion of $\sim 65^\circ$ with 180 N load in hands for lordotic and kyphotic lumbar postures. As it is noted, the inclination of the disc mid-height planes is much larger in the lordotic posture than in the kyphotic posture and that especially at the L5-S1 disc. Moreover, the relative magnitude of different loads due to muscle forces is also affected by the instantaneous line of action of muscles.....	105
Fig. 5.1 The FE model as well as the representation of global and local musculatures in the sagittal and frontal planes. Only fascicles on one side have been shown in the frontal plane. ICPL: Iliocostalis Lumborum pars lumborum, ICPT: Iliocostalis Lumborum pars thoracic, IP: Iliopsoas, LGPL: Longissimus Thoracis pars lumborum, LGPT: Longissimus Thoracis pars thoracic, MF: Multifidus, QL: Quadratus Lumborum, IO: Internal Oblique, EO: External oblique, and RA: Rectus Abdominus.....	135
Fig. 5.2 Normalized global muscle activities (ICPT and LGPT) for different flexion tasks predicted using eight different cost functions compared to measured normalized <i>in vivo</i> EMG data (mean \pm SD). All nonlinear cost functions (with the exception of Σ force ²) as well as the double linear method predicted muscle activities in relatively close agreement with experimental data.....	136
Fig. 5.3 Predicted axial compression (normal to disc mid-height planes) at different segmental levels based on eight optimization cost functions for different flexion tasks. The forces differ at most by $\sim 20\%$ at the lowest levels.....	137

Fig. 5.4 Predicted anterior shear force (parallel to disc mid-height planes) at different segmental levels based on eight optimization cost functions for different flexion tasks. The forces differ at most by ~14% at the L5-S1 level.....	138
Fig. 6.1 The FE model as well as global and local musculatures in the sagittal and frontal planes (only fascicles on one side have been shown). ICPL: Iliocostalis Lumborum pars lumborum, ICPT: Iliocostalis Lumborum pars thoracic, IP: Iliopsoas, LGPL: Longissimus Thoracis pars lumborum, LGPT: Longissimus Thoracis pars thoracic, MF: Multifidus, QL: Quadratus Lumborum, IO: Internal Oblique, EO: External oblique, and RA: Rectus Abdominus.....	165
Fig. 6.2 Axial compression (N) acting normal to different intervertebral disc levels (T12/S1) in reference cases (no IAP and no abdominal coactivity) and four cases with different abdominal coactivities along with IAP.....	166
Fig. 6.3 Anterior-posterior shear force (N) acting parallel to mid-planes of different intervertebral disc levels (T12/S1) in reference cases (no IAP and no abdominal coactivity) and four cases with different abdominal coactivities along with IAP....	167
Fig. 6.4 Normalized <i>in vivo</i> measured EMG activity (mean \pm SD) of thoracic extensor muscles (Longissimus Thoracis pars thoracic, LGPT, and Iliocostalis Lumborum pars thoracic, ICPT) for different lifting tasks. Predictions have also been shown in reference cases (no IAP and no abdominal coactivity) and four cases with different abdominal coactivities along with IAP of 4 kPa when lifting a load of 180 N in upright standing posture and of 9 kPa when lifting the same load in forward trunk flexions of 40 ° and 65°.....	168
Fig. 7.1 The FE model as well as global and local musculatures in the sagittal and frontal planes (only fascicles on one side are shown). ICPL: Iliocostalis Lumborum pars lumborum, ICPT: Iliocostalis Lumborum pars thoracic, IP: Iliopsoas, LGPL: Longissimus Thoracis pars lumborum, LGPT: Longissimus Thoracis pars thoracic, MF: Multifidus, QL: Quadratus Lumborum, IO: Internal Oblique, EO: External oblique, and RA: Rectus Abdominus.....	186

Fig. 7.2 Geometry of global muscles (Longissimus Thoracis pars thoracic, LGPT, and Iliocostalis Lumborum pars thoracic, ICPT) in upright standing posture with straight LOA and in flexion of 65° with curved LOA considering no reduction in LA or with a 10% reduction. No wrapping happens at L1-L3 levels for the case with 10% reduction as the LA distance did not decrease below the critical values set for wrapping at these levels..... 187

Fig. 7.3 Normalized *in vivo* measured EMG activity (mean \pm SD) of global muscles (Longissimus Thoracis pars thoracic, LGPT, and Iliocostalis Lumborum pars thoracic, ICPT) for different lifting tasks. Predictions (normalized by 0.6xPCSA) have also been shown for the cases with straight LOA, curved LOA with no reduction in LA, and curved LOA with a 10% reduction in LA for these muscles (F: free, L: lordotic, K: kyphotic)..... 188

Fig. 7.4 Horizontal translation of T1 vertebra under a unit horizontal perturbation force at deformed configurations as a function of q for the flexion task (40° with 180 N in hands, free style) with straight and curved LOA..... 189

Fig. 7.5 Magnitude and direction of wrapping contact forces on the spine due to wrapping of global muscles (Longissimus Thoracis pars thoracic, LGPT, and Iliocostalis Lumborum pars thoracic, ICPT) for the case with no reduction in LAs from upright posture under trunk flexion of 65° with 180 N in hands (free style)..... 190

Fig. 8.1 The FE model as well as global and local musculatures in the sagittal plane (only fascicles on one side are shown) in upright standing posture at initial undeformed configuration. ICPL: Iliocostalis Lumborum pars lumborum, ICPT: Iliocostalis Lumborum pars thoracic, LGPL: Longissimus Thoracis pars lumborum, LGPT: Longissimus Thoracis pars thoracic, MF: Multifidus, QL: Quadratus Lumborum, IP: Iliopsoas, IO: Internal Oblique, EO: External oblique, and RA: Rectus Abdominus (axes are not to the same scale)..... 210

Fig. 8.2 Deformed configuration of the spine and the global muscles (Longissimus Thoracis pars thoracic, LGPT, and Iliocostalis Lumborum pars thoracic, ICPT) with curved lines of action under flexion of 65°. The cutting transverse plane for the single-

level free body diagram (SLFBD) model at the L5-S1 disc level is also depicted (abdominal muscles are not shown).....	211
Fig. 8.3 Normalized (to 0.6 times physiological cross sectional area) activity of global muscles (Longissimus Thoracis pars thoracic, LGPT, and Iliocostalis Lumborum pars thoracic, ICPT) for both loading cases predicted using kinematics-driven (KD) approach and single-level free body diagram (SLFBD) models considered at different T12-L1 through L5-S1 levels. Normalized (to the MVC) <i>in vivo</i> measured EMG activity (mean \pm SD) of these muscles is also shown.....	212
Fig. 8.4 Index of Equilibrium Violation (IEV %) at different T12-L1 through L5-S1 levels when applying muscle forces calculated based on single-level free body diagram (SLFBD) model at the L5-S1 level. OCF-1 and 2 refer to optimization cost functions of sum of squared and linear muscle stresses, respectively, used to partition net moment at the L5-S1 level between muscles.....	213
Fig. 8.5 Relative error in axial compression forces estimated at different spinal levels when applying the muscle forces calculated by the single-level free body diagram (SLFBD) model at the L5-S1 level compared to those calculated using SLFBD models directly at the level under consideration.....	214
Fig. 9.1 Load-displacement response of the lumbar spine with published data of <i>in vitro</i> and finite element model studies.....	217
Fig. 9.2 Variation of computed T12 sagittal translation with the vertical applied load at T12 vertebra level using linear perturbation analysis at deformed configurations due to 1 N horizontal force at the T12.....	218
Fig. 9.3 Variation of computed T1 sagittal translation with the vertical applied load at T1 vertebra level using linear perturbation analysis at deformed configurations due to 1 N horizontal force at the T1.....	219
Fig. 9.4 Distribution of gravity load applied at different spinal levels in the finite element model compared with those of other studies.....	220
Fig. 9.5 Eccentricity of the applied gravity load relative to the center of corresponding vertebra in the finite element model compared with those of other studies.....	220

Fig. 9.6 Muscle passive force-length relationship considered in the model compared to other experimental data. Curves of McGill and Kippers (1996) and Nussbaum and Chaffin (1996) have been adapted from data of Deng and Goldsmith (1987) and McCully and Faulkner (1983), respectively..... 223

Fig. 9.7 Variation of computed T1 sagittal translation with the muscle stiffness coefficient, q , for two different lumbar rotation partitions (see text) under identical total trunk flexion of 40° using linear perturbation analysis at deformed configurations due to 1 N horizontal force at the T1. The smallest q in each case is the critical value below which the system becomes unstable..... 228

Fig. 9.8 Local and global muscle activities compared with their maximum values obtained by experimental studies under flexion of 40° plus 180 N carried in hands.. 235

Fig. 9.9 Local and global muscle activities compared with their maximum values obtained by experimental studies under flexion of 65° plus 180 N carried in hands... 236

List of Annexes

APPENDIX A: THE LIGAMENTOUS SPINE AND TRUNK MUSCLE ARCHITECTURE.....	275
APPENDIX B: OPTIMIZATION: LAGRANGE MULTIPLIERS METHOD....	286

CHAPTER 1

INTRODUCTION

1.1 Low Back Disorders (LBDs)

Spine disorders are the most prevalent cause of chronic disability in persons less than 45 years of age (Ashton-Miller and Schultz, 1997). As many as 85% of adults experience low back pain (LBP) that interfere with their work or recreational activity and up to 25% of the people between the ages of 30 to 50 years report low back symptoms when surveyed (Frymoyer, 1996). According to the Canadian Centre for Occupational Health and Safety, the largest lost time claim in Canada, accounting for 25% of all claims, is also due to back injuries (Canadian Task Force on Preventive Health Care, 2003). In 1992, the annual costs associated with back pain in the US ranged from \$20 to \$50 billion (Nachemson, 1992). In both prevalence and cost (treatment, absenteeism, compensation), low back disorders (LBDs) are, hence, recognized as the most significant disorders (Praemer et al., 1992; Webster and Snook, 1994).

Although the cause of most LBDs remains unknown, but both personal and environmental risk factors which include biomechanical and psychological factors need to be taken into account for an adequate understanding of the mechanism of LBP (Shirazi-Adl and Parnianpour, 2001). For the latter, the following factors are identified to be of significance: monotonous work, high perceived workload, time pressure, low control on the job, and lack of social support (Bongers, 1993). As for the former factors, the results of epidemiological studies have associated six occupational factors with LBP symptoms: (1) physically heavy work, (2) static work postures, (3) frequent bending and twisting, (4) lifting and sudden forceful incidents, (5) repetitive work, and (6) exposure to vibration (Frymoyer et al., 1983). In a large survey, lifting or bending episodes accounted for 33% of all work-related causes of back pain (Damkot et al., 1984).

Combination of lifting with lateral bending or twisting that occurs in asymmetric lifts has been identified as a frequent cause of back injury in the workplace (Marras et al., 1995; Kelsey et al., 1984; Hoogendoorn et al., 2000; Troup et al., 1981; Varma and Porter, 1995; Andersson, 1981). Among various work-related activities, lifting, awkward posture, and heavy physical work have been indicated to have strong relationship with lumbar musculoskeletal disorders (NIOSH, 1997). Several review studies on the epidemiology of LBP have also concluded that lifting, in general, is one of the major documented risk factors for LBD (Ferguson and Marras, 1997; Burdorf and Sorock, 1997; Frank et al., 1996).

1.2 Biomechanical Models of the Human Spine

There exists a general agreement that the major cause of injury is associated with the mechanical overload and/or overuse of the lumbar spine tissues. The above-mentioned studies confirming an association between heavy work and LBD justify biomechanical investigations of the human spine. Obviously, the most important mechanical function of the spine is to support external, gravity and inertial loads during various activities of daily living. Such Mechanical factors are often identified as the primary cause of LBD (Adams and Dolan, 1995; Bigos et al., 1986; Frymoyer et al., 1983; Kerr et al., 2001; Marras et al., 1995; McCowin et al., 1991). Knowledge of spinal loads, spinal movements, trunk muscle forces, and interactions between spinal pathologies and mechanical factors, hence, provides appropriate insight for the effective prevention and treatment of LBDs. Prevention and treatment programs, sport medicine, and performance enhancement programs would benefit from a more accurate knowledge of loads on spine and muscle forces.

Excessive mechanical loads likely induce injury (from micro damage to complete rupture) in the ligamentous spine (e.g., ligaments, intervertebral discs, vertebrae) and musculotendinous structures. Van Dieen et al. (1999) suggest that generally four mechanical loads are of more interest: axial compression and shear forces acting on the

spine, tensile stress in posterior spinal ligaments, and muscle forces. These loads, once calculated or measured, are to be compared with their tolerant limits in order to assess risk of injury to the spine. Based on *in vitro* measurements as well as finite element model studies some tolerant limits have been suggested for different mechanical loads which the spine should undergo. For instance, tolerant limits of 6.4 kN for axial compression (National Institute of Occupational Safety and Health), 1981), 2-2.8 kN for shear force (Cripton et al., 1995), and 60 Nm bending moment in passive ligamentous spine (Adams et al., 1980 and Adams and Dolan, 1991; Miller et al., 1986) have been suggested.

Unfortunately, none of foregoing mechanical parameters of interest can be measured directly. Therefore, other indicators of back load have been considered to indirectly estimate the parameters of interest. For instance, intradiscal pressure (IDP) (Nachemson, 1981; Wilke et al., 1999), intra-abdominal pressure (IAP) (Davis, 1981), and spinal shrinkage (Van Dieen and Toussaint, 1993; McGill et al., 1996a) have been suggested to be associated with the axial compression acting on intervertebral discs. There exist, however, some controversies about the validity of rather simple associations with spinal loads for these indicators (Van Dieen et al., 1999). Cost and ethical concerns have further limited the feasibility of indirect measurements. The infeasibility of direct quantification of muscle forces and spinal loads as well as the limitations of indirect measurement methods have persuaded researchers towards the use of biomechanical modeling techniques. Biomechanical models have been recognized as indispensable tools for evaluation of spinal loads in various occupational and recreational activities.

1.3 Biomechanical Models of the Spine and the Kinetic Redundancy

Biomechanical models, both static and dynamic, use the basic principles of mechanics to estimate muscle forces and spinal loads. Forces in different active (i.e., trunk muscles) and passive structures of the spine are calculated by satisfying equilibrium between external moments due to gravity-external loads and internal

moments produced by all active and passive structures of the spine (Fig. 1.1) as follow (limiting ourselves to sagittally symmetric isometric cases by neglecting dynamic loads in these equations as well as out-of-plane loads and movements, readers could consult Appendix A for general information on functional biomechanics of the spine):

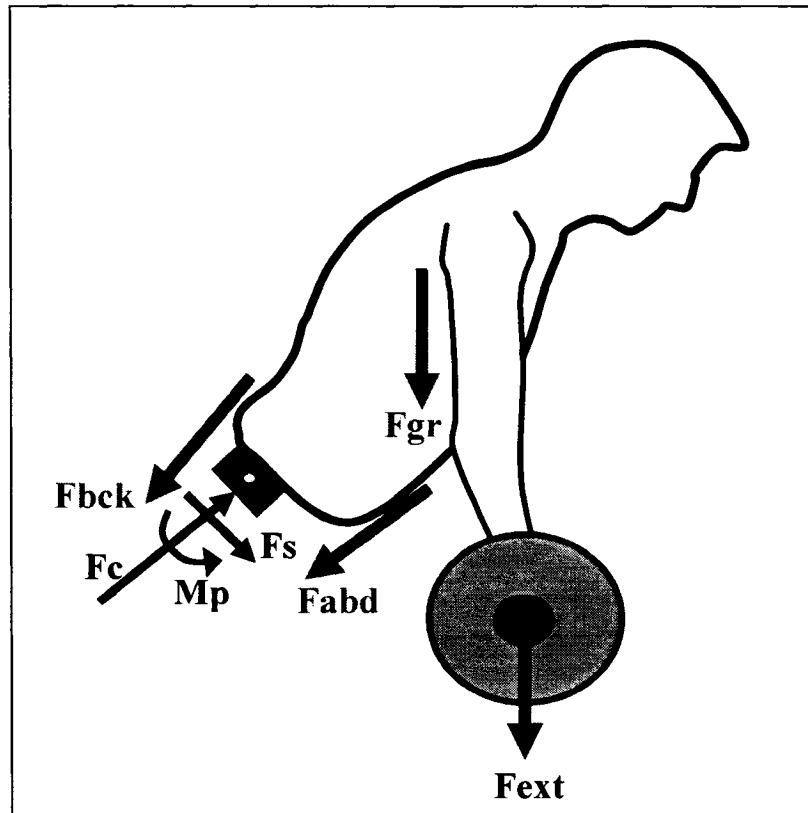


Fig. 1.1 Free-body diagram for calculating spinal and muscle loads at a typical lumbar disc during lifting.

$$\sum_{i=1}^n \mathbf{r}_{abd} \times \mathbf{F}_{abd} + \sum_{i=1}^m \mathbf{r}_{bck} \times \mathbf{F}_{bck} + \mathbf{M}_p = \mathbf{r}_{gr} \times \mathbf{F}_{gr} + \mathbf{r}_{ext} \times \mathbf{F}_{ext}. \quad (\text{Eq. 1.1})$$

in which r_{gr} , r_{ext} , r_{abd} , and r_{bck} are moment arms of gravity load (F_{gr}), external load (F_{ext}), different (total of n) abdominal muscle forces (F_{abd}), and different (total of m) back muscle forces (F_{bck}) with respect to the center of the disc where the free-body

diagram (FBD) is considered, respectively. $\mathbf{M_p}$ is the passive moment resisted by the ligamentous spine including disc and all passive tissues surrounding the spine which are cut by the FBD plane.

Moment of external loads ($\mathbf{r}_{gr} \times \mathbf{F}_{gr} + \mathbf{r}_{ext} \times \mathbf{F}_{ext}$) is usually estimated using a static or dynamic link segment model (for more details see Reeves and Cholewicki, 2003). $\mathbf{M_p}$ is generally estimated directly from the segmental rotation at the plane of cut using moment-rotation properties obtained by experimental *in vitro* or finite element modeling studies. The equilibrium equation is solved to calculate unknown abdominal and back muscle forces. Once muscle forces are calculated, equilibrium can be considered between external and internal forces to compute axial compression and shear forces acting on the spine as follow:

$$\mathbf{F}_{gr} + \mathbf{F}_{ext} + \sum_{i=1}^n \mathbf{F}_{abd} + \sum_{i=1}^m \mathbf{F}_{bck} + \mathbf{F}_s + \mathbf{F}_c = 0. \quad (\text{Eq. 1.2})$$

in which \mathbf{F}_s and \mathbf{F}_c are axial compression and anterior-posterior shear forces acting on the disc considered in this exemplary FBD.

The major problem in dealing with the foregoing equations is that Eq.1.1 can not be solved deterministically, since the number of unknown muscle forces ($n+m$) is much larger than the number of equilibrium equations (e.g., only one for the example in a sagittally symmetric lift). Numerous biomechanical models for estimation of spinal and muscle loads have been developed to tackle the kinetic redundancy in system of equilibrium equations. In doing so, generally four approaches have been reported in the literature; single-equivalent muscle approach, optimization-based approach, EMG-assisted approach, and Kinematics-driven model.

1.4 Single-Equivalent Approach

Earlier attempts to solve the redundancy problem have simplified the role of muscles by grouping them into synergistic groups, i.e. a single equivalent muscle represents all back muscles while ignoring abdominal ones (Chaffin, 1969; Leskinen et al., 1983; de Looze et al., 1996; Morris et al., 1961; van Dieen and de Looze, 1999). This reduces the number of unknown muscle forces allowing the number of equations and unknowns to become identical so one could obtain the unique solution to the muscle forces and, subsequently, spinal loads. Obviously, this method fails to estimate forces in individual trunk muscles including various fascicles of extensor back muscles each of which attach to a different spinal level and may play a different role during lumbar extension and lifting activities (Bogduk et al., 1992a). Besides, there is a wide range of data reported for moment arms (Bogduk et al., 1992a; Daggfeldt and Thorstensson, 2003; Jorgensen et al., 2001; McGill, 2002; Stokes and Gardner-Morse, 1999; Wood et al., 1996) and line of action (Cholewicki and McGill, 1996; Han et al., 1992; Stokes and Gardner-Morse, 1999) of the equivalent single muscle to which predicted muscle and spinal loads remain very sensitive (Nussbaum et al., 1995; van Dieen and de Looze, 1999). It has, however, been suggested that single-equivalent models could solely be useful for a crude estimation of spinal compression (van Dieen and Kingma, 2005; Bergmark, 1989). The error naturally will grow in presence of greater antagonistic muscle activities which are neglected in this model.

1.5 Optimization-Based Approach

The very widely-used mathematical modeling approach which has been proposed to resolve the kinetic redundancy is based on the assumption that there may be a cost (objective) function (or many cost functions) that could be minimized or maximized (optimized) by central nervous system (CNS) while satisfying the equilibrium conditions. Optimization was the first approach ever used to partition moment of external loads between muscles in a multi-muscle model of the spine (Schultz et al., 1982). In the optimization procedure, constraint equations on muscle forces are introduced enforcing that muscle forces remain greater than zero and smaller than some

maximum values corresponding to the maximum allowable stress in the muscles. Various linear and nonlinear cost functions have been used; two of the more common ones include minimization of intervertebral disc compression forces (Schultz et al., 1982; Seireg and Arvikar, 1973; Yettram and Jackman, 1982; Zetterberg et al., 1987) and minimization of summation of muscle stresses to different powers (Crowninshield and Brand, 1981; Hughes et al., 1994). In general, an optimization problem can be defined as follows:

$$\text{Minimize } (\mathbf{OF}) \text{ (e.g., } \mathbf{OF} = \sum_{i=1}^n \left(\frac{\mathbf{F}_i}{\mathbf{A}_i} \right)^3 \text{)} \quad (\text{Eq. 1.3})$$

where the objective function (OF) subject to the linear equality constrain corresponding to equilibrium equation:

$$\sum_{i=1}^n r_i \times F_i = M - M_p \quad (\text{Eq. 1.4})$$

and inequality constraints:

$$0 \leq F_i \leq \sigma_{\max} \times PCSA_i \quad (\text{Eq. 1.5})$$

where F_i , $PCSA_i$, σ_{\max} , n , r_i , and M denote unknown total force in muscle i , physiological cross-sectional area of i th muscle, maximum allowable active stress, number of muscles cut by the FBD, moment arm of the i th muscle, and the moment of external loads, respectively. Note that Eqs. 1.1 and 1.4 are vectorial representations of equilibrium equations accounting for the fact that the sagittal moment of abdominal muscles is opposite to that of extensor muscles. Naturally, in order to minimize the cost function considered in Eq. 1.3, the optimization procedure usually assigns no forces to abdominal (antagonistic) muscles. Inability of optimization approaches to predict activity of antagonistic muscles is recognized as one of the major shortcomings of this

approach. Co-contraction of antagonist muscles, however, has been introduced in optimization approach by assuming a non-zero lower bound for muscle forces in Eq. (1.5) (Hughes et al., 1995). The lack of physiological basis for the assumption that CNS uses an optimization approach to partition loads among muscles as well as the deterministic nature of optimization-based recruitment predictions despite the presence of inter and intra-individual variability in performance are other deficiencies of this approach (Shirazi-Adl and Parnianpour, 2001; Reeves and Cholewicki, 2003). Nevertheless, optimization methods are still the most common approach used to estimate individual muscle forces in mathematical models of various joints (Herzog, 1992).

Predicted muscle forces using an optimization approach are qualitatively validated by comparison with measured EMG activity of muscles. Cost functions whose predictions for muscle forces correlate with muscle activation in a selected task are considered adequate (Crowninshield and Brand, 1981; Hughes et al., 1994; Prilutsky et al., 1998; van Bolhuis and Gielen, 1999). It has been suggested that a single cost function of minimization of axial compression acting on the spine or intervertebral displacements would not predict muscle activities in good agreement with EMG data (Stokes and Gardner-Morse, 2001). A multi-criteria cost function in which sum of weighted cost functions is simultaneously optimized was instead proposed (see Chapter 5 and Appendix B for more details on optimization approaches).

1.6 EMG-Assisted Approach

In the light of foregoing criticisms, the use of processed electromyography (EMG) from trunk muscles has been advocated to drive biologic solution to the redundancy present in biomechanical models (McGill and Norman 1986; Marras and Granata, 1997; Gagnon et al., 2001). As a muscle contracts, electrical signals are created within the muscles (EMG) which could be measured by surface electrodes on the skin overlying the muscle or by deep fine wire electrodes inside the muscle. In order to calculate force in trunk muscles a relationship between EMG activity of trunk muscles

and their force has to be subsequently presumed. Obviously, the calculated muscle forces in this way will not necessarily assure the satisfaction of equilibrium equations (Eq. 1.4). Therefore, a gain factor to which all calculated muscle forces are multiplied is introduced to satisfy equilibrium conditions (i.e., Eq. 1.4). This type of strategy is referred to as EMG-assisted method which is given credit for its ability to predict force in antagonistic muscles and for its sensitivity to inter and intra-individual variability.

Apart from the difficulty in recording the activity of all existing muscle fascicles, a limitation of EMG-assisted modeling is the fact that deep muscles are not accessible using surface EMG electrodes. One must use intra-muscular wire electrodes to measure the activity of these muscles or as often done in EMG-assisted models, activities for these muscles should be assumed on the basis of the EMG collected from select superficial ones. This disagrees with recent *in vivo* evidence that deep and superficial fibers of trunk muscles are controlled independently (Moseley et al, 2002). It has been, however, shown that appropriately located surface EMG electrodes may adequately represent amplitude of deep muscle activities for a variety of tasks (McGill et al., 1996b).

Even for superficial larger flat muscles the EMG activity is measured from one site of the muscle, despite the existing regional differences in muscle activities (Strohl et al., 1981; Davis and Mirka, 2000; Mirka et al., 1997; Hodges et al., 1999). Besides, wide controversy exists regarding the nature of relations between muscle forces and associated EMG activity. Due to these difficulties, EMG-assisted approach has been described to be cumbersome (van Dieen and Kingma, 2005) or even impossible (Calisse et al., 1999) for precise prediction of muscle forces in terms of both data acquisition and EMG-force relationships.

To improve the accuracy of predictions in terms of providing better match between the predicted muscle forces and their EMG profiles a hybrid optimization-EMG

based model was suggested (Cholewicki and McGill, 1994; Cholewicki et al., 1995). The objective of this approach was to balance net moment and moment produced by muscles by applying the least possible adjustment to individual muscle forces. In other words, individual gain factors are calculated for muscles rather than considering one single gain factor to which all muscle forces, as is the case in a pure EMG-assisted approach, are multiplied to balance the net moment. It was concluded that using such hybrid approach would predict muscle activities in best possible match with EMG data (Cholewicki and McGill, 1994).

1.7 Kinematics-driven approach

Since this method is employed in the current work, it will be fully presented in a subsequent section.

1.8 Spinal Stability

Both *in vitro* experimental and mathematical model studies on isolated osteoligamentous lumbar spine without muscular support have estimated critical buckling loads of less than ~90 N (Crisco and Panjabi, 1992; Crisco et al., 1992; Shirazi-Adl and Parnianpour, 1993). On the other hand, the entire ligamentous thoracolumbar spine can support much smaller loads of <20 N (Lucas and Bresler; Shirazi-Adl and Parnianpour, 1996). This indicates that the isolated spine devoid of muscles is unable to sustain compressive loads and will buckle under very low loads compared to those due solely to body weight. It becomes, therefore, obvious that equilibrium analysis is not enough to study the safe load tolerance of the spine as a structure and consequently mechanical stability analysis is also required. Besides, the crucial role of trunk muscles in providing stability to the spine becomes clear.

To further illustrate the importance of stability analysis, Granata and Orishimo (2001) measured EMG activity of trunk muscles when stability of the spine was challenged by external loads generating the same lumbar moments. By increasing height

of the load carried in the hands and not the load moment arm, it was revealed that muscle activation increased in both trunk extensor and flexor muscles. This would not have been predicted with an equilibrium-based model. For this reason researchers have also considered stability analyses in order to better understand the mechanics of the lumbar spine. Complete structural analysis of the spine, thus, requires a two-stage approach: equilibrium analysis which is performed to estimate tissue loads including muscle forces and spinal loads, and then stability analyses employing earlier estimations to examine system stability margin in presence of a perturbation

It is important to differentiate between the term *mechanical instability* and *clinical instability* usually used in spine biomechanics literature. Panjabi (2003) defined the former one as inability of the spine to carry spinal loads while the latter refers to the clinical consequences of neurological deficit or pain. In current study wherever we refer to the term stability, only the mechanical definition is meant.

Simple inverted pendulum models in which spinal stiffness are represented by torsional springs have been proposed to simulate the spine structure for stability analysis (Reeves and Cholewicki, 2003). The system stability is subsequently verified by examination of the second variation of the total potential energy. Muscles are modeled as preloaded variable stiffness springs that store elastic energy upon perturbation and provide stability to the system. Stiffness of the muscles has been considered to be both linearly (Bergmark, 1989; Crisco and Panjabi, 1991) and nonlinearly (Cholewicki and McGill, 1995; Shadmehr and Arbib, 1992) related to the muscle force, although most modeling approaches assume a linear relationship (Reeves and Cholewicki, 2003). Bergmark (1989) used a muscle stiffness proportional to muscle force (F) and inversely proportional to its length (l) ($k=qF/l$) with the q as a non-dimensional muscle stiffness coefficient taken the same for all muscles. Using this relationship Crisco and Panjabi (1991) demonstrated that the overall stability of a five-vertebrae spinal column model depends on muscle architecture. In fact, the spine was always unstable if any vertebral

level was devoid of muscles. This elucidates that to accurately estimate spinal stability, multisegmental models of the spine considering all trunk muscles are necessary.

Bergmark (1989) was the first to develop a multiple muscle model with five lumbar rigid vertebrae, a rigid pelvis and rigid thoracic cage to study the spinal stability during sagittally-symmetric static lifting in upright standing posture. The rigid vertebrae were interconnected by torsional springs while neglecting axial and shear stiffness of the passive spine. Based on whether the muscles crossed a single intervertebral joint or spanned all joints from the pelvis to the ribcage, he divided trunk muscles into local and global systems. The critical muscle stiffness coefficient (q) for a stable equilibrium at a specific posture was evaluated. He found that for q values smaller than 37, stability at a given posture was not possible at all. He also found that for a given activation level of the local muscles, there exist a maximum limit of activation for global muscles above which the spine will buckle. This is because muscles, when activated, increase compression load on the spine, which could offset their beneficial increase in stiffness.

In a similar biomechanical model of the spine in which lumbar vertebrae, pelvis and thorax were all considered rigid while neglecting axial and shear stiffness of the passive spine, Cholewicki and McGill, 1996 investigated stability of the spine during dynamics activities. They found that there exists an ample stability safety margin in the tasks that required greater muscular efforts. However, tasks that demanded very little muscle activity, such as upright standing with no load, were found to be close to the buckling threshold. It appears that tasks that challenge spine stability the most are the ones in which the spine is maintained in a neutral posture with small muscle activities.

Using a linear finite element model of the spine with 132 unknown muscle forces and 36 unknown joint displacements, Gardner-Morse et al. (1995) analyzed stability of the spine in maximum voluntary trunk extension efforts performed in the upright standing posture. Critical Value of q was in the range of 3.7-4.7 in order to stabilize the

spine; implying that at maximal efforts, muscle stiffness is sufficient to stabilize the lumbar spine. In an additional analysis in which passive spine stiffness was decreased by 10%, it was observed that q must consequently increase from 4.5 to 4.7 in upright standing posture. This shows the importance of stiffness of ligamentous spine, besides the muscles, in providing stability to the spine (Stokes and Gardner-Morse, 2003). Intra-abdominal pressure (Cholewicki et al., 1999a, b; Essendrop et al., 2002; Gracovetsky et al., 1985; McGill and Norman, 1987; McGill and Sharratt, 1990) and co-activity of antagonistic muscles (Cholewicki et al., 1999; El-Rich and Shirazi-Adl, 2004, 2005) have been also indicated as parameters providing stability to the spine. Dysfunction of stabilizing systems is postulated to lead to LBP and injury (Panjabi, 1992a, b).

1.9 Lifting Techniques

Role of lifting in low-back injuries is well recognized in the literature as described before. In search of optimal lifting methods, two techniques have been proposed in the literature for lifting of low-lying objects; squat lift (i.e., knee bent and back straight) and the stoop lift (i.e., knee straight and back bent) (see Fig. 1.2). The literature on the safer lifting technique remains controversial; however, the squat lift is usually considered to be safer than the stoop one in bringing the load closer to the body and, hence, reducing the extra demand on back muscles to counterbalance additional moments (van Dieen et al., 1999 and Hsiang et al., 1997). The importance of the squat versus stoop lifting postures has, however, been downplayed due to the lack of a clear biomechanical rationale for the promotion of either style (McGill, 1997). Many workers, despite instruction to the contrary, prefer the stoop lift over squat lift. It is known that there is an increased physiological cost (Garg and Herrin, 1979) as well as more rapid fatigue development (Hagen et al., 1993) in squatting and that squat lift is not always possible due to the lift set up and load size (van Dieen et al., 1999).

In a recent review paper (van Dieen et al., 1999) and a biomechanical model study (Potvin et al., 1991) of the effect of squat and stoop lifting techniques on the

lumbar spine loading, it was suggested that the risk of injury may be influenced more by the lumbar posture (kyphotic, lordotic, or free styles) rather than the choice of stoop or squat technique. In a kyphotic lift the lumbar spine is flexed while in a lordotic one the lumbar lordosis is preserved (see Fig. 1.3). The advantages in preservation or flattening (i.e., flexing) of the lumbar lordosis during lifting tasks are, however, even less understood.

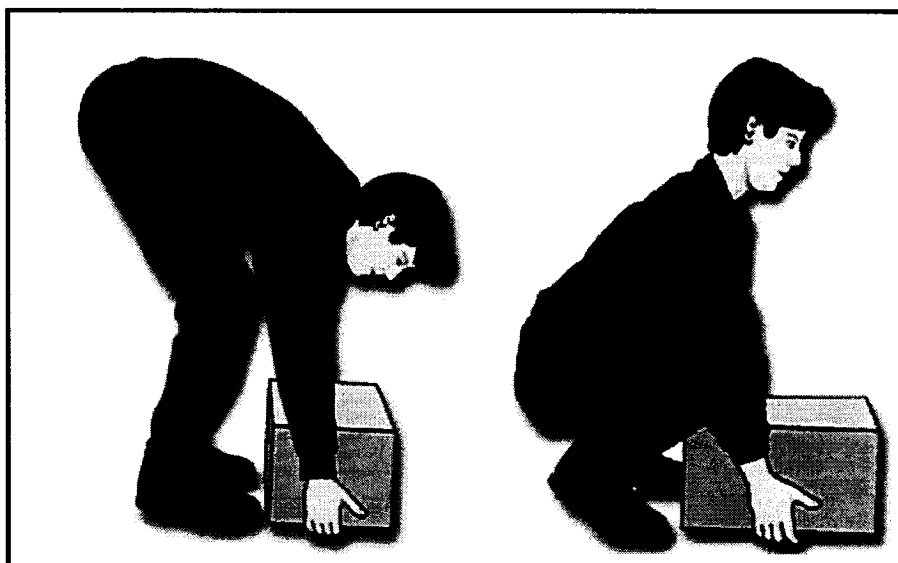


Fig. 1.2 Stoop (left) versus squat (right) lift

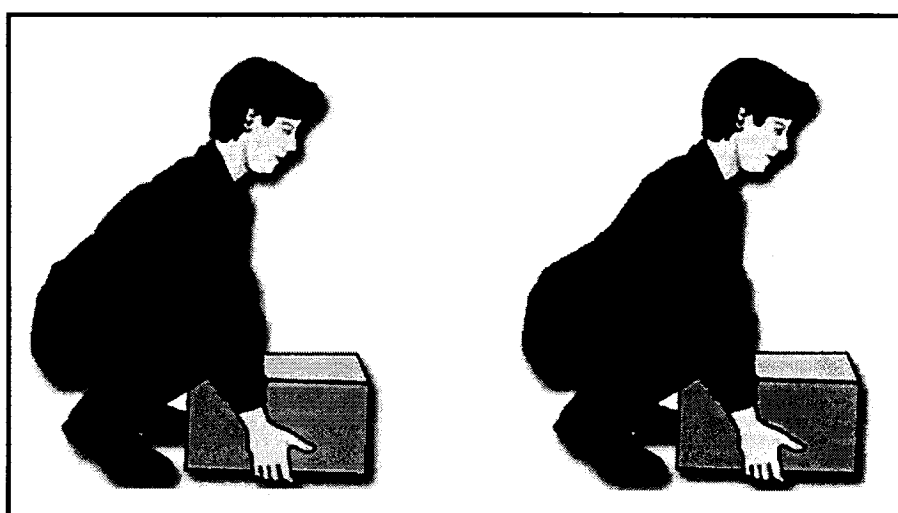


Fig. 1.3 Kyphotic (left) versus lordotic (right) lift during a squat lift.

A kyphotic lift (i.e., flexed lumbar spine) is recommended by some as it utilizes the passive ligamentous system (i.e., posterior ligaments and lumbodorsal fascia) to their maximum thus relieving the active extensor muscles (Gracovetsky et al., 1985). In contrast, however, others advocate lordotic postures indicating that posterior ligaments cannot effectively protect the spine and an increase in erector spinae activities is beneficial in augmenting spinal stability (McGill, 1997; Vakos et al., 1994) and in diminishing the anterior shear force on spine (Potvin et al., 1991).

The inability to accurately determine the loads on the trunk active and passive components as well as the system stability margin appears as a critical hindrance towards the development of ergonomic guidelines for the design of safer lifting tasks. Evidently, an improved assessment of risk of injury depends on a more accurate estimation of the load partitioning in the human trunk in forward flexion tasks.

1.10 Intra-Abdominal Pressure (IAP)

One parameter with the potential to influence spinal mechanics and stability is intra-abdominal pressure (IAP) that has been reported to increase during static and dynamics lifting tasks (Andersson et al., 1976; Bartelink, 1957; Marras et al., 1984; McGill et al., 1990; Hagins et al., 2004). In neutral standing posture without carrying any load in hands IAP has been measured as low as 0.2 kPa (Andersson et al., 1977), 0.3 kPa (Marras and Mirka, 1996), and 0.98 kPa (Nachemson et al., 1986). IAP has been reported to reach 50 kPa in power competitive lifters wearing belt (McGill et al., 1990).

For years, it has been argued that an increase in IAP could unload the spine both directly by pressing upwards on the ribcage via diaphragm and indirectly by generating an extensor moment on the lumbar spine that decreases back muscle activities (Bartelink, 1957; Daggfeldt and Thorstensson, 2003; Essendrop and Schibye, 2004; Hodges et al., 2001). This relief mechanism can be better understood by considering the

FBD depicted in Fig. 1.1 while taking into account the force generated due to IAP (Fig. 1.4). Eqs. 1.1 and 1.2 can now be re-written as follow:

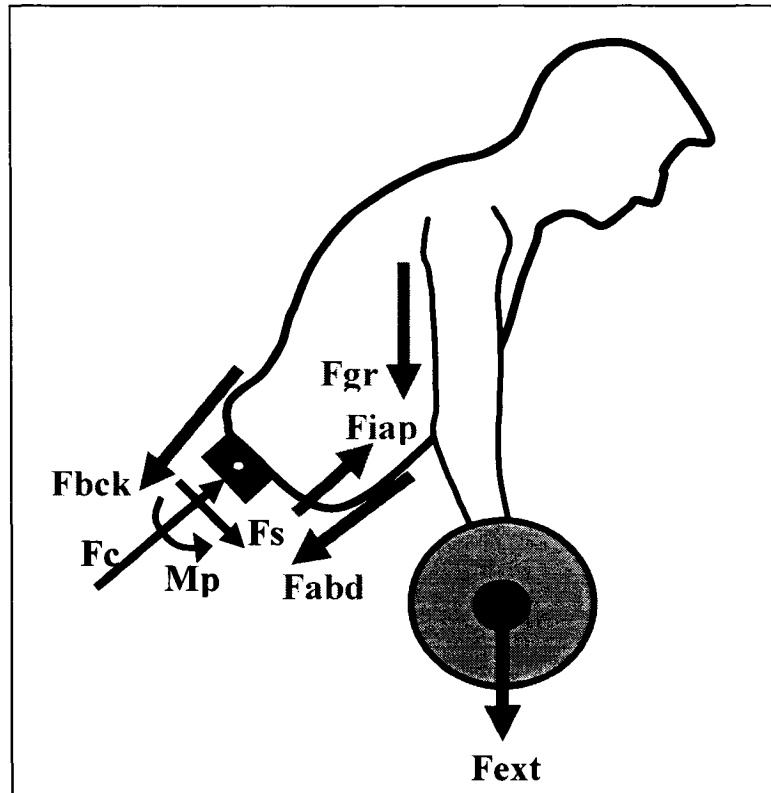


Fig. 1.4 Free-body diagram for calculating spinal and muscle loads on a lumbar disc during lifting while taking account for the IAP force.

$$\sum_{i=1}^n R_{gr} \times F_{gr} + \sum_{i=1}^m R_{ext} \times F_{ext} + \sum_{i=1}^n R_{iap} \times F_{iap} + \sum_{i=1}^n R_{abd} \times F_{abd} + \sum_{i=1}^m R_{bck} \times F_{bck} + M_p = 0. \quad (\text{Eq. 1.6})$$

$$F_{gr} + F_{ext} + F_{iap} + \sum_{i=1}^n F_{abd} + \sum_{i=1}^m F_{bck} + F_s + F_c = 0. \quad (\text{Eq. 1.7})$$

in which R_{iap} is the moment arm of generated force (F_{iap}) due to IAP. It becomes clear from these two equations that IAP has the potential to unload the spine both directly (Eq. 1.7) and indirectly (Eq. 1.6) by generating an extensor moment against moment of

external loads. According to this mechanism, abdominal belts have been recommended with the objective to increase IAP and unload spine (Harman et al., 1989; Lander et al., 1992); thus reducing risk of injury to the spine.

Using a biomechanical model of the lumbar spine in which IAP was introduced with no concurrent abdominal coactivities, it was claimed that IAP can unload the spine at all levels by ~400 N (34-40% of total compression) during maximal back extension in an extended posture when lying on the side (Daggfeldt and Thorstensson, 2003). This finding, however, has been challenged by other biomechanical models stating that the co-contraction of abdominal muscles occurring along with an increase in IAP produces a flexor moment large enough to offset or even exceed the IAP-generated extensor moment (McGill and Norman, 1987; McGill et al., 1990; Cholewicki et al., 2002). Besides, experimental studies have found that IAP increase is associated with a concurrent increase in the intradiscal pressure during Valsalva maneuvers (Nachemson et al., 1986) and no reduction in erector spinae EMG activity in lifting (Krag et al., 1986; McGill et al., 1990) thus raising questions on the unloading role of IAP.

It appears that studies that advocate the unloading effect of IAP usually consider a raise in IAP to be primarily due to the activity of transverse abdominis (TA) whose fibers are mostly oriented in the transverse plane thus imposing little or no compression penalty on the lumbar spine (Daggfeldt and Thorstensson, 2003, 2004; Hodges et al., 2001). On the other hand, others insist that no appreciable increase in IAP can develop without simultaneous coactivity of all abdominal muscles including internal oblique (IO), external oblique (EO), and rectus abdominis (RA) whose activity would counterbalance both the upward unloading force and the generated extensor moment due to IAP (Cholewicki et al., 2002; Cholewicki and Reeves, 2004).

The controversy on the unloading role of IAP is due partly to uncertainties about the magnitude and pattern of abdominal muscle coactivities that occur with an increase

in IAP. Inability of biomechanical models to accurately partition loads among the trunk active-passive components and evaluate spinal loads remains as another reason for the existing controversy. The predictions of EMG-driven models on the effect of IAP on spinal loading and stability are only as accurate as the many underlying assumptions made in their formulation and spine model used. Moreover, model studies advocating unloading role of IAP during maximum back exertions have considered the transverse abdominis (TA) as the only abdominal muscle generating IAP (Daggfeldt and Thorstensson, 2003).

In contrast to the unloading action of IAP, there exists a general consensus that an increase in IAP stabilizes the spine. Any increase in IAP is accompanied by the co-contraction of abdominal muscles which, in turn, increases spinal stiffness and stability (Cholewicki et al., 1999a, b). Generated abdominal coactivities due to a raise in IAP may further increase activity of extensor muscles thus increasing the overall stiffness of the system.

1.11 Geometry of Trunk Thoracic Extensor Muscles

For a detailed description on the geometry of back muscles see Appendix A. Wide ranges of data have been reported in the literature for the lever arm of erector spinae (ES) in the sagittal plane (~4-8 cm) (Bogduk et al., 1992a; Daggfeldt and Thorstensson, 2003; Jorgensen et al., 2001; McGill, 2002; Stokes and Gardner-Morse, 1999; Wood et al., 1996) as well as for their line of action (LOA) (Cholewicki and McGill, 1996; Han et al., 1992; Stokes and Gardner-Morse, 1999). Both the lever arm of ES (Jorgensen et al., 2003; Macintosh et al., 1993; Tveit et al., 1994) and the angle between their LOA and the longitudinal axis of vertebrae (Macintosh et al., 1993; McGill et al., 2000) have been observed to decrease as the spine flexes forward in the sagittal plane. The extent of such alterations, especially for thoracic fascicles of the ES, needs yet to be determined (Macintosh et al., 1993).

An equally crucial issue is the pathway of local (i.e., with upper attachments at lumbar vertebrae) and global (i.e., with upper attachments at the rib cage) ES muscles. Unlike in upright postures in which these pathways can accurately be assumed as straight lines between insertion points, such may not be assumed in tasks involving large lumbar flexions. In latter tasks, a straight line assumption for global muscles could violate kinematics constraints by penetrating into intervening hard/soft tissues. The local lumbar muscles have been suggested not to take significantly curved orientations in flexion (Macintosh et al., 1993). Curved rather than linear pathways have, however, to be considered for global muscles especially in tasks involving large trunk flexion if precise estimation of muscle forces and spinal loads are sought.

Some earlier biomechanical models (e.g. Cholewicki and McGill, 1996) report also to have considered curved pathways for extensor muscles that pass through several points at different vertebrae. These models, however, appear to have failed to account for reaction (contact) forces at these points of contact between muscles and vertebrae. These contact forces are due to changes in muscle orientation and would generate moment as well as shear/compression forces that need to be considered in associated equilibrium equations at different levels. Simulation of wrapping without the proper consideration of these contact forces at the deformed configuration of the spine is not, hence, adequate and would adversely affect the accuracy of estimations.

1.12 Free Body Diagram-based Models of the Spine

A major shortcoming in many current and earlier biomechanical model studies of multi-segment spinal structure lies in the consideration of the balance of net external moments only at a single cross section (typically at lowermost lumbar discs) (see Fig. 1.1) rather than along the entire length of the spine (e.g., Schultz et al. 1982, McGill and Norman 1986, Cholewicki et al. 1995, Parnianpour et al. 1997, van Dieen et al. 2003, Granata et al. 2005, Marras et al. 2005). These models are widely employed in ergonomic applications and in injury prevention and treatment programs. It has been

indicated, though with no details, that the muscle forces evaluated based on such single-level equilibrium models, once applied on the system along with external loads, may not necessarily satisfy equilibrium at remaining levels along the spine (Stokes and Gardner-Morse 1995). The extent of violations in equilibrium at different levels and their effects on the estimated muscle forces and spinal loads, however, have not yet been quantified.

1.13 Finite Element Models of the Spine and the Kinematics-Based Approach

As mentioned before, biomechanical models based on optimization or EMG-assisted approaches share often major deficiencies; the balance of net external moments is considered only at one cross-section rather than along the entire length of the spine. It has been indicated that the muscle forces evaluated based on such single-level equilibrium models, once applied on the system along with external loads, may not necessarily satisfy equilibrium at remaining levels along the spine (Stokes and Gardner-Morse 1995). Therefore, the evaluated muscle forces, once applied on the system along with external loads, may not necessarily generate the same spinal kinematics under which they were initially calculated. Naturally, accuracy in calculation of the stability margin of the active-passive system is also influenced by simplifying assumptions made in the model.

To overcome these shortcomings, linear finite element models along with optimization algorithms have been developed and used to evaluate muscle recruitment, internal loads, and stability margin (Dietrich et al., 1991; Gardner-Morse et al., 1995; Gardner-Morse and Stokes, 1998; Stokes and Gardner-Morse, 1995, 2001). A simplified geometrical model of the spine with rotational degrees-of-freedom and nonlinear stiffness properties along with EMG-assisted approach was used to evaluate muscle forces and stability margin in various tasks (Cholewicki and McGill, 1996). The translational degrees-of-freedom at various joints and, hence, associated shear/axial equilibrium equations were totally neglected in this latter model which would adversely

influence predictions on muscle forces and system stability (Stokes and Gardner-Morse, 1995).

Proper considerations of the nonlinear material properties of the thoraco-lumbar motion segments in different directions with load- and direction-dependent properties, of realistic distribution of gravity/external loads, and of verification of the stability using nonlinear analysis are important to obtain reliable results. Adequate nonlinear representation of passive spine particularly in presence of large compression forces and flexion rotations expected in lifting tasks (Patwardhan et al., 2003; Shirazi-Adl, 2006; Stokes and Gardner-Morse, 2003) is important not only in proper partitioning of the net moments among passive-active components but also in the stability analysis of the system. Besides, realistic consideration of spinal geometry and deformation under loading is crucial in proper determination of both active and passive spinal loads as well as spinal stability.

A novel iterative kinematics-based approach has, recently, been developed and validated in which the a-priori measured kinematics of the spine are prescribed in a nonlinear finite element model to evaluate muscle, spinal loads, and stability in neutral standing postures (Kiefer et al., 1997; El-Rich et al., 2004; El-Rich and Shirazi-Adl, 2005; Shirazi-Adl et al., 2002 and 2005). An advantage of this approach is in prescribing the *in vivo* kinematics data that constrain the spinal deformation under external loading and muscle exertions. Besides each prescribed kinematics on the spine provides an additional linear equilibrium equation between unknown muscle forces and external loads; thus decreasing the degree of redundancy of the system. If the number equilibrium equations at a particular spinal level reaches that of unknown muscle forces, the problem is solved deterministically. Such approach not only satisfies the equilibrium equations in all directions along the entire length of the spine but yields spinal postures in full accordance with external/gravity loads, muscle forces, and passive tissues with nonlinear properties. The stability margin of the spine under muscle forces, kinematics,

and gravity/external loads considered can subsequently be determined under deformed configuration.

This method has been employed to investigate muscle activities, spinal loads, and system stability in upright standing postures without load in hands or with a load of 380 N carried either in front or on sides (El-Rich et al.; 2004 and 2005). Predicted muscle activities were in satisfactory qualitative agreement with measured EMG activities. Intra-discal pressure in the L4-L5 disc, with or without load in hands, was predicted to be in excellent agreement with *in vivo* data measured under similar tasks. Large compression forces of approximately 2000 N were computed in lower lumbar levels when 380 N was held in front. Prescribed coactivity of abdominal muscles markedly increased internal loads and improved system stability. Large critical q values of about 75 was predicted in neutral upright standing posture which decreased to about 20 when carrying 380 N load in hands on sides or in front. Coactivity of only 3.5% in all abdominal muscles (rectus and obliques) further decreased critical q to about 4. This confirms previous finding of Cholewicki and McGill (1996) that during heavy efforts, muscle stiffness is ample to provide necessary stability to the lumbar spine.

The studies of El-Rich et al. (2004 and 2005) was nevertheless limited to investigation of static lifting tasks in upright standing postures while neglecting the effect of interaction between intra-abdominal pressure and abdominal coactivities on spinal loads and stability. They, however, studied the effect of lumbar posture (lordotic vs. kyphotic) on predictions and found that the lordotic posture is a safer one in terms of imposing smaller loads on the spine. Moreover, in agreement with Granata and Orishimo (2001), they found that the spinal stability substantially deteriorates as the height of the load in hands increases (El-Rich et al., 2005).

CHAPTER 2

OBJECTIVES AND THESIS ORGANIZATION

2.1 Application of the Kinematics-Based Approach for Lifting Tasks Involving Forward Trunk Flexion

One of the principal objectives of this thesis has been to develop and apply the Kinematics-based approach to compute muscle forces and spinal loads at different spinal levels in static lifting activities involving forward flexion of trunk. The system stability margin is also determined using nonlinear analysis, linear buckling, and perturbation analyses at deformed configurations assuming various muscle stiffness values. Moreover, as a part of this investigation to obtain input data for the model and to validate model predictions, existing measured trunk kinematics by skin markers and selected extensor/flexor muscle EMG activities by surface electrodes in normal subjects under isometric lifting postures are analyzed as a part of this investigation. This study has the specific objectives:

1- to determine the role of external load, trunk-pelvic flexion angles on muscle forces, internal ligamentous loads, and system stability which are crucial in understanding the risk of back injuries in lifting tasks;

2- to investigate the relative load-bearing role of passive (ligamentous spine and muscles) and active components in supporting the net trunk moment in flexion postures; and

3- to quantify the effect of changes in passive ligamentous properties which may occur due for example to injury to the spine on load partitioning and spinal stability in lifting tasks.

2.2 Addressing the Controversial Issue of Lifting Techniques Using the Kinematics-Based Approach

The second objective of the study was set to investigate the relative effect of changes in the lumbar posture (lordotic vs. kyphotic) on the load partitioning and stability of the human trunk in static lifting tasks by using the Kinematics-based approach. Again, in the experimental *in vivo* part of the investigation, kinematics of the spine (required as input data into the model) and EMG activity of major trunk muscles (required to qualitatively validate model predictions) were collected under same postures studied in the model study, i.e., static lifting during forward trunk flexion with three different lumbar postures of kyphotic, lordotic, and free style. Results of this study serve to recommend one of these lumbar postures as the safest one in terms reducing back loads or improving spinal stability.

2.3 Effect of Optimization Cost Function Used in the Kinematics-Based Approach on Predictions

In the Kinematics-Based approach, the measured kinematics data are prescribed into the finite element model of the spine to generate additional equations at each spinal level in order to alleviate the kinetic redundancy; each displacement component introduces an equilibrium equation in the form of $\Sigma r \times f = M$ where r , f , and M are lever arm of muscles with respect to the vertebra to which they are attached, unknown total forces in muscles attached to the level under consideration, and reaction moment at the vertebra under prescribed rotation, respectively. If the number of prescribed kinematics at a vertebral level reaches that of unknown muscle forces attached to that level, the problem can be solved deterministically, otherwise an optimization approach should also be employed. Since only sagittal rotations have been measured and prescribed in the current version of the Kinematics-based approach, the optimization criteria of sum of cubed muscle stresses were also employed to solve the existing redundancies at different levels.

Effect of different optimization criteria on estimated muscle forces and joint loads have been studied in models that consider equilibrium at only one cross-section

(Hughes et al., 1994; Hughes, 1995; Parnianpour et al., 1997; Herzog and Leonard, 1991). For instance, Parnianpour et al. (1997) investigated the effect of six different cost functions on spinal loads by using six different anatomical models of the spine under different loading conditions. Although in their study the effect of cost function on estimated compression and anterior-posterior shear forces was found statistically significant, but the fidelity of the anatomical models played a more dominant role than the choice of the cost function. Similar results were found by Hughes (1995) whose findings demonstrated as high a difference as 3600 N for predicted axial compression at the L2-L3 level between models based on four different cost functions.

Using a linear finite element model that considered equilibrium at all levels, unacceptable segmental displacements/forces were found with the cost function of sum of muscle stresses cubed which led authors to suggest that the trunk muscle activation strategy was likely controlled by a multi-criteria cost function and not a single one (Stokes and Gardner-Morse, 2001). In these formulations, both intervertebral displacements and muscle forces were treated as unknown so that when minimizing one set there existed no guarantee that plausible results could be predicted for another set.

The influence of various optimization criteria on spinal loads and stability has not been addressed in biomechanical models that consider equilibrium along the entire length of the spine such as the Kinematics-based approach in which the muscle forces are evaluated separately at each individual vertebral level in an iterative method using a nonlinear finite element model. This work, hence, aims to investigate:

1- to what extent the choice of optimization cost function used in the Kinematics-based biomechanical model could influence predicted trunk muscle forces, spinal loads, and sagittal spinal stability; and

2- which cost function(s) (total of eight) predicts muscle forces in qualitative agreement with the EMG activity of trunk muscles measured *in vivo* under the same posture and loading considered in the model.

Since measured vertebral rotations are prescribed into the current kinematics-based model and only muscle forces remain as unknowns of the problem, it is hypothesized that a single cost function is adequate enough to predict plausible muscle forces in qualitative agreement with measured EMG data.

2.4 Addressing the Controversial role of Intra-Abdominal Pressure (IAP) in Unloading and Stabilizing the Spine during Lifting Tasks

An investigation was set to delineate controversial role of IAP on muscle forces, spinal loads as well as on spinal stability during regular static lifting activities involving upright standing and forward flexed postures. The Kinematics-based approach combined with a nonlinear finite element model of spinal active-passive components was applied to estimate trunk muscle forces, spinal loads, and stability. Two hypotheses were examined:

- 1- the beneficial role of IAP in unloading the spine would depend on IAP magnitude and relative coactivity of abdominal muscles.
- 2- an increase in IAP with or without concurrent abdominal co-activation would stabilize the spine.

The study has also the specific objective of determination of the extent of abdominal coactivity beyond which the beneficial unloading and stabilizing effects of IAP disappear.

2.5 A Novel Approach for Proper Simulation of Wrapping of Trunk Thoracic Extensor Muscles around Vertebra

Another objective of the current work was to introduce a novel approach for proper simulation of wrapping phenomenon of global extensor muscles around vertebrae in the Kinematics-based approach while taking account for the contact forces between muscles and the spine. It is also to investigate the likely effects of the wrapping of global extensor muscles and of subsequent reduction in their lever arm on computed muscle forces, internal spinal loads and system stability in lifting tasks. The effect of lumbar posture on spinal loading and stability was re-evaluated using this new modified approach.

2.6 The Importance of Satisfaction of Equilibrium Conditions At All Spinal Levels and Not Only At One Single Level of the Spine on Model Predictions

The last objective of this study was set to quantify the extent to which the muscle/spinal loads and equilibrium requirements at different levels are influenced by results of wide-spread single-level free body diagram (SLFBD) model studies. In order to do this while considering two isometric symmetric lifting tasks, the results of our Kinematics-based model that satisfies kinematics and equilibrium requirements at all levels and directions are compared with those based on SLFBD models. Since the net external moments, lever arm of muscles, and number of muscles that cross each level change from a level to another, it is hypothesized that SLFBD models grossly violate equilibrium at remaining levels and that the estimated muscle forces and spinal loads would alter depending on the level considered and the posture (task) simulated.

2.7 Thesis Organization

Including the previous and current chapters, this thesis consists of nine chapters six of which (chapters 3 through 8) address each of the abovementioned studies (2.1-2.6) in the format of an article having its own abstract, introduction, method, results, discussion, and list of references (see section 2.8). In the last chapter a full discussion on the methodological issues, findings of this investigation, and implications is presented. Finally, two annexes are given at the end of thesis one of which deals with functional

anatomy of the spine and associated musculature while the second one is a brief explanation on the method used to analytically solve the optimization algorithm. Readers who are not acquainted with anatomical function of the spine are inspired to read Appendix A.

2.8 List of publications

The following articles have been submitted for publications during the course of my PhD five of which are already published:

1. **Arjmand N**, Shirazi-Adl A. Model and *in vivo* studies on human trunk load partitioning and stability in isometric forward flexions. *Journal of Biomechanics* 2006; 39(3):510-521.
2. **Arjmand N**, Shirazi-Adl A. Biomechanics of lumbar posture in static lifting tasks. *Spine* 2005; 30(23):2637-48.
3. **Arjmand N**, Shirazi-Adl A. Sensitivity of kinematics-based model predictions to optimization criteria in static lifting tasks. *Medical Engineering and Physics* 2006; 28 (6): 504-514.
4. **Arjmand N**, Shirazi-Adl A. Role of intra-abdominal pressure in unloading and stabilizing the spine during static lifting tasks. *European Spine Journal* 2006; 15 (8): 1265-75.
5. **Arjmand N**, Shirazi-Adl A., Bazrgari B. Wrapping of Trunk Thoracic Extensor Muscles Influences Muscle Forces and Spinal Loads in Lifting Tasks. *Clinical Biomechanics* 2006; 21(7): 668-675.
6. **Arjmand N**, Shirazi-Adl A., Parnianpour M. Trunk biomechanical models based on equilibrium at a single-level violate equilibrium at other levels. *Ergonomics* (submitted March 2006).

CHAPTER 3

MODEL AND *IN VIVO* STUDIES ON HUMAN TRUNK LOAD PARTITIONING AND STABILITY IN ISOMETRIC FORWARD FLEXIONS

N. Arjmand and A. Shirazi-Adl

Department of Mechanical Engineering, École Polytechnique
Montréal, Québec, Canada

Article published in ***Journal of Biomechanics*** 2006; 39 (3): 510-521

Keywords: Muscle Force; Finite Element Method; Kinematics; Stability; Flexion; EMG

3.1 ABSTRACT

To resolve the trunk redundancy to determine muscle forces, spinal loads, and stability margin in isometric forward flexion tasks, a combined *in vivo*-numerical model studies was undertaken. It was hypothesized that the passive resistance of both the ligamentous spine and the trunk musculature plays a crucial role in equilibrium and stability of the system. Fifteen healthy males performed free isometric trunk flexions of $\sim 40^\circ$ and $\sim 65^\circ \pm$ loads in hands while kinematics by skin markers and EMG activity of trunk muscles by surface electrodes were measured. A novel kinematics-based approach along with a nonlinear finite element model were iteratively used to calculate muscle forces and internal loads under prescribed measured postures and loads considered *in vivo*. Stability margin was investigated using nonlinear, linear buckling, and perturbation analyses under various postures, loads and alterations in ligamentous stiffness. Flexion postures significantly increased activity in extensor muscles when compared with standing postures while no significant change was detected in between flexed postures. Compression at the L5-S1 substantially increased from 570 and 771 N in upright posture, respectively for ± 180 N, to 1912 and 3308 N at $\sim 40^\circ$ flexion, and furthermore to 2332 and 3850 N at $\sim 65^\circ$ flexion. Passive ligamentous/muscle components resisted up to 77% of the net moment. In flexion postures, the spinal stability substantially improved due both to greater passive stiffness and extensor muscle activities so that, under 180 N, no muscle stiffness was required to maintain stability. The co-activity of abdominal muscles and the muscle stiffness were of lesser concern to maintain stability in forward flexion tasks as compared with upright tasks. An injury to the passive system, on one hand, required a substantial compensatory increase in active muscle forces which further increased passive loads and, hence, the risk of injury and fatigue. On the other hand, it deteriorated the system stability which in turn could require greater additional muscle activation. This chain of events would place the entire trunk active-passive system at higher risks of injury, fatigue and instability.

3.2 INTRODUCTION

Knowledge of load distribution among passive and active components of the human trunk during various occupational and athletic activities is essential both to assess risk of injury and to improve effective prevention, treatment, and rehabilitation of spinal disorders. Due to the difficulty and invasiveness of direct measurements, indirect estimation of muscle forces and internal loads has been attempted (Nachemson, 1981; Rohlmann et al., 2001, 2002; Wilke et al., 1999, 2001). Despite previous experimental and biomechanical model studies, satisfactory determination of active/passive loads and spinal stability in different tasks remains yet to be achieved. Biomechanical models have become indispensable tools in partitioning estimated net moments among various components of the human trunk. For this purpose, reduction methods, EMG-assisted models, optimization approaches or a combination thereof have been used (e.g., Dolan and Adams, 1993; Gagnon et al., 2001; Granata and Marras, 1995; Hughes et al., 1994). These biomechanical models share often major deficiencies; the balance of net external moments is considered only at one cross-section rather than along the entire length of the spine. Moreover, the evaluated muscle forces, once applied on the system along with external loads, may not necessarily generate the same spinal kinematics under which they were initially calculated. Naturally, accuracy in calculation of the stability margin of the active-passive system is also influenced by simplifying assumptions made in the model.

To overcome the foregoing shortcomings, linear finite element models along with optimization algorithms have been developed and used to evaluate muscle recruitment, internal loads, and stability margin (Dietrich et al., 1991; Gardner-Morse et al., 1995; Gardner-Morse and Stokes, 1998; Stokes and Gardner-Morse, 1995, 2001). A simplified geometrical model of the spine with rotational degrees-of-freedom and nonlinear stiffness properties along with EMG-assisted optimization approach was used to evaluate muscle forces and stability margin in various tasks (Cholewicki and McGill, 1996). The translational degrees-of-freedom at various joints and, hence, associated

shear/axial equilibrium equations were totally neglected in this latter model which would adversely influence predictions on muscle forces and system stability. Direct *in vivo* measurements of loads in internal fixators and of intradiscal pressure have also been used to estimate trunk muscle forces in experimental (Wilke et al., 2003) and finite element model studies (Calisse et al., 1999). Proper considerations of the nonlinear material properties of the thoracolumbar motion segments in different directions with load- and direction-dependent properties, of realistic distribution of gravity/external loads, and of verification of the stability using nonlinear analysis are important to obtain reliable results. Adequate nonlinear representation of passive spine particularly in presence of large compression forces and flexion rotations expected in lifting tasks (Patwardhan et al., 2003; Shirazi-Adl, 2004; Stokes and Gardner-Morse, 2003) is important not only in proper partitioning of the net moments among passive-active components but also in the stability analysis of the system.

We have recently developed and validated a novel iterative kinematics-based approach in which the a-priori measured kinematics of the spine are exploited in a nonlinear finite element model to evaluate muscle and internal loads in neutral standing postures resulting in a synergistic solution of the active-passive system (El-Rich et al., 2003; Kiefer et al., 1998; Shirazi-Adl et al., 2002, 2004). This iterative approach not only satisfies the equilibrium equations in all directions along the entire length of the spine but yields spinal postures in full accordance with external/gravity loads, muscle forces, and passive tissues with nonlinear properties. The stability margin of the spine under muscle forces, kinematics, and gravity/external loads considered has subsequently been determined.

In this study, the foregoing approach is applied to compute muscle forces and spinal internal loads at different levels at two isometric forward flexions of $\sim 40^\circ$ and $\sim 65^\circ$ under gravity ± 180 N held in hands. The system stability margin is also determined using nonlinear analysis as the gold standard as well as linear buckling and perturbation

analyses at deformed configurations assuming various muscle stiffness values. Moreover, as a part of this investigation to obtain input data for the model and to validate model predictions, trunk kinematics by skin markers and selected extensor/flexor muscle EMG activities by surface electrodes are measured in normal subjects under foregoing postures and loads. This study has the specific objectives: 1- to determine the role of external load and trunk flexion angles on muscle activations, internal ligamentous loads, and system stability which are crucial in understanding the risk of back injuries in lifting tasks; 2- to quantify the stability margin of the trunk in forward flexion tasks due to alterations in passive stiffness of the spine; and 3- to investigate the relative load-bearing role of passive (ligamentous spine and muscles) and active components in supporting the net trunk moment in flexion postures. It is hypothesized that the passive resistance of both the ligamentous spine and the trunk musculature plays a crucial role in equilibrium and stability of the system and that the extent of this role depends on the load carried, trunk flexion angle, and injury to ligamentous tissue.

3.3 METHODS

In Vivo Measurements: Fifteen healthy male with no recent back complications volunteered for the study after signing an informed consent form. Their mean age, body height and mass were 30 ± 6 years, 177 ± 7 cm, and 74 ± 11 kg. While bending slightly forward, infrared light emitting markers, LED, were placed on tip of the spinous processes at T1, T5, T10, T12, L1, L3, L5, and S1 levels. Three extra LED markers were placed on the ilium (left/right iliac crests) and posterior-superior iliac spine for evaluation of pelvic rotation and one on the bar to detect the position of weights in hands. A three-camera Optotrak system (NDI International, Waterloo/Canada) was used to collect 3D coordinates of LED markers. To record EMG signals, five pairs of surface electrodes were positioned bilaterally over the following trunk muscles (McGill, 1991; O'Sullivan et al., 2002): longissimus dorsi (~ 3 cm lateral to midline at the L1), iliocostalis (~ 6 cm lateral to midline at the L1), multifidus (~ 2 cm lateral to midline at

the L5), external obliques (~10 cm lateral to midline above umbilicus and aligned with muscle fibers), and rectus abdominis (~3 cm lateral to midline above the umbilicus). The raw EMG signals were collected at 1500 Hz, amplified, band-pass filtered at 10-400 Hz by a 2nd order Butterworth filter, rectified and RMS was calculated over 4s trial duration and averaged for both sides. For normalization, EMG data at maximum voluntary contraction (MVC) was collected in standing (in cardinal planes while loaded via a strapped harness (Sparto and Parnianpour, 1998)), prone, and supine positions.

In standing posture, subjects were handed load of 0, 90 N or 180 N symmetrically via dumbbells on sides. Subsequently, starting from the upright standing position with straight knees (\pm 90 N or 180 N in hands), subjects were asked to flex the trunk by \sim 40° and then 65° in the sagittal plane. During tests, subjects were instructed to keep arms extended in the gravity direction. Total trunk and pelvic rotation relative to the upright standing posture were computed (Table 3.1). EMG data were analyzed with two-way ANOVA with repeated measures on two factors (posture at 3 levels and load magnitude at 3 levels) using Tukey's post hoc multiple comparisons with $p<0.05$ as significance level (Statistica, StatSoft, Tulsa, OK).

Thoracolumbar Finite Element Model: A sagittally-symmetric T1-S1 beam-rigid body model (Kiefer et al., 1998; Pop, 2001; Shirazi-Adl et al., 2002, 2004) comprising of 6 deformable beams to represent T12-S1 discs and 7 rigid elements to represent T1-T12 (as a single body) and lumbosacral vertebrae (L1 to S1) was used (Fig. 3.1). The beams modeled the overall nonlinear stiffness of T12-S1 motion segments (i.e., vertebrae, disc, facets and ligaments) at different directions and levels. The nonlinear load-displacement response under single and combined axial/shear forces and sagittal/lateral/axial moments along with the flexion versus extension differences were represented in this model based on numerical and measured results of previous single- and multi-motion segment studies (Oxland et al., 1992; Pop, 2001; Shirazi-Adl et al., 2002; Yamamoto et al., 1989). Based on our recent studies (Shirazi-Adl, 2004), the

stiffness of motion segments in sagittal rotation was further modified to account for the stiffening effect observed in presence of moderate to large compression loads (Patwardhan et al., 2003; Stokes and Gardner-Morse, 2003). The insertion points of beams to rigid vertebrae were shifted posteriorly from the end-plate centers by 4 mm to account for the posterior movement in the disc axis of rotation observed under loads in different directions (Shirazi-Adl et al., 1986a, b). In all cases, gravity load of 387 N was distributed at different levels (Pearsall, 1994; Takashima et al., 1979) (Fig. 3.1). To simulate load in hands, 180 N was also considered in some cases.

Prescribed Postures: Mean measured trunk and pelvic rotations were prescribed on the T12 and S1 levels, respectively. As for the individual lumbar vertebrae, the total lumbar rotation was divided in accordance with proportions reported in earlier investigations (Dvorak et al., 1991; Pearcy et al., 1984; Plamondon et al., 1988; Potvin et al., 1991; Shirazi-Adl and Parnianpour, 1999; Yamamoto et al., 1989) and prescribed at individual segments (Table 3.1).

Muscle Model and Muscle Force Calculation: A sagittally-symmetric muscle architecture with 46 local (attached to lumbar vertebrae) and 10 global (attached to thoracic cage) muscles was used (Bogduk et al., 1992; Daggfeldt and Thorstensson, 2003; Stokes and Gardner-Morse, 1999) (Fig. 3.2 and Table 3.2). For the global muscles, since the entire T1-T12 was taken as a rigid body, each muscle was represented by a single fascicle inserted into the center of its attachment area. To evaluate muscle forces a novel kinematics-based algorithm (Fig. 3.3) was employed to solve for the redundant active-passive system under prescribed measured kinematics and external loads (El-Rich et al., 2003; Shirazi-Adl et al., 2002, 2004). In this manner, calculated muscle forces at each instance of loading were compatible with the prescribed kinematics (i.e., posture) and external loading while accounting for the nonlinear realistic stiffness of the passive system. This approach exploits kinematics data to generate additional equations at each level in order to alleviate the kinetic redundancy of

the problem. If, insufficient number of prescribed displacements is available at a level, which is the case in this study, then an optimization approach should also be employed. In the current study, the cost function of minimum sum of cubed muscle stresses was considered in the optimization with inequality equations of muscle stresses remaining positive but smaller than 0.6 MPa (Gagnon et al., 2001). The finite element program ABAQUS (Hibbit, Karlsson & Sorensen, Inc., Pawtucket, RI, version 6.3) was used to carry out nonlinear structural analyses while the optimization procedure was analytically solved using an in-house program based on Lagrange Multipliers Method (Raikova and Prilutsky, 2002). The total computed muscle force in each muscle was partitioned into active and passive components with the latter force evaluated based on a length-tension relationship (Davis et al., 2003).

Stability Analyses: The external load, when present, was applied at its measured height due to its effect on stability margin (Granata and Orishimo, 2001). In each simulation case, after the muscle forces were calculated, the model was modified with uniaxial elements to represent muscles between their insertion points. Nonlinear analyses were repeated under loads but with no prescribed segmental rotations (with the exception of the pelvic tilt). Stiffness of each uniaxial element, k , was assigned using the linear stiffness-force relation $k=qF/l$ (Bergmark, 1989; Crisco and Panjabi, 1991) in which the muscle stiffness was proportional to the muscle force, F , and inversely proportional to its current length, l , with the q as a non-dimensional muscle stiffness coefficient taken the same for all muscles. Nonlinear analyses were performed for different q values thus identifying the minimum (critical) q value above which a convergent solution in a force-controlled loading environment existed. In addition to nonlinear analyses, linear buckling and perturbation analyses at loaded, deformed, configurations were also carried out to estimate stability margin as a function of q .

3.4 RESULTS

In *in vivo* measurements, EMG activity of extensor muscles in forward flexions of $\sim 40^\circ$ and $\sim 65^\circ$ increased significantly ($p < 0.009$) when compared to those in standing posture under identical load in hands (Fig. 3.4A). Moreover, for the flexion postures, a significant increase ($p < 0.04$) in EMG activity of back muscles was observed at 180 N load when compared with 0 N. Bending forward from $\sim 40^\circ$ to $\sim 65^\circ$ under the same load, however, had no significant effect on EMG activities. In standing posture, no significant changes in EMG activity of back muscles were detected under loads. Both abdominal muscles (EO and RA), though relatively silent during the entire tests, showed a decrease in EMG activity during forward flexion tasks with identical load in hands, being significant only at the EO in 180 N ($p < 0.004$) (Fig. 3.4B).

Under prescribed segmental sagittal rotations based on the mean measurements (Table 3.1 and Fig. 3.5), both external load of 180 N (in flexion postures only) and flexion postures (when compared to standing posture only) substantially increased muscle forces as well as internal loads in ligamentous spine at all levels (Fig. 3.6 and Table 3.3). In the nonlinear stability analysis phase (Fig. 3.3), predicted kinematics, muscle forces, and internal loads remained identical to those computed in the earlier phase regardless of the stiffness coefficient (q) assigned to the muscle elements. These nonlinear and subsequent linear buckling and perturbation analyses at deformed configurations showed that small muscle stiffness coefficients, q , was needed to maintain stability of the spine in flexed postures without load in hands (Fig. 3.7A). On the contrary, no muscle stiffness was at all needed in the flexed postures while carrying 180 N. In this case, the stability of the spine was mainly provided by the passive stiffness of motion segments, an observation which was confirmed by additional analyses when altering the flexion stiffness of passive spine by up to $\pm 30\%$ (Fig. 3.7B).

3.5 DISCUSSION

The objectives of this study were to determine trunk muscle forces, spinal loads, and stability margin for different muscle and ligamentous stiffness values during

isometric forward flexion tasks \pm external loads. Such postures and loads are common in many activities such as athletic and manual material handling tasks and have been recognized as a risk factor for back injuries (Hoogendoorn et al., 2000). In this study, the application of the Kinematics-based approach to solve the redundant trunk system and the validation of its predictions required parallel *in vivo* measurements on normal subjects under same postures and loads.

3.5.1 Methodological Issues

The assumption of rigid body for the T1-T12 segments was confirmed by measuring nearly equal rotations from lines attaching T12 to T5 and T12 to T1, e.g., respectively $41.4 \pm 7.5^\circ$ and $41.0 \pm 7.3^\circ$ for flexion of $\sim 40^\circ$ without load in hands, in agreement with others (Nussbaum and Chaffin, 1996). The geometry of muscle fascicles was modeled by straight lines with no initial strain before applying gravity load. The transverse abdominus, latissimus dorsi, lumbodorsal fascia, intersegmental and multisegmental muscles were neglected. The transverse abdominus has been recognized to unload the spine indirectly by increasing intra-abdominal pressure (Daggfeldt and Thorstensson, 2003) as well as to play a role in controlling the spinal stability (Hodges, 1999; Hodges and Richardson, 1996; Pietrek et al., 2000). Latissimus dorsi has been known to produce trunk extensor moment via the lumbodorsal fascia, a contribution suggested not sizable during lifting tasks (Bogduk et al., 1998; McGill and Norman, 1988). The intersegmental and multisegmental muscles have been reported not to play important stabilizing role (Crisco and Panjabi, 1991). For qualitative validation of predicted muscle forces, the maximum allowable muscle stress was assumed for all muscles to be 0.6 MPa. The normalized passive tension-length relationship was also assumed to be the same for all muscles despite the fact that the specific architecture of each muscle could influence this relationship (Woittiez et al., 1984). Moreover, the effect of muscle activation level on this passive relationship (Lee and Herzog, 2002; Rassier et al., 1999, 2003) was neglected. For the stability analyses, the muscle stiffness coefficient, q , was chosen the same for all muscles while a linear stiffness-force relation, rather than a

nonlinear one (Cholewicki and McGill, 1995; Shadmehr and Arbib, 1992), was taken. The controversial mechanical role of the intra-abdominal pressure (IAP) in unloading the spine and generating a net extensor moment as well as its likely stabilizing role during flexion tasks was not considered (Arjmand et al., 2001; Cholewicki et al., 2002; Cresswell et al., 1992; Cresswell, 1993; Cresswell and Thorstensson, 1994; Daggfeldt and Thorstensson, 1997, 2003). The neglected co-activation, although measured to be small, could serve to increase the stability of the lumbar spine especially in standing postures (Cholewicki et al., 1997, 1999a, b; El-Rich et al., 2004).

Calculation of the trunk and pelvic rotations from skin markers, despite non-invasiveness and ease of measurements, is recognized to have important errors involving identification of anatomical landmarks, skin movement relative to the underlying bony landmarks, and deformability of vertebrae themselves (Lee et al., 1995; Shirazi-Adl, 1994; Zhang and Xiong, 2003). Due to inherent errors, in this work, the measurements were used only to evaluate pelvic tilt and trunk T1-T12 rotations with the intervening lumbar segmental rotations evaluated based on relative values reported in the literature. Study of the effect of alterations in lumbar rotations on results (e.g., lordosis versus kyphosis) is the subject of future works. Moreover, the measurement of the maximum EMG activity (MVC) in each muscle required for normalization depends amongst others on the task design, subject and electrode location (O'Sullivan et al., 2002; McGill, 1991). Since the electrodes for the multifidus at the L5 level are more likely to yield activity of adjacent longissimus (Stokes et al., 2003), comparisons between predictions and measurements were avoided for the Multifidus.

The kinetic redundancy of the trunk system can be deterministically resolved if the number of prescribed kinematics data at a level reaches the number of muscles inserted into the same level. In the current study, since only sagittal rotation of vertebrae was prescribed, an optimization approach based on minimum sum of cubed muscle stresses was also used. Although, this cost function was recognized to agree better with the EMG

data (Hughes et al., 1994; Van Dieen, 1997), it has been associated with unrealistic joint displacements (Stokes and Gardner-Morse, 2001), an issue that is irrelevant to our work in which *in vivo* kinematics were prescribed. Moreover, the convergence of the nonlinear optimization solution on a global minimum was assured by solving the problem analytically using Lagrange Multiplier Method.

3.5.2 Comparisons and Implications

Compared to neutral standing postures, forward flexions of $\sim 40^\circ$ and $\sim 65^\circ$ substantially increased extensor muscle forces and internal loads (Table 3.3 and Fig. 3.6). These loads further increased in presence of 180 N in hands. The axial compression at the L4/L5 level significantly increased by 251% at $\sim 40^\circ$ flexion and by 337% at $\sim 65^\circ$ flexion compared to the neutral standing with no external load. When holding 180 N in hands, these values further increased to 338% and 420% of those in neutral standing with 180 N, respectively (Table 3.3). In standing posture, however, the magnitude of load in hands had no significant effect on EMG activity of global extensor muscles (Fig. 3.4A). The maximum shear and compression forces in the tasks considered in this study, occurring at the lowermost L5/S1 level (Table 3.3), remained smaller than segmental tolerant limits (McGill, 1997; NIOSH, 1981). Accounting for the axial compression-disc pressure relations in lumbar specimens (Shirazi-Adl and Drouin, 1988), the current predicted compression loads at the L4-L5 level agree well with *in vivo* intradiscal pressure measurements reported under similar load magnitudes and postures (Wilke et al., 1999, 2001) (Fig. 3.8).

The computed total force in erector spinae, as the sum of ICpt and LGpt muscle forces, was 700 N and 950 N for flexion angles of $\sim 40^\circ$ and $\sim 65^\circ$ without external load and 1328 N and 1545 N in presence of 180 N in hands, respectively. The predicted active component of global muscle forces when normalized to their maximum values (i.e., $0.6 \times \text{PCSA}$) was in satisfactory agreement with normalized EMG activities under both flexion postures \pm 180 N (Fig. 3.9). In accordance with our *in vivo* measurements,

the model predicted only a slight change in active extensor muscle forces when flexing forward from $\sim 40^\circ$ to $\sim 65^\circ$ under identical load in hands while, in contrast, a large increase was noted under 180 N at the same posture (Fig. 3.9). These are due to the greater contribution of passive components under larger flexion angles (under same loads) and of the active components under larger net moments (at the same posture) (Fig. 3.10). The model confirmed the hypothesis on the important contribution of passive components to resist net moments under flexion tasks especially when no load was carried in hands (Fig. 3.10). This passive contribution likely becomes increasingly more important as trunk flexion further increases towards the full trunk flexion which is in accordance with the flexion-relaxation phenomenon (McGill and Kippers, 1994; Nussbaum and Chaffin, 1996). The ligamentous and muscle passive resistant moments were, respectively, ~ 22 Nm and 27 Nm at $\sim 40^\circ$ and ~ 35 Nm and 42 Nm at $\sim 65^\circ$ for cases without load in hands. These values are in very good agreement with reported maximum resistance of lumbar motion segments in flexion (Adams and Dolan, 1991; Miller et al., 1986) and estimated total passive extensor moment that increases with trunk flexion reaching ~ 100 Nm at full flexion during isometric exertions (Dolan et al., 1994; Nussbaum and Chaffin, 1996).

Abdominal muscles were measured to have rather small EMG activity in standing postures that further diminished with trunk flexion (statistically significant for EO under 180 N). Similarly, significant decrease in antagonistic muscle co-activations during isometric submaximal trunk flexion has been recorded (Tan et al., 1993). It has been suggested that the co-activity of abdominal muscles, despite a substantial increase in compression on spine, is essential to maintain stability in neutral standing postures (El-Rich et al., 2004; Granata and Orishimo, 2001; Granata and Wilson, 2001). The spine appears, however, to be adequately stabilized in forward flexion tasks by greater ligamentous stiffness and muscle activation with lesser need for muscle stiffness (Figs. 3.7A, B) or muscle co-activity (Fig. 3.4B).

3.5.3 Stability

The issue of structural stability of the human spine is recognized as an important consideration in avoiding injury and functioning safely (Bergmark, 1989; Cholewicki et al., 1997, 2000; Cholewicki and McGill SM, 1996; Cholewicki and VanVliet, 2002; Crisco III and Panjabi, 1991; El-Rich et al., 2003; Gardner-Morse et al., 1995; Gardner-Morse and Stokes, 1998; Granata and Orishimo, 2001; Kiefer et al., 1998). The nonlinear analysis under applied forces is the gold standard in evaluating the system stability. Other complementary approaches, as used in the present study, would be the linear stability and perturbation analyses on the deformed configurations of the structure. In these latter methods, the error involved in estimation of buckling loads is expected to diminish as the applied loads and deformed configurations approach the critical state. By varying the muscle stiffness coefficient, q , the critical value was found in the nonlinear analyses below which the system became unstable; i.e., no convergent solution existed under applied forces. These q values were further utilized in linear buckling and perturbation analyses at deformed configurations in order to estimate system stability margins.

In contrast to neutral standing postures, the spine appeared to be rather stable in forward flexion tasks due primarily to the greater stiffness of both active and passive sub-systems that significantly increased with flexion angles and compression forces (Fig. 3.7A), an observation in agreement with previous works (Cholewicki and McGill, 1996). The lowest q value required to maintain stability of the spine under $\sim 40^\circ$ and $\sim 65^\circ$ flexions with no load in hands was ~ 10 and 6 , respectively (Fig. 3.7A). In contrast, no muscle stiffness was at all required in flexed postures when carrying 180 N (Fig. 3.7A). In these cases, the system stability was primarily provided by passive stiffness of motion segments that nonlinearly increased with axial compression and flexion angle.

To further investigate the relative importance of motion segment stiffness on the spinal stability in flexion tasks, the nonlinear flexural stiffness of all passive segments

was altered by either $\pm 10\%$ or $\pm 30\%$ and analyses were repeated at $\sim 40^\circ$ flexion under 180 N. The system stability further increased with stiffer passive tissue whereas it decreased as the passive stiffness diminished (Fig. 3.7B). Interestingly, these trends in the system stability occurred despite opposite compensatory changes in muscle activation. The increase in stability margin despite smaller muscle activation and its deterioration despite larger muscle activation reiterates our hypothesis on the important role of passive stiffness in the system stability. Muscle forces increased as the passive stiffness diminished by 10 and 30% resulting in larger compression on L4-L5 disc by 4.9% and 14.4%, respectively. In contrast, larger passive stiffness decreased muscle forces and axial compression on the L4-L5 disc by 7.6% and 18% respectively. Such alterations in passive stiffness are expected due to spinal injuries and degenerations. These results confirm our hypothesis on the need for compensatory muscle activations in order to maintain equilibrium and stability in presence of injuries, degenerations, or alterations in ligamentous spine which in turn could increase the risk of fatigue and injury in active/passive tissues. It is to be noted that an increase in muscle activation, even in cases with no muscle stiffness $q=0$, would improve the system stability via its contribution through the stress stiffness matrix.

In conclusion, a novel kinematics-based finite element approach was used that simultaneously satisfied the kinematics, equilibrium and stability requirements at all levels and directions and not just the equilibrium at one level only. The proposed model allowed for the incorporation of realistic nonlinear load- and direction-dependent properties of spinal motion segments. The results confirmed our hypothesis that the passive resistance of both the ligamentous spine and the trunk musculature played a very important role in the system equilibrium and stability as the trunk flexion increased. The co-activity of abdominal muscles as well as muscle stiffness could, hence, be of lesser concern to maintain stability in such forward flexion tasks as compared with upright tasks. Moreover, any injury to the passive system, on one hand, requires a substantial compensatory increase in active muscle forces which would further increase passive

loads and, hence, the risk of injury and fatigue. It would, on the other hand, deteriorate the system stability which in turn may require greater additional muscle activation. Altogether, this chain of events would place the entire trunk active-passive system at higher risk of injury, fatigue and instability.

3.6 ACKNOWLEDGEMENTS

The research is supported by a grant from the Institut de recherche en santé et en sécurité du travail du Québec (IRSST-Québec) and the Natural Sciences and Engineering Research Council of Canada (NSERC-Canada). Authors also gratefully acknowledge A. Feldman for the use of the Motor Control Laboratory at the Montreal Institute of Rehabilitation and A. Mitnitsky and M. Trottier for assistance in data collection.

3.7 REFERENCES

Adams, M.A., Dolan, P., 1991. A technique for quantifying the bending moment acting on the lumbar spine in vivo. *Journal of Biomechanics* 24 (2), 117-26.

Arjmand, N., Shirazi-Adl, A., Parnianpour, M., 2001. A finite element model study on the role of trunk muscles in generating intra-abdominal pressure. *Biomedical Engineering-Applications, Basis & Communications* 13 (4), 23-31.

Bergmark, A., 1989. Stability of the lumbar spine -A study in mechanical engineering. *Acta Orthopaedica Scandinavica Supplementum* 230, 1-54.

Bogduk, N., Macintosh, J.E., Pearcy, M.J., 1992. A universal model of the lumbar back muscles in the upright position. *Spine* 17, 897-913.

Bogduk, N., Johnson, G., Spalding, D., 1998. The morphology and biomechanics of latissimus dorsi. *Clin Biomech* 13 (6), 377-385.

Calisse, J., Rohlmann, A., Bergmann, G., 1999. Estimation of trunk muscle forces using the finite element method and in vivo loads measured by telemeterized internal spinal fixation devices. *Journal of Biomechanics* 32 (7), 727-31.

Cholewicki, J., Ivancic, P.C., Radebold, A., 2002. Can increased intra-abdominal pressure in humans be decoupled from trunk muscle co-contraction during steady state isometric exertions? *European Journal of Applied Physiology* 87 (2),127-33.

Cholewicki, J., Juluru, K., McGill, S.M., 1999a. Intra-abdominal pressure mechanism for stabilizing the lumbar spine. *Journal of Biomechanics* 32 (1), 13-7.

Cholewicki, J., Juluru, K., Radebold, A., Panjabi, M.M., McGill, S.M., 1999b. Lumbar spine stability can be augmented with an abdominal belt and/or increased intra-abdominal pressure. *European Spine Journal* 8 (5), 388-95.

Cholewicki, J., McGill, S.M., 1995. Relationship between muscle force and stiffness in the whole mammalian muscle: A simulation study. *Journal of Biomechanical Engineering* 117, 339-342.

Cholewicki, J., McGill, S.M., 1996. Mechanical stability of the in vivo lumbar spine: Implications for injury and chronic low back pain. *Clinical Biomechanics* 11, 1-15.

Cholewicki, J., Panjabi, M.M., Khachatrian, A., 1997. Stabilizing function of trunk flexor-extensor muscles around a neutral spine posture. *Spine* 22, 2207-2212.

Cholewicki, J., Simons, A.P.D., Radebold, A., 2000. Effects of external trunk loads on lumbar spine stability. *Journal of Biomechanics* 33, 1377-1385.

Cholewicki, J., VanVliet, J.J., 2002. Relative contribution of trunk muscles to the stability of the lumbar spine during isometric exertions. *Clinical Biomechanics* 17, 99-105.

Cresswell, A.G., 1993. Responses of intra-abdominal pressure and abdominal muscle activity during dynamic trunk loading in man. *European Journal of Applied Physiology* 66 (4), 315-20.

Cresswell, A.G., Grundstrom, H., Thorstensson, A., 1992. Observations on intra-abdominal pressure and patterns of abdominal intra-muscular activity in man. *Acta Physiologica Scandinavica* 144 (4), 409-18.

Cresswell, A.G., Thorstensson, A., 1994. Changes in intra-abdominal pressure, trunk muscle activation and force during isokinetic lifting and lowering. *European Journal of Applied Physiology* 68 (4), 315-21.

Crisco III, J.J., Panjabi, M.M., 1991. The intersegmental and multisegmental muscles of the lumbar spine –A biomechanical model comparing lateral stabilizing potential. *Spine* 16, 793-799.

Daggfeldt, K., Thorstensson, A., 1997. The role of intra-abdominal pressure in spinal unloading. *Journal of Biomechanics* 30 (11-12), 1149-55.

Daggfeldt, K., Thorstensson, A., 2003. The mechanics of back-extensor torque production about the lumbar spine. *Journal of Biomechanics* 36, 815-25.

Davis, J., Kaufman, K.R., Lieber, R.L., 2003. Correlation between active and passive isometric force and intramuscular pressure in the isolated rabbit tibialis anterior muscle. *Journal of Biomechanics* 36, 505-12.

Dietrich, M., Kedzior, K., Zagrajek, T., 1991. A biomechanical model of the human spinal system. *Proceedings of the Institution of Mechanical Engineers. Part H*, 205 (1), 19-26.

Dolan, P., Adams, M.A., 1993. The relationship between EMG activity and extensor moment generation in the erector spinae muscles during bending and lifting activities. *Journal of Biomechanics* 26 (4-5), 513-22.

Dolan, P., Mannion, A.F., Adams, M.A., 1994. Passive tissues help the back muscles to generate extensor moments during lifting. *Journal of Biomechanics* 27 (8), 1077-85.

Dvorak, J., Panjabi, M.M., Chang, D.G., Theiler, R., Grob, D. 1991. Functional radiographic diagnosis of the lumbar spine. Flexion-extension and lateral bending. *Spine* 16 (5), 562-71.

El-Rich, M., Shirazi-Adl, A., Arjmand, N., 2004. Muscle activity, internal loads and stability of the human spine in standing postures: combined model-in vivo studies. *Spine*, in press.

Gagnon, D., Larivière, C., Loisel, P., 2001. Comparative ability of EMG, optimisation, and hybrid modelling approaches to predict trunk muscle forces and lumbar spine loading during dynamic sagittal plane lifting. *Clinical Biomechanics* 16, 359-372.

Gardner-Morse, M., Stokes, I.A.F., Laible, J.P., 1995. Role of muscles in lumbar spine stability in maximum extension efforts. *Journal of Orthopaedic Research* 13, 802-808.

Gardner-Morse, M., Stokes, I.A.F., 1998. The effects of abdominal muscle coactivation on lumbar spine stability. *Spine* 23, 86-92.

Granata, K.P., Marras, W.S., 1995. An EMG-assisted model of trunk loading during free-synergetic lifting. *Journal of Biomechanics* 28, 1309-1317.

Granata, K.P., Orishimo, K.F., 2001. Response of trunk muscle coactivation to changes in spinal stability. *Journal of Biomechanics* 34, 1117-1123.

Granata, K.P., Sanford, A.H., 2000. Lumbar-pelvic coordination is influenced by lifting task parameters. *Spine* 25 (11), 1413-8

Granata, K.P., Wilson, S.E., 2001. Trunk posture and spinal stability. *Clinical biomechanics* 16, 650-659.

Hodges, P.W., 1999. Is there a role for transversus abdominis in lumbo-pelvic stability? *Manual Therapy* 4, 74-86

Hodges, P.W., Richardson, C.A., 1996. Inefficient muscular stabilization of the lumbar spine associated with low back pain. A motor control evaluation of transversus abdominis. *Spine* 21(22), 2640-50.

Hoogendoorn, W.E., Bongers, P.M., de Vet, H.C., Douwes, M., Koes, B.W., Miedema, M.C., Ariens, G.A., Bouter, L.M., 2000. Flexion and rotation of the trunk and lifting at work are risk factors for low back pain: results of a prospective cohort study. *Spine* 25, 3087-92.

Hughes, R.E., Chaffin, D.B., Lavender, S.A., Andersson, G.B.J., 1994. Evaluation of muscle force prediction models of the lumbar trunk using surface electromyography. *Journal of Orthopaedic Research* 12, 689-698.

Kiefer, A., Shirazi-Adl, A., Parnianpour, M., 1998. Synergy of human spine in neutral postures. *European Spine Journal* 7, 471-479.

Lee, Y.H., Chiou, W.K., Chen, W.J., Lee, M.Y., Lin, Y.H., 1995. Predictive model of intersegmental mobility of lumbar spine in the sagittal plane from skin markers. *Clinical Biomechanics* 10 (8), 413-420.

Lee, H.D., Herzog, W., 2002. Force enhancement following muscle stretch of electrically stimulated and voluntarily activated human adductor pollicis. *Journal of Physiology* 545, 321-30.

McGill, S.M., 1991. Electromyographic activity of the abdominal and low back musculature during the generation of isometric and dynamic axial trunk torque: Implications for lumbar mechanics. *Journal of Orthopaedic Research* 9, 91-103.

McGill, S.M., 1997. The biomechanics of low back injury: implications on current practice in industry and the clinic. *Journal of Biomechanics* 30, 465-75.

McGill, S.M., Kippers, V., 1994. Transfer of loads between lumbar tissues during the flexion-relaxation phenomenon. *Spine* 19, 2190-96.

McGill, S.M., Norman, R.W., 1988. Potential of lumbodorsal fascia forces to generate back extension moments during squat lifts. *Journal of Biomedical Engineering* 10 (4), 312-8.

Miller, J.A., Schultz, A.B., Warwick, D.N., Spencer, D.L., 1986. Mechanical properties of lumbar spine motion segments under large loads. *Journal of Biomechanics* 19 (1), 79-84.

Nachemson, A., 1981. Disc pressure measurements. *Spine* 6, 93-97.

National Institute for Occupational Safety and Health, 1981. A work practices guide for manual lifting. Cincinnati, Ohio, U.S. Department of Health and Human Services (NIOSH), pp. 30-43 (Technical report no. 81-122).

Nussbaum, M.A., Chaffin, D.B., 1996. Development and evaluation of a scalable and deformable geometric model of the human torso. *Clinical Biomechanics* 11 (1), 25-34.

O'Sullivan, P.B., Grahamslaw, K.M., Kendell, M., Lapenskie, S.C., Moller, N.E., Richards, K.V., 2002. The effect of different standing and sitting postures on trunk muscle activity in a pain-free population. *Spine* 27, 1238-1244.

Oxland, T., Lin, R.M., Panjabi, M., 1992. Three-dimensional mechanical properties of the thoracolumbar junction. *Journal of Orthopaedic Research* 10, 573-580.

Patwardhan, A.G., Havey, R.M., Carandang, G., Simonds, J., Voronov, L.I., Ghanayem, A.J., Meade, K.P., Gavin, T.M., Paxinos, O., 2003. Effect of compressive follower preload on the flexion-extension response of the human lumbar spine. *Journal of Orthopaedic Research* 21 (3), 540-6.

Pearcy, M., Portek, I., Shepherd, J., 1984. Three-dimensional x-ray analysis of normal movement in the lumbar spine. *Spine* 9 (3), 294-7.

Pearsall, D.J., 1994. Segmental inertial properties of the human trunk as determined from computer tomography and magnetic resonance imagery. PhD thesis. Queen's University, Kingston, Ontario.

Pietrek, M., Sheikhzadeh, A., Nordin, M., and Hagins, M., 2000. Biomechanical modeling of intra-abdominal pressure generation should include the transversus abdominis. *Journal of Biomechanics* 33, 787-790.

Plamondon, A., Gagnon, M., Maurais, G., 1988. Application of a stereoradiographic method for the study of intervertebral motion. *Spine* 13 (9), 1027-32.

Pop, D.G., 2001. Analyse non linéaire par éléments finis du système actif passif de la colonne vertébrale humaine. M.Sc.A. Dissertation. Génie mécanique, École Polytechnique, Montréal, Québec.

Potvin, J.R., McGill, S.M., Norman, R.W., 1991. Trunk muscle and lumbar ligament contributions to dynamic lifts with varying degrees of trunk flexion. *Spine* 16 (9), 1099-107.

Raikova, R.T., Prilutsky, B.I., 2002. Sensitivity of predicted muscle forces to parameters of the optimization-based human leg model revealed by analytical and numerical analyses. *Journal of Biomechanics* 34, 1243-1255.

Rassier, D.E., Herzog, W., Wakeling, J., Syme, D.A., 2003. Stretch-induced, steady-state force enhancement in single skeletal muscle fibers exceeds the isometric force at optimum fiber length. *Journal of Biomechanics* 36 (9), 1309-16.

Rassier, D.E., MacIntosh, B.R., Herzog, W., 1999. Length dependence of active force production in skeletal muscle. *Journal of Applied Physiology* 86 (5), 1445-57.

Rohlmann, A., Arntz, U., Graichen, F., Bergmann, G., 2001. Loads on an internal spinal fixation device during sitting. *Journal of Biomechanics* 34, 989-993.

Rohlmann, A., Graichen, F., Bergmann, G., 2002. Loads on an internal spinal fixation device during physical therapy. *Physical Therapy* 82, 44-52.

Shadmehr, R., Arbib, M.A., 1992. A mathematical analysis of the force-stiffness characteristics of muscles in control of a single joint system. *Biological Cybernetics* 66, 463-477.

Shirazi-Adl, A., 1994. Analysis of the role of bone compliance on mechanics of a lumbar motion segment. *Journal of Biomechanical Engineering* 116, 408-412.

Shirazi-Adl, A., 2004. Stiffening role of compression on lumbar spine response in flexion/axial rotations- application of a novel wrapping element. 5th Combined Meeting of the Orthopaedic Research Societies of Canada, USA, Japan and Europe, No. 061, Banff, Alberta.

Shirazi-Adl, A., Ahmed, A.M., Shrivastava, S.C., 1986a. A finite element study of a lumbar motion segment subjected to pure sagittal plane moments. *Journal of Biomechanics* 19, 331-350.

Shirazi-Adl, A., Ahmed, A.M., Shrivastava, S.C., 1986b. Mechanical response of a lumbar motion segment in axial torque alone and combined with compression. *Spine* 11, 914-927.

Shirazi-Adl, A., Drouin, G., 1988. Nonlinear gross response analysis of a lumbar motion segment in combined sagittal loadings. *Journal of Biomechanical Engineering* 110, 216-222.

Shirazi-Adl, A., El-Rich, M., Pop, D.G., Parnianpour, M., 2004. Spinal Muscle forces, internal loads and stability in standing under various postures and loads: applications of kinematics-based algorithm. *European Spine Journal*, in press.

Shirazi-Adl, A., Parnianpour, M., 1999. Effect of changes in lordosis on mechanics of the lumbar spine-lumbar curvature in lifting. *Journal of Spinal Disorders* 12 (5), 436-47.

Shirazi-Adl, A., Sadouk, S., Parnianpour, M., Pop, D., El-Rich, M., 2002. Muscle force evaluation and the role of posture in human lumbar spine under compression. *European Spine Journal* 11, 519-526.

Sparto, P.J., Parnianpour, M., 1998. Estimation of trunk muscle forces and spinal loads during fatiguing repetitive trunk exertions. *Spine* 23, 423-429.

Stokes, I.A., Henry, S.M., Single, R.M., 2003. Surface EMG electrodes do not accurately record from lumbar multifidus muscles. *Clinical Biomechanics* 18, 9-13.

Stokes, I.A., Gardner-Morse, M., 1995. Lumbar spine maximum efforts and muscle recruitment patterns predicted by a model with multijoint muscles and joints with stiffness. *Journal of Biomechanics* 28, 173-186.

Stokes, I.A., Gardner-Morse, M., 1999. Quantitative anatomy of the lumbar musculature. *Journal of Biomechanics* 32, 311-316.

Stokes, I.A., Gardner-Morse, M., 2001. Lumbar spinal muscle activation synergies predicted by multi-criteria cost function. *Journal of Biomechanics* 34, 733-740.

Stokes, I.A., Gardner-Morse, M., 2003. Spinal stiffness increases with axial load: another stabilizing consequence of muscle action. *Journal of Electromyography and Kinesiology* 13 (4):397-402.

Takashima, S.T., Singh, S.P., Haderspeck, K.A., Schultz, A.B., 1979. A model for semi-quantitative studies of muscle actions. *Journal of Biomechanics* 12, 929-939.

Tan, J.C., Parnianpour, M., Nordin, M., Hofer, H., Willems, B., 1993. Isometric maximal and submaximal trunk extension at different flexed positions in standing. *Triaxial torque output and EMG. Spine* 18, 2480-90.

Van Dieen, J.H., 1997. Are recruitment patterns of the trunk musculature compatible with a synergy based on the maximization of endurance? *Journal of Biomechanics* 30, 1095-1100.

Wilke, H.J., Neef, P., Caimi, M., Hoogland, T., Claes, L.E., 1999. New in vivo measurements of pressures in the intervertebral disc in daily life. *Spine* 24, 755-763.

Wilke, H.J., Neef, P., Hinz, B., Seidel, H., Claes, L., 2001. Intradiscal pressure together with anthropometric data -A data set for the validation of models. *Clinical Biomechanics* 6, S111-S126.

Wilke, H.J., Rohlmann, A., Neller, S., Graichen, F., Claes, L., Bergmann, G., 2003. A novel approach to determine trunk muscle forces during flexion and extension: a comparison of data from an in vitro experiment and in vivo measurements. *Spine* 28 (23), 2585-93.

Woittiez, R.D., Huijing, P.A., Boom, H.B., Rozendal, R.H., 1984. A three-dimensional muscle model: a quantified relation between form and function of skeletal muscles. *Journal of Morphology* 182 (1), 95-113.

Yamamoto, I., Panjabi, M., Crisco, T., Oxland, T., 1989. Three-dimensional movements of the whole lumbar spine and lumbosacral joint. *Spine* 14, 1256-1260.

Zhang, X., Xiong, J., 2003. Model-guided derivation of lumbar vertebral kinematics in vivo reveals the difference between external marker-defined and internal segmental rotations. *Journal of Biomechanics* 36 (1), 9-17.

Table 3.1 Mean measured, prescribed thorax and pelvis rotations from the neutral standing posture as well as prescribed lumber rotations in the FE model assuming relative rotations of 8% at T12-L1, 13% at L1-L2, 16% at L2-L3, 23% at L3-L4, 26% at L4-L5, and 14% at L5-S1 level for both flexion postures of ~40° and 65° (based on reported *in vivo* kinematics measurements).

Vertebrae level	Prescribed kinematics in the FE model (deg)			
	Flexion 40°	Flexion 40° + 180 N	Flexion 65°	Flexion 65° + 180 N
Thorax (measurements)*	41.0	46.0	62.0	65.0
T1	39.2	43.8	59.5	62.2
T2	36.0	40.0	55.0	57.4
Total lumbar rotation†	31.9	35.1	49.3	51.2
L4	26.1	28.2	41.2	42.4
L5	19.6	20.3	32.0	32.4
Pelvis (measurements)‡	16.0	16.0	27.0	27.0

* The angle between T1-T12 and gravity lines was calculated as the trunk rotation in standing and flexed postures.

† Computed by evaluating the orientation of normal to the plane passing through the three markers on the pelvis.

‡ Was computed as the difference between the total thorax and pelvic rotations (Granata and Sanford, 2000).

Table 3.2 Physiological cross sectional areas (PCSA, mm²) and initial length (in brackets, mm) for muscles on each side of the spine at different insertion levels. ICpl: Iliocostalis Lumborum pars lumborum, ICpt: Iliocostalis Lumborum pars thoracic, IP: Iliopsoas, LGpl: Longissimus Thoracis pars lumborum, LGpt: Longissimus Thoracis pars thoracic, MF: Multifidus, QL: Quadratus Lumborum, IO: Internal Oblique, EO: External Oblique, and RA: Rectus Abdominus.

Local muscles	ICpl	IP	LGpl	MF	QL
L1	108 (170)	252 (276)	79 (172)	96 (158)	88 (137)
L2	154 (118)	295 (241)	91 (132)	138 (135)	80 (104)
L3	182 (84)	334 (206)	103 (88)	211 (106)	75 (74)
L4	189 (50)	311 (169)	110 (52)	186 (82)	70 (46)
L5	-	182 (132)	116 (25)	134 (51)	-
Global muscles	RA	EO	IO	ICpt	LGpt
T1-T12	567 (353)	1576 (239)	1345 (135)	600 (250)	1100 (297)

Table 3.3 Internal loads in passive ligamentous spine at various levels for neutral standing and flexed postures ± 180 N in hands.

Disc Level	Standing posture				Forward Flexion 40°				Forward Flexion 65°			
	0 N				180 N				0 N			
	*M	*S	M	C	S	M	C	S	M	C	S	M
L12-L1	8.4	337	-35	8.9	567	-133	18.5	933	250	22.4	1679	490
L1-L2	6.3	405	-46	6.3	633	-77	22.1	1171	224	28.3	2186	439
L2-L3	3.9	447	-63	3.1	668	-78	21.3	1414	111	28.7	2606	202
L3-L4	1.5	498	-7	0.7	702	-24	17.2	1669	173	24.7	2971	277
L4-L5	1.3	535	28	1.3	741	61	16.8	1862	95	24.1	3250	73
L5-S1	2.3	570	190	3.9	753	318	19.4	1912	502	27.1	3308	726
											31.8	2332
											506	3850
											38.1	708

* M: sagittal moment at mid-height, + ve in flexion (Nm); C: local axial compression at mid-height (N); S: local shear force at mid-height, +ve in anterior direction (N).

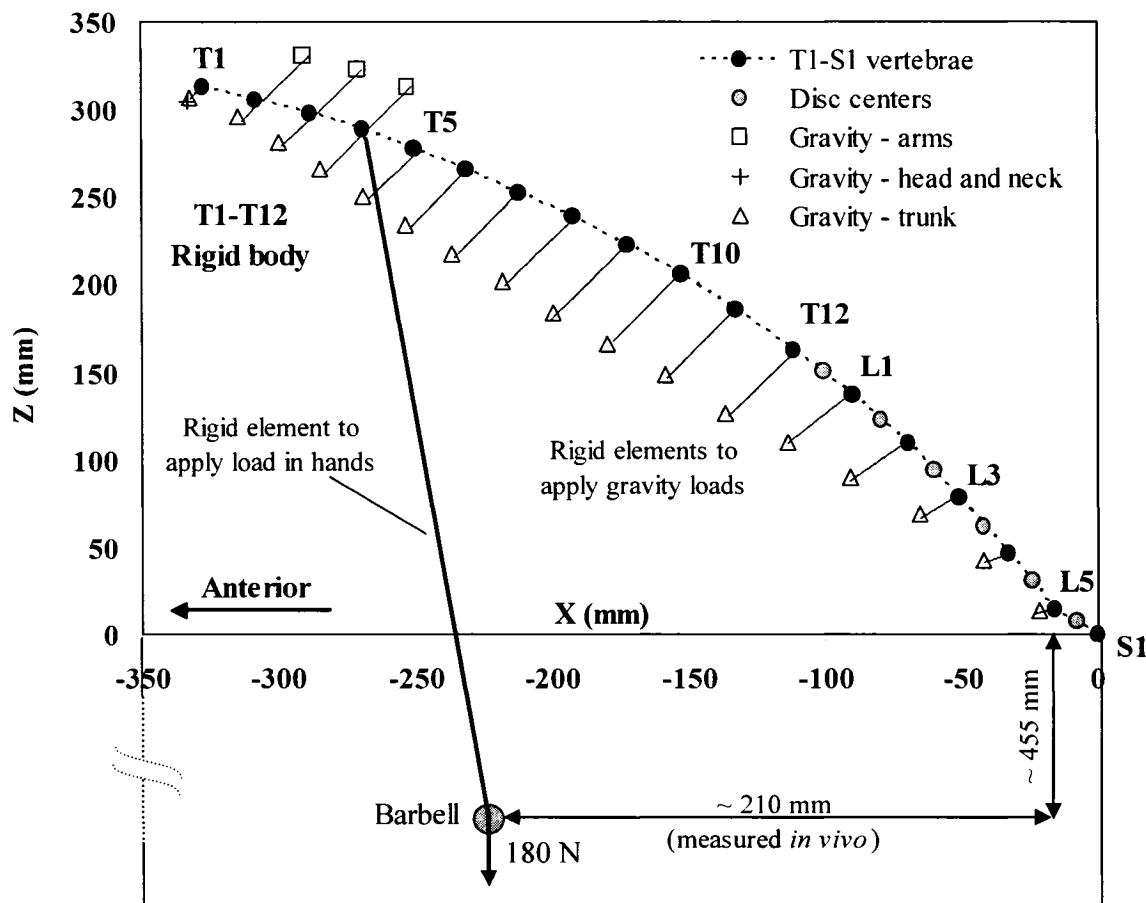


Fig. 3.1 Sagittal profile of the FE model at $\sim 40^\circ$ flexion prescribed based on measurements. Positions of distributed gravity loads (total of ~ 387 N: 256 N anteriorly at T1-L5 levels for the torso, 58.5 N for the head/neck at 1 cm anterior to T1, and 72.2 N for arms/shoulder at 3 cm posterior to T2-T4) and concentrated 180 N held in front via a barbell are shown. The external load is applied on the T4 at a location based on mean of measured data.

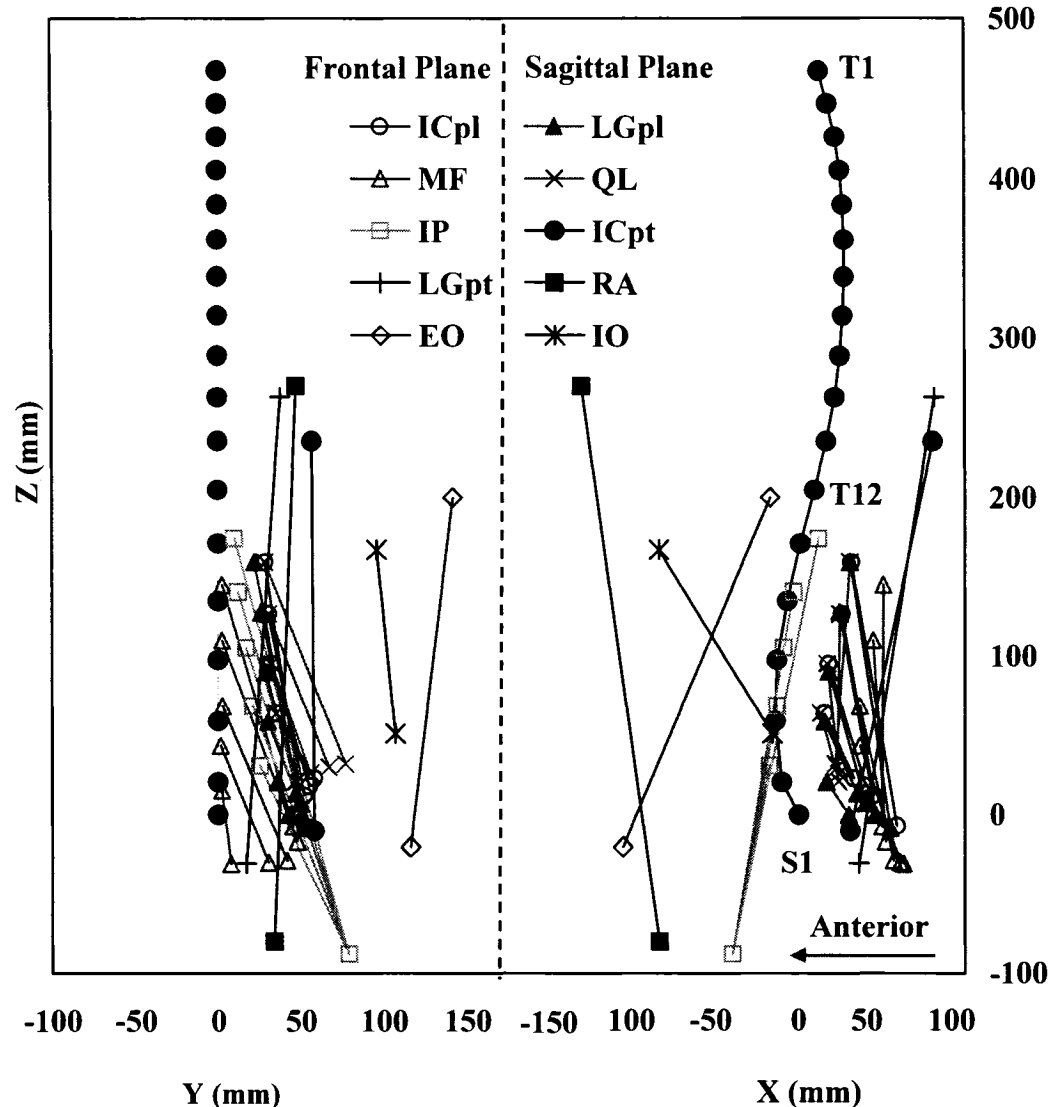


Fig. 3.2 Representation of global and local musculatures in the sagittal and frontal planes used in the FE model. Only fascicles at one side have been shown. ICpl: Iliocostalis Lumborum pars lumborum, ICpt: Iliocostalis Lumborum pars thoracic, IP: Iliopsoas, LGpl: Longissimus Thoracis pars lumborum, LGpt: Longissimus Thoracis pars thoracic, MF: Multifidus, QL: Quadratus Lumborum, IO: Internal Oblique, EO: External oblique, and RA: Rectus Abdominus.

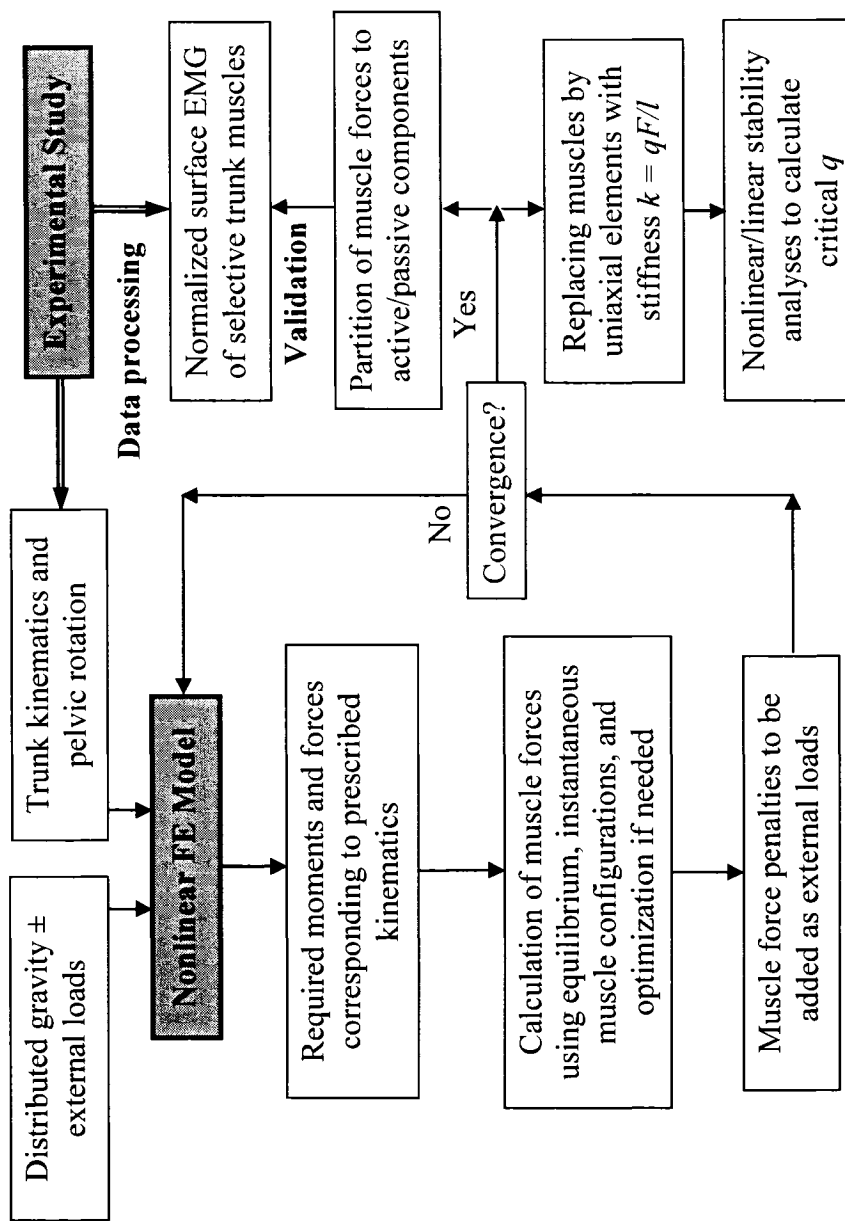


Fig. 3.3 Flow-chart for the application of the kinematics-based approach and determination/validation of trunk muscle forces, internal loads as well as stability margin of the spine. The moments required for the prescribed rotations were fed into a separate algorithm that calculated muscle forces at each level. Axial compression and horizontal shear penalties of these muscle forces were then fed back into the finite element model as additional updated external loads. This iterative approach was continued at each load step till convergence was reached.

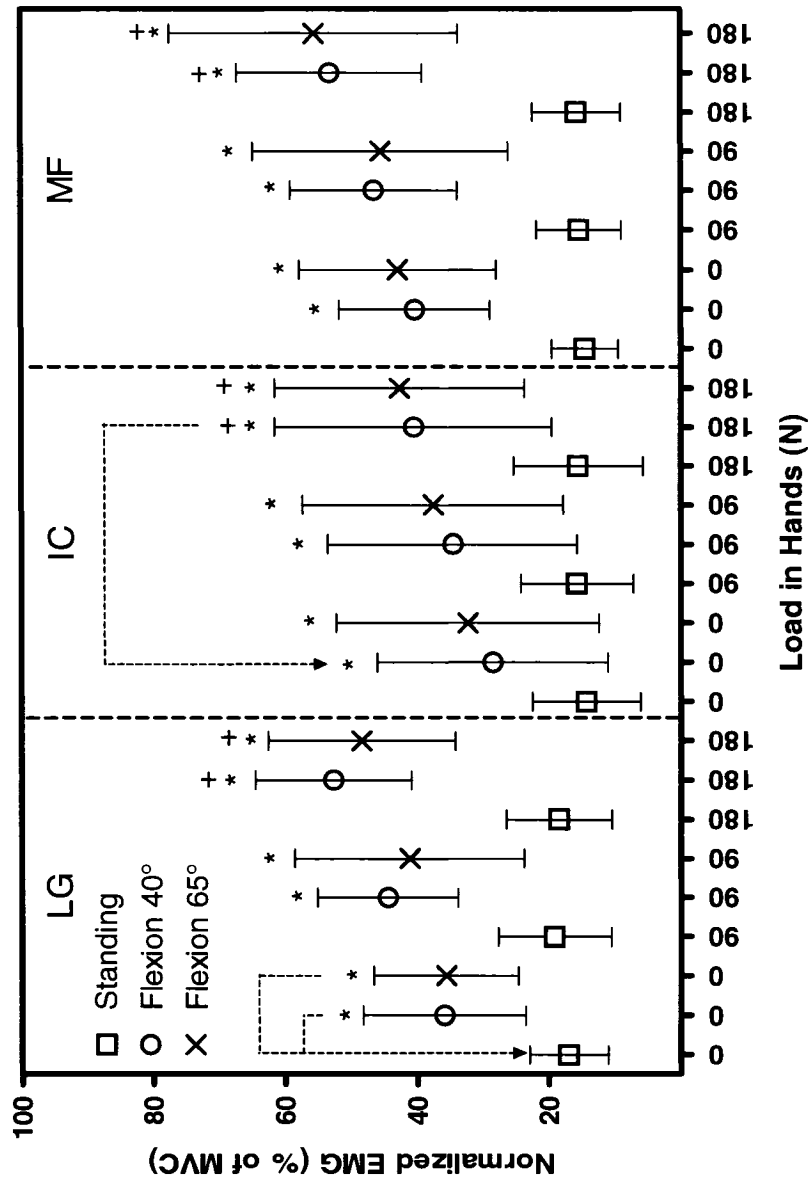


Fig. 3.4A *In vivo* measured normalized EMG activity (mean \pm S.D.) of extensor muscles in standing and flexed postures as a function of load carried symmetrically in hands. IC: Iliocostalis, LG: Longissimus, and MF: Multifidus. * Significant change in EMG activity compared to that of standing posture due to flexion under identical load in hands (as explicitly shown for LG). + Significant change in EMG activity compared to that of 0 N due to load magnitude under identical postures (as explicitly shown for IC muscle).

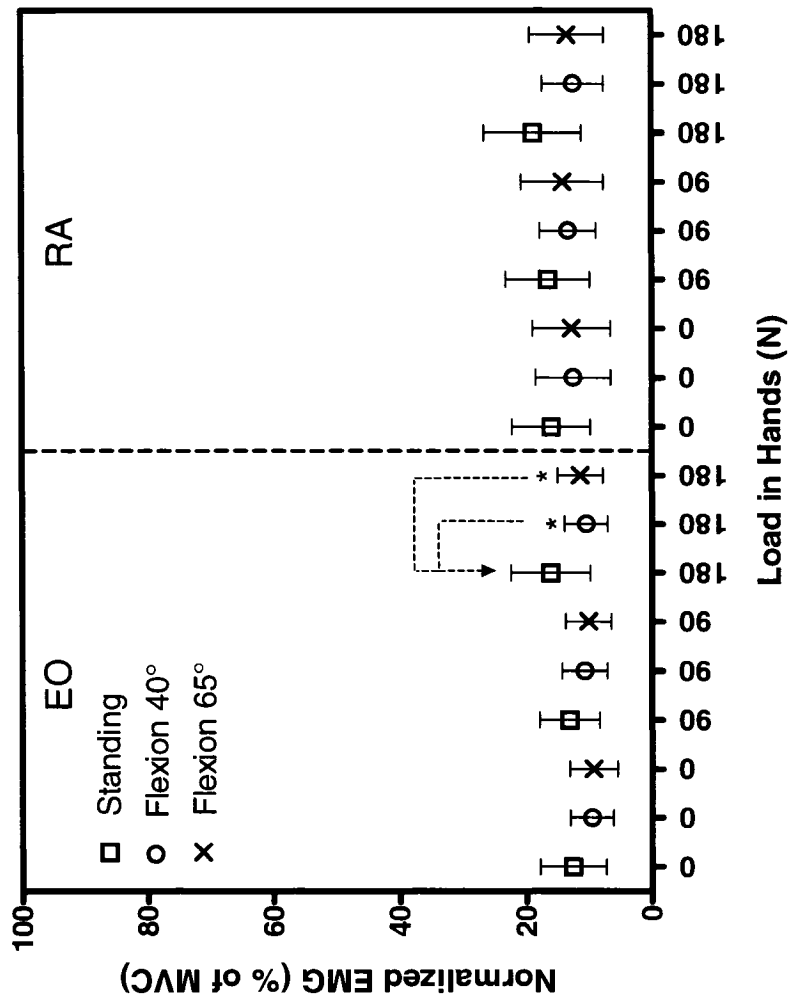


Fig. 3.4B *In vivo* measured normalized EMG activity (mean \pm S.D.) of abdominal muscles in standing and flexed postures as a function of load carried symmetrically in hands. EO: External oblique, and RA: Rectus Abdominus. * Significant change in EMG activity compared to that of standing posture due to flexion under identical load in hands (as explicitly shown for EO muscles). No significant change in EMG activity compared to that of 0 N due to load magnitude under identical postures was observed.

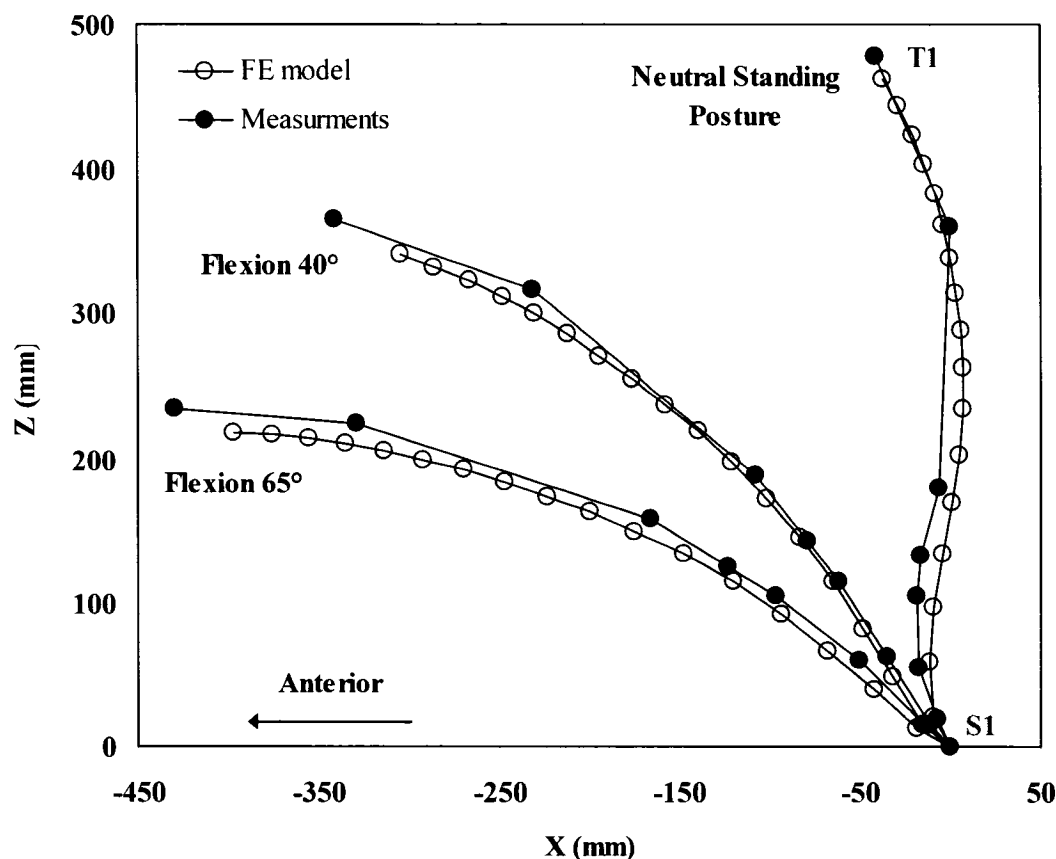


Fig. 3.5 Mean measured kinematics along with deformed finite element model in standing and flexed postures without load in hands.

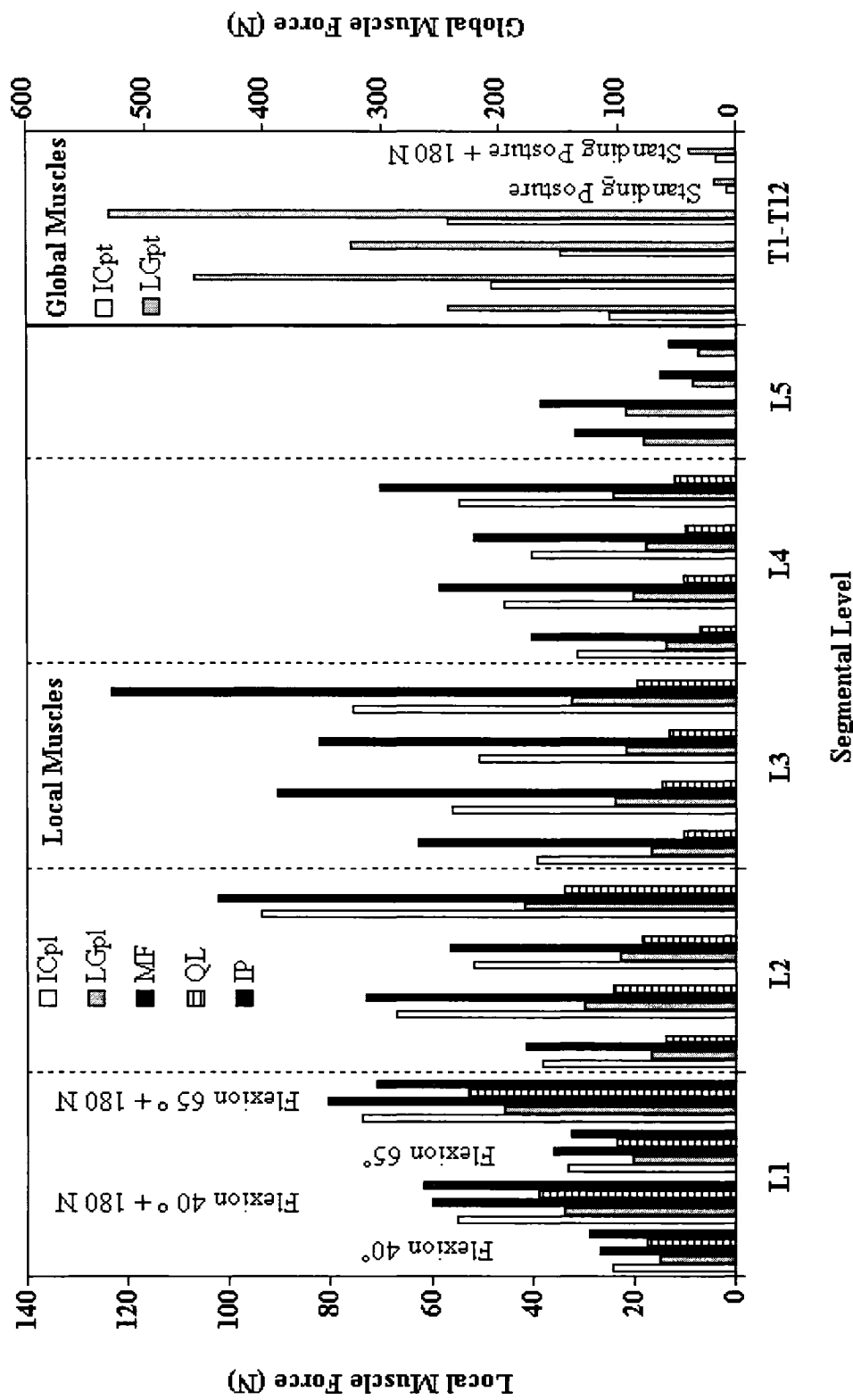


Fig. 3.6 Calculated trunk muscle forces in different fascicles, on each side, for flexed postures with and without load of 180N in hands. Global muscle forces in standing postures have also been shown.

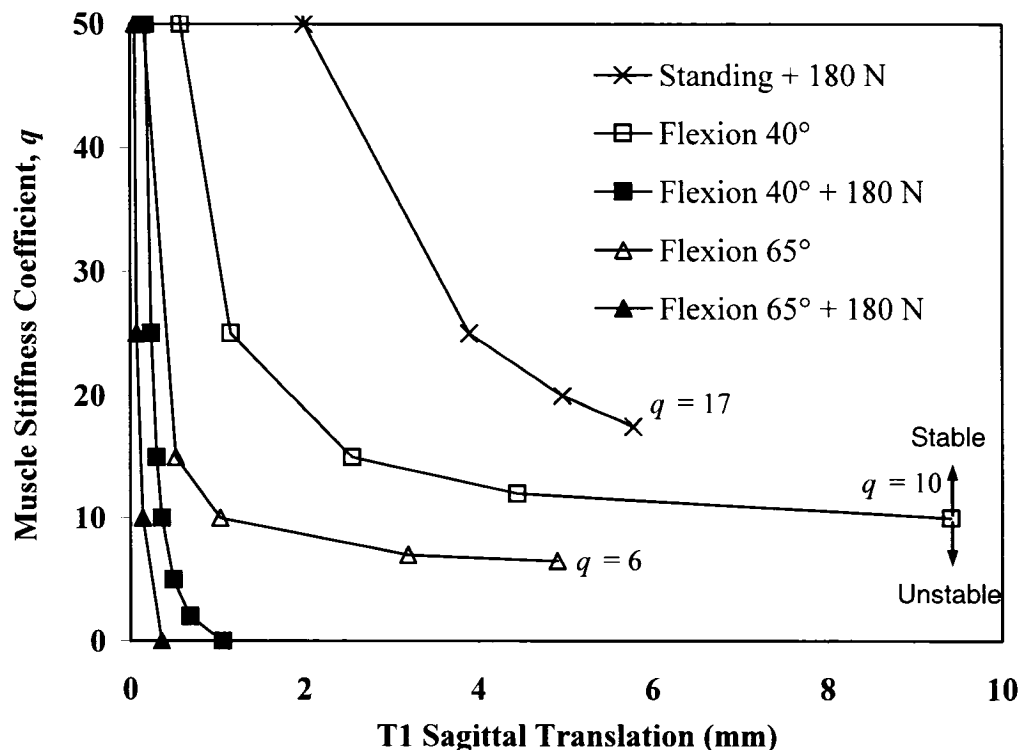


Fig. 3.7A Variation of computed T1 sagittal translation with the muscle stiffness coefficient, q , for different postures with and without load of 180 N in hands using linear perturbation analysis at deformed configurations due to 1 N horizontal force at the T1 (in agreement with nonlinear analyses). The smallest q in each case is the critical value below which the system becomes unstable.

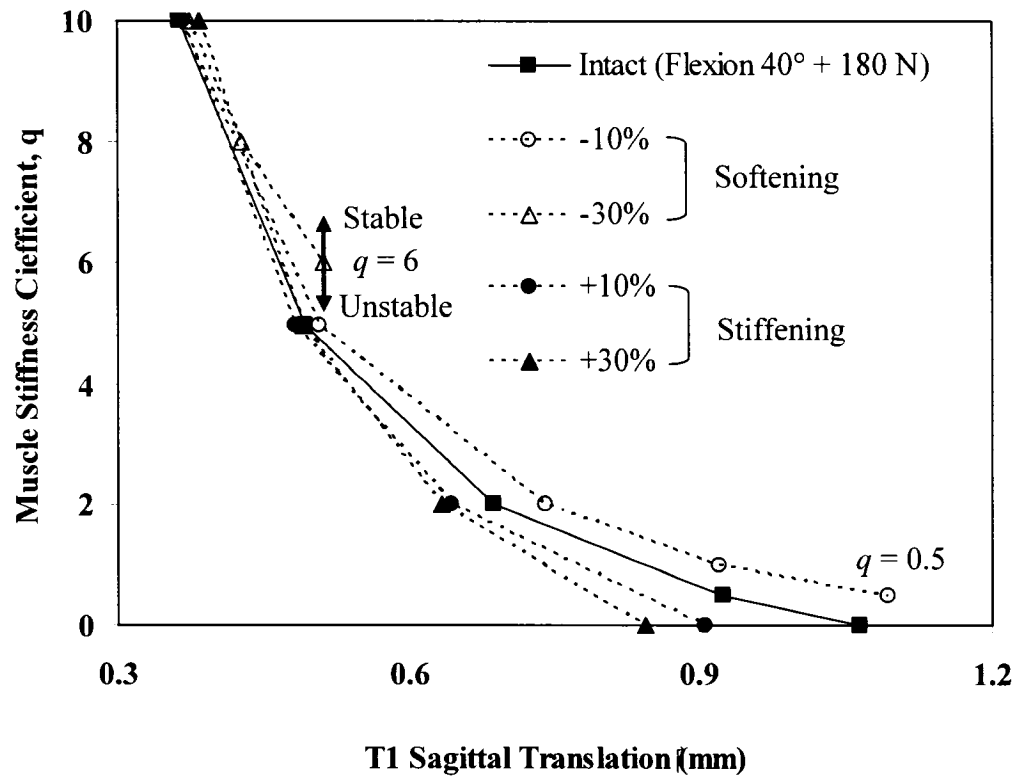


Fig. 3.7B Variation of computed T1 sagittal translation with the muscle stiffness coefficient, q , for the case with $\sim 40^\circ$ flexion and 180 N load in hands (while altering the flexion stiffness of passive ligamentous spine by up to $\pm 30\%$) using linear perturbation analysis at deformed configurations due to 1 N horizontal force at the T1 (in agreement with nonlinear analyses).

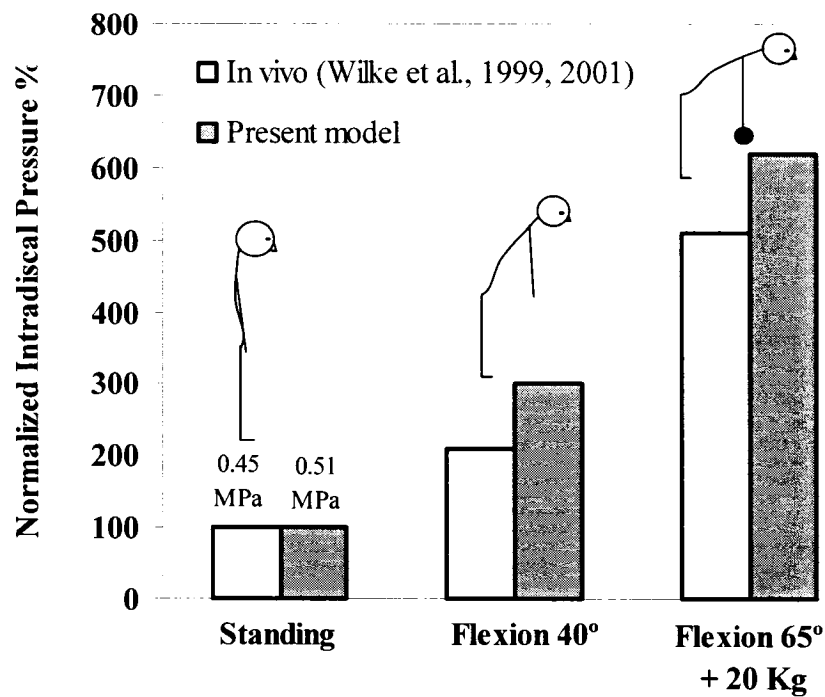


Fig. 3.8 Measured (*in vivo*) and computed intradiscal pressure values at the L4-L5 disc under different loads and postures. Values have been normalized to their respective values in the neutral standing posture.

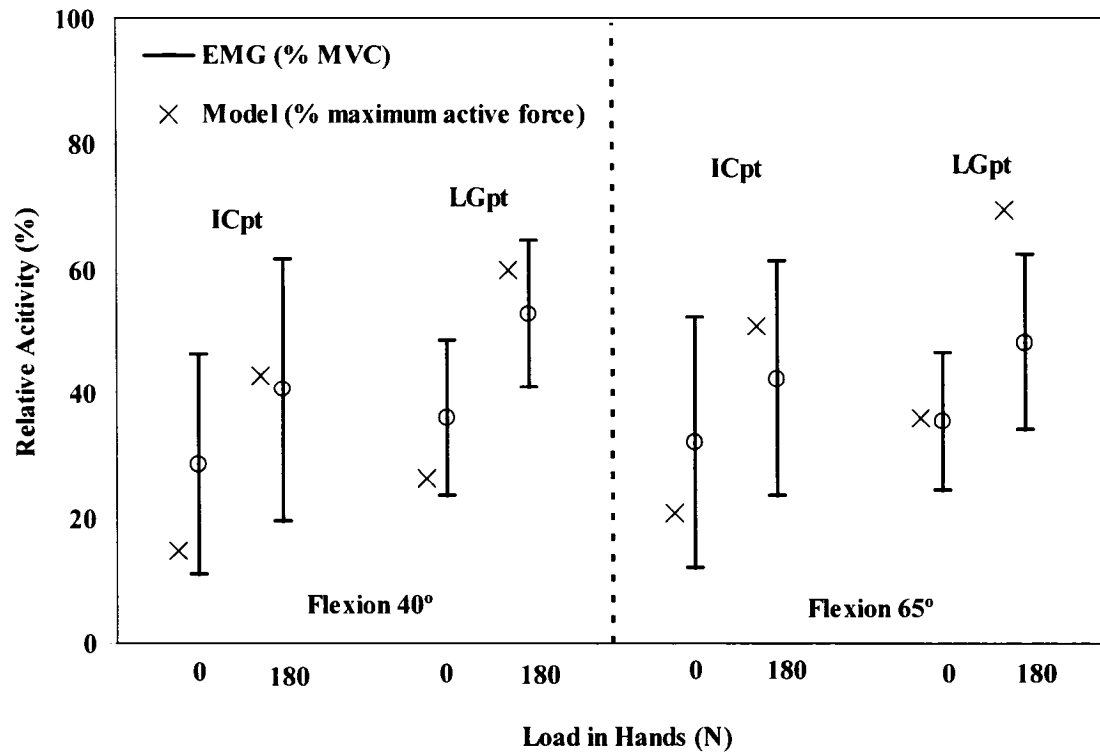


Fig. 3.9 Comparison of measured normalized EMG activity with computed muscle forces normalized to their respective maximum active force ($0.6 \times \text{PCSA}$, Table 2) for global muscles in flexed postures with and without load of 180 N in hands.

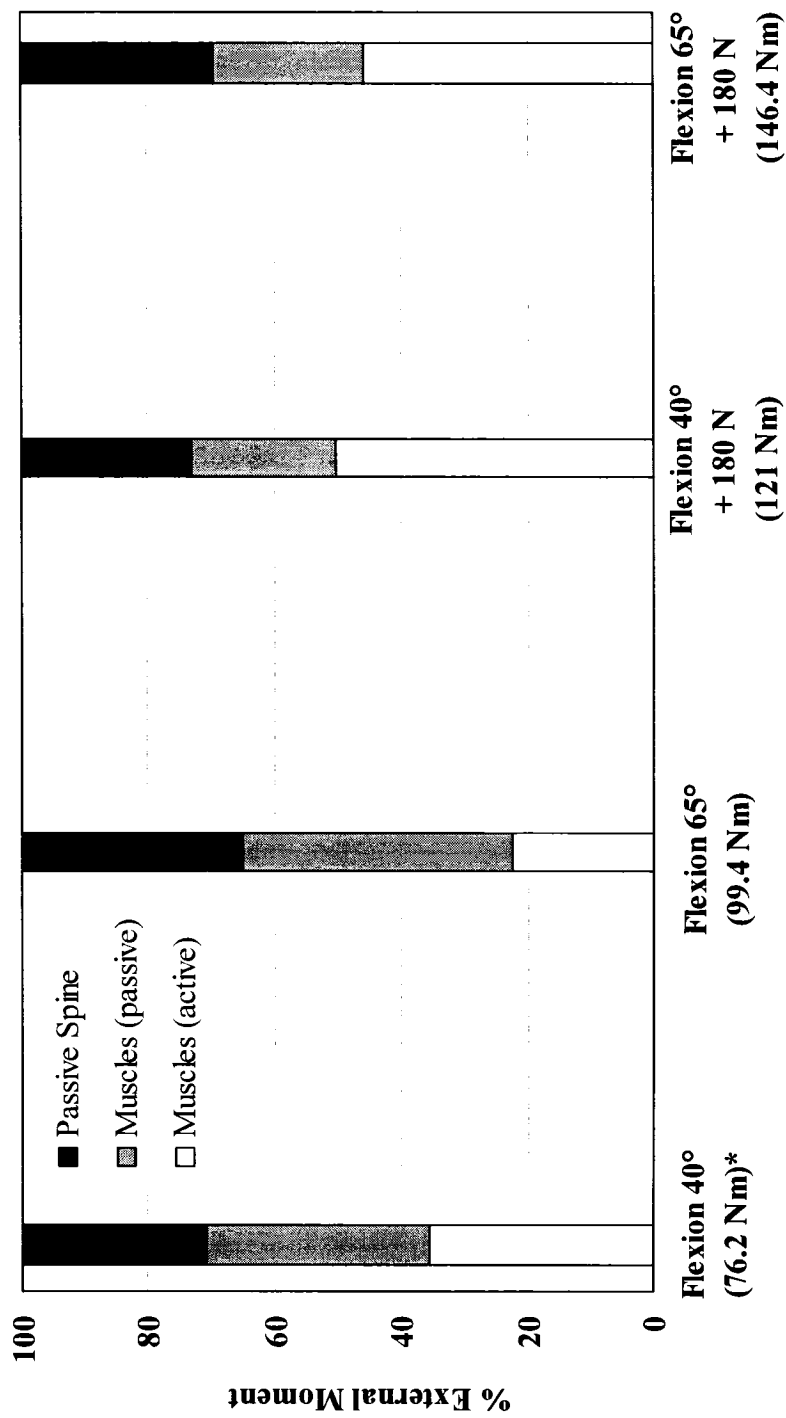


Fig. 3.10 Relative contribution of trunk muscles (passive and active) and of passive motion segments (ligamentous spine) to counterbalance the total moment of external/gravity loads (indicated by *) for flexed postures with or without load of 180 N in hands.

CHAPTER 4

BIOMECHANICS OF CHANGES IN LUMBAR POSTURE IN STATIC LIFTING

N. Arjmand and A. Shirazi-Adl

Department of Mechanical Engineering, École Polytechnique
Montréal, Québec, Canada

Article published in *Spine* 2005; 30 (23): 2637-48

Keywords: Trunk Muscles; Finite Element; Stability; Lumbar posture; EMG

4.1 ABSTRACT

Study Design: *In vivo* measurements and model studies are combined to investigate the role of lumbar posture in static lifting tasks.

Objectives: Identification of the role of changes in the lumbar posture on muscle forces, internal loads, and system stability in static lifting tasks with and without load in hands.

Summary of Background Data: Despite the recognition of the causal role of lifting in spinal injuries, the advantages of preservation or flattening of the lumbar lordosis while performing lifting tasks is not yet clear.

Methods: Kinematics of the spine and surface EMG activity of selected muscles were measured in 15 healthy subjects under different forward trunk flexion angles and load cases. Apart from the free style lumbar posture, subjects were instructed to take either lordotic or kyphotic posture as well. A Kinematics-based method along with a nonlinear finite element model were interactively used to compute muscle forces, internal loads and, system stability margin under postures and loads considered in *in vivo* investigations.

Results: In comparison with the kyphotic postures, the lordotic postures increased the pelvic rotation, active component of extensor muscle forces, segmental axial compression and shear forces at the L5-S1 level and spinal stability margin while decreasing the passive muscle forces and segmental flexion moments.

Conclusion: Alterations in the lumbar lordosis in lifting resulted in significant changes in the muscle forces and internal spinal loads. Spinal shear forces at different segmental levels were influenced by changes in both the disc inclinations and extensor muscle lines of action as the posture altered. Considering internal spinal loads and active/passive muscle forces, the current study supports the free style posture or a posture with moderate flexion as the posture of choice in static lifting tasks.

4.2 INTRODUCTION

Epidemiological studies have associated physically heavy work, static work postures, frequent bending, and lifting with low-back pain (LBP) symptoms (Frymoyer et al., 1983). In a large survey, lifting or bending episodes accounted for 33% of all work-related causes of back pain (Damkot et al., 1984). Combination of lifting with lateral bending or twisting has been identified as a frequent cause of back injury in the workplace (Andersson, 1981; Hoogendoorn et al., 2000; Kelsey et al., 1984; Marras et al., 1995; Troup et al., 1981; Varma and Porter, 1995). Among various work-related activities, lifting, awkward posture, and heavy physical work have been indicated to have strong relationship with lumbar musculoskeletal disorders (MSDs) (NIOSH, 1997). Trunk motion and velocity of trunk movement have also been identified as significant risk factors for occupational low-back disorders (Davis and Marras, 2000; Marras et al., 1995; Norman et al., 1998). Search for a safe lifting technique has, thus, attracted considerable attention due to the high risk of injury and LBP associated with frequent lifting specially in industrial manual material handling (MMH) tasks. Compression force limits have been recommended (NIOSH, 1981; Waters et al., 1993) for safer MMH manoeuvres based on the premise that excessive compression loads could cause injury.

Despite the well-recognized role of lifting in low-back injuries, the literature on safer lifting techniques remains controversial. In search of optimal lifting methods, squat lift (i.e., knee bent and back straight) is generally considered to be safer than the stoop lift (i.e., knee straight and back bent) in bringing the load closer to the body and, hence, reducing the extra demand on back muscles to counterbalance additional moments. The importance of the squat versus stoop lifting postures has, however, been downplayed due to the lack of a clear biomechanical rationale for the promotion of either style (McGill, 1997). Many workers, despite instruction to the contrary, prefer the stoop lift over squat lift. It is known that there is an increased physiological cost (Garg and Herrin, 1979) as well as more rapid fatigue development (Hagen et al., 1993) in squatting and that squat lift is not always possible due to the lift set up and load size (Van Dieen et al.,

1999). In a recent review paper (Van Dieen et al., 1999) and a biomechanical model study (Potvin et al., 1991a) of the effect of squat and stoop lifting techniques on the lumbar spine loading, it was suggested that the risk of injury may be influenced more by the lumbar posture rather than the choice of stoop or squat technique.

The advantages in preservation or flattening (i.e., flexing) of the lumbar lordosis during lifting tasks are even less understood. A kyphotic lift (i.e., flexed lumbar spine) is recommended by some as it utilizes the passive ligamentous system (i.e., posterior ligaments and lumbodorsal fascia) to their maximum thus relieving the active extensor muscles (Gracovetsky et al., 1981, 1985). In contrast, however, others advocate lordotic and straight-back postures indicating that posterior ligaments cannot effectively protect the spine and an increase in erector spinae activities is beneficial in augmenting spinal stability (Aspden, 1989; Delitto et al., 1987; Hart et al., 1987; McGill, 1997; Vakos et al., 1994) and in diminishing the anterior shear force on spine (McGill et al., 2000; Potvin et al., 1991a, b). In an earlier *in vivo* study, it was noted that professional power lifters accomplished their heavy lifts with remarkably small intersegmental flexion angles (Cholewicki and McGill, 1992). Experimental studies have advocated a moderate lumbar flexion under high compressive forces (Adams et al., 1994). The lever arm of erector spinae muscle group has been measured from MRI to decrease significantly by 10-24% from a lordotic to a kyphotic posture (Tveit et al., 1994) indicating its greater moment-resistant capacity in the former posture.

The inability to accurately determine the loads on the trunk active and passive components as well as the system stability margin appears as a critical hindrance towards the development of ergonomic guidelines for the design of safer lifting tasks. Evidently, an improved assessment of risk of injury depends on a more accurate estimation of the load partitioning in the human trunk in forward flexion tasks. Spinal loads have indirectly been estimated by measurement of intradiscal pressure (Nachemson, 1981; Wilke et al., 1999), load on spinal instruments (Rohlmann et al.,

2001, 2002), spinal shrinkage (Van Dieen and Toussaint, 1993; McGill et al., 1996), and EMG activity of trunk muscles (Mouton et al., 1991; Potvin et al., 1996). Due to the limitations in foregoing methods, biomechanical models have been recognized as indispensable tools for evaluation of spinal loads and system stability in various occupational and athletic activities.

The current work aims to employ a combined model studies-*in vivo* measurements approach to investigate the relative effect of changes in the lumbar posture on the load partitioning and stability of the human trunk in static lifting tasks. In the *in vivo* part of the investigation, kinematics of the spine (required as input data into the model) and EMG activity of major trunk muscles (required to qualitatively validate model predictions) are collected under isometric trunk flexions of $\sim 40^\circ$ and 65° with and without a load of 180 N in hands. Volunteers carry out the sagittally-symmetric tasks with three different lumbar postures; kyphotic, lordotic, and free style (with no instruction on posture). Subsequently, the biomechanical model study uses a nonlinear thoracolumbar finite element model coupled with a Kinematics-based approach (Arjmand and Shirazi-Adl, 2006; El-Rich et al., 2004; Kiefer et al., 1998; Shirazi-Adl et al., 2002; Shirazi-Adl et al., 2005) that calculates muscle forces, spinal loads and stability under prescribed measured postures and loads considered *in vivo*.

4.3 MATERIALS AND METHODS

4.3.1 *In vivo* measurement

Fifteen healthy males with no recent back complications volunteered for the study after signing an informed consent form approved by the Institut de réadaptation de Montréal. Their mean (\pm S.D.) age, body height, and mass were 30 ± 6 years, 177 ± 7 cm, and 74 ± 11 kg. While bending slightly forward, infrared light emitted markers, LED, were attached on the skin at the tip of T1, T5, T10, T12, L1, L3, L5, and S1 spinous processes for evaluation of lumbar and torso flexions. Three extra LED markers were placed on the posterior-superior iliac spine and ilium (left/right iliac crests) for

evaluation of pelvic rotation, and one on the load to track the position of weights in hands. A three-camera Optotrak system (NDI International, Waterloo, Ontario) was employed to collect 3D coordinates of LED markers. Simultaneously, five pairs of surface electrodes were positioned bilaterally (McGill, 1991; O'Sullivan et al., 2002) over longissimus dorsi (~3cm lateral to midline at the L1), iliocostalis (~6cm to midline at the L1), multifidus (~2cm to midline at the L5), external obliques (~10cm to midline above umbilicus and aligned with muscle fibers), and rectus abdominis (~3cm to midline above the umbilicus). The raw EMG signals were amplified, band-pass filtered at 10-400 Hz by a 2nd order Butterworth filter, rectified over 4s trial duration and averaged for both sides. For normalization, EMG data at maximum voluntary contraction (MVC) was collected in standing (in cardinal planes while loaded via a strapped harness (Sparto and Parnianpour, 1998)), prone, and supine positions.

Subjects held either no load or 180 N in hands via a bar during isometric forward flexion tasks with torso at ~40° or ~65°. These tasks were performed either with no instruction on the posture (free style) or with specific instruction that subjects voluntarily take lordotic and kyphotic lumbar postures by controlling their pelvic tilt. In all three postures, the overall trunk forward rotations were kept nearly unchanged as subjects primarily altered their pelvic tilt to achieve various lumbar postures. During measurements, subjects were also instructed to keep knees straight and arms extended in the gravity direction. Three-way analyses of variance (ANOVA) for repeated measure factors were performed to study the effect of lumbar posture (3 levels: lordotic, free, and kyphotic), load magnitude (2 levels: 0 N and 180 N), and torso flexion (2 levels: ~40° and 65°) on EMG activities. Besides, one-way ANOVA for repeated measure factors were used to study the effect of lumbar posture on the pelvic rotation, torso flexion, and load position. *Tukey's post hoc* tests were performed to further reveal any significant trends ($p<0.05$).

4.3.2 Thoracolumbar Finite Element Model

The details of the model have been given elsewhere (Arjmand and Shirazi-Adl, 2006; El-Rich et al., 2004; Kiefer et al., 1998; Shirazi-Adl et al., 2002; Shirazi-Adl et al., 2005) and are briefly described here. A sagittal-symmetric T1-S1 beam-rigid body model consisting of 6 deformable beams to represent T12-S1 segments and 7 rigid elements to represent T1-T12 (as a single body) and lumbosacral vertebrae (L1 to S1) was used (Fig. 4.1). The nonlinear load-displacement response under single and combined axial/shear forces and moments along with the flexion versus extension differences were represented in this model based on numerical and measured results of previous single- and multi-motion segment studies (Oxland et al., 1992; Patwardhan et al., 2003; Pop, 2001; Shirazi-Adl, 2006; Shirazi-Adl et al., 2002; Stokes and Gardner-Morse, 2003; Yamamoto et al., 1989). The nonlinear response in flexion moment and axial compression is given for different segmental levels in Fig. 4.2 while the shear modulus (kGA) is assumed constant varying from 5502 N at the T12-L1 level to 6736 N at the L5-S1 level. In all cases, based on the mean body weight of our subjects and percentage of body weight at each motion segment level reported elsewhere (Pearsall, 1994; Takashima et al., 1979), a gravity load of 387 N was considered and distributed eccentrically at different levels. To simulate the cases with an external load in hands, 180 N was applied at the location measured *in vivo* via a rigid element attached to the T3 vertebra.

4.3.3 Prescribed Postures

Mean measured sagittal rotations at the upper torso (evaluated based on the change in the inclination of the line attaching the T1 marker to the T12 one) and pelvis (evaluated based on the change in the orientation of the normal to the plane passing through the pelvis markers) were prescribed onto the model at the T12 and S1 levels, respectively. As for the individual lumbar vertebrae, the total lumbar rotation, calculated as the difference between the foregoing two rotations, was partitioned in accordance with proportions reported in earlier investigations (8% at T12-L1, 13% at L1-L2, 16% at L2-L3, 23% at L3-L4, 26% at L4-L5, and 14% at L5-S1) (Dvorak et al., 1991; Frobin et

al., 1996; Pearcy et al., 1984; Plamondon et al., 1988; Potvin et al., 1991a; Shirazi-Adl and Parnianpour, 1999; Yamamoto et al., 1989).

4.3.4 Muscle Model and Muscle Force Calculation

A sagittally-symmetric muscle architecture with 46 local (attached to lumbar vertebrae) and 10 global (attached to thoracic cage) muscles was used (Fig. 4.1 and Table 4.1) (Bogduk et al., 1992; Daggfeldt and Thorstensson, 2003; Stokes and Gardner-Morse, 1999). To evaluate muscle forces a novel Kinematics-based algorithm (Fig. 4.3) was employed to solve the redundant active-passive system subjected to prescribed measured kinematics and external loads (Arjmand and Shirazi-Adl, 2006; El-Rich et al., 2004; Shirazi-Adl et al., 2002; Shirazi-Adl et al., 2005). In this manner, calculated muscle forces at each instance of loading were compatible with the prescribed kinematics (i.e., posture) and external loading while accounting for the realistic nonlinear stiffness of the passive system. This approach exploits kinematics data to generate additional equilibrium equations at each level in order to alleviate the kinetic redundancy of the problem. If, insufficient number of prescribed displacements is available at a level, then an optimization approach should also be employed. In the current study, the cost function of minimum sum of cubed muscle stresses was considered in the optimization with inequality equations of unknown muscle forces remaining positive and greater than their passive force components (calculated based on muscle strain and a tension-length relationship (Davis et al., 2003)) but smaller than the sum of maximum physiological active forces (i.e., 0.6 PCSA) and the passive force components (Gagnon et al., 2001; Guzik et al., 1996). The finite element program ABAQUS (Hibbit, Karlsson & Sorensen, Inc., Pawtucket, RI, version 6.4) was used to carry out nonlinear structural analyses while the optimization procedure was analytically solved using an in-house program based on Lagrange Multipliers Method (Raikova and Prilutsky, 2001). For the sake of comparison with our *in vivo* measurements, the active muscle force was initially computed for each muscle by subtracting the passive force

(using a tension-length relation (Davis et al., 2003)) from the calculated total muscle force and was then normalized to its own maximum physiological force.

4.3.5 Stability Analyses

In each simulation case, after the muscle forces were calculated, the model was modified with uniaxial elements replacing muscles between their insertion points. Stiffness of each uniaxial element, k , was assigned using the linear stiffness-force relationship $k=qF/l$ (F : known muscle force, l : instantaneous muscle length, q : muscle stiffness coefficient chosen a priori) (Bergmark, 1989; Crisco and Panjabi, 1991). Nonlinear analyses under same external loads and prescribed pelvic tilt were performed for different q values thus identifying the critical q for which the system ceased to be stable. In addition to nonlinear analyses, linear buckling and perturbation analyses (Reeves and Cholewicki, 2003) at loaded, deformed, configurations were also carried out as complementary approaches to estimate trunk stability margin as a function of q .

4.4 RESULTS

4.4.1 *In vivo* study

In accordance with instructions, torso rotations remained nearly the same irrespective of changes in the lumbar posture from the free style to either lordotic or kyphotic curvature (Fig. 4.4). Similarly, location of the load in hands was negligibly influenced by changes in the lumbar posture. The pelvic rotation was, however, significantly decreased from the lordotic posture to the kyphotic one (Fig. 4.4) with that for the free style remaining in between. The lumbar flexion evaluated as the difference between the torso rotation and the pelvic tilt, hence, significantly increased from the lordotic posture to the kyphotic one. The change in the lumbar curvature in between these two postures was larger in the absence of the external load (Fig. 4.4).

EMG activities in global extensor muscles (LGPT and ICPT) increased, though not significantly, in the lordotic lumbar posture compared with those in the kyphotic

posture for the cases with no load in hands (Fig. 4.5 and Table 4.2). EMG activity of extensor muscles significantly increased in all cases as 180 N was added in hands (Table 4.2). Abdominal muscles, though relatively quiet in all tasks (with means remaining < 20% of MVC) (Fig. 4.5), demonstrated a significant change with both lumbar posture and load in hands (Table 4.2). The EMG activity of abdominal muscles increased as the posture was altered from the free style. Tukey's tests revealed that the EO activity significantly increased from the free style to the kyphotic posture. For the RA, the difference between the kyphotic and free postures was significant only under 180 N while the difference between lordotic and free styles was significant regardless of the load magnitude.

4.4.2 FE model study

Due to the measured small and non-significant variations in torso rotation in various postures (Fig. 4.4), in the FE simulations and under each load condition, the mean torso rotation measured in the free style posture (listed in Fig. 4.4) was considered for all three lumbar postures. The pelvic tilt was, however, different and taken as the mean of measured values (listed in Fig. 4.4). In agreement with our *in vivo* measurements, active component of force in global muscles (LGPT and ICPT) increased in the lordotic posture compared with that in the kyphotic posture when no load was carried in hands. This variation, however, disappeared in presence of 180 N in hands (Table 4.3 and Fig. 4.5). For all conditions considered, the passive components of extensor muscle forces increased in the kyphotic posture and decreased in the lordotic posture (Table 4.3) in accordance with the computed changes in their lengths.

Under identical torso rotation and external load, change in the lumbar posture had a greater relative effect on the segmental flexion moment and shear force than on the axial compression force (<14%) (Table 4.4). Maximum local segmental shear and compression forces were computed at the L5-S1 disc and were found to be greater in lordotic postures. In contrast, segmental moments were much larger in kyphotic postures

(Table 4.4). For all postures, the system stability substantially increased as torso flexion increased from $\sim 40^\circ$ to 65° and as load increased from 0 to 180 N. In cases without load in hands, the spinal stability further improved from a kyphotic to a lordotic posture (Fig. 4.6). No muscle stiffness was at all required to maintain system stability in all postures when holding 180 N in hands.

4.5 DISCUSSION

In an attempt to search for the safer lumbar posture in static lifting tasks, this study aimed to investigate the relative effect of alterations in the lumbar posture on load partitioning and system stability. Subjects performed different isometric lifting tasks either with no instruction on the lumbar posture or instructed to take lordotic or kyphotic posture. It is to be noted that the findings of this study should be applicable to both squat and stoop static lifting techniques.

Despite several studies on the effect of changes in the lumbar posture on the EMG signals of the trunk and hip muscles (Delitto and Rose, 1992; Delitto et al., 1987; Hart et al., 1987; Holmes et al., 1992; Vakos et al., 1994) the issue of the safest lumbar posture during lifting activities remain controversial. This is partly due to the lack of a comprehensive biomechanical model that can accurately determine passive-active load partitioning and spinal stability under different postural and loading conditions. Towards such goal, a combined model studies-*in vivo* measurements investigation was employed in this work. The Kinematics-based finite element approach simultaneously satisfied kinematics, equilibrium, and stability requirements at all levels and directions while accounting for realistic nonlinear load- and direction-dependent properties of the passive spine. The results indicated that under identical torso rotation and load in hands, the lordotic posture as compared with the kyphotic posture significantly increased pelvic rotation, slightly increased net total moment at the S1 level, markedly increased active component of global (in absence of 180 N only) and local extensor muscle forces, substantially decreased passive component of extensor muscle forces, decreased the

inclination of extensor muscles with respect to the horizontal plane, slightly increased segmental axial compression at the distal L5-S1 level, significantly increased anterior shear force at the distal L4-S1 levels while decreasing them at upper levels, considerably decreased segmental flexion moment/rotation at all levels, and improved spinal stability. In lordotic postures due partly to an increase in the lever arm of global muscles, the muscle forces had a greater relative role in balancing net external moment. Finally, measured and computed results with the free style posture in which subjects performed static lifting with no instruction on the lumbar posture were generally much closer to those with the kyphotic posture than those with the lordotic one.

4.5.1 Methodological Issues

Calculation of the segmental rotations from skin markers is recognized to involve errors in identification of vertebral positions, skin movement relative to the underlying vertebrae, and deformability of vertebrae themselves (Lee et al., 1995; Zhang et al., 2003). Due to these inherent errors, the measurements were used in this work only to evaluate pelvic tilt and torso rotations with the intervening lumbar segmental rotations evaluated based on relative values reported in the literature. The foregoing proportions remained the same in all three lumbar postures considered. Moreover, measurement of the maximum EMG activity (MVC) required for normalization depends amongst others on the task design, subject, and electrode location (McGill, 1991; O'Sullivan, 2002). The electrodes for the multifidus at the L5 level more likely yield activity of adjacent longissimus (Stokes et al., 2003), therefore comparisons between predictions and measurements were avoided for the Multifidus. The collected data for these electrodes, however, demonstrated exactly the same trends as those observed for the data of other electrodes at the L1 level (Fig. 4.5) with mean normalised values being almost always greater (at most by 6%) than those measured for the LGPT markers (Fig. 4.5).

Regarding the model study, the assumption of rigid body motion at the T1-T12 segments (upper torso) was confirmed, in agreement with others (Nussbaum and

Chaffin, 1996), by measuring nearly equal rotations at lines attaching either the markers T12 to T5 or markers T12 to T1 (Arjmand and Shirazi-Adl, 2006). The geometry of muscle fascicles was modeled by straight lines with no initial strain before applying gravity load. This assumption might be a crude one for global extensor muscles attaching the pelvis to the upper thorax when the lumbar spine approaches full flexion in which case these muscles wrap around the other surrounding tissues. The likely effect of wrapping on results is currently under investigation in an on going project. The transverse abdominus, latissimus dorsi, lumbodorsal fascia, and intersegmental/multisegmental muscles were neglected. The transverse abdominus has been recognized both to unload the spine indirectly by increasing intra-abdominal pressure (Daggfeldt and Thorstensson, 2003) and to contribute to the spinal stability during lifting (Hodges, 1999; Hodges and Richardson, 1996; Pietrek et al., 2002). Latissimus dorsi has been known to produce trunk extensor moment via the lumbodorsal fascia, a contribution suggested not to be sizable during lifting tasks (Bogduk et al., 1998; McGill and Norman, 1988). The intersegmental and multisegmental muscles have been reported not to play important stabilizing role (Crisco and Panjabi, 1991).

For qualitative validation of predicted muscle forces, the maximum allowable muscle stress of 0.6 MPa was assumed for all muscles. The passive tension-length relationship was also assumed to be the same despite the fact that the specific architecture of each muscle could influence this relationship (Woittiez et al., 1984). Moreover, the effect of muscle activation level on this passive relationship was neglected (Lee and Herzog, 2002; Rassier et al., 1999, 2003). For the stability analyses, the muscle stiffness coefficient, q , was chosen the same for all muscles while a linear stiffness-force relation, rather than a nonlinear one (Cholewicki and McGill, 1995; Shadmehr and Arbib, 1992), was considered. It is important to emphasize that the passive load-length and stiffness relationships considered for muscles in the current study have absolutely no bearing at all on the predicted spinal loads (shear and compression forces, sagittal moments) and total muscle forces. The partitioning of the

calculated muscle forces into active and passive components in post-processing of the data would, however, be influenced by the choice of passive force-length relation while the muscle stiffness coefficient q would only affect the system stability margin. The controversial mechanical role of the intra-abdominal pressure (IAP) in unloading the spine and generating a net extensor moment as well as its likely stabilizing role during flexion tasks were not considered (Arjmand et al., 2001; Cholewicki et al., 2002; Daggfeldt and Thorstensson, 1997, 2003). The relatively low co-activity of abdominal muscles observed in this work, specially in free style postures (Fig. 4.5), was not considered in this study. The cost function of minimum sum of cubed muscle stresses used in the optimization algorithm has been recognized to be in agreement with the EMG data (Hughes et al., 1994; Van Dieen, 1997). Moreover, the convergence of the nonlinear optimization solution on a global minimum was assured in this study by solving the optimization problem analytically using Lagrange Multiplier Method.

4.5.2 Lumbar posture and muscle activities

Active force in almost all extensor muscles increased from the kyphotic postures to the lordotic ones (Table 4.3 and Fig. 4.5), a trend that disappeared for the global muscles when 180 N was added in hands. It appeared that the local muscles attached to lumbar vertebrae acted primarily to control the lumbar posture and, hence, experienced substantially greater activities in lordotic postures. To resist only slightly smaller net external moments, the smaller active force in kyphotic postures was, however, compensated by larger contributions from passive components (Table 4.3 and Fig. 4.7). The moment-carrying role of the ligamentous spine was much greater in kyphotic postures (27 to 44 N-m) than that in lordotic postures (16 to 37 N-m) (Fig. 4.7). The contribution of passive muscle forces in kyphotic postures was also crucial (Table 4.3 and Fig. 4.7); a role that has been neglected in previous works when suggesting that in kyphotic postures the subjects hang on their ligaments (Hart et al., 1987) or the spine is without much muscular support (Holmes et al., 1992). In agreement with previous observations (Tveit et al., 1994), the lever arm of global muscles increased in lordotic

postures (by 6-15% compared to the free style) whereas they decreased in kyphotic postures (by 3-7% compared to the free style). Finally, *in vivo* measurements indicated that EMG activities in abdominal muscles were the least in the free style posture as compared with lordotic and kyphotic postures which could partly be due to the fact that the subjects lacked training in efficient voluntary control of their lumbar curvature.

4.5.3 Lumbar posture and spinal loads

Maximum compression and shear forces primarily occurred at the distal L5-S1 segmental level and were larger in lordotic postures than in kyphotic ones (Table 4.4). The shear forces decreased substantially by 23-36% while the compression forces decreased by only 2-14% as the lordotic posture changed to a kyphotic one. At the L5-S1 level and under identical external loading, an increase in trunk flexion substantially increased compression force and flexion moment while the shear force remained nearly unchanged. On the other hand, under identical trunk flexion angle, all these loads significantly increased as the external load of 180 N was added in hands (Table 4.4).

At the uppermost T12-L2 and lowermost L5-S1 disc mid-height planes, muscle forces generated shear forces in the anterior direction adding to those due to external load/gravity (Fig. 4.8). At the L4-L5 disc mid-height plane, however, global thoracic and local lumbar muscles generated posterior shear forces in opposition to the anterior shear force of gravity/external loads (Fig. 4.8). This alteration from the L5-S1 level to the L4-L5 level was due to the less oblique inclination (by $\sim 10-12^\circ$) of the disc mid-height plane at the latter level. The beneficial role of the lumbar extensor muscles in reducing the anterior shear force in lordotic postures as suggested elsewhere (Potvin et al., 1991a, b) does not, hence, hold true at the L5-S1 level which is subjected to the greatest shear force and, hence, risk of shear injury. In fact at this level, the lordotic posture, by causing much greater pelvic rotation, substantially increased the disc inclination and, hence, the shear component of muscle forces and gravity/external loads in the anterior direction (Fig. 4.8). The beneficial role of back muscles in counterbalancing the

gravity/external load-caused anterior shear forces appeared to decrease from the L4-L5 level upward to L2-L3 level and then to reverse at the uppermost T12-L2 levels.

Apart from the disc inclination, the relative magnitude of shear and compression forces is also influenced by the changes in the line of action (LOA) of extensor muscles in the sagittal plane which varies as the lumbar posture changes. For instance, the LOA of both global and local extensor muscles, in accordance with *in vivo* data (McGill et al., 2000), became more horizontal (by up to $\sim 4^\circ$ in global muscles and $\sim 8^\circ$ in local muscles) as the kyphotic posture changed to the lordotic one. These changes diminish the ability of extensor muscles in supporting segmental anterior shear force in kyphotic postures. The prediction of greater anterior shear forces at the upper levels (Table 4.4 and Fig. 4.8) in kyphotic postures is in accordance with these changes as the disc inclination at these levels remained nearly the same in both lordotic and kyphotic postures.

4.5.4 Lumbar posture and spinal stability

Calculation of relatively small critical q values in lifting irrespective of the lumbar posture (Fig. 4.6), as compared with those in standing postures (Arjmand and Shirazi-Adl, 2006; El-Rich et al., 2004), demonstrate that the spinal stability is of a lesser concern in tasks involving forward flexion. In the presence of 180 N in hands, no muscle stiffness was at all required as the system stability was adequately maintained by passive stiffness of motion segments that nonlinearly increased with axial compression and flexion angle. As far as the lumbar postures are concerned, the lordotic posture was found to somewhat improve the system stability, in agreement with earlier suggestions (Vakos et al., 1994), which could be due to the greater activity of extensor muscles recorded in these postures (Fig. 4.5). The system stability, however, should not be associated solely with the activity in muscles as the passive stiffness of the ligamentous spine and muscles as well as the position of load also play important roles (Arjmand and Shirazi-Adl, 2006).

4.5.5 Lordotic, kyphotic, or free-style posture?

Under the loads and trunk flexion angles considered in this study, the maximum segmental anterior shear and compression forces occurred in the lordotic posture while the maximum segmental flexion moment occurred in the kyphotic posture. None of these loads, however, exceeded the injury tolerant levels of lumbar segments reported in the literature (Cripton et al., 1995; McGill, 1997). Neither posture can, hence based on the results of this study, be indicated as the one to be associated with a substantial increase in the risk of injury to the ligamentous spine. The greater activity in extensor muscles found in lordotic postures suggests the vulnerability of these muscles to fatigue under repetitive or sustained loading conditions when carried out with lordotic lumbar spine. The kyphotic postures exploited primarily the passive ligamentous/muscle force components while the active muscle forces played more important role in lordotic postures. Although the system stability was of a lesser concern in forward flexion postures as compared with upright postures, the lordotic posture was found to somewhat improve the stability margin. Finally, kinematics, muscle forces and internal loads for the free style posture in which subjects performed static lifting with no instruction on the lumbar posture appeared to be much closer to results for the kyphotic postures than to those for the lordotic ones. Notwithstanding the need for additional investigations, the current study appears to advocate the free style posture or a posture with moderate flexion as the posture of choice in static lifting tasks when considering both internal spinal loads and active/passive muscle forces.

4.6 ACKNOWLEDGEMENT

The work is supported by grants from the NSERC-Canada and the IRSST-Québec. The assistance of M. Trottier and A. Mitnitski in collection and analysis of *in vivo* data is gratefully appreciated.

4.7 REFERENCES

Adams MA, McNally DS, Chinn H, Dolan P. Posture and the compressive strength of the lumbar spine. *Clin Biomech* 1994;9(1):5-14.

Andersson GB. Epidemiologic aspects on low-back pain in industry. *Spine* 1981;6(1):53-60.

Arjmand N, Shirazi-Adl A. Model and in vivo studies on human trunk load partitioning and stability in isometric forward flexions. *J Biomech* 2006; 39(3):510-21.

Arjmand N, Shirazi-Adl A, Parnianpour M. A finite element model study on the role of trunk muscles in generating intra-abdominal pressure. *Biomedical Engineering-Applications, Basis & Communications* 2001;13:23-31.

Aspden RM. The spine as an arch. A new mathematical model. *Spine* 1989; 14:266-74.

Bergmark A. Stability of the lumbar spine -A study in mechanical engineering. *Acta Orthopaedica Scandinavia Supplementum* 1989;230:1-54.

Bogduk N, Johnson G, Spalding D. The morphology and biomechanics of latissimus dorsi. *Clin Biomech* 1998;13(6):377-385.

Bogduk N, Macintosh JE, Pearcy MJ. A universal model of the lumbar back muscles in the upright position. *Spine* 1992;17:897-913.

Cholewicki J, Ivancic PC, Radebold A. Can increased intra-abdominal pressure in humans be decoupled from trunk muscle co-contraction during steady state isometric exertions? *European Journal of Applied Physiology* 2002;87:127-33.

Cholewicki J, McGill SM. Lumbar posterior ligament involvement during extremely heavy lifts estimated from fluoroscopic measurements. *J Biomech* 1992;25(1):17-28.

Cholewicki J, McGill SM. Relationship between muscle force and stiffness in the whole mammalian muscle: A simulation study. *J Biomech Eng* 1995;117:339-342.

Cripton P, Berlemen U, Visarino H, Begeman PC, Nolte LP, Prasad P. Response of the lumbar spine due to shear loading. Proc. Symp. On Injury Prevention through Biomechanics, 4-5 May 1995, Wayne State University.

Crisco III JJ, Panjabi MM. The intersegmental and multisegmental muscles of the lumbar spine –A biomechanical model comparing lateral stabilizing potential. *Spine* 1991;16:793-799.

Daggfeldt K, Thorstensson A. The role of intra-abdominal pressure in spinal unloading. *J Biomech* 1997;30:1149-55.

Daggfeldt K, Thorstensson A. The mechanics of back-extensor torque production about the lumbar spine. *J Biomech* 2003;36:815-25.

Damkot DK, Pope MH, Lord J, Frymoyer JW. The relationship between work history, work environment and low-back pain in men. *Spine* 1984;9(4):395-9.

Davis J, Kaufman KR, Lieber RL. Correlation between active and passive isometric force and intramuscular pressure in the isolated rabbit tibialis anterior muscle. *J Biomech* 2003;36:505-12.

Davis KG, Marras WS. The effects of motion on trunk biomechanics. *Clin Biomech* 2000;15:703-17.

Delitto RS, Rose SJ. An electromyographic analysis of two techniques for squat lifting and lowering. *Phys Ther* 1992;72:438-48.

Delitto RS, Rose SJ, Apts DW. Electromyographic analysis of two techniques for squat lifting. *Phys Ther* 1987;67:1329-34.

Dvorak J, Panjabi MM, Chang DG, Theiler R, Grob D. Functional radiographic diagnosis of the lumbar spine. Flexion-extension and lateral bending. *Spine* 1991;16:562-71.

El-Rich M, Shirazi-Adl A, Arjmand N. Muscle activity, internal loads and stability of the human spine in standing postures: combined model-in vivo studies. *Spine* 2004; 29: 2633-42.

Frobin W, Brinckmann P, Leivseth G, Biggemann M, Reikeras O. Precision measurement of segmental motion from flexion-extension radiographs of the lumbar spine. *Clin Biomech* 1996;11:457-465.

Frymoyer JW, Pope MH, Clements JH, Wilder DG, MacPherson B, Ashikaga T. Risk factors in low-back pain. An epidemiological survey. *J Bone Joint Surg Am* 1983;65(2):213-8.

Gagnon D, Larivière C, Loisel P. Comparative ability of EMG, optimisation, and hybrid modelling approaches to predict trunk muscle forces and lumbar spine loading during dynamic sagittal plane lifting. *Clin Biomech* 2001;16:359-372.

Garg A, Herrin GD. Stoop or squat, a biomechanical and metabolical evaluation. *A.I.I.E. Transactions* 1979;11:293-302.

Gracovetsky S, Farfan H, Helleur C. The abdominal mechanism. *Spine* 1985;10:317-24.

Gracovetsky S, Farfan HF, Lamy C. The mechanism of the lumbar spine. *Spine* 1981;6:249-62.

Guzik DC, Keller TS, Szpalski M, Park JH, Spengler DM. A biomechanical model of the lumbar spine during upright isometric flexion, extension, and lateral bending. *Spine* 1996;21:427-33.

Hagen KB, Hallen J, Harms-Ringdahl K. Physiological and subjective responses to maximal repetitive lifting employing stoop and squat technique. *Eur J Appl Physiol Occup Physiol* 1993;67:291-7.

Hart DL, Stobbe TJ, Jaraiedi M. Effect of lumbar posture on lifting. *Spine* 1987;12:138-45.

Hodges PW. Is there a role for transversus abdominis in lumbo-pelvic stability? *Manual Therapy* 1999;4:74-86.

Hodges PW, Richardson CA. Inefficient muscular stabilization of the lumbar spine associated with low back pain. A motor control evaluation of transversus abdominis. *Spine* 1996;21:2640-50.

Holmes JA, Damaser MS, Lehman SL. Erector spinae activation and movement dynamics about the lumbar spine in lordotic and kyphotic squat-lifting. *Spine* 1992;17:327-34.

Hoogendoorn WE, Bongers PM, de Vet HC, Douwes M, Koes BW, Miedema MC, Ariens GA, Bouter LM. Flexion and rotation of the trunk and lifting at work are risk

factors for low back pain: results of a prospective cohort study. *Spine* 2000;25:3087-92.

Hughes RE, Chaffin DB, Lavender SA, Andersson GBJ. Evaluation of muscle force prediction models of the lumbar trunk using surface electromyography. *J Orthop Res* 1994;12:689-698.

Kelsey JL, Githens PB, White AA 3rd, Holford TR, Walter SD, O'Connor T, Ostfeld AM, Weil U, Southwick WO, Calogero JA. An epidemiologic study of lifting and twisting on the job and risk for acute prolapsed lumbar intervertebral disc. *J Orthop Res* 1984;2(1):61-6.

Kiefer A, Shirazi-Adl A, Parnianpour M. Synergy of human spine in neutral postures. *European Spine J* 1998;7:471-479.

Lee YH, Chiou WK, Chen WJ, Lee MY, Lin YH. Predictive model of intersegmental mobility of lumbar spine in the sagittal plane from skin markers. *Clin Biomech* 1995;10:413-420.

Lee HD, Herzog W. Force enhancement following muscle stretch of electrically stimulated and voluntarily activated human adductor pollicis. *Journal of Physiology* 2002;545,321-30.

Marras WS, Lavender SA, Leurgans SE, Fathallah FA, Ferguson SA, Allread WG, Rajulu SL. Biomechanical risk factors for occupationally related low back disorders. *Ergonomics* 1995;38(2):377-410.

McGill SM. Electromyographic activity of the abdominal and low back musculature during the generation of isometric and dynamic axial trunk torque: Implications for lumbar mechanics. *J Orthop Res* 1991;9:91-103.

McGill SM. The biomechanics of low back injury: implications on current practice in industry and the clinic. *J Biomech* 1997;30:465-75.

McGill SM, Hughson RL, Parks K. Changes in lumbar lordosis modify the role of the extensor muscles. *Clin Biomech* 2000;15:777-80.

McGill SM, Norman RW. Potential of lumbodorsal fascia forces to generate back extension moments during squat lifts. *J Biomed Eng* 1988;10(4):312-8.

McGill SM, van Wijk MJ, Axler CT, Gletsu M. Studies of spinal shrinkage to evaluate low-back loading in the workplace. *Ergonomics* 1996;39:92-102.

Mouton LJ, Hof AL, Jongh HJD, Eisma WH. Influence of posture on the relation between surface electromyogram amplitude and back muscle moment: consequences for the use of surface electromyogram to measure back load. *Clin Biomech* 1991;6:245-51.

Nachemson A. Disc pressure measurements. *Spine* 1981;6:93-97.

National Institute for Occupational Safety and Health. A work practices guide for manual lifting. Cincinnati, Ohio, U.S. Department of Health and Human Services (NIOSH), 1981, pp. 30-43 (Technical report no. 81-122).

National Institute for Occupational Safety and Health (NIOSH). Musculoskeletal disorders and workplace factors. U.S. Dept. of Health and Human Services, 1997.

Norman R, Wells R, Neumann P, Frank J, Shannon H, Kerr M. A comparison of peak vs cumulative physical work exposure risk factors for the reporting of low back pain in the automotive industry. *Clin Biomech* 1998;13(8):561-573.

Nussbaum MA, Chaffin DB. Development and evaluation of a scalable and deformable geometric model of the human torso. *Clin Biomech* 1996;11:25-34.

O'Sullivan PB, Grahamslaw KM, Kendell M, Lapenskie SC, Moller NE, Richards KV. The effect of different standing and sitting postures on trunk muscle activity in a pain-free population. *Spine* 2002;27:1238-1244.

Oxland T, Lin RM, Panjabi M. Three-dimensional mechanical properties of the thoracolumbar junction. *J Orthop Res* 1992;10:573-580.

Patwardhan AG, Havey RM, Carandang G, Simonds J, Voronov LI, Ghanayem AJ, Meade KP, Gavin TM, Paxinos O. Effect of compressive follower preload on the flexion-extension response of the human lumbar spine. *J Orthop Res* 2003;21:540-6.

Pearcy M, Portek I, Shepherd J. Three-dimensional x-ray analysis of normal movement in the lumbar spine. *Spine* 1984;9:294-7.

Pearsall DJ. Segmental inertial properties of the human trunk as determined from computer tomography and magnetic resonance imagery. PhD thesis. Queen's University, Kingston, Ontario;1994.

Pietrek M, Sheikhzadeh A, Nordin M, Hagins M. Biomechanical modeling of intra-abdominal pressure generation should include the transversus abdominis. *J Biomech* 2000;33,787-790.

Plamondon A, Gagnon M, Maurais G. Application of a stereoradiographic method for the study of intervertebral motion. *Spine* 1988;13:1027-32.

Pop DG. Analyse non linéaire par éléments finis du système actif passif de la colonne vertébrale humaine. M.Sc.A. Dissertation. Génie mécanique, École Polytechnique, Montréal, Québec; 2001.

Potvin JR, McGill SM, Norman RW. Trunk muscle and lumbar ligament contributions to dynamic lifts with varying degrees of trunk flexion. *Spine* 1991a;16:1099-107.

Potvin JR, Norman RW, McGill SM. Reduction in anterior shear forces on the L4/L5 disc by the lumbar musculature. *Clin Biomech* 1991b;6(2):88-96.

Potvin JR, Norman RW, McGill SM. Mechanically corrected EMG for the continuous estimation of erector spinae muscle loading during repetitive lifting. *Eur J Appl Physiol Occup Physiol* 1996;74:119-32.

Raikova RT, Prilutsky BI. Sensitivity of predicted muscle forces to parameters of the optimization-based human leg model revealed by analytical and numerical analyses. *J Biomech* 2001;34:1243-1255.

Rassier DE, Herzog W, Wakeling J, Syme DA. Stretch-induced, steady-state force enhancement in single skeletal muscle fibers exceeds the isometric force at optimum fiber length. *J Biomech* 2003;36(9):1309-16.

Rassier DE, MacIntosh BR, Herzog W. Length dependence of active force production in skeletal muscle. *Journal of Applied Physiology* 1999;86(5),1445-57.

Reeves NP, Cholewicki J. Modeling the human lumbar spine for assessing spinal loads, stability, and risk of injury. *Crit Rev Biomed Eng* 2003;31:73-139.

Rohlmann A, Arntz U, Graichen F, Bergmann G. Loads on an internal spinal fixation device during sitting. *J Biomech* 2001;34:989-993.

Rohlmann A, Graichen F, Bergmann G. Loads on an internal spinal fixation device during physical therapy. *Physical Therapy* 2002;82:44-52.

Shadmehr R, Arbib MA. A mathematical analysis of the force-stiffness characteristics of muscles in control of a single joint system. *Biological Cybernetics* 1992;66:463-477.

Shirazi-Adl A. Analysis of large compression loads on lumbar spine in flexion and in torsion using a novel wrapping element. *J Biomech* 2006, 39(2):267-75.

Shirazi-Adl A, El-Rich M, Pop DG, Parnianpour M. Spinal Muscle forces, internal loads and stability in standing under various postures and loads: applications of kinematics-based algorithm. *European Spine J* 2005, 14(4):381-92.

Shirazi-Adl A, Parnianpour M. Effect of changes in lordosis on mechanics of the lumbar spine-lumbar curvature in lifting. *J Spinal Disord* 1999;12:436-47.

Shirazi-Adl A, Sadouk S, Parnianpour M, Pop D, El-Rich M. Muscle force evaluation and the role of posture in human lumbar spine under compression. *European Spine J* 2002;11:519-526.

Sparto PJ, Parnianpour M. Estimation of trunk muscle forces and spinal loads during fatiguing repetitive trunk exertions. *Spine* 1998;23:423-429.

Stokes IA, Gardner-Morse M. Quantitative anatomy of the lumbar musculature. *J Biomech* 1999;32:311-316.

Stokes IA, Gardner-Morse M. Spinal stiffness increases with axial load: another stabilizing consequence of muscle action. *Journal of Electromyography and Kinesiology* 2003;13:397-402.

Stokes IA, Henry SM, Single RM. Surface EMG electrodes do not accurately record from lumbar multifidus muscles. *Clin Biomech* 2003;18:9-13.

Takashima ST, Singh SP, Haderspeck KA, Schultz AB. A model for semi-quantitative studies of muscle actions. *J Biomech* 1979;12:929-939.

Troup JD, Martin JW, Lloyd DC. Back pain in industry. A prospective survey. *Spine* 1981;6(1):61-9.

Tveit P, Daggfeldt K, Hetland S, Thorstensson A. Erector spinae lever arm length variations with changes in spinal curvature. *Spine* 1994;19:199-204.

Vakos JP, Nitz AJ, Threlkeld AJ, Shapiro R, Horn T. Electromyographic activity of selected trunk and hip muscles during a squat lift: Effect of varying the lumbar posture. *Spine* 1994;19:687-95.

Van Dieen JH. Are recruitment patterns of the trunk musculature compatible with a synergy based on the maximization of endurance? *J Biomech* 1997;30:1095-1100.

Van Dieen JH, Hoozemans MJ, Toussaint HM. Stoop or squat: a review of biomechanical studies on lifting technique. *Clin Biomech* 1999;14:685-96.

Van Dieen JH, Toussaint HM. Spinal shrinkage as a parameter of functional load. *Spine* 1993;18:1504-14.

Varma KM, Porter RW. Sudden onset of back pain. *Eur Spine J* 1995;4(3):145-7.

Waters TR, Putz-Anderson V, Garg A, Fine LJ. Revised NIOSH equation for the design and evaluation of manual lifting tasks. *Ergonomics* 1993;36(7):749-76.

Wilke HJ, Neef P, Caimi M, Hoogland T, Claes LE. New in vivo measurements of pressures in the intervertebral disc in daily life. *Spine* 1999;24:755-763.

Woittiez RD, Huijing PA, Boom HB, Rozendal RH. A three-dimensional muscle model: a quantified relation between form and function of skeletal muscles. *Journal of Morphology* 1984;182(1):95-113.

Yamamoto I, Panjabi M, Crisco T, Oxland T. Three-dimensional movements of the whole lumbar spine and lumbosacral joint. *Spine* 1989;14:1256-1260.

Zhang X, Xiong J. Model-guided derivation of lumbar vertebral kinematics in vivo reveals the difference between external marker-defined and internal segmental rotations. *J Biomech* 2003;36:9-17.

Table 4.1 Physiological cross sectional area (PCSA, mm²) and initial length (in brackets, mm) for muscles on each side of the spine at different insertion levels. ICPL: Iliocostalis Lumborum pars lumborum, ICPT: Iliocostalis Lumborum pars thoracic, IP: Iliopsoas, LGPL: Longissimus Thoracis pars lumborum, LGPT: Longissimus Thoracis pars thoracic, MF: Multifidus, QL: Quadratus Lumborum, IO: Internal Oblique, EO: External Oblique, and RA: Rectus Abdominus.

Local Muscles	ICPL	IP	LGPL	MF	QL
L1	108 (170)	252 (276)	79 (172)	96 (158)	88 (137)
L2	154 (118)	295 (241)	91 (132)	138 (135)	80 (104)
L3	182 (84)	334 (206)	103 (88)	211 (106)	75 (74)
L4	189 (50)	311 (169)	110 (52)	186 (82)	70 (46)
L5	-	182 (132)	116 (25)	134 (51)	-
Global Muscles	RA	EO	IO	ICPT	LGPT
T1-T12	567 (353)	1576 (239)	1345 (135)	600 (250)	1100 (297)

Table 4.2 Three-way analysis of variance for repeated measures for trunk muscle EMG activities during lifting tasks (values with statistical significance at $p<0.05$ are highlighted). ICPT: Iliocostalis Lumborum Pars Thoracic, LGPT: Longissimus Thoracis Pars Thoracic, MF: Multifidus, EO: External Oblique, and RA: Rectus Abdominus.

ANOVA	LGPT	ICPT	MF	EO	RA
T* (40° vs 65°)	0.91896	0.58610	0.80385	0.45781	0.17174
W* (0 vs 180N)	0.01555	0.00731	0.00967	0.00006	0.00331
P* (F† vs L† vs K†)	0.49660	0.08425	0.16325	0.04417	0.02556
T×W	0.60527	0.51487	0.92422	0.49953	0.56191
T×P	0.60426	0.88741	0.67970	0.64106	0.32868
W×P	0.64897	0.41444	0.40476	0.57909	0.03705
T×W×P	0.33142	0.49928	0.24299	0.55038	0.71228

*T: torso flexion, W: weight in hands, P: lumbar posture (free, lordotic and kyphotic)

† F: free, L: lordotic, K: kyphotic

Table 4.3 Predicted total (Ft), passive (Fp), and active (Fa=Ft - Fp; listed for global muscles) muscle forces at different segmental levels for various tasks (N). LGPT: Longissimus Thoracis Pars Thoracic, ICPT: Iliocostalis Lumborum Pars Thoracic, IP: Iliopsoas, GPL: Longissimus Thoracis Pars Lumborum, ICPL: Iliocostalis Lumborum Pars Lumborum, MF: Multifidus, QL: Quadratus Lumborum.

Muscle	Upper Attachment Level	Flexion 40°						Flexion 65°						
		0 N			180 N			0 N			180 N			
		F*	L*	K*	F	L	K	F	L	K	F	L	K	
LGPT	RIB	Ft	242	245	228	458	428	458	326	324	297	530	501	514
		Fp	68	41	84	64	45	74	88	63	98	71	57	75
ICPT	RIB	Fa	174	204	144	394	383	384	237	261	199	459	444	439
		Ft	107	106	103	205	188	208	149	144	138	243	224	238
IP	L1	Fp	54	31	68	51	35	62	74	49	84	60	46	65
		Ft	29	38	29	62	64	70	32	42	34	71	70	76
L1		Fp	0	0	0	0	0	0	0	0	0	0	0	0
		Ft	15	19	14	34	34	39	20	25	21	46	45	50
L2		Fp	10	5	13	10	6	13	16	9	18	14	10	14
		Ft	17	18	15	30	29	30	23	25	23	42	40	43
L3		Fp	10	4	14	10	6	13	16	9	19	14	9	15
		Ft	17	16	15	24	25	21	22	23	21	32	33	31
L4		Fp	10	4	15	11	5	14	18	9	21	15	9	16
		Ft	14	19	15	20	27	17	18	22	20	24	30	24
L5		Fp	10	4	14	10	5	13	18	9	20	14	8	15
		Ft	18	41	8	22	61	10	9	35	7	7	41	4
		Fp	3	1	4	3	1	3	5	2	6	4	2	4

ICPL	L1	Ft	24	31	23	55	55	64	33	40	36	74	73	81
	L2	Fp	16	8	21	17	11	21	25	15	29	22	16	24
	Ft	Ft	38	40	35	67	65	67	52	56	51	94	91	97
	L3	Fp	23	10	33	25	14	32	39	21	46	34	23	37
	L4	Ft	31	43	29	46	61	39	40	49	41	54	67	54
		Fp	20	8	29	21	11	28	36	18	41	30	19	32
	L1	Ft	27	34	30	60	60	70	36	44	41	81	80	88
	L2	Fp	22	11	30	24	15	30	35	21	41	31	22	34
	L3	Fp	26	12	37	29	16	37	44	24	51	39	26	42
	L4	Ft	63	61	52	91	93	81	82	88	74	123	123	120
MF	L1	Fp	28	11	42	32	16	43	51	26	61	45	28	49
	L2	Ft	40	54	34	58	77	51	52	63	49	70	86	69
	L3	Fp	15	6	23	17	9	23	28	14	33	25	15	26
	L4	Ft	32	72	15	39	80	17	15	61	12	13	73	6
	L5	Fp	4	2	5	4	2	5	6	3	7	5	3	5
	L1	Ft	17	22	19	39	39	45	24	29	23	53	53	57
	L2	Fp	6	3	9	6	3	8	11	5	13	8	5	9
	L3	Ft	14	14	13	24	24	24	19	20	19	34	33	35
	L4	Fp	7	10	8	10	14	9	11	5	14	9	5	10
		Fp	5	2	8	5	2	7	10	4	12	7	4	8

*F: free, L: lordotic, K: kyphotic

Table 4.4 Predicted internal loads in passive ligamentous spine at various levels for static lifting tasks $\pm 180\text{ N}$ in hands for different lumbar postures.

Disc	Spinal Loads	Flexion 40°						Flexion 65°					
		0 N			180 N			0 N			180 N		
		F*	L*	K*	F	L	K	F	L	K	F	L	K
T12-L1	S†	250	215	264	490	423	523	408	355	412	672	600	685
	C†	933	940	895	1679	1592	1680	1101	1095	1021	1781	1696	1738
	M†	18	15	22	22	18	27	24	19	29	27	23	31
L1-L2	S	224	194	238	439	379	477	380	338	388	637	566	654
	C	1171	1231	1143	2186	2103	2265	1406	1456	1350	2444	2345	2460
	M	22	16	26	28	22	32	31	23	35	36	29	39
L2-L3	S	111	92	121	202	173	220	224	192	229	338	298	343
	C	1414	1476	1370	2606	2505	2690	1737	1803	1682	3039	2908	3078
	M	21	14	26	29	20	34	33	22	37	39	30	42
L3-L4	S	173	195	163	277	294	266	256	267	245	365	369	352
	C	1669	1718	1592	2971	2871	3020	2067	2148	1993	3528	3396	3556
	M	17	10	23	25	16	32	30	18	35	36	26	40
L4-L5	S	95	172	54	73	170	7	73	153	41	17	108	-24
	C	1862	1957	1771	3250	3218	3271	2319	2436	2250	3859	3796	3884
	M	17	9	22	24	15	30	29	18	33	35	25	38
L5-S1	S	502	649	413	726	883	622	506	677	441	708	858	659
	C	1912	2089	1797	3308	3376	3290	2332	2545	2266	3850	3943	3865
	M	19	12	24	27	19	31	32	21	34	38	29	39

* F: free, L: lordotic, K: kyphotic

† S: local shear force (N), positive for anterior; C: local axial compression (N); M: sagittal moment, positive for flexion (Nm).

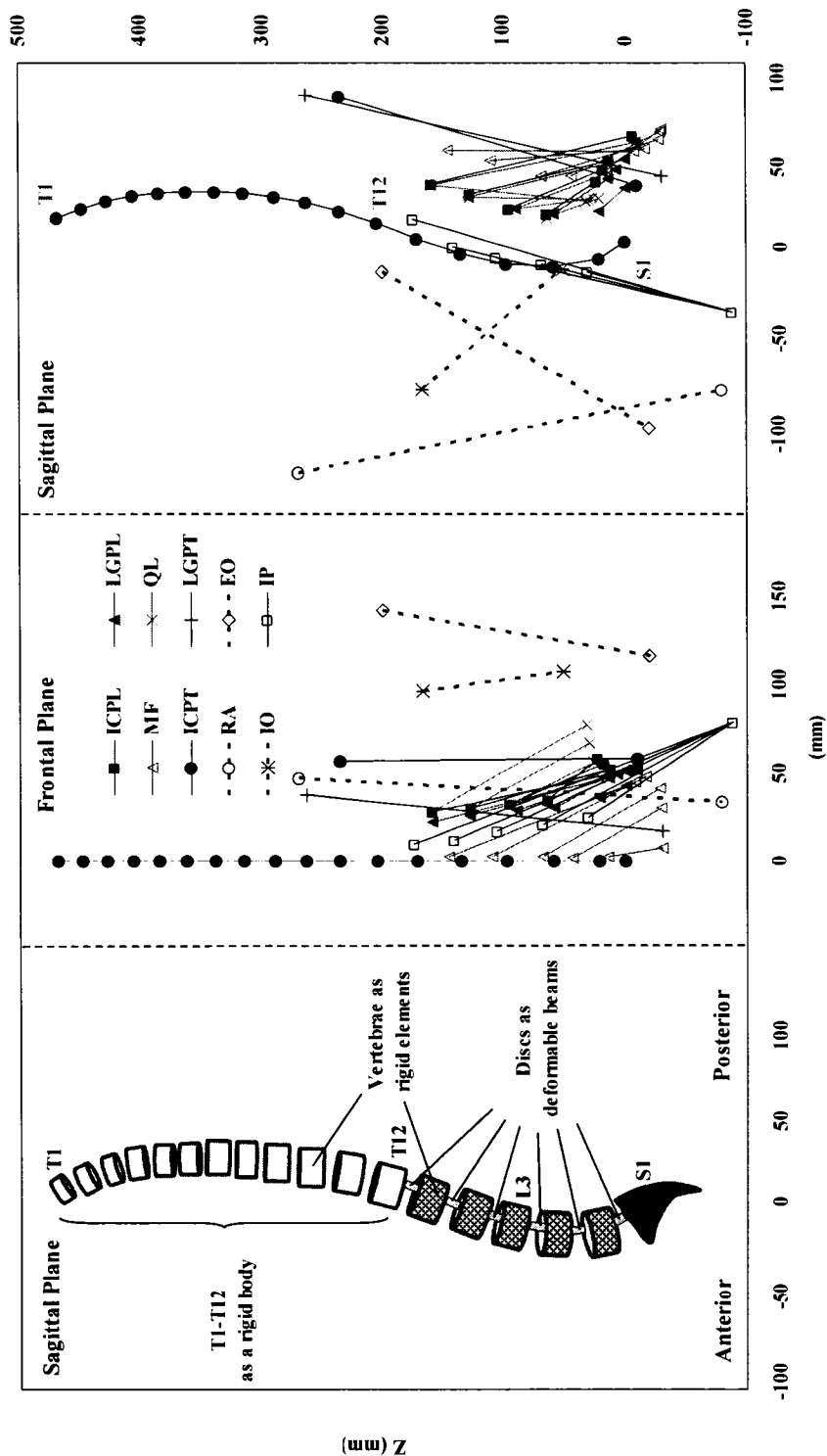


Fig. 4.1 The FE model as well as representation of global and local musculatures in the sagittal and frontal planes used in the model. Only fascicles on one side have been shown. ICPL: Iliocostalis Lumborum pars lumborum, ICPT: Iliocostalis Lumborum pars thoracic, IP: Iliopsoas, GPL: Longissimus Thoracis pars lumborum, LGPT: Longissimus Thoracis pars thoracic, MF: Multifidus, QL: Quadratus Lumborum, IO: Internal Oblique, EO: External oblique, and RA: Rectus Abdominus.

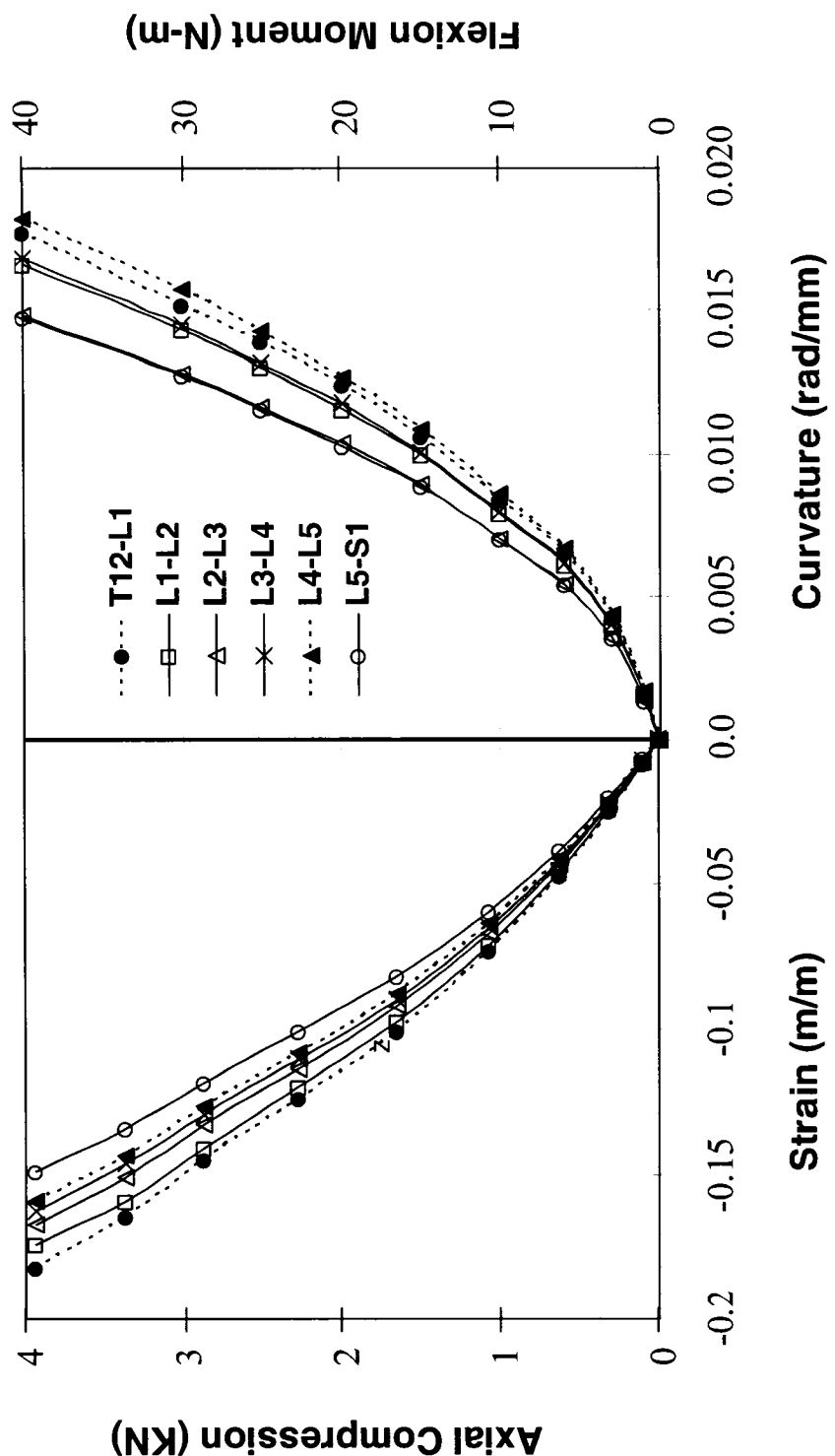


Fig. 4.2 Nonlinear stiffness properties of motion segments at different levels; axial compression force-axial strain on the left and flexion moment-curvature under large compression preloads (~2700 N) on the right.

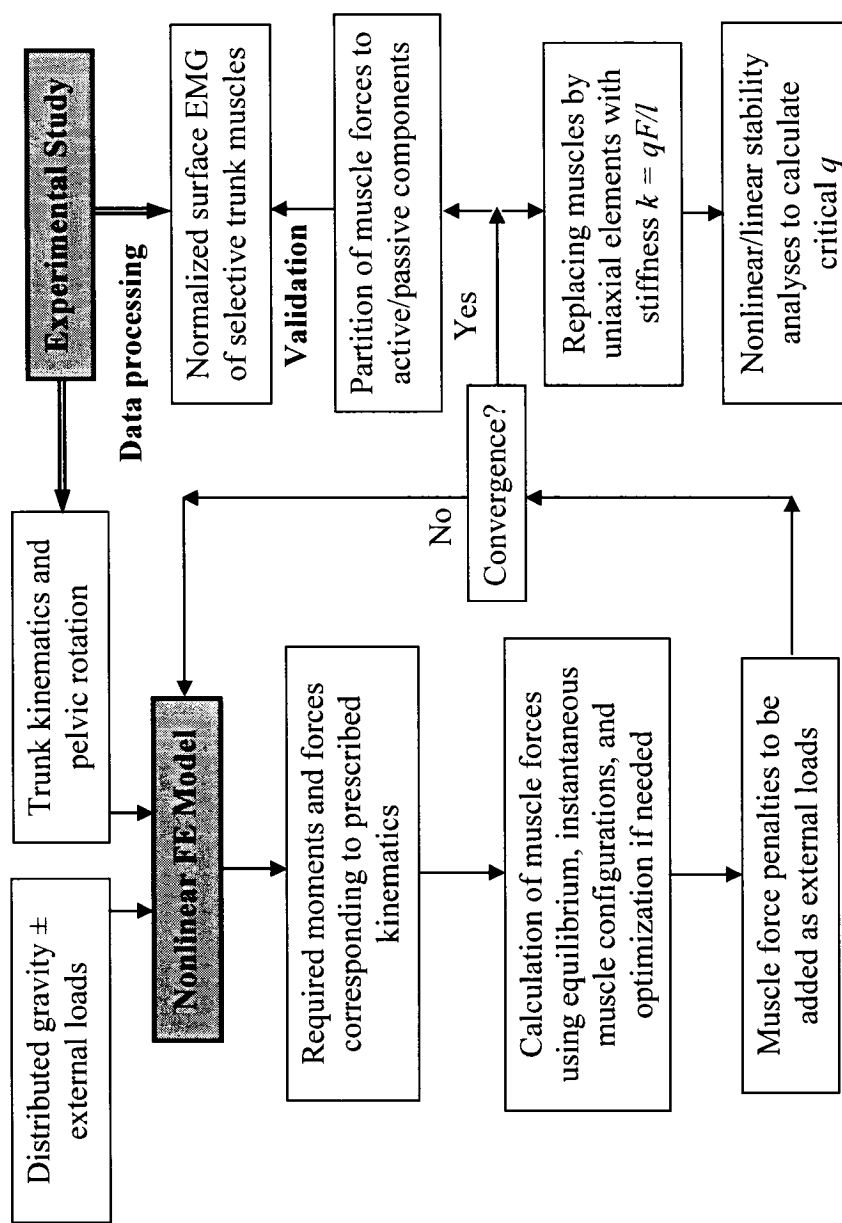


Fig. 4.3 Flow-chart for the application of the Kinematics-based approach and determination of trunk muscle forces, internal loads and stability margin of the spine. The moments required for the prescribed rotations were used in a separate algorithm to calculate muscle forces at each level. Axial compression and horizontal shear force components (i.e., penalties) of these muscle forces were then considered in the finite element model as additional updated external loads. This iterative approach was continued at each load step till convergence was reached.

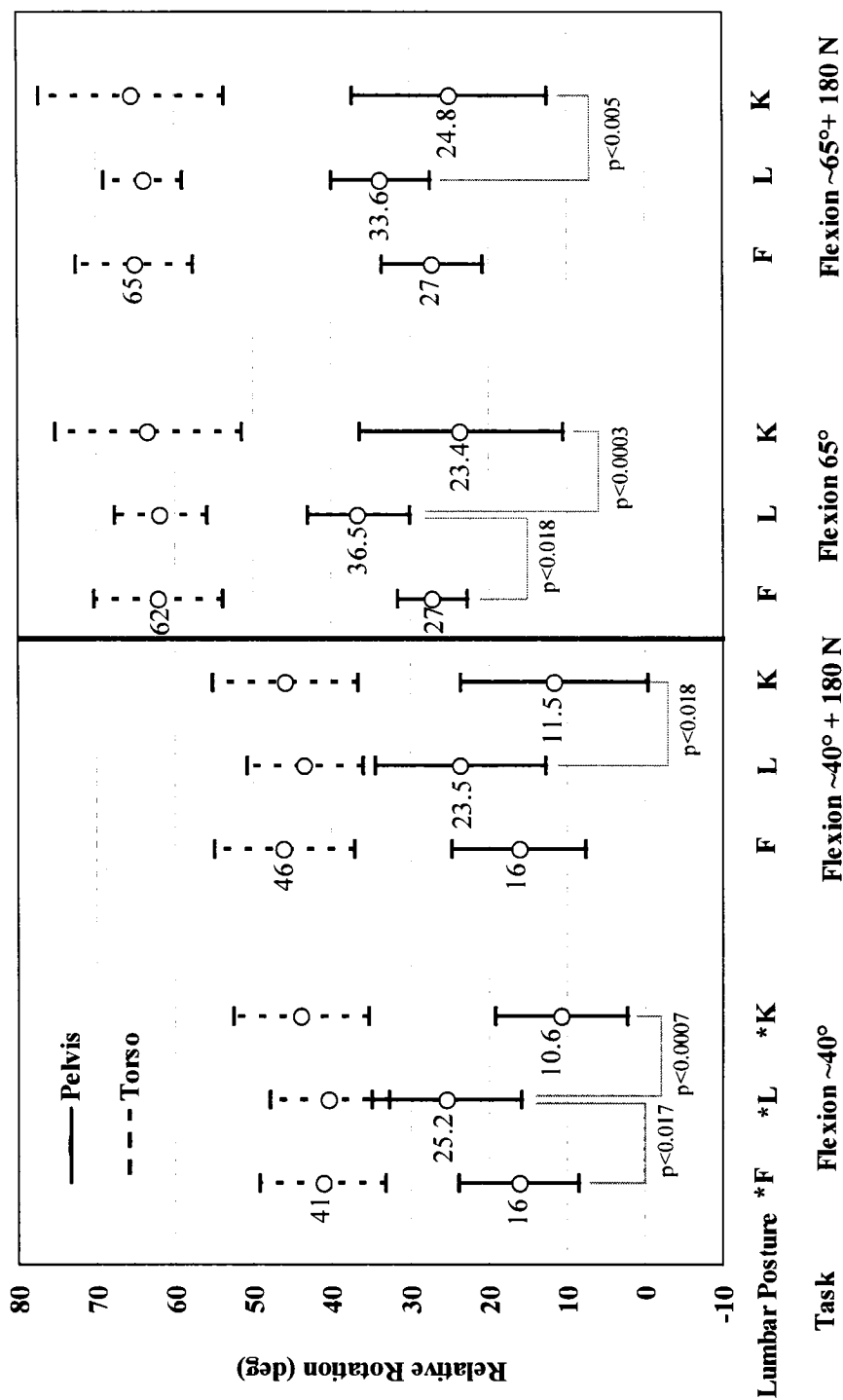


Fig. 4.4 *In vivo* measured (mean \pm SD) pelvic and torso rotations for different lifting tasks and postures. Mean rotation values as prescribed in the FE model for various cases as well as significant p-levels are also listed.

*F: free, L: lordotic, K: kyphotic

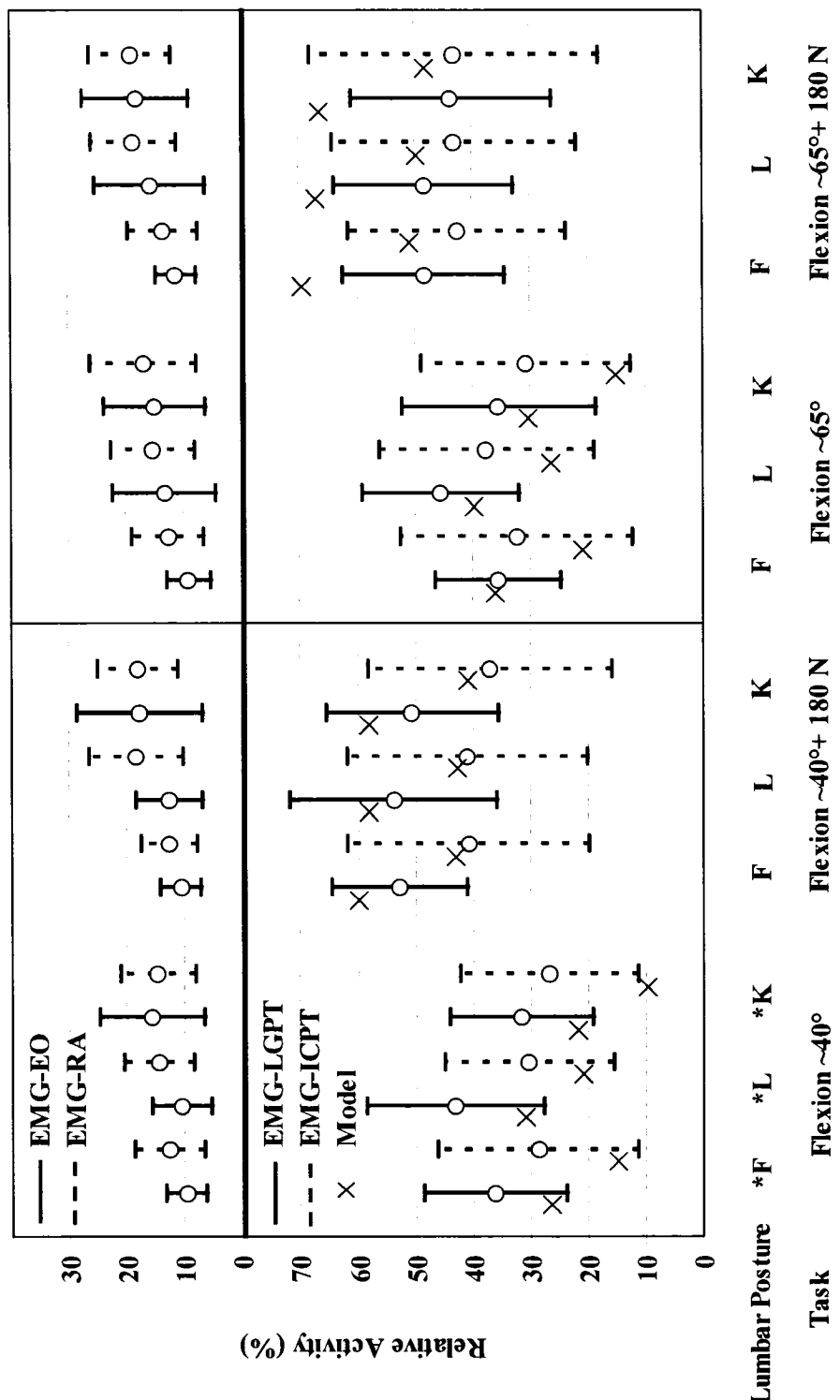


Fig. 4.5 *In vivo* measured normalized EMG activity (mean \pm SD) of extensor and abdominal muscles for different lifting tasks. The predicted normalized force in extensor muscles is also shown. ICPT: Iliocostalis Lumborum Pars Thoracic, LGPT: Longissimus Thoracis Pars Thoracic, EO: External Oblique, and RA: Rectus Abdominus. *F: free, L: lordotic, K: kyphotic

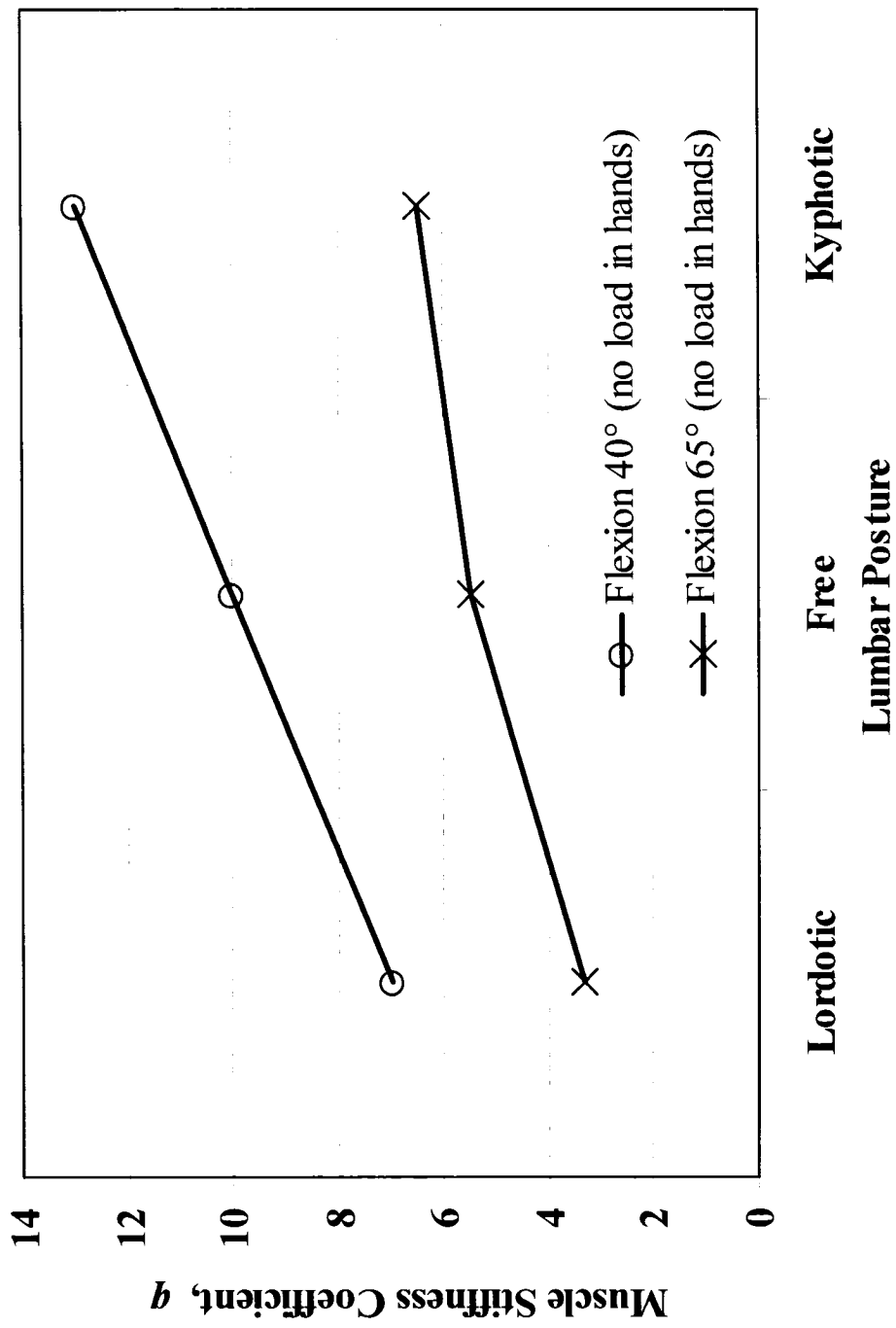


Fig. 4.6 Variation of the critical muscle stiffness coefficient, q , with lumbar posture for two flexed tasks (~ 40 and 65°) without external load in hands

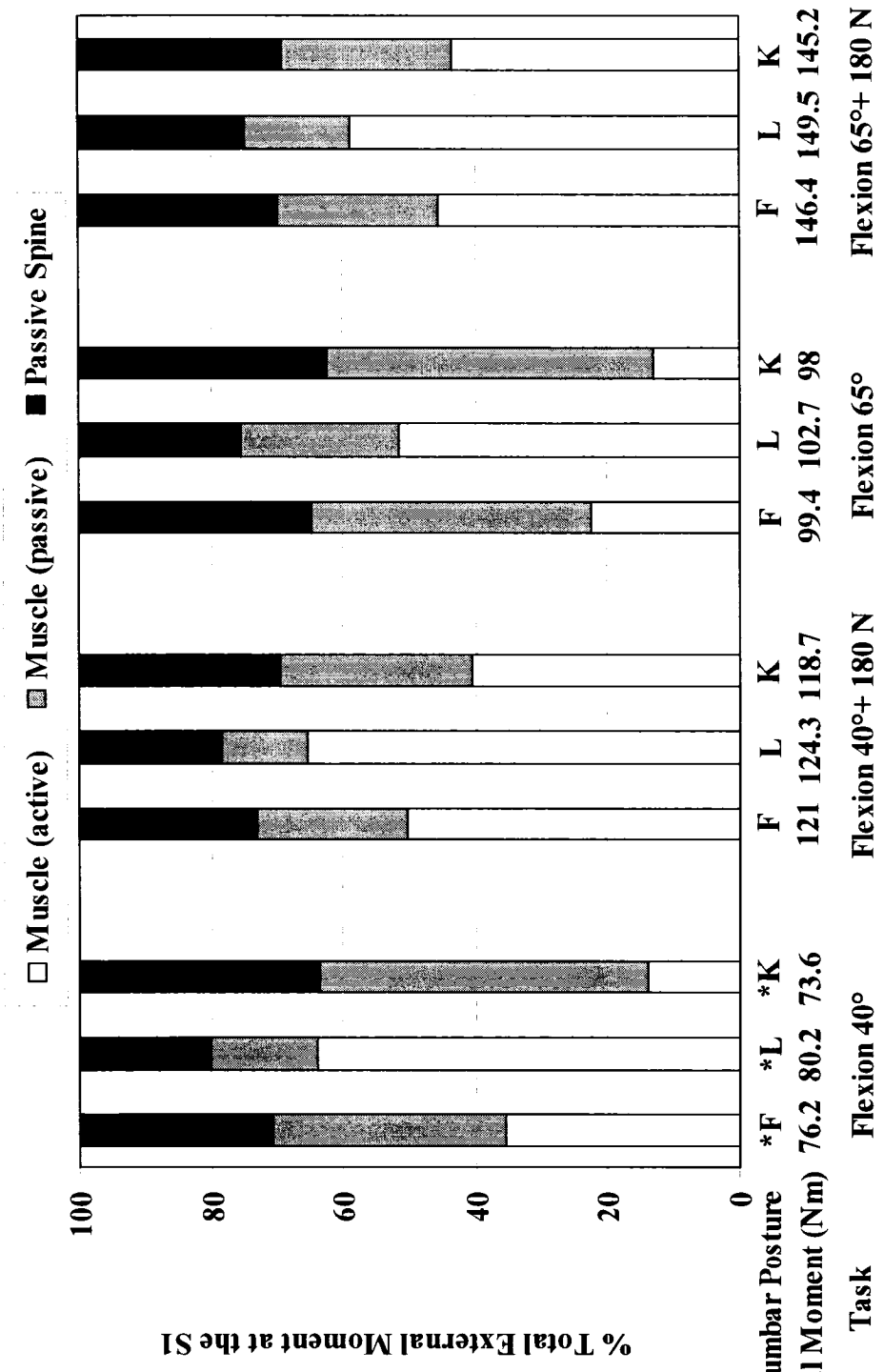
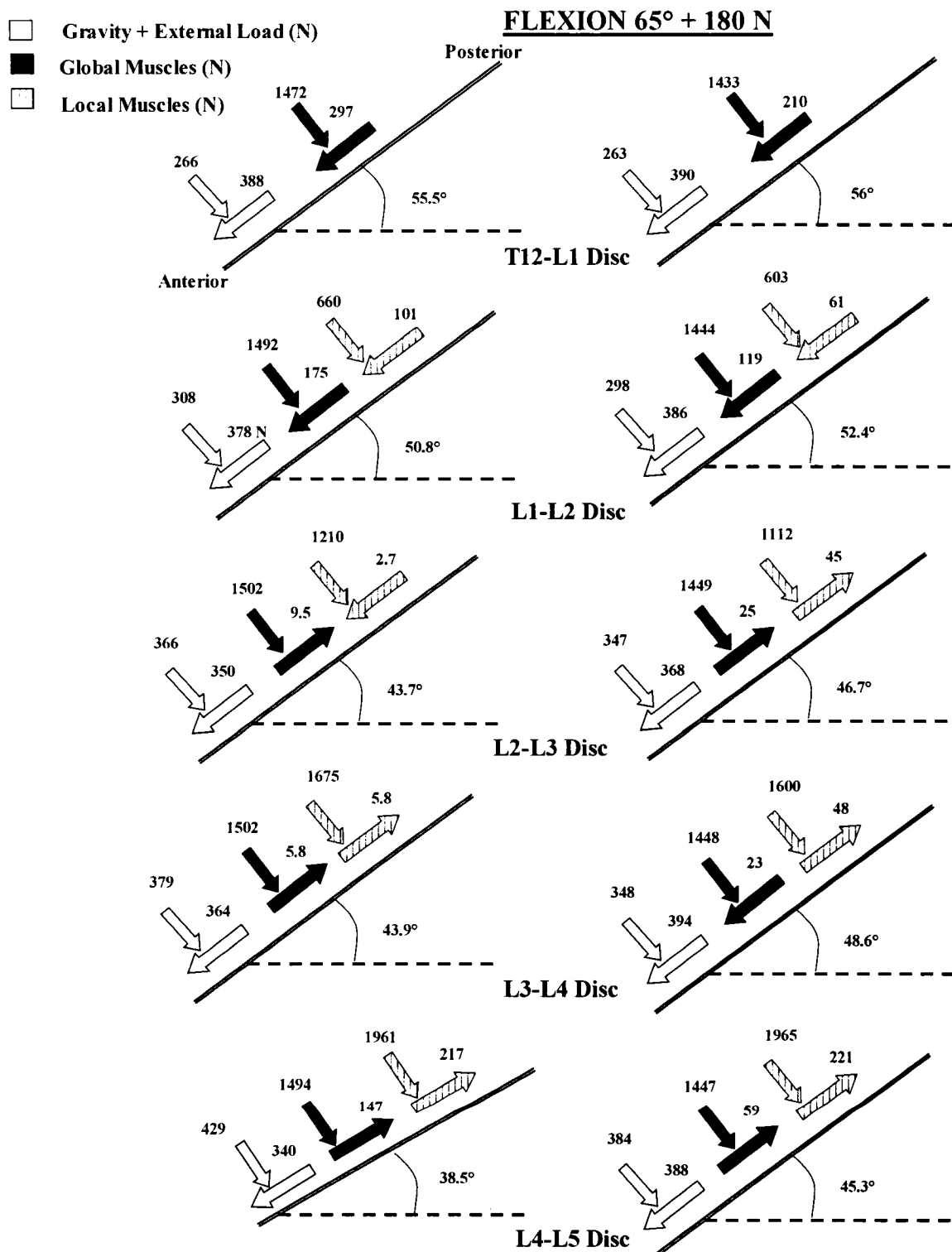


Fig. 4.7 Relative contribution of trunk muscles (passive and active) and of passive motion segments (ligamentous spine) to offset the net total moment of external/gravity loads at the S1 level for different tasks and lumbar postures. *F: free, L: lordotic, K: kyphotic



See next page

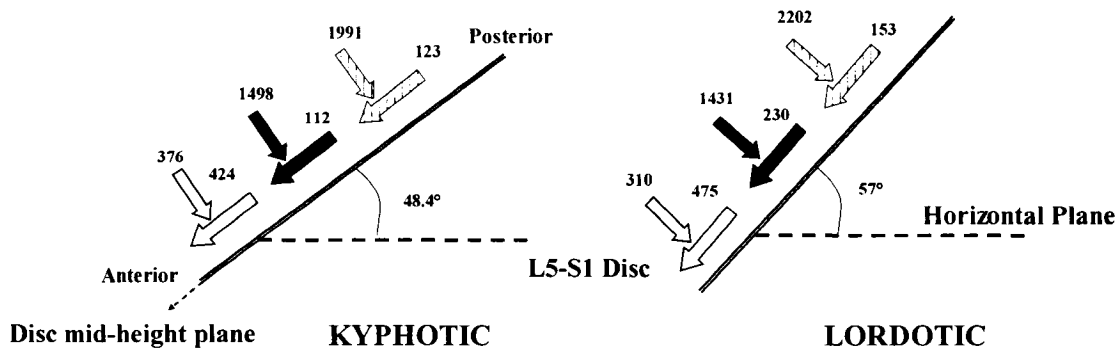


Fig. 4.8 Axial compression and anterior shear force components acting on the L4-L5 and L5-S1 disc mid-height planes presented separately due to gravity, global muscle and local muscle forces in static flexion of $\sim 65^\circ$ with 180 N load in hands for lordotic and kyphotic lumbar postures. As it is noted, the inclination of the disc mid-height planes is much larger in the lordotic posture than in the kyphotic posture and that especially at the L5-S1 disc. Moreover, the relative magnitude of different loads due to muscle forces is also affected by the instantaneous line of action of muscles.

CHAPTER 5

SENSITIVITY OF KINEMATICS-BASED MODEL PREDICTIONS TO OPTIMIZATION CRITERIA IN STATIC LIFTING TASKS

N. Arjmand, A. Shirazi-Adl

Department of Mechanical Engineering, École Polytechnique, Montréal, Québec,
Canada

Article published in *Medical Engineering & Physics* 2006; 28 (6): 504-14

Keywords: Muscle force; Internal loads; Optimization; Finite element; Kinematics-based approach; Stability; EMG

5.1 ABSTRACT

The effect of eight different cost functions on trunk muscle forces, spinal loads and stability was investigated. Kinematics-based approach combined with nonlinear finite element modeling and optimization were used to model *in vivo* measurements on isometric forward flexions at $\sim 40^\circ$ and $\sim 65^\circ$ in sagittal plane with or without a load of 180 N in hands. Four nonlinear (Σstress^3 , Σstress^2 , Σforce^2 , and muscle fatigue) and four linear (Σstress , Σforce , axial compression, and double-linear) criteria were considered. Predicted muscle activities were compared with measured EMG data. All predictions, irrespective of the cost function used, satisfied required kinetic, kinematics and stability conditions all along the spine. Four criteria (Σstress^3 , Σstress^2 , fatigue, and double-linear) predicted muscle activities that qualitatively matched measured EMG data. The fatigue and double-linear criteria were inadequate in predicting greater forces in larger lumbar muscles with no consideration for their moment arms. Nearly the same stability margin was computed under these four cost functions. At the lower lumbar levels, the compression forces differed by $<20\%$ and the shear forces by $<14\%$ as various cost functions were considered. Smaller axial compression and anterior shear forces (by $<\sim 6\%$) were computed when only the active components rather than the total muscle forces were taken as unknowns in the Σstress^3 cost function. Overall, one single cost function of Σstress^2 or Σstress^3 rather than a multi-criteria one was found sufficient and adequate in yielding plausible results comparable with measured EMG activities and disc pressure.

5.2 INTRODUCTION

Accurate evaluation of trunk muscle forces, spinal loads and stability margin is crucial in effective injury prevention and rehabilitation programs, especially in industrial manual material handling tasks. Spinal loads have indirectly been estimated by measurement of intradiscal pressure (IDP) (Nachemson, 1981, Wilke et al., 1999), load on spinal implants (Rohlmann et al., 2001, 2002), spinal shrinkage (McGill et al., 1996; van Dieen and Toussaint, 1993), or EMG activity of select trunk muscles (Mouton et al., 1991; Potvin et al., 1996). Due to the limitations in indirect measurement methods (van Dieen et al., 1999), biomechanical models are recognized as effective tools in evaluation of spinal loads and system stability in different occupational and recreational activities (Reeves and Cholewicki, 2003).

Trunk kinetic redundancy creates a hindrance in determination of muscle forces and joint loads. Several prediction models using reduction methods, optimization approaches, EMG-assisted models, or a combination thereof have been used to overcome this indeterminate problem (Callaghan and McGill, 1995; Dolan and Adams, 1993; Gagnon et al., 2001; Hughes et al., 1994; Reeves and Cholewicki, 2003; Schultz et al., 1983). These model studies with some exceptions (Cholewicki and McGill, 1996; Stokes and Gardner-Morse, 1995, 2001), however, have considered the balance of net external moments at only one single cross-section (often at the lower lumbar levels) rather than along the entire length of the spine; a simplification that likely results in inaccurate estimation of muscle forces, spinal loads and stability margin.

To improve predictions, we have recently introduced and applied a novel Kinematics-based nonlinear finite element approach in which the measured kinematics and passive nonlinear properties are incorporated into a finite element model to analyze various tasks (Arjmand and Shirazi-Adl, 2005, 2006; El-Rich et al., 2004; Shirazi-Adl et al., 2002, 2005). The final solution of this iterative procedure verifies stability and satisfies kinematics and kinetic conditions at all spinal levels and directions. This

approach exploits measured kinematics data to generate additional equations at each spinal level in order to alleviate the kinetic redundancy; each displacement component introduces an equilibrium equation. If the number of prescribed kinematics at a vertebral level reaches that of unknown muscle forces attached to that level, the problem can be solved deterministically, otherwise an optimization approach should also be employed. Since only sagittal rotations were prescribed in these model studies, the optimization criteria of sum of cubed muscle stresses were also employed to solve the existing redundancies at different levels (Arjmand and Shirazi-Adl, 2005, 2006; El-Rich et al., 2004).

Numerical optimization is a popular technique employed in biomechanical models to resolve the redundancy by optimizing some performance criteria presumed to be in accordance with the central nervous system (CNS) in controlling muscle activation patterns (Bean et al., 1988; Crowninshield and Brand, 1981; Dul et al., 1984; Seireg and Arvikar, 1973; Wynarsky and Schultz, 1991). Effect of different optimization criteria on estimated muscle forces and joint loads have been studied in models that consider equilibrium at only one cross-section (Buchanan and Shreeve, 1996; Herzog and Leonard, 1991; Hughes, 1995, 2000; Hughes et al., 1994; Parnianpour et al., 1997). Using a linear finite element model that considered equilibrium at all levels, unacceptable segmental displacements/forces were found with the cost function of sum of muscle stresses cubed which led the authors to suggest that the trunk muscle activation strategy was likely controlled by a multi-criteria cost function and not a single one (Stokes and Gardner-Morse, 2001). In these formulations, both intervertebral displacements and muscle forces were treated as unknown so that when minimizing one set there existed no guarantee that plausible results could be predicted for another set.

The influence of various optimization criteria on spinal loads and stability has not been addressed in biomechanical models that consider equilibrium along the entire length of the spine such as the Kinematics-based approach in which the muscle forces

are evaluated separately at each individual vertebral level in an iterative method using a nonlinear finite element. This work, hence, aims to investigate

- (a) to what extent the choice of optimization cost function used in the Kinematics-based biomechanical model could influence predicted trunk muscle forces, spinal loads, and spinal stability; and
- (b) which cost function(s) predicts muscle forces in qualitative agreement with the EMG activity of trunk muscles measured *in vivo* under the same posture and loading considered in the model.

Since measured vertebral rotations are prescribed into the current kinematics-based model and only muscle forces remain as unknowns of the problem, it is hypothesized that a single cost function is adequate enough to predict plausible muscle forces in qualitative agreement with measured EMG data.

5.3 METHODS

5.3.1 *In vivo*-biomechanical model studies

The Kinematics-based algorithm was used to solve the trunk redundant active-passive system under static symmetric lifting tasks involving trunk flexions of $\sim 40^\circ$ and $\sim 65^\circ$ in the sagittal plane with or without a load of 180 N in hands (Arjmand and Shirazi-Adl, 2005, 2006; El-Rich et al., 2004; Shirazi-Adl et al., 2005). Infrared light emitted markers, LED, were attached on the skin at the tip of T1, T5, T10, T12, L1, L3, L5, and S1 spinous processes for evaluation of lumbar and torso flexions. Three extra LED markers were placed on the posterior-superior iliac spine and ilium (left/right iliac crests) for evaluation of pelvic rotation, and one on the load to track the position of weights in hands. A three-camera Optotrak system (NDI International, Waterloo, Ontario) was employed to collect 3D coordinates of LED markers. Surface EMG electrodes bilaterally recorded the activity of superficial muscles; longissimus, iliocostalis, multifidus, external oblique and rectus abdominis. After data processing, EMG activities were normalized to their maximum values registered in MVC tests.

During tests, subjects were instructed to keep arms extended in the gravity direction. All data were recorded for a period of 4 seconds and then were averaged over time.

The details of the model have been given elsewhere (Arjmand and Shirazi-Adl, 2005, 2006; El-Rich et al., 2004; Shirazi-Adl et al., 2002, 2005) and are briefly described here. A sagittally-symmetric model of the T1-S1 spine with 46 local (attached to lumbar vertebrae) and 10 global (attached to thoracic cage) muscles was used to investigate the foregoing isometric flexion tasks (Fig. 5.1 and Table 5.1) (Arjmand and Shirazi-Adl, 2005; Bogduk et al., 1992; Daggfeldt and Thorstensson, 2003; Shirazi-Adl et al., 2002; Stokes and Gardner-Morse, 1999). The nonlinear and direction-dependent mechanical properties of T12-S1 segments were represented by deformable beams while the T1-T12 segments were taken as a single rigid body. A gravity load of 387 N based on the mean body weight of our subjects and percentage of body weight at each motion segment level was distributed eccentric to the center of vertebrae at different levels (Arjmand and Shirazi-Adl, 2006). To simulate load in hands, 180 N was applied at the location measured in vivo via a rigid element attached to the T3 vertebra. Mean measured sagittal rotations at the upper torso (evaluated based on the change in the inclination of the line attaching the T1 marker to the T12 one) and pelvis (evaluated based on the change in the orientation of the normal to the plane passing through the markers on the pelvis) were prescribed onto the model at the T12 and S1 levels, respectively. As for the individual lumbar vertebrae, the total lumbar rotation, calculated as the difference between the foregoing two rotations, was partitioned in accordance with proportions reported in earlier investigations (8% at T12-L1, 13% at L1-L2, 16% at L2-L3, 23% at L3-L4, 26% at L4-L5, and 14% at L5-S1) (Dvorak et al., 1991; Pearcy et al., 1984; Plamondon et al., 1988; Potvin et al., 1991; Shirazi-Adl and Parnianpour, 1999; Yamamoto et al., 1989). The finite element program ABAQUS (Hibbit, Karlsson & Sorensen, Inc., Pawtucket, RI, version 6.4) was used to carry out nonlinear structural analyses.

5.3.2 Optimization approaches

Since the number of prescribed displacements at each vertebral level (i.e., flexion rotation) is less than that of unknown muscle forces directly acting on the same level, an optimization approach must also be used. Eight different cost functions, four nonlinear (sum of cubed muscle stresses Σ stress³, sum of squared muscle stresses Σ stress², sum of squared muscle forces Σ force², and muscle fatigue) and four linear (sum of muscle stresses Σ stress, sum of muscle forces Σ force, axial compression at disc mid-heights, and maximum muscle intensity known as the double linear method (Bean et al., 1988)) functions, were used. The muscle fatigue criteria determines muscle forces such that the activity endurance time as a nonlinear function of muscle forces, maximum muscle forces, and percentage of slow twitch fibers is maximized (Dul et al., 1984). Value of slow twitch fibers, in the current study, was taken as 40% in all muscles (Buchanan and Shreeve, 1996; Johnson et al., 1973). The coupled iterative optimization problem within the Kinematics-based approach is formulated at each level as:

$$\text{Minimize (Cost Function)} \quad (\text{Eq. 5.1})$$

subject to the linear equality constrain corresponding to the prescribed sagittal rotation:

$$\sum_{i=1}^n r_i \times F_i = M \quad (\text{Eq. 5.2})$$

and inequality constraints:

$$F_{pi} \leq F_i \leq \sigma_{max} \times PCSA_i + F_{pi} \quad (\text{Eq. 5.3})$$

where F_i , F_{pi} , $PCSA_i$, σ_{max} , n , r_i , M denote unknown total force in muscle i , passive component of the force in muscle i , physiological cross-sectional area of i th muscle, maximum allowable active stress in muscles (taken as 0.6 MPa for all muscles), number of muscles attached to the vertebra, moment arm of the i th muscle, and the required moment in the sagittal plane, respectively. F_{pi} is calculated based on instantaneous muscle strain obtained from the finite element model and a tension-length relationship (Davis et al., 2003).

An in-house program based on Lagrange Multipliers Method (Raikova and Prilutsky, 2001) was developed to analytically solve the nonlinear optimization for cost functions of Σ stress³, Σ stress², and Σ force². Since only one equality constraint equation (Eq. 5.2) was considered, the solution for the double linear and fatigue criteria could also analytically be determined (Bean et al., 1988; Dul et al., 1984) in which case the double linear method became equivalent to minimizing maximum muscle intensity by using a single linear program (Bean et al., 1988). The MATLAB[®] (the MathWorks Inc., Natick, MA, USA, version 6.1) optimization toolbox (i.e. *linprog* procedure) was used to solve remaining linear optimization criteria. Solutions of the nonlinear optimization problems were further validated by MATLAB[®] optimization toolbox (i.e. *quadprog* and *fmincon* procedures).

Thirty two cases in total (4 tasks and 8 different cost functions) were analyzed to compute trunk muscle forces, internal loads and stability margin. For the sake of comparison with *in vivo* EMG measurements, the active force in each muscle was initially computed by subtracting the passive force (estimated using a tension-length relation (Davis et al., 2003)) from the calculated total force which was subsequently normalized to its own maximum physiological force (0.6 \times PCSA).

5.3.3 Stability analyses

In each case, after the muscle forces and internal loads were calculated, the model was modified with uniaxial spring elements replacing muscles between their insertion points. Stiffness of each uniaxial element, k , was assigned using the linear stiffness-force relationship $k=qF/l$ (F : total muscle force, l : instantaneous muscle length, q : muscle stiffness coefficient) (Bergmark, 1989; Crisco and Panjabi, 1991). Nonlinear analyses under external loads and prescribed pelvic tilt were performed for different q values thus identifying the critical q . In addition, linear buckling and perturbation analyses at loaded configurations were also carried out to estimate trunk stability margin as a function of q .

Alternatively, additional analyses were also performed in which the muscle passive stiffness, k_p , was calculated directly from the slope of the passive tension-length relationship (Davis et al., 2003). The total muscle stiffness was subsequently calculated as the sum of this passive stiffness (k_p) and the active muscle stiffness calculated as before ($k_a = qFa/l$ with F_a as active component of muscle force). Analyses were carried out only for the cost function of Σstress^3 to calculate critical q using this modified approach.

5.3.4 Passive-active separation in optimization

In foregoing optimization methods, the total muscle force was treated as the unknown in the optimization. Active muscle force was then computed for each muscle by subtracting the passive force from the calculated total muscle force. One, however, can argue that the CNS (or the optimization method) controls only the active component of muscle forces while the passive component is a muscle property as a function of muscle elongation. In order to investigate the effect of this latter consideration on results, the analyses were repeated, for the cost function of Σstress^3 , by considering only active muscle components in the cost function. The total muscle force was then calculated as the sum of the unknown active component and the passive one evaluated a-priori using the tension-length relationship (Davis et al., 2003) independent of optimization procedure. In this manner, mathematical formulation of the optimization procedure (Eqs.5.1-5.3) would be modified as follows:

$$\text{Minimize (Cost Function} = \sum_{i=1}^n \left(\frac{F_{ai}}{PCAS_i} \right)^3 \text{)} \quad (\text{Eq. 5.4})$$

subject to the equality constrain:

$$\sum_{i=1}^n r_i \times F_{ai} = M - M_p \quad (\text{Eq. 5.5})$$

and inequality constraints:

$$0 \leq F_{ai} \leq \sigma_{max} \times PCSA_i \quad (\text{Eq. 5.6})$$

where F_{ai} is active force component in i th muscle and $M_p = \sum_{i=1}^n r_i \times F_{pi}$.

5.3.5 Statistical analyses

Three-way analyses of variance (ANOVA) for repeated measure factors were performed to investigate effect of trunk flexion angle (2 levels: 40° and 65°), load magnitude (2 levels: 0 N and 180 N), and optimization cost function used (8 levels) on the axial compression and anterior shear forces at all segmental levels. *Tukey's post hoc* tests were performed to further reveal any significant trends ($p<0.05$).

5.4 RESULTS

5.4.1 Effect of cost function

All nonlinear optimization approaches (except Σ force²) and the double linear method predicted active muscle forces that, when normalized, were qualitatively in good agreement with measured normalized EMG activity in global muscles (ICPT, LGPT) (Fig. 5.2, Table 5.2). The predictions based on the cost function of minimization of muscle fatigue were similar to those using the double linear method. The results of ANOVA analyses demonstrated that the main effect of trunk flexion, load magnitude, and cost function on axial compression force was statistically significant (Fig. 5.3). The interaction effect of cost function and each of trunk flexion and load variables was also significant. Tukey's post hoc test revealed the cost functions with significant differences in prediction of axial compression (Table 5.3). When considering the anterior shear force, only the main effect of carried load was statistically significant (Fig. 5.4).

Predicted q value as the index of spinal stability was influenced by the optimization cost function used (Table 5.4). No muscle stiffness was at all required ($q=0$) to maintain system stability under trunk flexion of 40° and 65° when load of 180

N was carried in hands. Predicted q for the cost function of Σ stress³ substantially diminished from 9 to 2 in 40° and from 5 to 0 in 65° forward flexion angles (both cases with no load in hands) when muscle passive stiffness was calculated from the nonlinear tension-length relationship.

5.4.2 Passive-active separation in optimization

Optimization procedure defined based on Eqs. (5.4-5.6) predicted, at all spinal levels, smaller axial compression (by <139 N or ~6%) and anterior shear forces (by <32 N or ~6%) when compared to the strategy based on Eqs. (5.1-5.3) (Table 5.5). Total force predicted in local muscles was only slightly influenced while differences in the predicted global muscle forces were more pronounced (Table 5.5).

5.5 DISCUSSION

The main goals of this study were to determine (i) the effect of 8 different optimization cost functions on computed muscle forces, internal loads and system stability under static lifting tasks in the Kinematics-based biomechanical approach, and (ii) cost function(s) that yield muscle activities in better qualitative agreement with *in vivo* measured EMG activity. All predictions, irrespective of the cost function used, satisfied the kinematics, equilibrium and stability requirements at all levels and directions along the entire length of the spine and not just the equilibrium at one specific cross-section only.

5.5.1 Methodological Issues

Additional details on the Kinematics-based finite element model studies and *in vivo* measurements along with assumptions made were presented elsewhere (Arjmand and Shirazi-Adl, 2005, 2006). The assumption of rigid body for the T1-T12 segments was confirmed by our measurements of nearly equal rotations from lines attaching markers T12 to T5 and T12 to T1, an observation in agreement with others (Nussbaum and Chaffin, 1996). The geometry of muscle fascicles was modeled by straight lines

which could influence muscle length and line of action which in turn would influence predictions (Nussbaum et al., 1995) especially at larger flexion angles. The maximum allowable active muscle stress was assumed to be 0.6 MPa in all muscles. The normalized passive tension-length relationship was assumed to be the same in all muscles despite the fact that the specific architecture of each muscle (Woittiez et al., 1984) and the activation level (Lee and Herzog, 2002; Rassier et al., 2003) could influence this relationship. It is to be noted that although the optimization equations accounted for the contribution of muscle forces in equilibrium of moments at different levels, the penalty of muscle forces in shear and axial directions were taken into account by the finite element approach in an iterative procedure. Thus the equilibrium of the spine in deformed configuration under external, gravity and muscle forces was satisfied in all directions and at all levels.

Based on the EMG measurements (not presented here), both abdominal muscles (RA and EO), though relatively silent in the entire test, demonstrated a decrease in EMG activity during forward flexion tasks as compared to the standing postures with identical load in hands (Arjmand and Shirazi-Adl, 2005, 2006). For the isometric flexion tasks investigated in this study, the negligence of co-activity in abdominal muscles for all cost functions could, hence, be justified. The abdominal co-activity could enhance stability (El-Rich et al., 2004; Shirazi-Adl et al., 2005) and unload the spine via the activation of the intra-abdominal pressure (IAP) (Daggfeldt and Thorstensson, 1997, 2003). The co-activity in abdominal muscles could, however, be introduced via incorporation of non-zero lower bounds on the muscle stresses (El-Rich et al., 2004; Forster et al., 2004; Hughes et al., 1995; Shirazi-Adl et al., 2005). In this work and for each task, model and muscle input parameters (i.e. moment arm and PCSA) remained the same for different optimization algorithms. Changes in the muscle parameters have been reported to have substantial influence on muscle forces (Brand et al., 1986; Buchanan and Shreeve, 1996; Herzog, 1992; Parnianpour et al., 1997; Raikova and Prilutsky, 2001).

5.5.2 Adequacy of one cost function

The hypothesis of this study regarding the adequacy of a single cost function to predict plausible muscle activities that also match EMG data was confirmed by the nonlinear cost functions (with the exception of Σ force²) and the double linear method (Fig. 5.2). The computed compression forces were also in general agreement with *in vivo* intradiscal pressure measurements (Wilke et al., 1999, 2001) when accounting for the disc pressure-compression relationships (Shirazi-Adl, 2006). The hypothesis that one single cost function is adequate enough to predict plausible muscle activities in agreement with EMG data has been confirmed by earlier works (Crowninshield and Brand, 1981; Dul et al., 1984; Hughes et al., 1994; Prilutsky et al., 1998; van Dieen, 1997) while refuted by others (Buchanan and Shreeve, 1996; Stokes and Gardner-Morse, 2001). One likely reason for failing to predict muscle activities in accordance with EMG data has been reported to be the high sensitivity of estimated muscle forces to model input parameters, i.e. moment arms and PCSAs (Nussbaum et al., 1995; Raikova, 2000; Raikova and Prilutsky, 2001). Another reason is the treatment of joint displacements/forces and muscle stresses both as unknowns in the optimization problem (Stokes and Gardner-Morse, 2001) as minimization of one would yield unrealistic values for the other. In the current study, however, the intervertebral rotations were prescribed based on direct measurements while the computed intervertebral translations or associated compressive and anterior shear forces were in reasonable physiological ranges (Figs. 5.3 and 5.4).

5.5.3 Effect of cost functions

All nonlinear cost functions (with the exception of Σ force²) as well as the double linear method predicted muscle activities in qualitative agreement with experimental data; being larger in the LGPT than in the ICPT (Fig. 5.2). In contrast, the cost functions of Σ force², Σ force, and axial compression in mid-disc heights assigned more activity to the ICPT. The latter two cost functions did not indeed activate the LGPT until the ICPT was fully saturated (Fig. 5.2). The cost function of Σ stress, on the other hand, activated

the ICPT only after the LGPT was fully saturated. This demonstrates the high dependency of predictions in these cost functions on the lower/upper limits of muscle forces considered in the optimization. In contrast, predictions of Σstress^2 and Σstress^3 cost functions were least dependent on these extreme limits.

Effect of all linear cost functions (with the exception of the double linear method) as well as the nonlinear cost function of Σforce^2 on the relative activity of global muscles with respect to each other was task dependent; i.e., modified as the load and trunk flexion changed. For example, considering the flexion task of 40° with the cost function of Σstress , the relative magnitude of the predicted LGPT and ICPT activities was much larger when subjects carried load in hands. This disagrees with our own EMG measurements as well as those of others (Lavender et al., 1992) indicating small changes in relative trunk muscle activities from a task to another. This observation questions the validity of foregoing cost functions. Effect of remaining cost functions on the predicted relative activity of trunk muscles, in contrast, remained nearly the same in various tasks.

All cost functions that qualitatively compared well with EMG data predicted larger force in the LGPT than in the ICPT (Table 5.2). The criteria of minimizing muscle fatigue and the double linear method generated more force in muscles with larger PCSA regardless of muscle moment arms while the criteria of Σstress^2 and Σstress^3 yielded more force in muscles with larger $r \times PCSA^2$ and $r \times PCSA^3$, respectively. Therefore, the local ICPL muscles were subjected to maximum forces in former two criteria while the MF carried the greatest forces in latter ones. The argument that for a cost function of a general form $\sum c_i F_i^n$, larger forces are predicted in muscles with smaller c_i (Raikova, 1999), did not hold true in our study in which greater forces were computed in muscles with smaller c_i/r_i , i.e. larger $r_i \times PCSA_i^n$ with c_i taken as $1/PCSA_i^n$ (in cases of Σstress , Σstress^2 , and Σstress^3) and larger r_i with c_i taken as 1 (in cases of Σforce and Σforce^2). Since the simulated tasks in this study were planar movements, the double

linear method became equivalent to minimizing the maximum intensity in muscles (Bean et al., 1988) yielding results identical also to those obtained with the minimization of muscle fatigue (maximization of muscle endurance time) (Dul et al., 1984).

Maximum values of axial compression and anterior shear forces occurred, respectively, at the L4/S1 levels and L5-S1 level irrespective of the optimization cost function used and tasks considered (Figs. 5.3 and 5.4). Effect of the optimization cost function used in the Kinematics-based approach on the predicted compression was statistically significant. The maximum difference in compression force remained $\sim 20\%$ (maximum between the double linear method and the minimization of axial compression) (Fig. 5.3 and Table 5.3) which was much smaller than 160% reported elsewhere (Hughes et al., 1994). In contrast, anterior shear forces were not significantly affected by the optimization cost function used ($\sim 14\%$ at the L5-S1 level) (Fig. 5.4). These observations suggest a more careful consideration of the cost function when the axial compression force (NIOSH, 1981) rather than the anterior shear force (McGill, 1997) is considered as the primary measure to evaluate the risk to injury.

The spine appeared rather stable in all tasks studied (Table 5.4). This was due primarily to the greater stiffness of both active and passive sub-systems that significantly increased with flexion angles and compression forces. The index of stability (q) was influenced by the choice of cost function being smaller (more stable spine) for the cases when Σ force, Σ force 2 , and axial compression were minimized. Almost no difference in estimation of stability margin was found between the four cost functions whose predictions matched reasonably well the measured EMG data (Table 5.4). Decomposition of the muscle force into passive and active and subsequent evaluation of the passive stiffness from the tension-length relationship (rather than the linear force-stiffness used for the active stiffness) resulted in a much more stable configuration associated with smaller q values.

5.5.4 Passive-active separation in optimization

This issue is important for flexion tasks in which changes in muscle length are not negligible and passive forces constitute non-negligible proportions of total muscle forces. If the passive component of muscle force disappears, as expected in neutral sitting and standing postures, both approaches would then predict identical results (Eqs. (5.1-5.3) and (5.4-5.6)). In this study, all optimization cost functions were initially applied using the total (active plus passive) muscle forces as unknowns in Eqs. (5.1-5.3) yielding predictions independent of the assumed passive length-tension relationship. The strategy based upon Eqs. (5.4-5.6), however, appears to be a plausible one in which only the active component of the muscle forces enter into optimization methods as unknowns while the passive components are determined a priori based on muscle properties. Naturally, the relative accuracy in these approaches depends directly on the adequacy both of the length-tension relationships chosen for trunk muscles and of the cost functions used. Comparison of results for the cost function of Σ stress³ indicated slightly smaller axial compression and anterior shear forces (by $\sim 6\%$) at all spinal levels when only the active muscle forces were taken as unknowns. Total force predicted in local muscles was only slightly influenced by the strategy adopted while differences were more pronounced in global muscles being smaller in the LGPT and larger in the ICPT when the 2nd strategy was considered (Table 5.5).

5.5.5 Cost function(s) to use

Predictions of optimization approaches in which the relative muscle forces are not dependent either on the moment arm magnitudes (i.e., the minimization of fatigue and double linear method when moment equilibrium is considered in one plane) or on muscle PCSAs (i.e., Σ force and axial compression) remain questionable. The former two methods were reported to be promising (Bean et al., 1988; Dul et al., 1984; Prilutsky and Zatsiorsky, 2002; Schultz et al., 1983) and predicted global muscle activities in agreement with experimental data of this study (Fig. 5.2). As for local lumbar muscles, for instance in the IP with a large PCSA but very small moment arm (see Table 5.1 and Fig. 5.1), large forces were computed when using these cost functions in all tasks

considered in this study (up to 100% activity when at 65° with 180 N). Reported small EMG activity measured in the IP during trunk flexions (Andersson et al., 1996) as well as anatomical considerations (Bogduk et al., 1992) suggest that the IP cannot be a major contributor in balancing trunk sagittal moment. As a consequence of large forces assigned to large muscles with small lever arms, segmental axial compression forces reached maximum when using these two cost functions (Fig. 5.3). Large axial compression has also been reported elsewhere when using the double linear approach for moment equilibrium condition at a single section (Hans et al., 1991; Hughes, 1995; Hughes et al., 1994). Force in the IP (as an example of a muscle with large PCSA but small moment arm) is predicted more reasonably when using cost functions of Σstress^2 or Σstress^3 in which larger share is given to muscles with greater $r \times \text{PCSA}^2$ and $r \times \text{PCSA}^3$, respectively. In addition, it has been reported that the double linear method does not compare as well with EMG data as the Σstress^3 criterion does (Hughes and Chaffin, 1995; Hughes et al., 1994). This corroborates our findings that, despite good agreement with measured activities in global muscles, the double linear and fatigue criteria yield unreliable forces in local muscles. Predictions based on minimization of Σforce , Σforce^2 , and axial compression failed to match neither trends nor magnitude of normalized EMG activity measured in global muscles (Fig. 5.2). Predictions of cost function of Σstress matched pattern of EMG activity of global muscles but not their magnitudes. This cost function yields more activity in the muscles with larger $r \times \text{PCSA}$.

The cost functions of Σstress^2 and Σstress^3 appeared most adequate with results in good agreement with measured EMG activity in global muscles under all tasks considered. Predictions of these two cost functions remained within the lower/upper limits of muscle forces in the optimization approach; same results would have been obtained had limits not been introduced. Besides, force-sharing in between muscles accounted for both muscle lever arm and PCSA. No significant difference in spinal loads was found between predictions of these two cost functions (Table 5.3, Figs. 5.3 and 5.4). Although predictions of Σstress^3 was even less dependent on the inequality constraint

equations but the criteria of Σ stress² would be easier to analytically implement especially when equilibrium is considered in more than one plane (Crowninshield and Brand, 1981; Hughes et al., 1994; Prilutsky et al., 1998; van Bolhuis and Gielen, 1999; van Dieen, 1997).

In the Kinematics-based approach, the diverse choice of cost functions considered in this work appeared to have significant effect on muscle forces. The spinal compression forces varied by <~20% while the shear forces changed by <~14% at the L5-S1 level. In prevention and rehabilitation programs in which a more accurate estimation of muscle forces and spinal loads is needed, one single cost function of Σ stress² or Σ stress³ appears to be sufficient when compared with multi-criteria ones and adequate when compared with other cost functions used here.

5.6 ACKNOWLEDGMENT

The work is supported by grants from the Natural Sciences and Engineering Research Council of Canada (NSERC) and the Institut de recherche en santé et en sécurité du travail du Québec (IRSST).

5.7 REFERENCES

Andersson, E.A., Oddsson, L.I., Grundstrom, H., Nilsson, J., Thorstensson, A. EMG activities of the quadratus lumborum and erector spinae muscles during flexion-relaxation and other motor tasks. *Clin Biomech* 1996;11:392-400.

Arjmand, N., Shirazi-Adl, A. Biomechanics of changes in lumbar posture in static lifting. *Spine* 2005; 30(23):2637-48.

Arjmand, N., Shirazi-Adl, A. Model and in vivo studies on human trunk load partitioning and stability in isometric forward flexions. *J Biomech* 2006; 39(3):510-21.

Bean, J.C., Chaffin, D.B., Schultz, A.B. Biomechanical model calculation of muscle contraction forces: a double linear programming method. *J Biomech* 1988;21:59-66.

Bergmark, A. Stability of the lumbar spine –A study in mechanical engineering. *Acta Orthopaedica Scandinavia Supplementum* 1989;230:1-54.

Bogduk, N., Macintosh, J.E., Pearcy, M.J. A universal model of the lumbar back muscles in the upright position. *Spine* 1992;17:897-913.

Bogduk, N., Pearcy, M., Hadfield, G. Anatomy and biomechanics of the psoas major. *Clin Biomech* 1992;7:109–119.

Brand, R.A., Pedersen, D.R., Friederich, J.A. The sensitivity of muscle force predictions to changes in physiologic cross-sectional area. *J Biomech* 1986;19:589-96.

Buchanan, T.S., Shreeve, D.A. An evaluation of optimization techniques for the prediction of muscle activation patterns during isometric tasks. *J Biomech Eng* 1996;118:565-74.

Callaghan, J.P., McGill, S.M. Muscle activity and low back loads under external shear and compressive loading. *Spine* 1995;20:992-8.

Cholewicki, J., McGill, S.M. Mechanical stability of the in vivo lumbar spine: Implications for injury and chronic low back pain. *Clinical Biomechanics* 1996;11:1-15.

Crisco III, J.J., Panjabi, M.M. The intersegmental and multisegmental muscles of the lumbar spine –A biomechanical model comparing lateral stabilizing potential. *Spine* 1991;16:793-799.

Crowninshield, R.D., Brand, R.A. A physiologically based criterion of muscle force prediction in locomotion. *J Biomech* 1981;14:793-801.

Daggfeldt, K., Thorstensson, A. The role of intra-abdominal pressure in spinal unloading. *J Biomech* 1997;30 (11-12):1149-55.

Daggfeldt, K., Thorstensson, A. The mechanics of back-extensor torque production about the lumbar spine. *J Biomech* 2003;36:815-25.

Davis, J., Kaufman, K.R., Lieber, R.L., Correlation between active and passive isometric force and intramuscular pressure in the isolated rabbit tibialis anterior muscle. *J Biomech* 2003; 36:505-12.

Dolan, P., Adams, M.A. The relationship between EMG activity and extensor moment generation in the erector spinae muscles during bending and lifting activities. *J Biomech* 1993;26(4-5):513-22.

Dul, J., Johnson, G.E., Shiavi, R., Townsend, M.A. Muscular synergism-II. A minimum-fatigue criterion for load sharing between synergistic muscles. *J Biomech* 1984;17:675-84.

Dvorak, J., Panjabi, M.M., Chang, D.G., Theiler, R., Grob, D. Functional radiographic diagnosis of the lumbar spine. Flexion-extension and lateral bending. *Spine* 1991;16:562-71.

El-Rich, M., Shirazi-Adl, A., Arjmand, N. Muscle activity, internal loads and stability of the human spine in standing postures: combined model-in vivo studies. *Spine* 2004;29:2633-42.

Forster, E., Simon, U., Augat, P., Claes, L. Extension of a state-of-the-art optimization criterion to predict co-contraction. *J Biomech* 2004; 37:577-81.

Gagnon, D., Larivière, C., Loisel, P. Comparative ability of EMG, optimization, and hybrid modelling approaches to predict trunk muscle forces and lumbar spine loading during dynamic sagittal plane lifting. *Clin Biomech* 2001;16:359-372.

Hans, J.S., Goel, V.K., Kumar, S. A nonlinear optimization force model for human lumbar spine. *International Journal of Industrial Ergonomics* 1991;8:289-301.

Herzog, W. Sensitivity of muscle force estimations to changes in muscle input parameters using nonlinear optimization approaches. *J Biomech Eng* 1992;114:267-8.

Herzog, W., Leonard, T.R. Validation of optimization models that estimate the forces exerted by synergistic muscles. *J Biomech* 1991;24 Suppl 1:31-9.

Hughes, R.E. Choice of optimization models for predicting spinal forces in a three-dimensional analysis of heavy work. *Ergonomics* 1995;38:2476-2484.

Hughes, R.E. Effect of optimization criterion on spinal force estimates during asymmetric lifting. *J Biomech* 2000;33:225-9.

Hughes, R.E., Bean, J.C., Chaffin, D.B. Evaluating the effect of co-contraction in optimization models. *J Biomech* 1995;28:875-8.

Hughes, R.E., Chaffin, D.B. The effect of strict muscle stress limits on abdominal muscle force predictions for combined torsion and extension loadings. *J Biomech* 1995;28:527-33.

Hughes, R.E., Chaffin, D.B., Lavender, S.A., Andersson, G.B. Evaluation of muscle force prediction models of the lumbar trunk using surface electromyography. *J Orthop Res* 1994;12:689-98.

Johnson, M.A., Polgar, J., Weightman, D., Appleton, D. Data on the distribution of fibre types in thirty-six human muscles. An autopsy study. *J Neurol Sci* 1973;18:111-29.

Lavender SA, Tsuang YH, Andersson GB, Hafezi A, Shin CC. Trunk muscle cocontraction: the effects of moment direction and moment magnitude. *J Orthop Res*. 1992 Sep;10(5):691-700.

Lee, H.D., Herzog, W. Force enhancement following muscle stretch of electrically stimulated and voluntarily activated human adductor pollicis. *Journal of Physiology* 2002;545:321-30.

McGill, S.M. The biomechanics of low back injury: implications on current practice in industry and the clinic. *J Biomech* 1997;30:465-75.

McGill, S.M., van Wijk, M.J., Axler, C.T., Gletsu, M. Studies of spinal shrinkage to evaluate low-back loading in the workplace. *Ergonomics* 1996;39:92-102.

Mouton, L.J., Hof, A.L., Jongh, H.J.d., Eisma, W.H. Influence of posture on the relation between surface electromyogram amplitude and back muscle moment: consequences for the use of surface electromyogram to measure back load. *Clin Biomech* 1991;6:245-51.

Nachemson, A. Disc pressure measurements. *Spine* 1981;6:93-97.

National Institute for Occupational Safety and Health, 1981. A work practices guide for manual lifting. Cincinnati, Ohio, U.S. Department of Health and Human Services (NIOSH), pp. 30-43 (Technical report no. 81-122).

Nussbaum, M.A., Chaffin, D.B., Rechtien, C.J. Muscle lines-of-action affect predicted forces in optimization-based spine muscle modeling. *J Biomech* 1995;28:401-9.

Nussbaum, M.A., Chaffin, D.B. Development and evaluation of a scalable and deformable geometric model of the human torso. *Clinical Biomechanics* 1996; 11:25-34.

Parnianpour, M., Wang, J.L., Shirazi-Adl, A., Sparto, P., Wilke, H.J. The effect of variations in trunk models in predicting muscle strength and spinal loads. *Journal of Musculoskeletal Research* 1997;1:55-69.

Pearcy, M., Portek, I., Shepherd, J. Three-dimensional x-ray analysis of normal movement in the lumbar spine. *Spine* 1984;9:294-7.

Plamondon, A., Gagnon, M., Maurais, G. Application of a stereoradiographic method for the study of intervertebral motion. *Spine* 1988;13:1027-32.

Potvin, J.R., McGill, S.M., Norman, R.W. Trunk muscle and lumbar ligament contributions to dynamic lifts with varying degrees of trunk flexion. *Spine* 1991;16:1099-107.

Potvin, J.R., Norman, R.W., McGill, S.M. Mechanically corrected EMG for the continuous estimation of erector spinae muscle loading during repetitive lifting. *Eur J Appl Physiol Occup Physiol* 1996;74:119-32.

Prilutsky, B.I., Isaka, T., Albrecht, A.M., Gregor, R.J. Is coordination of two-joint leg muscles during load lifting consistent with the strategy of minimum fatigue? *J Biomech* 1998; 31;1025-34.

Prilutsky, B.I., Zatsiorsky, V.M. Optimization-based models of muscle coordination. *Exerc Sport Sci Rev* 2002;30:32-8.

Raikova, R. About weight factors in the non-linear objective functions used for solving indeterminate problems in biomechanics. *J Biomech* 1999;32:689-94.

Raikova, R. Prediction of Individual Muscle Forces Using Lagrange Multipliers Method - A Model of the Upper Human Limb in the Sagittal Plane: II. Numerical Experiments and Sensitivity Analysis. *Comput Methods Biomed Engin* 2000;3: 167-182.

Raikova, R.T., Prilutsky, B.I. Sensitivity of predicted muscle forces to parameters of the optimization-based human leg model revealed by analytical and numerical analyses. *J Biomech* 2001;34:1243-55.

Rassier, D.E., Herzog, W., Wakeling, J., Syme, D.A. Stretch-induced, steady-state force enhancement in single skeletal muscle fibers exceeds the isometric force at optimum fiber length. *J Biomech* 2003;36:1309-16.

Reeves, N.P., Cholewicki, J. Modeling the human lumbar spine for assessing spinal loads, stability, and risk of injury. *Crit Rev Biomed Eng* 2003;31:73-139.

Rohlmann, A., Arntz, U., Graichen, F., Bergmann, G. Loads on an internal spinal fixation device during sitting. *J Biomech* 2001;34:989-993.

Rohlmann, A., Graichen, F., Bergmann, G. Loads on an internal spinal fixation device during physical therapy. *Physical Therapy* 2002;82:44-52.

Schultz, A., Haderspeck, K., Warwick, D., Portillo, D. Use of lumbar trunk muscles in isometric performance of mechanically complex standing tasks. *J Orthop Res* 1983;1:77-91.

Seireg, A., Arvikar, R.J. A mathematical model for evaluation of forces in lower extremities of the musculo-skeletal system. *J Biomech* 1973;6:313-26.

Shirazi-Adl, A. Analysis of large compression loads on lumbar spine in flexion and in torsion using a novel wrapping element. *J Biomech* 2006;39(2):267-75.

Shirazi-Adl, A., El-Rich, M., Pop, D.G., Parnianpour, M. Spinal Muscle forces, internal loads and stability in standing under various postures and loads: applications of kinematics-based algorithm. *European Spine J* 2005; 14(4):381-92.

Shirazi-Adl, A., Parnianpour, M. Effect of changes in lordosis on mechanics of the lumbar spine-lumbar curvature in lifting. *J Spinal Disord* 1999;12:436-47.

Shirazi-Adl, A., Sadouk, S., Parnianpour, M., Pop, D., El-Rich, M. Muscle force evaluation and the role of posture in human lumbar spine under compression. *European Spine J* 2002;11:519-526.

Stokes, I.A., Gardner-Morse, M. Lumbar spine maximum efforts and muscle recruitment patterns predicted by a model with multijoint muscles and joints with stiffness. *J Biomech* 1995;28:173-186.

Stokes, I.A., Gardner-Morse, M. Quantitative anatomy of the lumbar musculature. *J Biomech* 1999;32:311-316.

Stokes, I.A., Gardner-Morse, M. Lumbar spinal muscle activation synergies predicted by multi-criteria cost function. *J Biomech* 2001;34:733-40.

van Bolhuis, B.M., Gielen, C.C. A comparison of models explaining muscle activation patterns for isometric contractions. *Biol Cybern* 1999; 81:249-61.

van Dieen, J.H. Are recruitment patterns of the trunk musculature compatible with a synergy based on the maximization of endurance? *J Biomech* 1997;30:1095-100.

van Dieen, J.H., Hoozemans, M.J., Toussaint, H.M. Stoop or squat: a review of biomechanical studies on lifting technique. *Clin Biomech* 1999;14:685-96.

van Dieen, J.H., Toussaint, H.M. Spinal shrinkage as a parameter of functional load. *Spine* 1993;18:1504-14.

Wilke, H.J., Neef, P., Caimi, M., Hoogland, T., Claes, L.E. New in vivo measurements of pressures in the intervertebral disc in daily life. *Spine* 1999;24:755-763.

Wilke, H.J., Neef, P., Hinz, B., Seidel, H., Claes, L. Intradiscal pressure together with anthropometric data -A data set for the validation of models. *Clin Biomech* 2001;6:S111-S126.

Woittiez, R.D., Huijing, P.A., Boom, H.B., Rozendal, R.H. A three-dimensional muscle model: a quantified relation between form and function of skeletal muscles. *Journal of Morphology* 1984;182 (1):95-113.

Wynarsky, G.T., Schultz, A.B. Optimization of skeletal configuration: studies of scoliosis correction biomechanics. *J Biomech* 1991;24:721-32.

Yamamoto, I., Panjabi, M., Crisco, T., Oxland, T. Three-dimensional movements of the whole lumbar spine and lumbosacral joint. *Spine* 1989;14:1256-1260.

Table 5.1 Physiological cross sectional area (PCSA, mm²) and initial length (in brackets, mm) of muscles on each side of the spine at different insertion levels. ICPL: Iliocostalis Lumborum pars lumborum, IP: Iliopsoas, LGPL: Longissimus Thoracis pars lumborum, MF: Multifidus, QL: Quadratus Lumborum, RA: Rectus Abdominus, EO: External Oblique, IO: Internal Oblique, ICPT: Iliocostalis Lumborum pars thoracic, and LGPT: Longissimus Thoracis pars thoracic.

Local Muscles	ICPL	IP	LGPL	MF	QL
L1	108 (170)	252 (276)	79 (172)	96 (158)	88 (137)
L2	154 (118)	295 (241)	91 (132)	138 (135)	80 (104)
L3	182 (84)	334 (206)	103 (88)	211 (106)	75 (74)
L4	189 (50)	311 (169)	110 (52)	186 (82)	70 (46)
L5	-	182 (132)	116 (25)	134 (51)	-
Global Muscles	RA	EO	IO	ICPT	LGPT
T1-T12	567 (353)	1576 (239)	1345 (135)	600 (250)	1100 (297)

Table 5.2 Predicted total force in global muscles (ICPT and LGPT) for different cost functions and tasks (each side of the spine, N)

Optimization Cost Function	Flexion 40°				Flexion 65°			
	0 N		180N		0 N		180N	
	ICPT	LGPT	ICPT	LGPT	ICPT	LGPT	ICPT	LGPT
Σstress³	107	242	205	458	149	326	243	530
Σstress⁴	93	259	181	490	133	347	218	567
Fatigue	122	224	230	422	165	302	268	490
Σforce⁵	182	150	348	281	249	194	408	315
Σstress	55	307	53	653	75	425	93	734
Compression	248	70	415	195	327	92	425	291
Σforce	248	70	415	194	327	92	425	291
Double-Linear	122	224	230	422	165	302	269	492

Table 5.3 Tukey's post hoc tests preceded by three-way analysis of variance (ANOVA) to determine significant differences in predicted axial compression based on eight different cost functions during lifting tasks (statistical significance at $p<0.05$ is highlighted)

Table 5.4 Predicted critical muscle stiffness coefficient (q) based on different cost functions used in simulation of various lifting tasks

Table 5.5 Spinal loads and global muscle (ICPT and LGPT) forces predicted based on cost function of sum of cubed muscle stresses using two optimization strategies; (1) with and (2) without the muscle passive force components considered also as unknowns in optimization

Task	Stra	Spinal Loads	Segmental Levels						Stra	Muscle Force	
			T12/L 1	L1/L 2	L2/L 3	L3/L 4	L4/L5	L5/S 1		ICP T	LGPT
Flexion 40°	1	Comp	933	1171	1414	1669	1862	1912	1	107	242
	2	Comp	928	1122	1352	1603	1789	1831			
	1	Shear†	250	224	111	173	95	502	2	123	223
	2	Shear†	251	212	104	162	86	478			
Flexion 40° + 180° N	1	Comp	1679	2186	2606	2971	3250	3308	1	205	458
	2	Comp	1675	2138	2544	2900	3168	3216			
	1	Shear†	490	439	202	277	73	726	2	221	440
	2	Shear†	491	426	195	267	68	705			
Flexion 65°	1	Comp	1101	1406	1737	2067	2319	2332	1	149	326
	2	Comp	1090	1337	1647	1970	2204	2193			
	1	Shear†	408	380	224	256	73	506	2	170	298
	2	Shear†	409	357	210	238	62	474			
Flexion 65° + 180° N	1	Comp	1781	2444	3039	3528	3859	3850	1	243	530
	2	Comp	1775	2377	2946	3422	3747	3731			
	1	Shear†	672	637	338	365	17	708	2	261	509
	2	Shear†	674	618	330	355	14	686			

* Strategy 1: based on equations (5.1-5.3), 2: based on equations (5.4-5.6)

†Axial compression at disc mid-height, ‡ Anterior shear force at disc mid-height

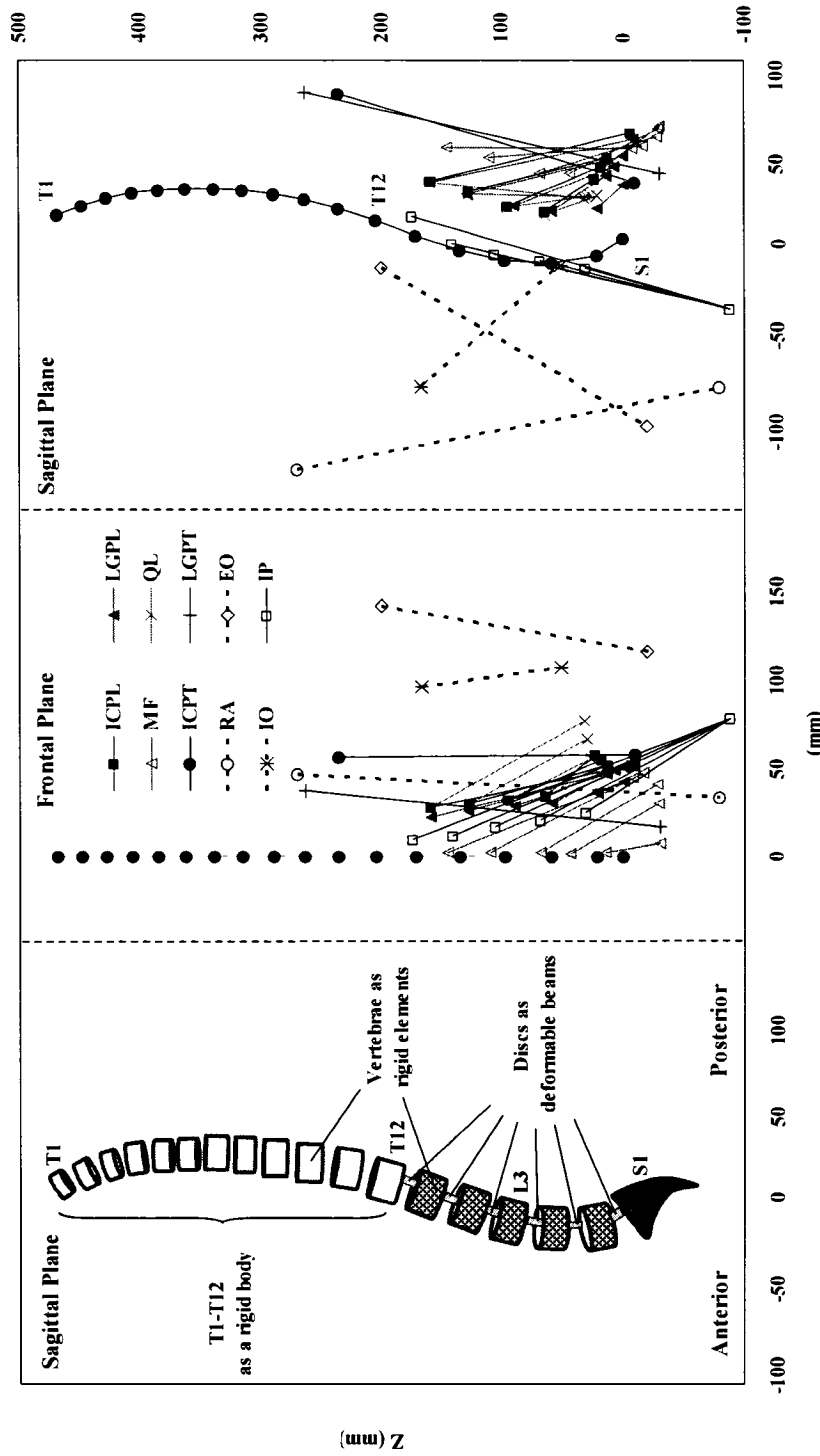


Fig. 5.1 The FE model as well as the representation of global and local musculature in the sagittal and frontal planes. Only fascicles on one side have been shown in the frontal plane. ICPL: Iliocostalis Lumborum pars lumborum, ICPT: Iliocostalis Lumborum pars thoracic, IP: Iliopsoas, LGPT: Longissimus Thoracis pars lumborum, LGPT: Longissimus Thoracis pars thoracic, MF: Multifidus, QL: Quadratus Lumborum, IO: Internal Oblique, EO: External oblique, and RA: Rectus Abdominus.

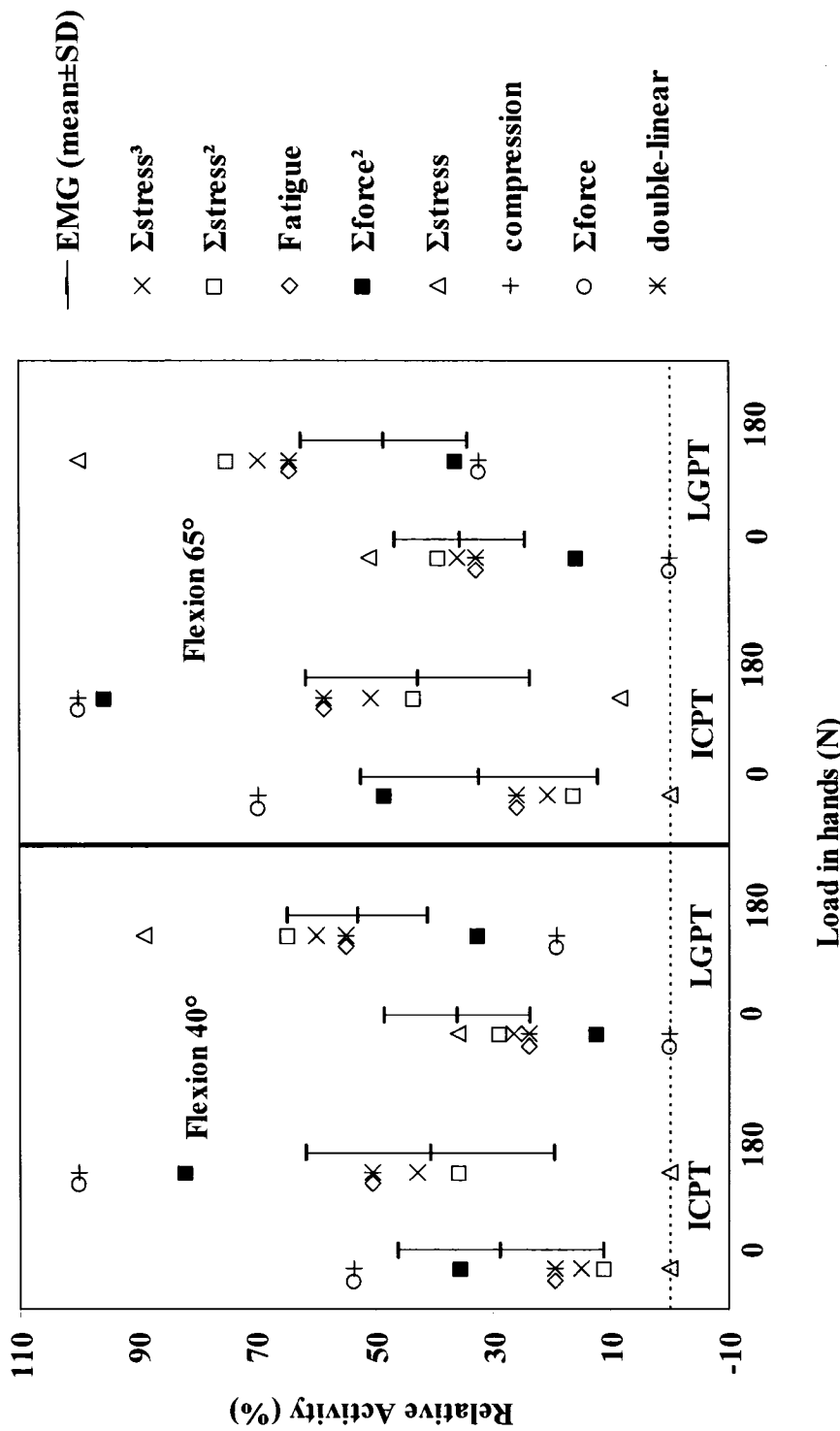


Fig. 5.2 Normalized global muscle activities (ICPT and LGPT) for different flexion tasks predicted using eight different cost functions compared to measured normalized *in vivo* EMG data (mean \pm SD). All nonlinear cost functions (with the exception of Σ force²) as well as the double linear method predicted muscle activities in relatively close agreement with experimental data.

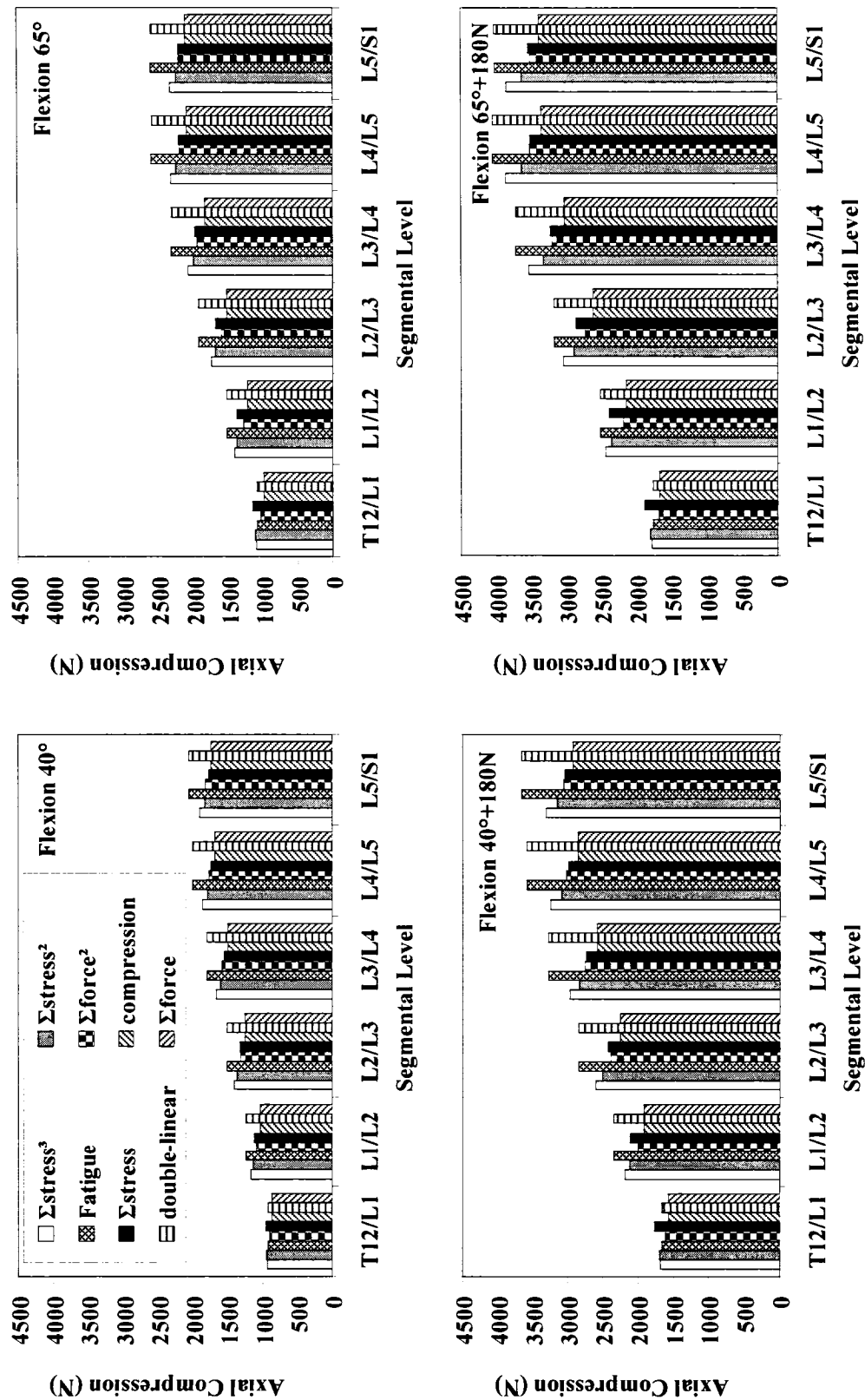


Fig. 5.3 Predicted axial compression (normal to disc mid-height planes) at different segmental levels based on eight optimization cost functions for different flexion tasks. The forces differ at most by ~20% at the lowest levels.

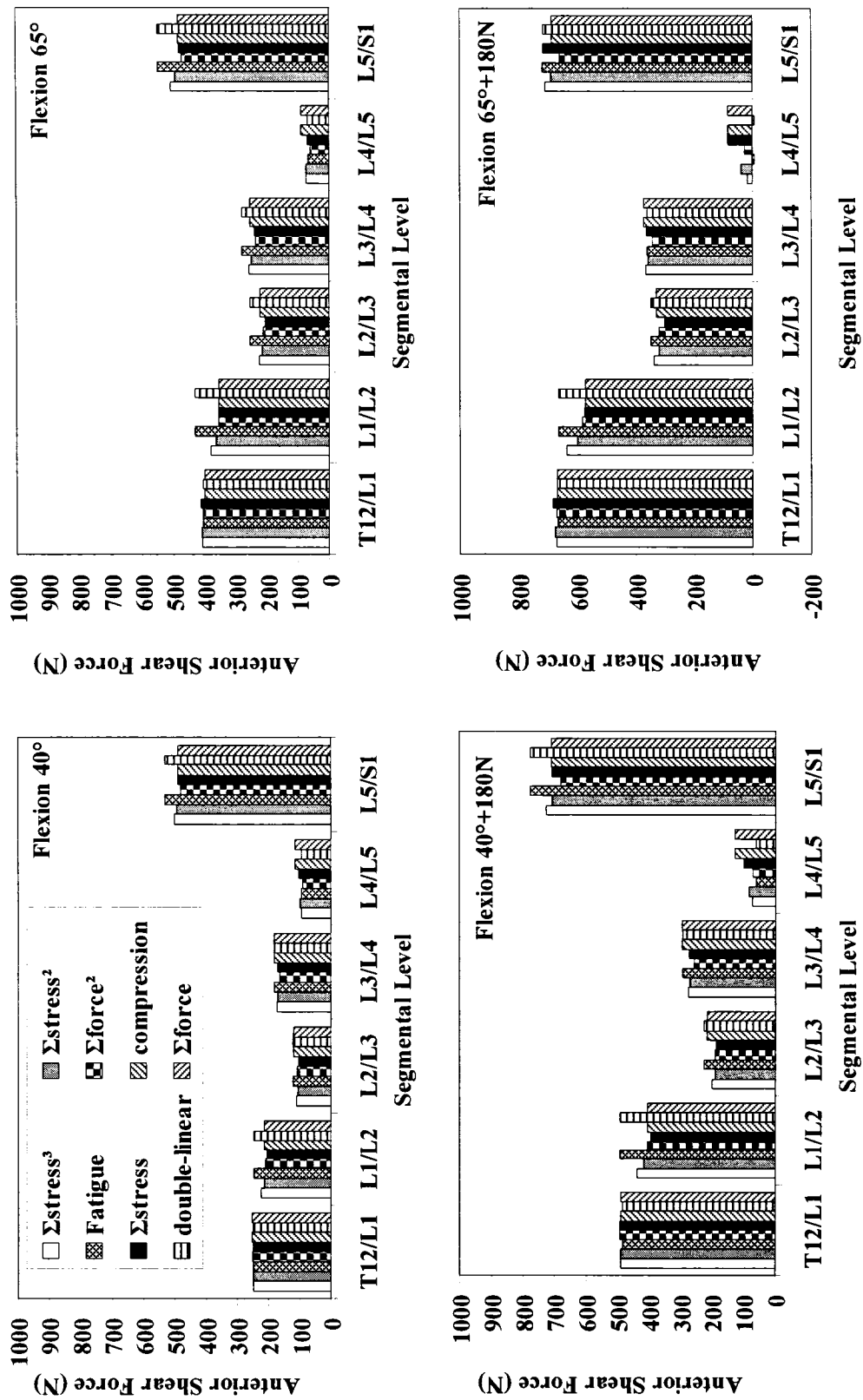


Fig. 5.4 Predicted anterior shear force (parallel to disc mid-height planes) at different segmental levels based on eight optimization cost functions for different flexion tasks. The forces differ at most by ~14% at the L5-S1 level.

CHAPTER 6

ROLE OF INTRA-ABDOMINAL PRESSURE IN UNLOADING AND STABILIZATION OF THE HUMAN SPINE DURING STATIC LIFTING TASKS

N. Arjmand and A. Shirazi-Adl

Article accepted for publication in *European Spine Journal* 2006; 15 (8): 1265-75.

Keywords: Intra-abdominal Pressure; Abdominal Coactivity; Finite Element Method; Lifting; Stability; Compression

6.1 ABSTRACT

The role of Intra-abdominal pressure (IAP) in unloading the spine has remained controversial. In the current study, a novel kinematics-based approach along with a nonlinear finite element model were iteratively used to calculate muscle forces, spinal loads, and stability margin under prescribed postures and loads measured in *in vivo* studies. Four coactivity levels (none, low, moderate, and high) of abdominal muscles (RA, EO, and IO) were considered concurrently with a raise in IAP from zero to 4 kPa when lifting a load of 180 N in upright standing posture and to 9 kPa when lifting the same load in forward trunk flexions of 40° and 65°. For comparison, reference cases with neither abdominal coactivity nor IAP were investigated as well. A raise in IAP unloaded and stabilized the spine when no coactivity was considered in foregoing abdominal muscles for all lifting tasks regardless of the posture considered. In the upright standing posture, the unloading action of IAP faded away even in presence of low level of abdominal coactivity while its stabilizing action continued to improve as abdominal coactivity increased to moderate and high levels. For lifting in forward flexed postures, the unloading action of IAP disappeared only with high level of abdominal coactivities while its stabilizing action deteriorated as abdominal coactivities increased. The IAP unloading and stabilizing actions, hence, appear to be posture and task specific.

6.2 INTRODUCTION

Estimation of spinal loads, trunk muscle forces, and stability of the human trunk during various activities, especially lifting that has been associated with higher incidence of back disorders (Damkot et al., 1984; Hoogendoorn et al., 2000), is essential to properly assess risk of injury in various loading conditions and postures. The prevention, treatment, and rehabilitation programs would subsequently benefit from such improved knowledge. One parameter with the potential to influence spinal mechanics and stability is intra-abdominal pressure (IAP) that has been reported to increase during static and dynamics lifting tasks (Andersson et al., 1976; Bartelink, 1957; Davis, 1956; Davis and Troup, 1964; Hagins et al., 2004; Marras and Mirka, 1996; Marras et al., 1984; McGill et al., 1990; Morris et al., 1961). For years, it has been argued that an increase in IAP could unload the spine both directly by pressing upwards on the rib cage via diaphragm and indirectly by generating an extensor moment on the lumbar spine that decreases back muscle activities (Bartelink, 1957; Daggfeldt and Thorstensson, 1997, 2003, 2004; Essendrop and Schibye, 2004; Harman et al., 1989; Hodges et al., 2001; Hodges and Gandevia, 2000; Keith, 1923; Morris et al., 1961). This relief mechanism has also been suggested as a remedy to the paradox in biomechanical model predictions in which spinal loads exceed tissue tolerant limits during heavy lifts (Chaffin, 1969; Cyron et al., 1975). Accordingly, abdominal belts have been recommended with the objective to increase IAP and unload spine (Harman et al., 1989; Lander et al., 1992).

Experimental studies, however, have found that IAP increase is associated with a concurrent increase in the intradiscal pressure during Valsalva maneuvers (Nachemson et al., 1986) and no reduction in erector spinae activity in lifting (Krag et al., 1986; McGill et al., 1990); thus raising questions on the unloading role of IAP. The co-contraction of abdominal muscles occurring along with an increase in IAP produces a flexor moment large enough to offset or even exceed the IAP-generated extensor moment (Cholewicki et al., 2002; McGill and Norman, 1987; McGill et al., 1990). Large cross sectional area of diaphragm and moment arm of the net IAP force considered in

biomechanical model studies have been suggested to be the reason for over estimation of auxiliary extensor moment generated by IAP (McGill and Norman, 1987; McGill and Norman, 1993).

The controversy on the unloading role of IAP (Cholewicki and Reeves, 2004; Daggfeldt and Thorstensson, 2004) is due partly to uncertainties about the magnitude and pattern of abdominal muscle coactivities that occur with an increase in IAP. Studies that advocate the unloading effect of IAP usually consider a raise in IAP to be primarily due to the activity of transverse abdominis (TA) whose fibers are mostly oriented in the transverse plane thus imposing little or no compression penalty on the lumbar spine (Daggfeldt and Thorstensson, 1997, 2003, 2004; Hodges et al., 2001). On the other hand, others insist that no appreciable increase in IAP can develop without simultaneous coactivity of all abdominal muscles including internal oblique (IO), external oblique (EO), and rectus abdominis (RA) whose activity would counterbalance the upward unloading force and generated extensor moment due to IAP (Cholewicki et al., 2002; Cholewicki and Reeves, 2004). Inability of biomechanical models to accurately partition loads among the trunk active-passive components and evaluate spinal loads remains as another reason for the existing controversy. The predictions of EMG-driven models on the effect of IAP on spinal loading and stability (Cholewicki et al., 2002; McGill and Norman, 1987) are only as accurate as the many underlying assumptions made in their formulation and spine model used. Moreover, model studies advocating unloading role of IAP during maximum back exertions have considered the TA as the only abdominal muscle generating IAP and have neglected spinal passive moment even in forward flexed postures (Daggfeldt and Thorstensson, 2003).

Normal function of IAP in unloading of the spine cannot adequately be investigated during the Valsalva maneuver or maximum voluntary strength exertions in which the concurrent presence of abdominal coactivities and IAP at high levels likely offset one another (Hodges et al., 2001). The current study was set to delineate IAP role

on muscle forces and spinal loads during regular static lifting activities involving standing and forward flexed postures. The Kinematics-based approach combined with a nonlinear finite element model of spinal active-passive components was applied to estimate trunk muscle forces, spinal loads, and stability (Arjmand and Shirazi-Adl, 2006; El-Rich et al., 2004; Shirazi-Adl et al., 2002). This realistic nonlinear finite element model circumvents many shortcomings in other biomechanical models by accounting for kinematics and kinetics conditions as well as passive-active synergies at all spinal levels. Direct *in vivo* measurements under same postures and loads are used to both provide prescribed kinematics into the model and validate model predictions with measured EMG activities. It is hypothesized that (a) the beneficial role of IAP in unloading the spine would depend on IAP magnitude and relative coactivity of abdominal muscles and (b) an increase in IAP with or without concurrent abdominal co-activation would stabilize the spine. Determination of the extent of abdominal coactivity beyond which the beneficial unloading and stabilizing effects of IAP disappear is the objective of this work.

6.3 METHODS

6.3.1 *In vivo* Measurement

More details for both *in vivo* and finite element model studies can be found elsewhere (Arjmand and Shirazi-Adl, 2006; El-Rich et al., 2004; Shirazi-Adl et al., 2002). Kinematics of the spine under standing posture as well as trunk flexions of 40° and 65° with 180 N in hands were measured in fifteen healthy males (age: 30±6 years, height: 177±7 cm, mass: 74±11 kg) using infrared light emitted markers, LED, attached on the skin at the tip of T1, T5, T10, T12, L1, L3, L5, and S1 spinous processes. Three extra LED markers were placed on the posterior-superior iliac spine and ilium (left/right iliac crests) for evaluation of pelvic rotation, and one on the load to track the position of weights in hands. A three-camera Optotrak system (NDI International, Waterloo, Ontario) was used to collect 3D coordinates of LED markers. Simultaneously, five pairs of surface electrodes were positioned bilaterally over longissimus dorsi (~3cm lateral to

midline at the L1), iliocostalis (~6cm to midline at the L1), multifidus (~2cm to midline at the L5), external obliques (~10cm to midline above umbilicus and aligned with muscle fibers), and rectus abdominis (~3cm to midline above the umbilicus). The raw EMG signals were amplified, band-pass filtered at 10-400 Hz by a 2nd order Butterworth filter, rectified over 4s trial duration and averaged for both sides. For normalization, EMG data at maximum voluntary contraction (MVC) was collected in standing (in cardinal planes while loaded via a strapped harness), prone, and supine positions.

6.3.2 Thoracolumbar Finite Element Model

A sagittally-symmetric T1-S1 beam-rigid body model consisting of 6 deformable beams to represent T12-S1 segments and 7 rigid elements to represent T1-T12 (as a single body) and lumbosacral vertebrae (L1 to S1) was used (Fig. 6.1). The nonlinear load-displacement response under single and combined axial/shear forces and moments along with the flexion versus extension differences were represented in this model based on numerical and measured results of previous single- and multi-motion segment studies (Oxland et al., 1992; Patwardhan et al., 2003; Shirazi-Adl, 2006; Shirazi-Adl et al., 2002; Yamamoto et al., 1989). In all cases, based on the mean body weight of our subjects and percentage of body weight at each motion segment level reported elsewhere (Pearsall, 1994; Takashima et al., 1979), a gravity load of 387 N was distributed eccentrically at different segmental levels. To simulate the external load carried symmetrically in hands, 180 N was applied at the location measured *in vivo* via a rigid element attached to the T3 vertebra (Fig. 6.1).

6.3.3 Prescribed Postures

Mean measured sagittal rotations at the upper torso (evaluated based on the change in the inclination of the line attaching the T1 marker to the T12 one) and pelvis (evaluated based on the change in the orientation of the normal to the plane passing through the markers on the pelvis) were prescribed onto the model at the T12 and S1

levels, respectively. As for the individual lumbar vertebrae, the total lumbar rotation, calculated as the difference between the foregoing two rotations, was partitioned in accordance with proportions reported in earlier investigations; i.e., 8 % at T12-L1, 13 % at L1-L2, 16 % at L2-L3, 23 % at L3-L4, 26 % at L4-L5, and 14 % at L5-S1 (Dvorak et al., 1991; Pearcy et al., 1984; Plamondon et al., 1988; Potvin et al., 1991; Yamamoto et al., 1989).

6.3.4 Intra-abdominal Pressure (IAP)

Magnitude of IAP while holding 180 N in hands was taken as 4 kPa in standing posture (Mueller et al., 1998) and 9 kPa at trunk flexions of 40° and 65° (Essendrop and Schibye, 2004; Mueller et al., 1998) (Table 6.1). The diaphragm areas and total force magnitudes/lever arms considered in different cases are also listed in Table 6.1. The IAP was represented by an upward force applied to the thorax via a rigid element attached to the T12 level. The direction of this force was taken in the vertical direction in the case simulating the upright posture. For the forward flexion simulations, however, this force changed direction to follow the thorax rotation (Fig. 6.1).

6.3.5 Abdominal Muscle Coactivity

Among abdominal muscles (IO, EO, and RA), the largest and smallest coactivity during lifting tasks has been observed in IO and RA, respectively (Cresswell, 1993; De Looze et al., 1999; Essendrop and Schibye, 2004; Ng et al., 2002; Silfies et al., 2005). To simulate a wide-range of likely situations in the model, therefore, three different levels of relative coactivity were considered in abdominal muscles: low level 1) RA: 0.5%, EO: 1%, IO: 2%, intermediate level 2) RA: 1%, EO: 2%, IO: 4%, and high level 3) RA: 2%, EO: 4%, IO: 8%. These activities were considered as a % of the maximum active force which in turn was calculated for each abdominal muscle as its physiological cross section area (PCSA) (Table 6.2) times the maximum active stress (taken as 0.6 MPa) (see Table 6.3). Additional cases were also studied in which the above coactivities were neglected altogether in which cases IAP was assumed to be solely generated by the

TA activation. Moreover, reference cases were considered for comparison where neither IAP nor abdominal coactivity was represented.

6.3.6 Muscle Model and Muscle Force Calculation

A sagittally-symmetric muscle architecture with 46 local (attached to lumbar vertebrae) and 10 global (attached to thoracic cage) muscle fascicles was used (Fig. 6.1 and Table 6.2) (Bogduk et al., 1992; Stokes and Gardner-Morse, 1999). To evaluate muscle forces, Kinematics-based algorithm was employed to solve the redundant active-passive system subjected to prescribed measured kinematics and external loads. In this manner, calculated muscle forces at each instance of loading were compatible with the prescribed kinematics (i.e., posture) and external loading while accounting for the realistic nonlinear stiffness of the passive system. Each sagittal rotation applied a priori at all spinal levels of the model generated an equilibrium equation at that level in the form of $\sum r_i \times f_i = M$ (r: muscle lever arm, f: muscle force, and M: required sagittal moment due to the applied rotation). To resolve the redundancy problem an optimization approach with the cost function of minimum sum of cubed muscle stresses was used along with inequality equations of unknown muscle forces remaining positive and greater than their passive force components (calculated based on muscle strain and a tension-length relationship (Davis et al., 2003)) but smaller than the sum of their respective maximum forces (i.e., 0.6 PCSA) and the passive force components. Once muscle forces were calculated, the axial compression and horizontal shear penalties of these muscle forces were fed back into the finite element model as additional updated external loads. This iterative approach was continued till convergence was reached. The finite element program ABAQUS (Hibbit, Karlsson & Sorensen, Inc., Pawtucket, RI, version 6.5) was used to carry out nonlinear structural analyses while the optimization procedure was analytically solved using an in-house program based on Lagrange Multipliers Method (Raikova and Prilutsky, 2001).

6.3.7 Stability Analyses

In each simulation case, after the muscle forces were calculated, the model was modified with uniaxial elements replacing muscles between their insertion points. Stiffness of each uniaxial element, k , was assigned using the linear stiffness-force relationship $k=qF/l$ (F : known muscle force, l : instantaneous muscle length, q : muscle stiffness coefficient chosen a priori) (Bergmark, 1989; Crisco and Panjabi, 1991). Nonlinear analyses under same external loads and prescribed pelvic tilt were performed for different q values thus identifying the critical q below which the system ceased to be stable. These nonlinear analyses under applied forces serve as the gold standard to evaluate the system stability and to verify validity of the calculated muscle forces under the prescribed kinematics performed in the earlier stage of the analysis. In addition to the nonlinear analyses, linear buckling and perturbation analyses at loaded, deformed, configurations were also carried out as complementary approaches to estimate trunk stability margin as a function of q .

6.4 RESULTS

Forces in abdominal muscles and associated moments at the T12 level were calculated based on prescribed % coactivities, muscle PCSAs, and lever arms at deformed configurations (Table 6.3). In all tasks, when IAP was introduced into the model without any concurrent coactivity in abdominal muscles, the spine was markedly unloaded in compression at all levels and under all tasks considered (Fig. 6.2). Shear forces decreased at all levels in upright posture whereas they generally increased in flexion tasks (Fig. 6.3). Furthermore, activity of thoracic (global) extensor muscles considerably dropped due to the extensor moment generated by IAP (Fig. 6.4).

When coactivity of abdominal muscles was also introduced into the model along with IAP, the foregoing decreasing trend in the axial compression reversed at all spinal levels and under all tasks (Fig. 6.2). As a result of changes in global extensor muscle activity (Fig. 6.4), the beneficial role of IAP actually disappeared and even reversed in upright standing posture for all coactivity levels and in flexion postures under highest

activity considered. Although larger abdominal coactivity increased segmental shear forces in standing posture, but the effect was less pronounced in flexion tasks (Fig. 6.3).

Neglecting IAP and abdominal coactivity (i.e., in reference cases), the spinal stability substantially improved as trunk flexed forward from upright standing (critical $q=17$) to 40° and 65° positions (critical $q=0$). Introduction of IAP alone into the model without any abdominal coactivity improved spinal stability in all tasks considered (e.g., q decreased from 17 to 14 in the standing posture). The presence of abdominal (RA, EO, and IO) coactivity consistently increased the spinal stability in standing posture (e.g. q decreased to 10 and further to 8 for the low and intermediate levels of abdominal coactivities, respectively). In flexion tasks, critical q remained always equal to zero while linear stability analyses demonstrated a slight decrease in the system stability margin. The stability margin in flexion tasks, however, slightly improved in all cases when compared with the reference cases in which neither IAP nor abdominal coactivity were considered.

6.5 DISCUSSION

The main objective of this study was to investigate the effect of IAP in concurrence with different activity levels of abdominal muscles on extensor muscle forces, spinal loads and system stability during static lifting tasks in both upright standing and forward flexed postures carrying 180 N in hands. A novel kinematics-based finite element approach was used in which the a-priori measured kinematics of the spine were prescribed into a nonlinear finite element model to evaluate muscle and internal loads resulting in a synergistic solution of the active-passive system (Arjmand and Shirazi-Adl, 2006; El-Rich et al., 2004; Shirazi-Adl et al., 2002). This iterative approach not only satisfied the equilibrium equations in all directions along the entire length of the spine but yielded spinal postures in full accordance with IAP/external/gravity loads, muscle forces, and nonlinear ligamentous stiffness properties. The stability margin of the

spine under muscle forces, kinematics, and IAP/gravity/external loads considered were subsequently determined.

In agreement with other studies (Daggfeldt and Thorstensson, 2003), IAP values considered in this study (i.e., 4 kPa in standing and 9 kPa in flexion tasks) unloaded compression on the spine by a mean value of ~19% at all levels when no concurrent coactivity was considered in abdominal muscles (RA, EO, and IO). In these cases, activity of both thoracic extensor muscles (LG and IC) decreased by ~55% in standing and ~30% in flexion tasks. In presence of low coactivity in abdominal muscles (level 1: RA: 0.5%, EO: 1%, IO: 2%), the unloading effect of IAP in standing posture faded away while that in flexion tasks reduced to a mean of ~13% at all levels (Fig. 6.2). In this case in standing posture, the activity of thoracic extensors very slightly exceeded their reference values computed under no IAP and no abdominal coactivity (Fig. 6.4). In flexion tasks, as the abdominal coactivity further increased to the moderate level, IAP unloaded the spine by an average of only ~7% (level 2: RA: 1%, EO: 2%, IO: 4%) while at the highest level of abdominal coactivity (level 3: RA: 2%, EO: 4%, IO: 8%), compression on the spine actually increased in average by ~5% at all levels (Fig. 6.2). Accordingly, the activity in extensor muscles increased beyond that in the reference case only in the case with highest abdominal coactivity (Fig. 6.4). These results confirm the first hypothesis of the study that IAP has the potential to substantially unload the spine in standing and flexion tasks; a role that depends directly on the IAP magnitude and concurrent level of coactivity in abdominal muscles in such tasks. That is, IAP could indeed even increase back muscle forces when large coactivity is generated in IO, EO, and RA muscles. The hypothesis of the study regarding the stabilizing effect of abdominal coactivities in various tasks in presence of IAP, however, was only confirmed in standing postures and not in flexion tasks in which a slightly lower stability margin was predicted when higher levels of abdominal coactivity were considered.

6.5.1 Methodological Remarks

The assumption of rigid body motion at the T1-T12 segments (upper torso) was confirmed, in agreement with others (Nussbaum and Chaffin, 1996), by measuring nearly equal rotations at lines attaching either the markers T12 to T5 or markers T12 to T1. The assumption of global extensor muscles as straight lines attaching the pelvis to the upper thorax may be a crude one when the lumbar spine approaches full flexion in which case these muscles wrap around the surrounding tissues. Although the simulated tasks in this study involved rotations of the thorax much smaller than those at full flexion, determination of the extent of such consideration on results needs additional studies. The Latissimus dorsi, lumbodorsal fascia, and intersegmental/multisegmental muscles were neglected. Latissimus dorsi has been known to produce trunk extensor moment via the lumbodorsal fascia; a contribution suggested not being sizable during lifting tasks (Bogduk et al., 1988; McGill and Norman, 1988). For the reference cases in which no coactivity was assumed in concurrence with IAP, this latter was assumed to be generated solely by TA coactivity. In this case, fascicles of TA were considered to be oriented in the transverse plane without having any axial compressive force penalty despite the fact that some of its fascicles especially in middle and lower regions are somewhat oblique (Urquhart et al., 2005). Other abdominal muscles (RA, EO, and IO) were all modeled by a single fascicle. Consideration of several fascicles instead of just one for oblique muscles (EO and IO) has influenced the estimated spinal loads significantly in asymmetric lifting tasks but only slightly in symmetric ones (Davis and Mirka, 2000). The values for IAP, Intra-abdominal area, and level arm of intra-abdominal force were all selected from those reported in the literature for the tasks similar to the ones considered in this study (Table 6.1).

For qualitative comparison of predicted extensor muscle activities with EMG data (Fig. 6.4) as well as to calculate abdominal muscle forces, the maximum allowable muscle stress of 0.6 MPa was assumed for all muscles which is in the mid-range of those in the literature (0.3-1.0 MPa) (Davis and Mirka, 2000; Farfan, 1973). It is important to emphasize that any changes in this maximum stress value would directly influence

forces considered in abdominal muscles for different cases. The passive tension-length relationship was also assumed to be the same for all muscles despite the fact that the specific architecture of each muscle could influence this relationship (Woittiez et al., 1984). The passive tension-length curve used in the current study was adapted from recent experimental data (Davis et al., 2003) which is in the range of those reported by others (McGill SM, Norman, 1986; Nussbaum MA, Chaffin, 1996; van Dieen, 1997). It is important to emphasize that the passive force-length and stiffness relations considered for muscles in the current study have absolutely no bearing at all on the predicted spinal loads and muscle forces. The partitioning of the calculated muscle forces into active and passive components in post-processing of the data (Fig. 6.4) would, however, be influenced by the choice of passive force-length relationship. The cost function of minimum sum of cubed muscle stresses used in the optimization algorithm has been recognized to predict muscle activities in agreement with the EMG data (Hughes et al., 1994; van Dieen, 1997).

6.5.2 IAP and Abdominal Coactivity Values

The IAP during maximum voluntary exertion or Valsalva manoeuvre has reached as high as 26.2 ± 9.6 (mean \pm sd) kPa (Cholewicki et al., 2002), 28 kPa (Essendrop et al., 2002), $\sim 19 \pm 6$ kPa (Daggfeldt K, Thorstensson, 2003), 26.6 ± 6.7 kPa (Harman et al., 1988), and 38.8 ± 5.2 kPa (Essendrop and Schibye, 2004). It has been reported to reach 50 kPa in power competitive lifters wearing belt (McGill et al., 1990). In neutral standing posture without carrying any load in hands IAP has been measured as low as 0.2 kPa (Andersson et al., 1977), 0.3 kPa (Marras and Mirka, 1996), and 0.98 kPa (Nachemson et al., 1986). The magnitude of 4 kPa considered in this study for IAP in standing posture with 180 N in hands is in the upper range of reported values (~ 0.5 -4 kPa) (Andersson et al., 1977; Mueller et al., 1998; Nachemson et al., 1986). Different IAP measurement techniques could influence the recorded data (Andersson et al., 1977). Although the choice of this value would undoubtedly influence the predictions but the conclusion regarding the ineffectiveness of IAP in unloading the spine in standing

postures based on the assumed value of 4 kPa would remain unchanged. This is due to the large flexor moment produced by abdominal muscles, especially IO, even in presence of low coactivity levels.

Large scatter also exists in IAP magnitudes reported for forward flexed postures; however there is a general consensus in that IAP increases as trunk flexion and moment increase (Andersson et al., 1977; Chaffin, 1969; Daggfeldt and Thorstensson, 2003; McGill and Norman, 1987; Mueller et al., 1998; Nachemson et al., 1986). The magnitude of 9 kPa considered in this study for IAP in flexion tasks with load in hands is at the middle range of mean values reported in the literature (1-21) kPa (Andersson et al., 1977; Essendrop and Schibye, 2004; Harman et al., 1989; Mairiaux et al., 1988; McGill et al., 1990; Mueller et al., 1998; Nachemson et al., 1986).

Despite general accord in the literature that IO is much more active than RA in lifting tasks; there is a large variation in reported normalized activity in abdominal muscles (Cresswell, 1993; De Looze, 1999; Essendrop and Schibye, 2004; Ng et al., 2002; Silfies et al., 2005). This discrepancy could partly be due to different techniques used to measure MVC activities required for EMG normalization. In the present study, the forces considered in abdominal muscles could correspond to much greater muscle activity levels had a smaller allowable stress been assumed; the same forces would correspond to abdominal activities increased by twofold when the maximum stress of 0.6 MPa is replaced by 0.3 MPa.

6.5.3 Unloading Effect of IAP in Standing Postures

Our results suggest that IAP could hardly unload the spine in standing postures unless if no or very low coactivity occurs in abdominal muscles. The lowest abdominal activity in this study (RA: 0.5%, EO: 1% and IO: 2%) generated ~4 Nm flexor moment (Table 6.3) that exceeded 3.2 Nm extensor moment due to IAP (Table 6.1). To compensate this additional flexor moment, slightly larger forces were needed in extensor

muscles which exceeded those in the reference case with no IAP/coactivity (Fig. 6.4). This, in turn, resulted in an increase in spine compression at all levels that offset almost all beneficial unloading action of IAP (Fig. 6.2).

The foregoing flexor moment of 4 Nm is mainly produced by IO (~3.2 Nm) due to its relatively large lever arm with respect to the thorax and large PCSA. In vivo studies demonstrate that TA and IO are the most active muscles during back extension activities (Bartelink, 1957; Cresswell, 1993; De Looze, 1999; Essendrop and Schibye, 2004; McGill and Norman, 1987; Ng et al., 2002; Silfies et al., 2005). Fascicles of IO are suggested to be primarily oriented transversely in which case, similar to TA, would not cause appreciable flexor moment and axial compression penalties on the spine (Daggfeldt K, Thorstensson, 1997, 2004). Although this might be true for IO fascicles at lower regions (Ng et al., 1998; Urquhart et al., 2005) but remaining fascicles attaching iliac crest and rib cage are oriented obliquely at ~50° to 75° to the horizontal plane (Stokes and Gardner-Morse, 1999; Urquhart et al., 2005) which can generate considerable flexor moment and axial compression on the spine. Those fascicles of IO which are oriented more transversely may redirect their force to RA sheath via linea semilunaris to enhance their effective moment arm (McGill, 1996).

Using a biomechanical model of the lumbar spine in which IAP was introduced with no concurrent abdominal coactivities, it was claimed that IAP can unload the spine at all levels by ~400 N (34-40% of total compression) during maximal back extension in an extended posture when lying on the side (Daggfeldt K, Thorstensson, 2003). In direct contrast, in another biomechanical model study in which only coactivity of abdominal muscles was incorporated into the model without IAP, abdominal coactivities were found to overload the spine by ~500 N at the L5-S1 level (22% of total compression) when holding 22.5 Kg in hands in erect posture (De Looze et al., 1999). Our results demonstrate that it is extremely important to consider both abdominal coactivities and IAP into a biomechanical model of upright standing postures. In support of others

(Cholewicki et al., 2002), our results refute the unloading role of IAP in standing postures in presence of even low coactivity in IO acting alone or along with other abdominal muscles.

6.5.4 Unloading Effect of IAP in Flexion Tasks

Based on the results of this study it appears that the unloading effect of IAP is more prevalent in flexion tasks in which only the highest abdominal coactivity level (RA: 2%, EO: 4%, IO: 8%) erased the beneficial unloading effect of IAP (Fig. 6.2). This relative effectiveness in flexion as compared with the upright posture is mainly due to the larger IAP, greater IAP area and lever arm in flexion which generate ~ 11.3 Nm extension moment. Given that the coactivity of IO, as the primary flexor generating abdominal muscle, decreases in forward flexion as reported in the literature (De Looze et al., 1999; McGill and Norman, 1986), the possible unloading effect of IAP under flexion could then become more important. The coactivity of both RA and EO has been measured by some to decrease in forward flexion tasks compared to the standing postures (Arjmand and Shirazi-Adl, 2006; Chen et al., 1998; Tan et al., 1993) while others report an opposite trend (De Looze et al., 1999; Nachemson et al., 1986). If indeed a fall in abdominal muscle (RA, EO, and IO) coactivities occur from standing to flexed postures, then the increase in IAP from standing posture to flexed posture should be provided mainly by contraction of the TA, diaphragm and pelvis floor muscles. Intramuscular EMG measurements (Cresswell, 1993; Cresswell and Thorstensson, 1989; Cresswell et al., 1992) as well as model studies (Arjmand et al., 2001; Daggfeldt and Thorstensson, 2003) have also provided evidence that the TA is the most significant contributor to raising IAP during back extension.

6.5.5 Stability

There is a general consensus that an increase in IAP stabilizes the spine; however the mechanism behind this stabilizing action is not yet well understood. One such mechanism is based on the premise that any increase in IAP is accompanied by the co-

contraction of abdominal muscles which in turn increase spinal stiffness and stability (Cholewicki et al., 1999a, b). In this case, it is assumed that the generated flexor moment due to abdominal coactivities cancel out the extensor moment produced by IAP thus requiring no additional activity in extensor muscles. Our results demonstrate that, in the upright standing posture, the combination of IAP and abdominal coactivity generates a net flexion moment that is offset by additional back muscle activity. Therefore, the associated improvement in stability observed in the current study is due to increases in both abdominal and extensor muscle activities in presence of IAP. On the other hand, such was not the case for lifting tasks in flexion in which spinal stability slightly deteriorated as abdominal coactivities increased. In these postures, since no muscle stiffness was needed to provide the stability (critical $q=0$), any increase in muscle activities would augment compression on the spine causing a drop in the critical load of the structure.

6.6. CONCLUSION

The IAP unloading and stabilizing actions seem to be posture and task specific. While the stabilizing effect of IAP and concurrent abdominal coactivity in the upright standing posture is evident but the IAP ability to unload the spine holds true only for very low abdominal coactivities or for the case in which only TA is responsible for any IAP increase. In contrast, the unloading action of IAP appears more effective in forward lifting tasks while its stabilizing role disappears. This study is the first to satisfy all kinetics, kinematics and stability requirements at all spinal levels in presence of gravity, external load, extensor/flexor muscle activations and IAP.

6.7 ACKNOWLEDGEMENT

The work is supported by grants from the NSERC-Canada and the IRSST-Québec. The protocol for *in vivo* measurements was approved by the local ethics committee and all participants signed an informed consent.

6.8 REFERENCES

Andersson GB, Ortengren R, Nachemson A (1976) Quantitative studies of back loads in lifting. *Spine* 1: 178-85.

Andersson GB, Ortengren R, Nachemson A (1977) Intradiskal pressure, intra-abdominal pressure and myoelectric back muscle activity related to posture and loading. *Clin Orthop Relat Res* 129: 156-64.

Arjmand N, Shirazi-Adl A, (2006) Model and in vivo studies on human trunk load partitioning and stability in isometric forward flexions. *J Biomech* 39(3):510-21.

Arjmand N, Shirazi-Adl A, Parnianpour M (2001) A finite element model study on the role of trunk muscles in generating intra-abdominal pressure. *Biomedical Engineering-Applications, Basis & Communications* 13 (4): 23-31.

Bartelink DL, (1957) The role of abdominal pressure in relieving the pressure on the lumbar intervertebral discs. *J Bone Joint Surg Br* 39:718-725.

Bergmark A (1989) Stability of the lumbar spine –A study in mechanical engineering. *Acta Orthop Scand Suppl* 230:1-54.

Bogduk N, Johnson G, Spalding D (1998) The morphology and biomechanics of latissimus dorsi. *Clin Biomech* 13 (6):377-385.

Bogduk N, Macintosh JE, Pearcy MJ (1992) A universal model of the lumbar back muscles in the upright position. *Spine* 17:897-913.

Chaffin DB (1969) Computerized biomechanical models-development of and use in studying gross body actions. *J Biomech* 2:429-441.

Chen WJ, Chiou WK, Lee YH, Lee MY, Chen ML (1998) Myo-electric behavior of the trunk muscles during static load holding in healthy subjects and low back pain patients. *Clin Biomech* 13 (1 Suppl 1):S9-S15.

Cholewicki J, Ivancic PC, Radebold A (2002) Can increased intra-abdominal pressure in humans be decoupled from trunk muscle co-contraction during steady state isometric exertions? *Eur J Appl Physiol* 87 (2):127-33.

Cholewicki J, Juluru K, McGill SM (1999a) Intra-abdominal pressure mechanism for stabilizing the lumbar spine. *J Biomech* 32 (1):13-7.

Cholewicki J, Juluru K, Radebold A, Panjabi MM, McGill SM (1999b) Lumbar spine stability can be augmented with an abdominal belt and/or increased intra-abdominal pressure. *Eur Spine J* 8:388-95.

Cholewicki J, Reeves NP (2004) All abdominal muscles must be considered when evaluating the intra-abdominal pressure contribution to trunk extensor moment and spinal loading. *J Biomech* 37: 953-4.

Cresswell AG (1993) Responses of intra-abdominal pressure and abdominal muscle activity during dynamic trunk loading in man *Eur J Appl Physiol* 66 (4):315-20.

Cresswell AG, Grundstrom H, Thorstensson A (1992) Observations on intra-abdominal pressure and patterns of abdominal intra-muscular activity in man. *Acta Physiol Scand* 144 (4):409-18.

Cresswell AG, Thorstensson A (1989) The role of the abdominal musculature in the elevation of the intra-abdominal pressure during specified tasks. *Ergonomics* 32:1237-46.

Crisco III JJ, Panjabi MM (1991) The intersegmental and multisegmental muscles of the lumbar spine –A biomechanical model comparing lateral stabilizing potential. *Spine* 16: 793-799.

Cyron BM, Hutton WC, Stott JRR (1975) The mechanical properties of the lumbar spine. *Mech E* 8 (2):63-68.

Daggfeldt K, Thorstensson A (1997) The role of intra-abdominal pressure in spinal unloading. *J Biomech* 30:1149-55.

Daggfeldt K, Thorstensson A (2003) The mechanics of back-extensor torque production about the lumbar spine. *J Biomech* 36:815-25.

Daggfeldt K, Thorstensson A (2004) Author's response to: "All abdominal muscles must be considered when evaluating the intra-abdominal pressure contribution to trunk extensor moment and spinal loading". *J Biomech* 37:955-6.

Damkot DK, Pope MH, Lord J, Frymoyer JW (1984) The relationship between work history, work environment and low-back pain in men. *Spine* 9(4):395-9.

Davis PR (1956) Variations of the human intra-abdominal pressure during weightlifting in different postures. *J Anat* 90:601.

Davis J, Kaufman KR, Lieber RL (2003) Correlation between active and passive isometric force and intramuscular pressure in the isolated rabbit tibialis anterior muscle. *J Biomech* 36:505-12.

Davis JR, Mirka GA (2000) Transverse-contour modeling of trunk muscle-distributed forces and spinal loads during lifting and twisting. *Spine* 25(2):180-9.

Davis PR, Troup JDG (1964) Pressures in the trunk cavities when pulling, pushing and lifting. *Ergonomics* 7:465-74.

De Looze MP, Groen H, Horemans H, Kingma I, van Dieen JH (1999) Abdominal muscles contribute in a minor way to peak spinal compression in lifting. *J Biomech* 32(7):655-62.

Dvorak J, Panjabi MM, Chang DG, Theiler R, Grob D (1991) Functional radiographic diagnosis of the lumbar spine. Flexion-extension and lateral bending. *Spine* 16 (5):562-71.

El-Rich M, Shirazi-Adl A, Arjmand N (2004) Muscle activity, internal loads and stability of the human spine in standing postures: combined model-in vivo studies. *Spine* 29:2633-42.

Essendrop M, Schibye B (2004) Intra-abdominal pressure and activation of abdominal muscles in highly trained participants during sudden heavy trunk loadings. *Spine* 29(21):2445-51.

Essendrop M, Schibye B, Hye-Knudsen C (2002) Intra-abdominal pressure increases during exhausting back extension in humans. *Eur J Appl Physiol* 87(2):167-73.

Farfan HF (1973) Mechanical disorders of low back. Philadelphia, Lea and Febiger, pp 182-189.

Hagins M, Pietrek M, Sheikhzadeh A, Nordin M, Axen K (2004) The effects of breath control on intra-abdominal pressure during lifting tasks. *Spine* 29(4):464-9.

Harman EA, Frykman PN, Clagett ER, Kraemer WJ (1988) Intra-abdominal and intra-thoracic pressures during lifting and jumping. *Med Sci Sports Exerc* 20(2):195-201.

Harman EA, Rosenstein RM, Frykman PN, Nigro GA (1989) Effects of a belt on intra-abdominal pressure during weight lifting. *Med Sci Sports Exerc* 21(2):186-90.

Hodges PW, Cresswell AG, Daggfeldt K, Thorstensson A (2001) In vivo measurement of the effect of intra-abdominal pressure on the human spine. *J Biomech* 34:347-53.

Hodges PW, Gandevia SC (2000) Changes in intra-abdominal pressure during postural and respiratory activation of the human diaphragm. *J Appl Physiol* 89(3):967-76.

Hoogendoorn WE, Bongers PM, de Vet HC, Douwes M, Koes BW, Miedema MC, Ariens GA, Bouter LM (2000) Flexion and rotation of the trunk and lifting at work are risk factors for low back pain: results of a prospective cohort study. *Spine* 25:3087-92.

Hughes RE, Chaffin DB, Lavender SA, Andersson GBJ (1994) Evaluation of muscle force prediction models of the lumbar trunk using surface electromyography. *J Orthop Res* 12:689-698.

Keith A (1923) Man's posture: its evolution and disorders. *Brit Med J* 1:587-590.

Krag MH, Byrne KB, Gilbertson LG, Haugh LD (1986) Failure of intra-abdominal pressurization to reduce erector spinae loads during lifting tasks. In: Proceedings of the 10th Annual Congress of the North American Society of Biomechanics. Montreal, Canada.

Lander JE, Hundley JR, Simonton RL (1992) The effectiveness of weight-belts during multiple repetitions of the squat exercise. *Med Sci Sports Exerc* 24(5):603-9.

Mairiaux P, Malchaire J, Vandiepenbeeck D, Bellelahom L (1988) Reproducibility of intra-abdominal pressure when lifting. *Scand J Rehabil Med* 20(2):83-8.

Marras WS, King AI, Joynt RL (1984) Measurements of loads on the lumbar spine under isometric and isokinetic conditions. *Spine* 9:176-88.

Marras WS, Mirka GA (1996) Intra-abdominal pressure during trunk extension motions. *Clin Biomech* 11:267–74.

McGill SM (1996) A revised anatomical model of the abdominal musculature for torso flexion efforts. *J Biomech* 29(7):973-7.

McGill SM, Norman RW (1986) Partitioning of the L4L5 dynamic moment into disc, ligaments and muscular components during lifting. *Spine* 11:666-678.

McGill SM, Norman RW (1987) Reassessment of the role of intra-abdominal pressure in spinal compression. *Ergonomics* 30:1565–1588

McGill SM, Norman RW (1988) Potential of lumbodorsal fascia forces to generate back extension moments during squat lifts. *J Biomed Eng* 10 (4):312-8.

McGill SM, Norman RW (1993) Low back biomechanics in industry: The prevention of injury through safer lifting. In M.D. Grabiner (Ed.). *Current issues in biomechanics*. (pp. 69-120). Human Kinetics: Champaign, Il.

McGill SM, Norman RW, Sharratt MT (1990) The effect of an abdominal belt on trunk uscle activity and intra-abdominal pressure during squat lifts. *Ergonomics* 33:147–60.

Mueller G, Morlock MM, Vollmer M, Honl M, Hille E, Schneider E (1998) Intramuscular pressure in the erector spinae and intra-abdominal pressure related to posture and load. *Spine* 23(23):2580-90.

Morris JM, Lucas DM, Bresler B (1961) Role of the trunk in stability of the spine. *J Bone Joint Surg Am* 43:327-351.

Nachemson AL, Andersson GBJ, Schultz AB (1986) Valsalva maneuver biomechanics. Effects on lumbar trunk loads of elevated intraabdominal pressures. *Spine* 11:476–479.

Ng JKF, Kippers V, Richardson CA (1998) Muscle fibre orientation of abdominal muscles and suggested surface EMG electrode positions. *Electromyogr Clin Neurophysiol* 38:51–58.

Ng JK, Kippers V, Parnianpour M, Richardson CA (2002) EMG activity normalization for trunk muscles in subjects with and without back pain. *Med Sci Sports Exerc* 34(7) :1082-6.

Nussbaum MA, Chaffin DB (1996) Development and evaluation of a scalable and deformable geometric model of the human torso. *Clin Biomech* 11 (1):25-34.

Oxland T, Lin RM, Panjabi M (1992) Three-dimensional mechanical properties of the thoracolumbar junction. *J Orthop Res* 10:573-580.

Patwardhan AG, Havey RM, Carandang G, Simonds J, Voronov LI, Ghanayem AJ, Meade KP, Gavin TM, Paxinos O (2003) Effect of compressive follower preload on the flexion-extension response of the human lumbar spine. *J Orthop Res* 21 (3): 540-6.

Pearcy M, Portek I, Shepherd J (1984) Three-dimensional x-ray analysis of normal movement in the lumbar spine. *Spine* 9 (3):294-7.

Pearsall DJ (1994) Segmental inertial properties of the human trunk as determined from computer tomography and magnetic resonance imagery. PhD thesis. Queen's University, Kingston, Ontario.

Plamondon A, Gagnon M, Maurais G (1988) Application of a stereoradiographic method for the study of intervertebral motion. *Spine* 13 (9):1027-32.

Potvin JR, McGill SM, Norman RW (1991) Trunk muscle and lumbar ligament contributions to dynamic lifts with varying degrees of trunk flexion. *Spine* 16:1099-107.

Raikova RT, Prilutsky BI (2001) Sensitivity of predicted muscle forces to parameters of the optimization-based human leg model revealed by analytical and numerical analyses. *J Biomech* 34:1243-1255.

Shirazi-Adl A (2006) Analysis of large compression loads on lumbar spine in flexion and in torsion using a novel wrapping element. *J Biomech* 39(2):267-75.

Shirazi-Adl A, Sadouk S, Parnianpour M, Pop D, El-Rich M (2002) Muscle force evaluation and the role of posture in human lumbar spine under compression. *Eur Spine J* 11:519-526.

Silfies SP, Squillante D, Maurer P, Westcott S, Karduna AR (2005) Trunk muscle recruitment patterns in specific chronic low back pain populations. *Clin Biomech* 20 (5):465-473.

Stokes IA, Gardner-Morse M (1999) Quantitative anatomy of the lumbar musculature. *J Biomech* 32:311-316.

Takashima ST, Singh SP, Haderspeck KA, Schultz AB (1979) A model for semi-quantitative studies of muscle actions. *J Biomech* 12:929-939.

Tan JC, Parnianpour M, Nordin M, Hofer H, Willems B (1993) Isometric maximal and submaximal trunk extension at different flexed positions in standing. Triaxial torque output and EMG. *Spine* 18:2480-90.

Urquhart DM, Barker PJ, Hodges PW, Story IH, Briggs CA (2005) Regional morphology of the transversus abdominis and obliquus internus and externus abdominis muscles. *Clin Biomech* 20:233-41.

van Dieen JH (1997) Are recruitment patterns of the trunk musculature compatible with a synergy based on the maximization of endurance? *J Biomech* 30:1095-1100.

Woittiez RD, Huijing PA, Boom HB, Rozendal RH (1984) A three-dimensional muscle model: a quantified relation between form and function of skeletal muscles. *J Morphol* 182 (1):95-113.

Yamamoto I, Panjabi M, Crisco T, Oxland T (1989) Three-dimensional movements of the whole lumbar spine and lumbosacral joint. *Spine* 14:1256-1260.

Table 6.1 Characteristics considered for the application of IAP in the model

Task (+180 N in Hands)	IAP (kPa)	Area (cm ²)*	Total Force (N)	Lever Arm @ T12 (cm) *	Extensor Moment (Nm) @ T12
Standing Posture	4	200	80	4.0	3.2
Flexion 40° and 65 °	9	250	225	5.0	11.25

* Daggfeldt and Thorstensson, 2003

Table 6.2 Physiological cross sectional area (PCSA, mm²) and initial length (in parentheses, mm) for muscles on each side of the spine at different insertion levels. ICPL: Iliocostalis Lumborum pars lumborum, ICPT: Iliocostalis Lumborum pars thoracic, IP: Iliopsoas, LGPL: Longissimus Thoracis pars lumborum, LGPT: Longissimus Thoracis pars thoracic, MF: Multifidus, QL: Quadratus Lumborum, IO: Internal Oblique, EO: External Oblique, and RA: Rectus Abdominus.

Local Muscles	ICPL	IP	LGPL	MF	QL
L1	108 (170)	252 (276)	79 (172)	96 (158)	88 (137)
L2	154 (118)	295 (241)	91 (132)	138 (135)	80 (104)
L3	182 (84)	334 (206)	103 (88)	211 (106)	75 (74)
L4	189 (50)	311 (169)	110 (52)	186 (82)	70 (46)
L5	-	182 (132)	116 (25)	134 (51)	-
Global Muscles	RA	EO	IO	ICPT	LGPT
T1-T12	567 (353)	1576 (239)	1345 (135)	600 (250)	1100 (297)

Table 6.3 Three levels of abdominal muscle coactivities and the generated force/flexor moment

Level	% Coactivity	Force on Each Side (N) [†]	Lever Arm @ T12 (mm)		Flexor Moment (Nm) @ T12
1- Low	RA: 0.5	1.7	S‡	140.0	0.48
			F40‡	150.0	0.51
			F65‡	151.2	0.51
	EO: 1	9.5	S	17.7	0.33
			F40	12.0	0.23
			F65	10.9	0.21
	IO: 2	16.1	S	98.7	3.19
			F40	98.4	3.18
			F65	98.8	3.19
2-Moderate	RA: 1	3.4	S	139.9	0.95
			F40	150.0	1.02
			F65	151.2	1.03
	EO: 2	18.9	S	17.7	0.67
			F40	12.0	0.45
			F65	10.9	0.41
	IO: 4	32.3	S	98.8	6.38
			F40	98.5	6.36
			F65	98.9	6.38
3- High	RA: 2	6.8	S	140.0	1.91
			F40	149.9	2.04
			F65	151.1	2.06
	EO: 4	37.8	S	17.6	1.33
			F40	12.0	0.91
			F65	10.9	0.82
	IO: 8	64.6	S	98.7	12.75
			F40	98.6	12.74
			F65	99.0	12.79

† (0.6 MPa)*PCAS*(% Coactivity)

‡ S: Standing posture, F40: Flexion posture at 40°, F65: Flexion posture at 65°

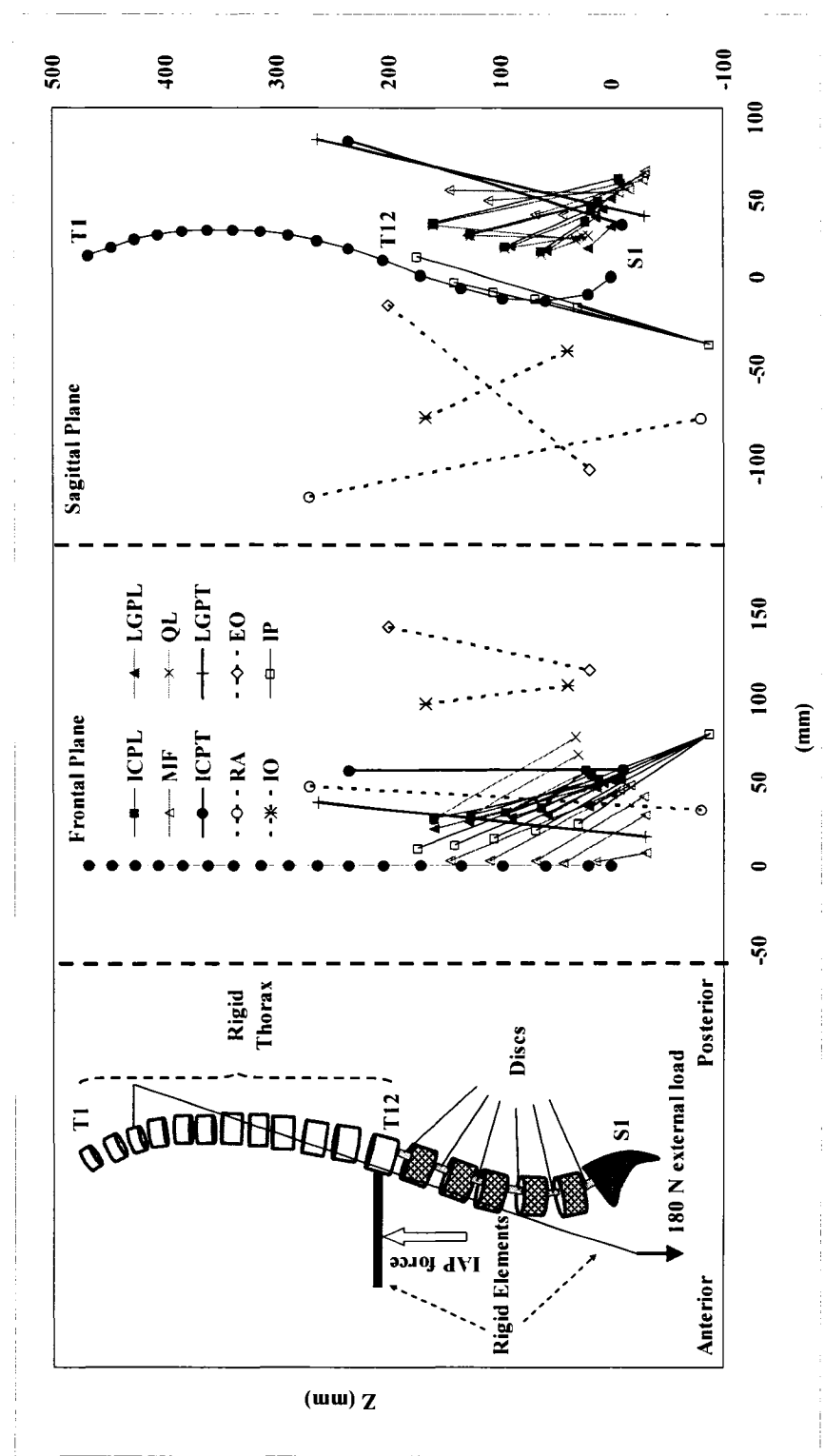


Fig. 6.1 The FE model as well as global and local musculatures in the sagittal and frontal planes (only fascicles on one side have been shown). ICPL: Iliocostalis Lumborum pars lumborum, ICPT: Iliocostalis Lumborum pars thoracic, IP: Iliopsoas, LGPL: Longissimus Thoracis pars lumborum, LGPT: Longissimus Thoracis pars thoracic, MF: Multifidus, QL: Quadratus Lumborum, IO: Internal Oblique, EO: External oblique, and RA: Rectus Abdominus.

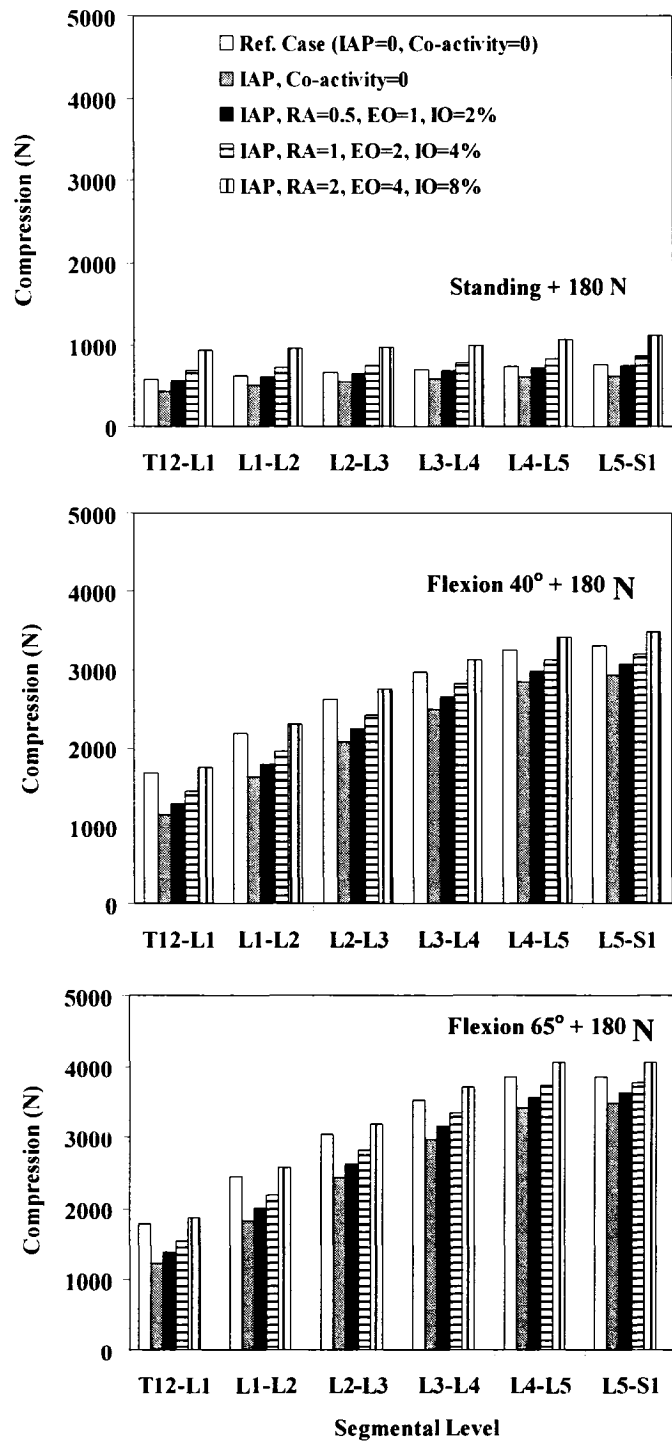


Fig. 6.2 Axial compression (N) acting normal to different intervertebral disc levels (T12/S1) in reference cases (no IAP and no abdominal coactivity) and four cases with different abdominal coactivities along with IAP.

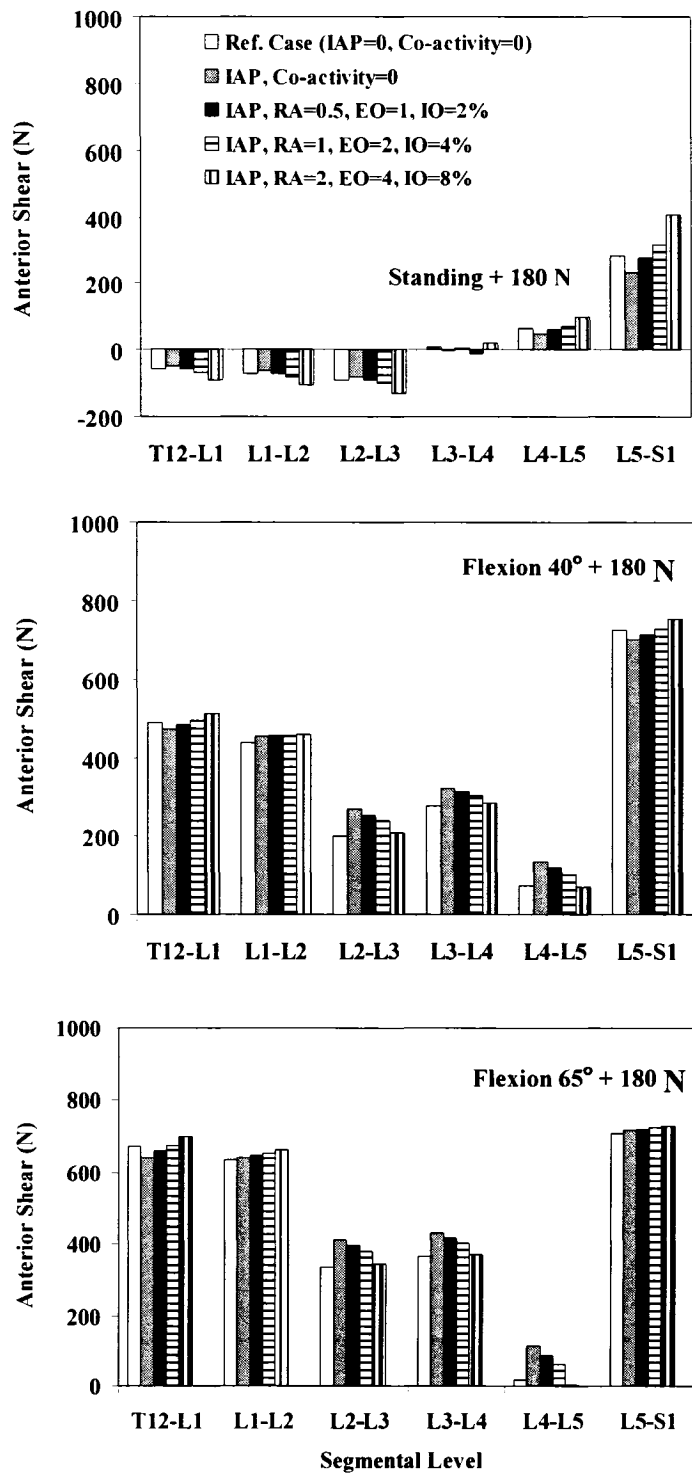


Fig. 6.3 Anterior-posterior shear force (N) acting parallel to mid-planes of different intervertebral disc levels (T12/S1) in reference cases (no IAP and no abdominal coactivity) and four cases with different abdominal coactivities along with IAP.

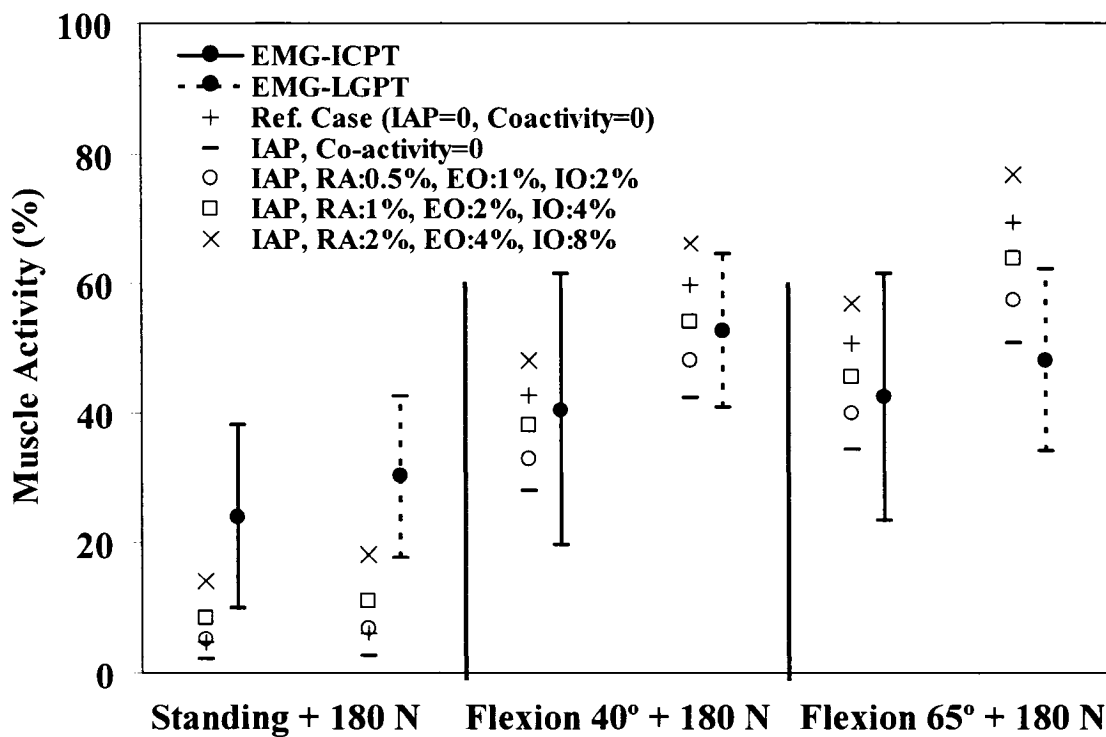


Fig. 6.4 Normalized *in vivo* measured EMG activity (mean \pm SD) of thoracic extensor muscles (Longissimus Thoracis pars thoracic, LGPT, and Iliocostalis Lumborum pars thoracic, ICPT) for different lifting tasks. Predictions have also been shown in reference cases (no IAP and no abdominal coactivity) and four cases with different abdominal coactivities along with IAP of 4 kPa when lifting a load of 180 N in upright standing posture and of 9 kPa when lifting the same load in forward trunk flexions of 40° and 65°.

CHAPTER 7

Wrapping of Trunk Thoracic Extensor Muscles Influences Muscle Forces and Spinal Loads in Lifting Tasks

N. Arjmand, A. Shirazi-Adl, and B. Bazrgari

Article published in *Clinical Biomechanics* 2006; 21 (7): 668-675

Keywords: Lever arm; Line of action; Muscle; Finite element method; Kinematics; Lifting

7.1 ABSTRACT

Background: An improved assessment of risk of spinal injury during lifting activities depends on an accurate estimation of trunk muscle forces, spinal loads and stability margin which in turn requires, amongst others, an accurate description of trunk muscle geometries. The lines of action of erector spinae muscles are often assumed to be linear despite the curved paths of these muscles in forward flexion postures.

Methods: A novel approach was introduced that allowed for the proper simulation of curved paths for global extensor muscles in our Kinematics-driven finite element model. The lever arms of global muscles at different levels were restrained either to remain the same or decrease only by 10% relative to their respective values in upright posture. Based on our earlier measurements, static lifting tasks at two trunk flexions (40° and 65°) and three lumbar postures (free style, lordotic and kyphotic) with 180 N in hands were analyzed.

Findings: Muscle forces and spinal compression at all levels substantially decreased as the global extensor muscles took curved paths. In contrast, the shear force at lower levels increased. Allowing for a 10% reduction in these lever arms during flexion increased muscle forces and compression forces at all levels. Despite smaller muscle forces, wrapping of global muscles slightly improved the spinal stability.

Interpretation: Consideration of global extensor muscles with curved paths and realistic lever arms is important in biomechanical analysis of lifting tasks. Reduction in the erector spinae lever arms during flexion tasks could vary depending on the lumbar posture. Results advocate small flattening of the lumbar curvature in isometric lifts yielding smaller compression and shear forces at the critical L5-S1 level.

7.2 INTRODUCTION

Accurate estimation of trunk muscle forces and spinal loads in various activities is essential for a better assessment of risk of tissue injury towards improvements in manual material handling techniques as well as prevention and treatment procedures. The infeasibility of direct quantification of muscle forces and spinal loads has led researchers to exploit biomechanical modeling techniques. For an improved estimation of spinal loads in lifting activities, biomechanical models require precise data on the geometry of trunk extensor muscles such as lever arm (LA) magnitude and line of action (LOA) with a straight or curved pathway.

Wide ranges of data, however, have been reported in the literature for the LA of erector spinae (ES) in the sagittal plane (~4-8 cm) (Bogduk et al., 1992; Daggfeldt and Thorstensson, 2003; Jorgensen et al., 2001; McGill, 2002; Stokes and Gardner-Morse, 1999; Wood et al., 1996) as well as for their LOA (Cholewicki and McGill, 1996; Han et al., 1992; Stokes and Gardner-Morse, 1999). The discrepancy exists partly due to different descriptions for the ES muscles themselves. Traditionally, ES group has been defined as a collection of fascicles originating from the sacroiliac region and running up to insert into vertebrae and the rib cage (Jorgensen et al., 2001, 2003; Moga et al., 1993; Wood et al., 1996). In some studies while not including the multifidus, the ES group is divided into four parts (longissimus thoracis pars thoracis/lumborum and iliocostalis lumborum pars thoracis/lumborum) each possessing several fascicles with different LOAs and LAs (Bogduk et al., 1992; Macintosh et al., 1993). As for the muscle LA, some studies (e.g., Jorgensen et al., 2001, 2003) have considered the distance in a transverse plane between the disc and ES centroid while others (Tveit et al., 1994) measure it as the perpendicular distance between the disc center and LOA of the ES. The former naturally ignores the effect of muscle fiber orientation resulting in overestimation of its LA. Both the LA of ES (Jorgensen et al., 2003; Macintosh et al., 1993; Tveit et al., 1994) and the angle between their LOA and the longitudinal axis of vertebrae (Macintosh et al., 1993; McGill et al., 2000) have been observed to decrease as the spine

flexes forward in the sagittal plane. The extent of such alterations, especially for thoracic fascicles of the ES, needs yet to be determined (Macintosh et al., 1993). Neglecting such variations in model studies simulating flexion tasks has resulted in a substantial underestimation of the compression force (by up to 46%) and overestimation of anterior-posterior shear force (by up to 300%) at the L5/S1 level (van Dieen and de Looze, 1999).

An equally crucial issue is the pathway of local (i.e., with upper attachments at lumbar vertebrae) and global (i.e., with upper attachments at the rib cage) ES muscles. Unlike in upright postures in which these pathways can accurately be assumed as straight lines between insertion points, such may not be assumed in tasks involving large lumbar flexions. In latter tasks, a straight line assumption for global muscles could violate kinematics constraints by penetrating into intervening hard/soft tissues. The local lumbar muscles have been suggested not to take significantly curved orientations in flexion (Macintosh et al., 1993). Curved rather than linear pathways have, however, to be considered for global muscles especially in tasks involving large trunk flexion if precise estimation of muscle forces and spinal loads are sought.

In our earlier investigations modeling static lifting activities with different lumbar postures (Arjmand and Shirazi-Adl, 2005, 2006a), detailed description of the ES was used (Bogduk et al., 1992; Macintosh et al., 1993; Stokes and Gardner-Morse, 1999). Although the LA of both global and local ES muscles diminished as the spine flexed forward from the standing upright posture, they remained, nevertheless, linear in between their insertion points. Magnitude of the LA of local muscles under flexion tasks were in overall agreement with those reported under flexed lumbar postures (Macintosh et al., 1993). The assumption of global ES muscles (i.e., iliocostalis and longissimus) remaining straight even in large forward flexion postures needs, however, to be critically investigated. The objective of the current work was, hence, to study the likely effects of the wrapping of global ES muscles and of subsequent reduction in their LA on computed

muscle forces, internal spinal loads and system stability in lifting tasks. It is hypothesized that the wrapping (i.e., curved path) of global muscles in larger trunk flexion angles markedly influences the model predictions, the extent of which depends on the trunk flexion angle and lumbar posture. For this purpose, a novel approach was introduced that accounted for the wrapping of global ES muscles in our Kinematics-driven finite element model (Arjmand and Shirazi-Adl, 2005, 2006a) by allowing these muscles to alter orientation while passing over various T12-L5 levels. Results were compared with our earlier predicted (assuming straight paths for global ES muscles) and measured results under same isometric lifting tasks.

7.3 METHODS

7.3.1 Tasks Simulated

Fifteen healthy male with no recent back complications volunteered for the study after signing an informed consent form. Their mean age, body height and mass were 30 ± 6 years, 177 ± 7 cm, and 74 ± 11 kg. While bending slightly forward, infrared light emitting markers, LED, were placed on tip of the spinous processes at T1, T5, T10, T12, L1, L3, L5, and S1 levels. Three extra LED markers were placed on the ilium (left/right iliac crests) and posterior-superior iliac spine for evaluation of pelvic rotation and one on the bar to detect the position of weights in hands. A three-camera Optotrak system (NDI International, Waterloo/Canada) was used to collect 3D coordinates of LED markers. To record EMG signals, five pairs of surface electrodes were positioned bilaterally over the following trunk muscles: longissimus dorsi (~ 3 cm lateral to midline at the L1), iliocostalis (~ 6 cm lateral to midline at the L1), multifidus (~ 2 cm lateral to midline at the L5), external obliques (~ 10 cm lateral to midline above umbilicus and aligned with muscle fibers), and rectus abdominis (~ 3 cm lateral to midline above the umbilicus). The raw EMG signals were collected at 1500 Hz, amplified, band-pass filtered at 10-400 Hz by a 2nd order Butterworth filter, and RMS was calculated over 4s trial duration and averaged for both sides. For normalization, EMG data at maximum voluntary

contraction (MVC) was collected in standing (in cardinal planes while loaded via a strapped harness, prone, and supine positions.

Subjects held 180 N in hands via a bar during isometric forward flexion tasks with torso at $\sim 40^\circ$ or $\sim 65^\circ$. These tasks were performed either with no instruction on the posture (free style) or with specific instruction that subjects voluntarily take lordotic and kyphotic lumbar postures by controlling their pelvic tilt. In all three postures, the overall trunk forward rotations were kept nearly unchanged as subjects primarily altered their pelvic tilt to achieve various lumbar postures. During measurements, subjects were also instructed to keep knees straight and arms extended in the gravity direction.

7.3.2 Model Study

A sagittally-symmetric T1-S1 beam-rigid body model consisting of 6 deformable beams with nonlinear properties to represent T12-S1 segments and 7 rigid elements to represent T1-T12 (as a single body) and lumbosacral vertebrae (L1 to S1) was used to estimate muscle forces, spinal loads, and system stability during the aforementioned tasks (Fig. 7.1) (Arjmand and Shirazi-Adl, 2005, 2006a). In all cases, based on the mean body weight of our subjects and percentage of body weight at each motion segment level reported elsewhere (Pearsall, 1994; Takashima et al., 1979), a gravity load of 387 N was considered and distributed eccentrically at different levels. The weight of 180 N was applied at the location measured *in vivo* via a rigid element attached to the T3 vertebra. Mean measured sagittal rotations at the upper torso (evaluated based on the change in the inclination of the line attaching the T1 marker to the T12 one) and pelvis (evaluated based on the change in the orientation of the normal to the plane passing through the pelvis markers) were prescribed onto the model at the T12 and S1 levels, respectively. As for the individual lumbar vertebrae, the total lumbar rotation, calculated as the difference between the foregoing two rotations, was partitioned in accordance with proportions reported in earlier investigations (Dvorak et al., 1991; Pearcy et al., 1984; Plamondon et al., 1988; Potvin et al., 1991; Yamamoto et al., 1989).

A sagittally-symmetric muscle architecture with 46 local and 10 global fascicles having straight LOAs in neutral standing posture was used (Bogduk et al., 1992; Stokes and Gardner-Morse, 1999) (Fig. 7.1). The Kinematics-driven approach was employed to evaluate trunk muscle forces subject to prescribed measured kinematics and external loads (Arjmand and Shirazi-Adl; 2005, 2006a; El-Rich et al, 2004; Shirazi-Adl et al., 2002). This approach exploits kinematics data to generate additional equilibrium equations at each level in order to alleviate the kinetic redundancy of the problem. Sagittal rotations applied a priori at different spinal levels generated an equilibrium equation at each level in the form of $\sum r_i \times f_i = M$ (r: muscle lever arm, f: muscle force, and M: required sagittal moment due to the prescribed rotation). To resolve the redundancy problem an optimization approach with the cost function of minimum sum of cubed muscle stresses (Arjmand and Shirazi-Adl, 2006b) was used along with inequality equations of unknown muscle forces remaining positive and greater than their passive force components (calculated based on muscle strain and a tension-length relationship (Davis et al., 2003) but smaller than the sum of maximum physiological active forces (i.e., 0.6 PCSA) and the passive force components. The finite element program ABAQUS Inc. version 6.5 was used to carry out nonlinear structural analyses while the optimization procedure was analytically solved using an in-house program based on Lagrange Multipliers Method (Raikova and Prilutsky, 2001).

To simulate curved paths in forward flexion tasks, global muscles (i.e., thoracic iliocostalis and longissimus) were assumed to wrap around pre-defined points that were located on and moved with T12-L5 vertebral levels. During the iterative analyses, the wrapping contact at each T12-L5 level occurred only when the instantaneous LA distance at that level decreased below its corresponding (critical) value in the neutral standing posture; being 58, 56, 56, 56, 52 and 44 mm for global iliocostalis and 53, 53, 55, 56, 54 and 48 mm for global longissimus at T12, L1, L2, L3, L4, and L5 vertebral levels, respectively. In these cases, no reduction in the LA distances was, hence, allowed

as the trunk flexed from the upright posture. To investigate the likely effect of alterations in these critical LA values set for beginning of the contact on results, an additional case under trunk flexion of 65° was also studied assuming 10% smaller critical LAs. Nonlinear finite element formulation of the curved paths was performed based on our earlier works on modeling of wrapping elements (Shirazi-Adl, 1989, 2006; Shirazi-Adl and Parnianpour, 2000). The wrapping reaction forces at each T12-L5 level was calculated in each iteration of the analysis by application of equilibrium at instantaneous deformed configurations taking identical muscle force in adjacent segments (i.e., frictionless contact). These wrapping reaction forces along with the axial and horizontal force penalties of the calculated muscle forces were fed back into the finite element model as additional updated external loads. This iterative approach was continued till convergence was reached. Once muscle forces were computed, the model was modified with uniaxial elements to represent muscles between their insertion points. Stiffness of each uniaxial element, k , was assigned using the linear stiffness-force relation $k=qF/L$ where q is the muscle stiffness coefficient, F is the muscle force and L is the muscle length. Nonlinear stability and linear perturbation analyses (Arjmand and Shirazi-Adl, 2005, 2006a) were performed to properly investigate the system stability. In the linear perturbation analyses, a unit force was applied at the T1 vertebra at deformed configuration and resulting horizontal displacement was calculated at different q values.

7.4. RESULTS

As the trunk flexed from the upright standing to 40° or 65° forward flexion, the global muscles followed a curved path while wrapping at different lumbar levels (Fig. 7.2). For the case allowing a 10% reduction in LA, no wrapping however occurred at L1-L3 levels in all postures as the LA distances at these levels did not fall below their corresponding critical values for contact. The muscle and spinal compression forces at all levels substantially decreased in both trunk flexion angles and in all three lumbar postures as the global ES took curved paths by wrapping around the T12-L5 levels while preserving their LA distances (Table 7.1). In contrast, the segmental shear forces at

distal L3-S1 levels increased in these cases (Table 7.1). A 10% reduction in critical LA of wrapping global muscles substantially increased compression forces at all levels. Wrapping of global muscles resulted in smaller muscle activities as compared with the cases with straight muscles, as depicted in Fig. 7.3 where the normalized active component of predicted muscle forces are compared with the normalized EMG data. When allowing for a 10% reduction in global muscle LAs for the case with the trunk flexion of 65°, the muscle activities increased to magnitudes in between the foregoing values for cases with either straight or curved global ES (Fig. 7.3).

Contact forces at wrapping points generally increased with trunk flexion but decreased from kyphotic postures to lordotic ones regardless of the task considered (Table 7.2). In linear perturbation analyses, with identical q values, slightly smaller T1 translations were computed when curved LOA was considered for global muscles (Fig. 7.4); the spinal stability was slightly improved in the case with curved global muscles. The relative effect of changes in lumbar posture (i.e., lordotic vs. kyphotic) on results remained nearly the same in both cases with straight or curved global ES muscles; lordotic posture increased active muscle forces as well as maximum compression and shear forces occurring at the lowermost L5-S1 level (Table 7.1). The segmental moments, however, were much greater in the kyphotic posture regardless of the global muscle path.

7.5 DISCUSSION

In earlier works assuming linear paths for global ES muscles (Arjmand and Shirazi-Adl, 2005, 2006a), excessive reductions in the LA of global muscle fascicles were evaluated compared with those reported (Tveit et al., 1994); e.g., 25%, 28%, and 20% at the T12 vertebra in free, kyphotic, and lordotic lumbar postures, respectively. An unrealistically close muscle path could also violate the kinematics requirement by passing through intervening hard/soft tissues. A novel approach was subsequently introduced in the current study in order to allow for global ES muscles with curved paths

while still assuming local muscles to have straight LOAs. Two cases with wrapping global muscles were considered in which as the spine flexed from the neutral standing posture the critical LAs of global muscles required for wrapping either remained as their initial values at upright standing or allowed to reduce by 10% from these initial values. The hypothesis of this study regarding the importance of wrapping of global muscles in large flexion postures was confirmed by predicting substantially smaller axial compression and muscle forces at all levels whereas greater shear forces at lower levels (Table 7.1 and Fig. 7.3). The former predictions are expected as larger LAs of global muscles in cases with wrapping muscles demand smaller muscle forces and, hence, smaller compression force at different levels while the latter predictions are due to the presence of wrapping contact forces. The mechanical effect of the wrapping of global ES muscles increased at greater trunk angles. Despite much smaller forces in global muscles in cases with wrapping global muscles, the system stability was only slightly improved which could be due to smaller compression forces on the spine in these cases.

Wrapping contact forces, with the exception of that at the L5/S1 level, acted approximately perpendicular to the compressive axis of the spine (Fig. 7.5) thus primarily increasing anterior shear forces with smaller effect on the axial compression. The effect of contact forces in increasing anterior shear force was especially obvious at the lower levels (L3-S1) (Table 7.1) while at the upper levels this effect disappeared due to more horizontal LOA of global muscles in cases with curved paths (Fig. 7.2). The wrapping contact forces generally increased as the trunk flexion angle increased and kyphotic posture was adopted (Table 7.2). These are due to the fact that the magnitude of the contact force depends not only on the muscle force but on the change in LOA of the muscle at a contact point; the larger this change is the greater the contact will become. The curved muscle LOA and associated wrapping contact forces resulted in a slight improvement in the system stability and that despite much smaller muscle forces when wrapping muscles were considered. Irrespective of the paths of global muscles,

straight or curved with or without 10% reduction in LAs, maximum compression and shear forces occurred at the distal L5-S1 segmental level and were larger in lordotic postures than in kyphotic ones.

Some earlier biomechanical models (e.g. Cholewicki and McGill, 1996) report also to have considered curved pathways for extensor muscles that pass through several points at different vertebrae. These models, however, appear to have failed to account for reaction (contact) forces at these points of contact between muscles and vertebrae. These contact forces are due to changes in muscle orientation and would generate moment as well as shear/compression forces that need to be considered in associated equilibrium equations at different levels. Simulation of wrapping without the proper consideration of these contact forces at the deformed configuration of the spine is not, hence, adequate adversely affecting the accuracy of estimations.

Since the exact extent of reduction in LAs of global muscles in flexion tasks remains unknown (Jorgensen et al., 2003; Macintosh et al., 1993; Tveit et al., 1994), a case was simulated with a 10% reduction which remained the same at all levels and in both kyphotic and lordotic postures. This resulted in a considerable increase in spinal compression and muscle forces compared to the case in which no reduction in LA was allowed (Table 7.1 and Fig 7.3). Comparison of trends in predicted active forces in global muscles with their measured EMG as posture changed (Fig. 7.3) would appear to indicate a better qualitative agreement had the reduction of 10% in LAs of global muscles been considered only for free and kyphotic postures and not for the lordotic postures. In other words, though not considered in this work, the reduction in the LAs of wrapping global muscles may be posture dependent; being greater in kyphotic postures than in lordotic ones, an observation that is in agreement with earlier works (Tveit et al., 1994). Results also reiterate, in agreement with others (Nussbaum et al., 1995; Parnianpour et al., 1997; van Dieen and de Looze, 1999), the sensitivity of the estimated spinal loads to anatomical assumptions including LOA and LA of global muscles.

It must be noted that, in this work, the EMG data were normalized with their measured MVC values whereas the predicted active muscle forces were normalized with their maximum value of 0.6^*PCSA . Due to major concerns on the EMG data collected at the MVC tasks, the EMG data collected on the skin at one level for each muscle, the maximum stress value of 0.6 MPa taken for normalization of predicted active muscle forces, the passive force-length relationship used for muscles in the model, and the existence of EMG-force relationships, no attempt was made to adjust input data to arrive at specific activation values in better agreement with measurements. It is evident that changing the maximum active stress from 0.6 MPa to, for example, 0.5 MPa or inversely to 0.7 MPa, while remaining still in the range of reported values in the literature, would shift all predicted values in Fig. 7.3 substantially upward or downward, respectively.

In conclusion, the assumption of straight and not curved LOA for global muscles in biomechanical models simulating lifting tasks results in much greater spinal compression forces and muscle activities whereas smaller shear forces at lower levels. The spinal stability is slightly improved by the wrapping of global muscles and that despite much smaller muscle activities. While providing almost the same spinal stability margin, the kyphotic lift decreases active muscle forces as well as maximum spinal compression and shear forces. Therefore, a posture with moderate flexion is preferable during lifting activities which agrees with the same finding in our previous study assuming linear paths for global muscles (Arjmand and Shirazi-Adl, 2005). The extent of reduction in the LA of global muscles during flexion that maybe posture dependent also influences results as such reductions substantially increase muscle forces and spinal compression.

7.6 ACKNOWLEDGEMENT

The work was supported by grants from the NSERC-Canada and the IRSST-Québec.

7.7 REFERENCES

Arjmand, N., Shirazi-Adl, A., 2006a. Model and in vivo studies on human trunk load partitioning and stability in isometric forward flexions. *J Biomech* 39, 510-521.

Arjmand, N., Shirazi-Adl, A., 2006b. Sensitivity of kinematics-based model predictions to optimization criteria in static lifting tasks. *Med Eng Phys.*, in press (available online).

Arjmand, N., Shirazi-Adl, A., 2005. Biomechanics of changes in lumbar posture in static lifting. *Spine* 30, 2637-48.

Bogduk, N., Macintosh, J.E., Pearcy, M.J., 1992. A universal model of the lumbar back muscles in the upright position. *Spine* 17, 897-913.

Cholewicki, J., McGill, S.M., 1996. Mechanical stability of the in vivo lumbar spine: implications for injury and chronic low back pain. *Clin Biomech* 11, 1-15.

Daggfeldt, K., Thorstensson, A., 2003. The mechanics of back-extensor torque production about the lumbar spine. *J Biomech*. 36, 815-25.

Davis, J., Kaufman, K.R., Lieber, R.L., 2003. Correlation between active and passive isometric force and intramuscular pressure in the isolated rabbit tibialis anterior muscle. *J Biomech* 36, 505-12.

Dvorak, J., Panjabi, M.M., Chang, D.G., Theiler, R., Grob, D., 1991. Functional radiographic diagnosis of the lumbar spine. Flexion-extension and lateral bending. *Spine* 16, 562-71.

El-Rich, M., Shirazi-Adl, A., Arjmand, N., 2004. Muscle activity, internal loads and stability of the human spine in standing postures: combined model-in vivo studies. *Spine* 29, 2633-42.

Han, J.S., Ahn, J.Y., Goel, V.K., Takeuchi, R., McGowan, D., 1992. CT-based geometric data of human spine musculature. Part I. Japanese patients with chronic low back pain. *J Spinal Disord*. 5, 448-58.

Jorgensen, M.J., Marras, W.S., Granata, K.P., Wiand, J.W., 2001. MRI-derived moment-arms of the female and male spine loading muscles. *Clin Biomech* 16, 182-93.

Jorgensen, M.J., Marras, W.S., Gupta, P., Waters, T.R., 2003. Effect of torso flexion on the lumbar torso extensor muscle sagittal plane moment arms. *The Spine J.* 3, 363-9.

Macintosh, J.E., Bogduk, N., Pearcy, M.J., 1993. The effects of flexion on the geometry and actions of the lumbar erector spinae. *Spine* 18, 884-93.

McGill S.M., 2002. Low Back Disorders: Evidence-Based Prevention and Rehabilitation. Human Kinetics Publishers; 1st Edition.

McGill, S.M., Hughson, R.L., Parks, K., 2000. Changes in lumbar lordosis modify the role of the extensor muscles. *Clin Biomech* 15, 777-80.

Moga, P.J., Erig, M., Chaffin, D.B., Nussbaum, M.A., 1993. Torso muscle moment arms at intervertebral levels T10 through L5 from CT scans on eleven male and eight female subjects. *Spine* 18, 2305-9.

Nussbaum, M.A., Chaffin, D.B., Rechtien, C.J., 1995. Muscle lines-of-action affect predicted forces in optimization-based spine muscle modeling. *J Biomech.* 28, 401-9.

Parnianpour, M., Wang, J.L., Shirazi-Adl, A., Sparto, P., Wilke, H.J., 1997. The effect of variations in trunk models in predicting muscle strength and spinal loads. *Journal of Musculoskeletal Research* 1, 55-69.

Pearcy, M., Portek, I., Shepherd, J., 1984. Three-dimensional x-ray analysis of normal movement in the lumbar spine. *Spine* 9, 294-7.

Pearsall, D.J., 1994. Segmental inertial properties of the human trunk as determined from computer tomography and magnetic resonance imagery. PhD thesis. Queen's University, Kingston, Ontario.

Plamondon, A., Gagnon, M., Maurais, G., 1988. Application of a stereoradiographic method for the study of intervertebral motion. *Spine* 13, 1027-32.

Potvin, J.R., McGill, S.M., Norman, R.W., 1991. Trunk muscle and lumbar ligament contributions to dynamic lifts with varying degrees of trunk flexion. *Spine* 16, 1099-107.

Raikova, R.T., Prilutsky, B.I., 2001. Sensitivity of predicted muscle forces to parameters of the optimization-based human leg model revealed by analytical and numerical analyses. *J Biomech.* 34, 1243-1255.

Seo, A., Lee, J.H., Kusaka, Y., 2003. Estimation of trunk muscle parameters for a biomechanical model by age, height and weight. *J Occup Health.* 45, 197-201.

Shirazi-Adl, A., 2006. Analysis of large compression loads on lumbar spine in flexion and in torsion using a novel wrapping element. *J Biomech.*, 39, 267-275.

Shirazi-Adl, A., 1989. Nonlinear finite element analysis of wrapping uniaxial elements. *Computers & Structures* 32, 119-123

Shirazi-Adl, A., Parnianpour, M., 2000. Load-bearing and stress analysis of the human spine under a novel wrapping compression loading. *Clin Biomech* 15, 718-25.

Shirazi-Adl, A., Sadouk, S., Parnianpour, M., Pop, D., El-Rich, M., 2002. Muscle force evaluation and the role of posture in human lumbar spine under compression. *European Spine J.* 11, 519-526.

Stokes, I.A., Gardner-Morse, M., 1999. Quantitative anatomy of the lumbar musculature. *J Biomech.* 32, 311-6.

Takashima, S.T., Singh, S.P., Haderspeck, K.A., Schultz, A.B., 1979. A model for semi-quantitative studies of muscle actions. *J Biomech.* 12, 929-939.

Tveit, P., Daggfeldt, K., Hetland, S., Thorstensson, A., 1994. Erector spinae lever arm length variations with changes in spinal curvature. *Spine* 19, 199-204.

van Dieen, J.H., de Looze, M.P., 1999. Sensitivity of single-equivalent trunk extensor muscle models to anatomical and functional assumptions. *J Biomech.* 32, 195-8.

Wood, S., Pearsall, D.J., Ross, R., Reid, J.G., 1996. Trunk muscle parameters determined from MRI for lean to obese males. *Clin Biomech* 11, 139-144.

Yamamoto, I., Panjabi, M., Crisco, T., Oxland, T., 1989. Three-dimensional movements of the whole lumbar spine and lumbosacral joint. *Spine* 14, 1256-1260.

Table 7.1 Spinal loads including axial compression, anterior-posterior shear force, and passive moment for different lifting tasks and lumbar postures without and with (no reduction or 10% reduction in lever arm) wrapping of global muscles

Disc	Task Global Muscles Posture	Flexion 65° + 180° N						Flexion 65° + 180° N					
		Straight (No Wrapping)			Curved (+ Wrapping)			Straight (No Wrapping)			Curved (+ Wrapping)		
		F*	L*	K*	F	L	K	F	L	K	F	L	K
T12-L1	S**	490	423	523	269	273	270	672	600	685	358	370	358
	C**	1679	1592	1680	1287	1332	1237	1781	1696	1738	1222	1275	1167
	M**	22	18	27	22	18	26	27	23	31	26	22	29
L1-L2	S	439	379	477	279	276	281	637	566	654	395	372	397
	C	2186	2103	2265	1540	1645	1505	2444	2345	2460	1505	1623	1472
	M	28	22	32	27	21	30	36	29	39	34	28	37
L2-L3	S	202	173	220	187	172	188	338	298	343	306	286	306
	C	2606	2505	2690	1824	1979	1778	3039	2908	3078	1886	2031	1863
	M	29	20	34	28	20	32	39	30	42	36	29	39
L3-L4	S	277	294	266	319	322	310	365	369	352	428	417	419
	C	2971	2871	3020	2202	2341	2092	3528	3396	3556	2337	2517	2303
	M	25	16	32	23	15	30	36	26	40	33	24	37
L4-L5	S	73	170	7	247	288	213	17	108	-24	287	318	262
	C	3250	3218	3271	2592	2787	2498	3859	3796	3884	2878	3069	2846
	M	24	15	30	22	13	28	35	25	38	32	22	34
L5-S1	S	726	883	622	829	949	760	708	858	659	899	1006	856
	C	3308	3376	3290	2751	2917	2625	3850	3943	3865	3009	3191	3000
	M	27	19	31	27	21	32	38	29	39	38	31	39

* F: free, L: lordotic, K: kyphotic

** S: local shear force (N), positive for anterior; C: local axial compression (N); M: sagittal moment, positive for flexion (Nm)

Table 7.2 Wrapping contact forces at various vertebral levels for different lifting tasks and lumbar postures without and with (no reduction or 10% reduction in lever arm) wrapping of global muscles

Vertebra	Task	Flexion 40°+ 180 N			Flexion 65°+ 180 N			Flexion 90°+ 180 N			
		Curved + Wrapping			Curved + Wrapping			Curved + 10% reduced LA			
	Global Muscles	Posture	F*	L*	K*	F	L	K	F	L	K
T12	Cx**		2.8	1.4	6.1	1.1	0.3	3.1	6.9	3.9	9.0
	Cy**		2.3	1.2	5.0	1.7	0.4	4.8	8.9	5.1	11.3
L1	Cx		45.1	34.1	49.0	45.1	35.5	46.7	0.0	0.0	0.0
	Cy		34.5	26.8	36.7	65.2	52.6	66.3	0.0	0.0	0.0
L2	Cx		59.0	45.9	63.0	57.8	52.0	59.0	0.0	0.0	0.0
	Cy		38.9	32.3	39.9	69.3	65.9	68.7	0.0	0.0	0.0
L3	Cx		74.9	54.9	84.0	77.5	62.0	79.7	95.6	74.0	99.9
	Cy		40.7	33.6	42.3	75.5	65.9	74.4	101.6	84.9	102.3
L4	Cx		109.3	84.6	120.6	121.9	100.2	123.4	139.8	85.1	144.8
	Cy		44.6	42.8	42.5	90.2	85.5	85.8	115.2	81.3	113.0
L5	Cx		79.3	53.8	90.1	107.9	85.8	106.5	54.4	45.7	55.7
	Cy		22.8	22.3	19.5	58.3	57.7	52.7	36.1	37.1	34.0

* F: free, L: lordotic, K: kyphotic

** Cx: contact force in global horizontal direction (N), positive for anterior; Cy: contact force in global vertical direction (N), positive for downward direction;

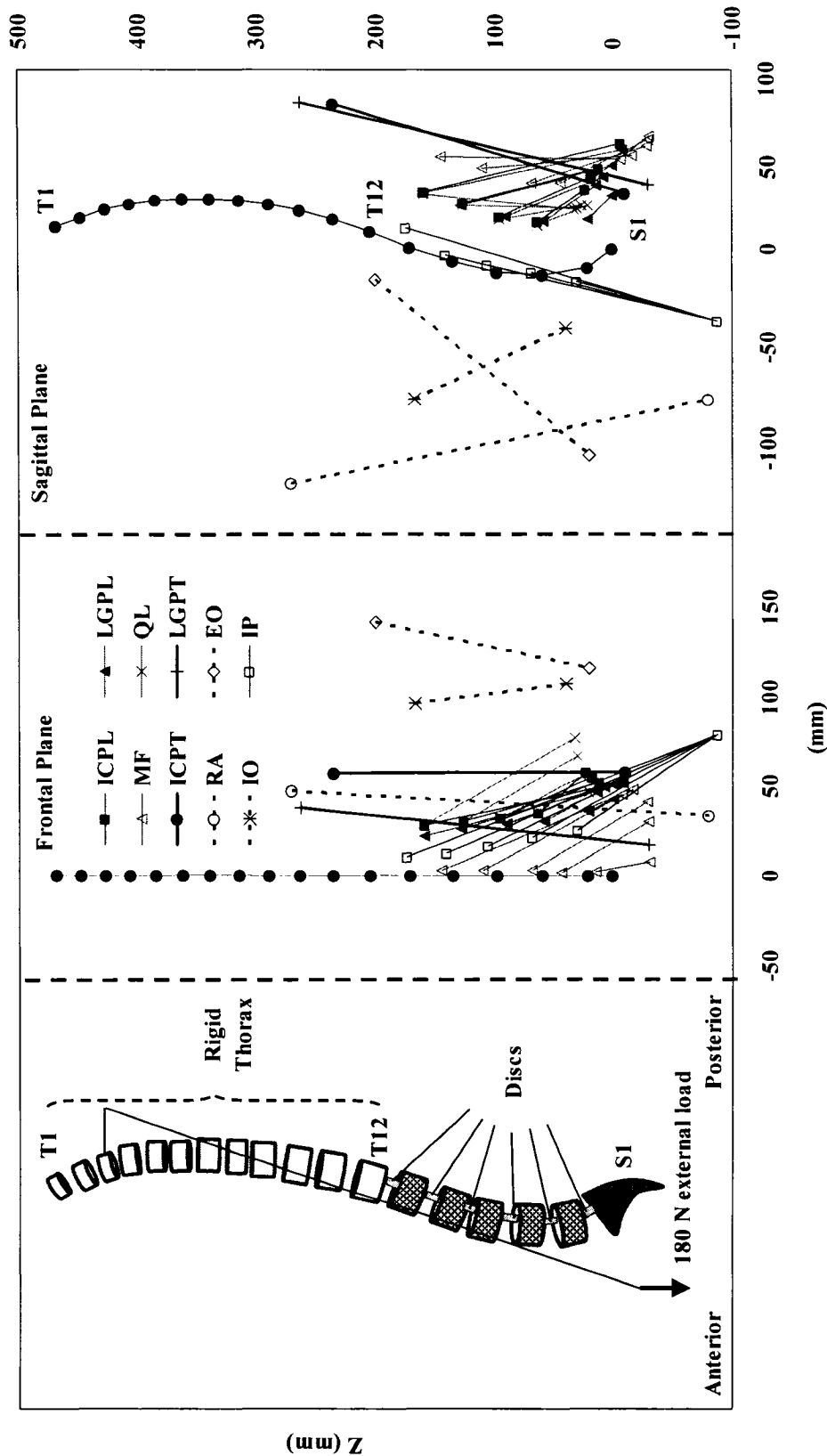


Fig. 7.1 The FE model as well as global and local musculatures in the sagittal and frontal planes (only fascicles on one side are shown). ICPL: Iliocostalis Lumborum pars thoracum, ICPT: Iliocostalis Lumborum pars thoracic, IP: Iliopsoas, GPL: Longissimus Thoracis pars thoracis, LGPT: Longissimus Thoracis pars thoracic, MF: Multifidus, QL: Quadratus Lumborum, IO: Internal Oblique, EO: External oblique, and RA: Rectus Abdominus.

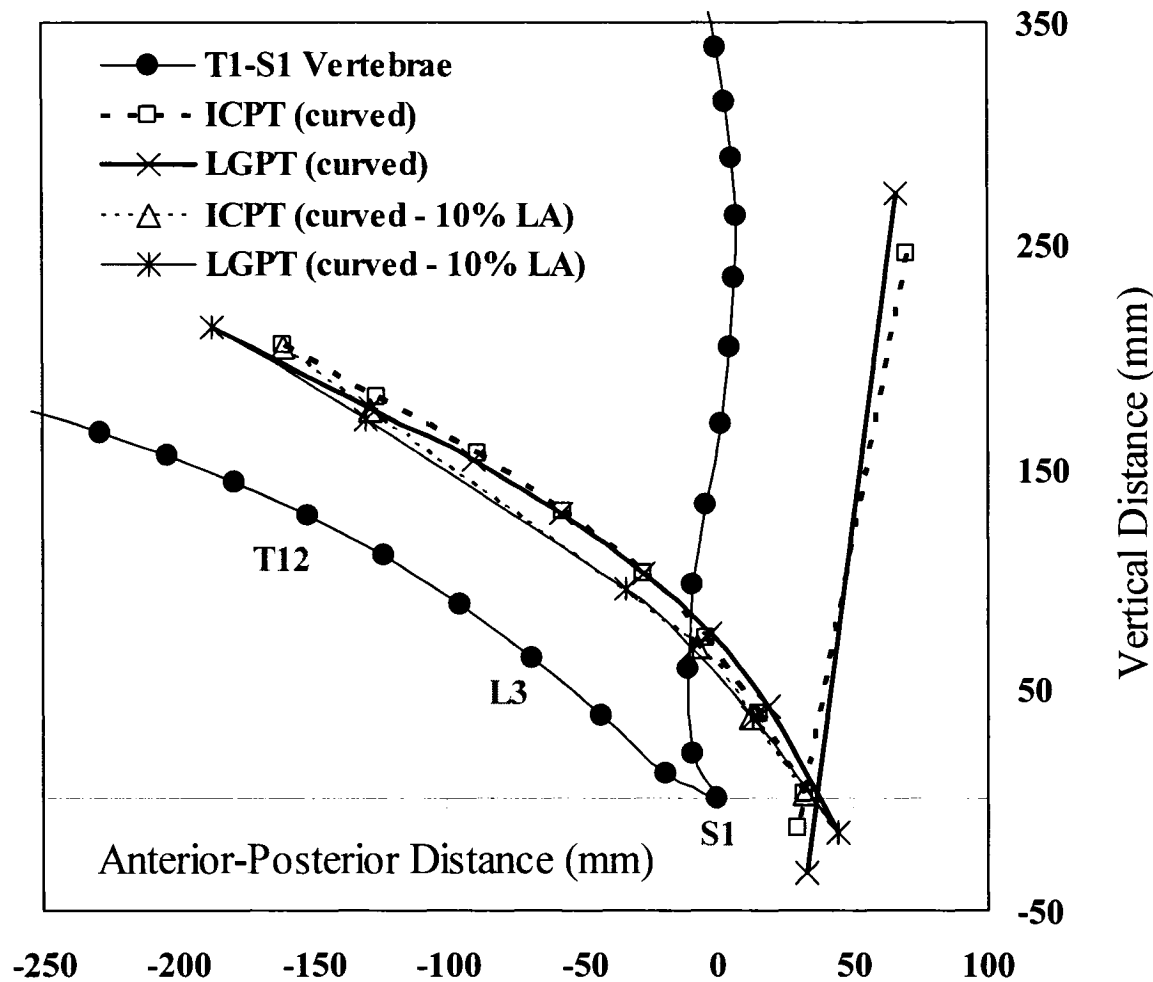


Fig. 7.2 Geometry of global muscles (Longissimus Thoracis pars thoracic, LGPT, and Iliocostalis Lumborum pars thoracic, ICPT) in upright standing posture with straight LOA and in flexion of 65° with curved LOA considering no reduction in LA or with a 10% reduction. No wrapping happens at L1-L3 levels for the case with 10% reduction as the LA distance did not decrease below the critical values set for wrapping at these levels.

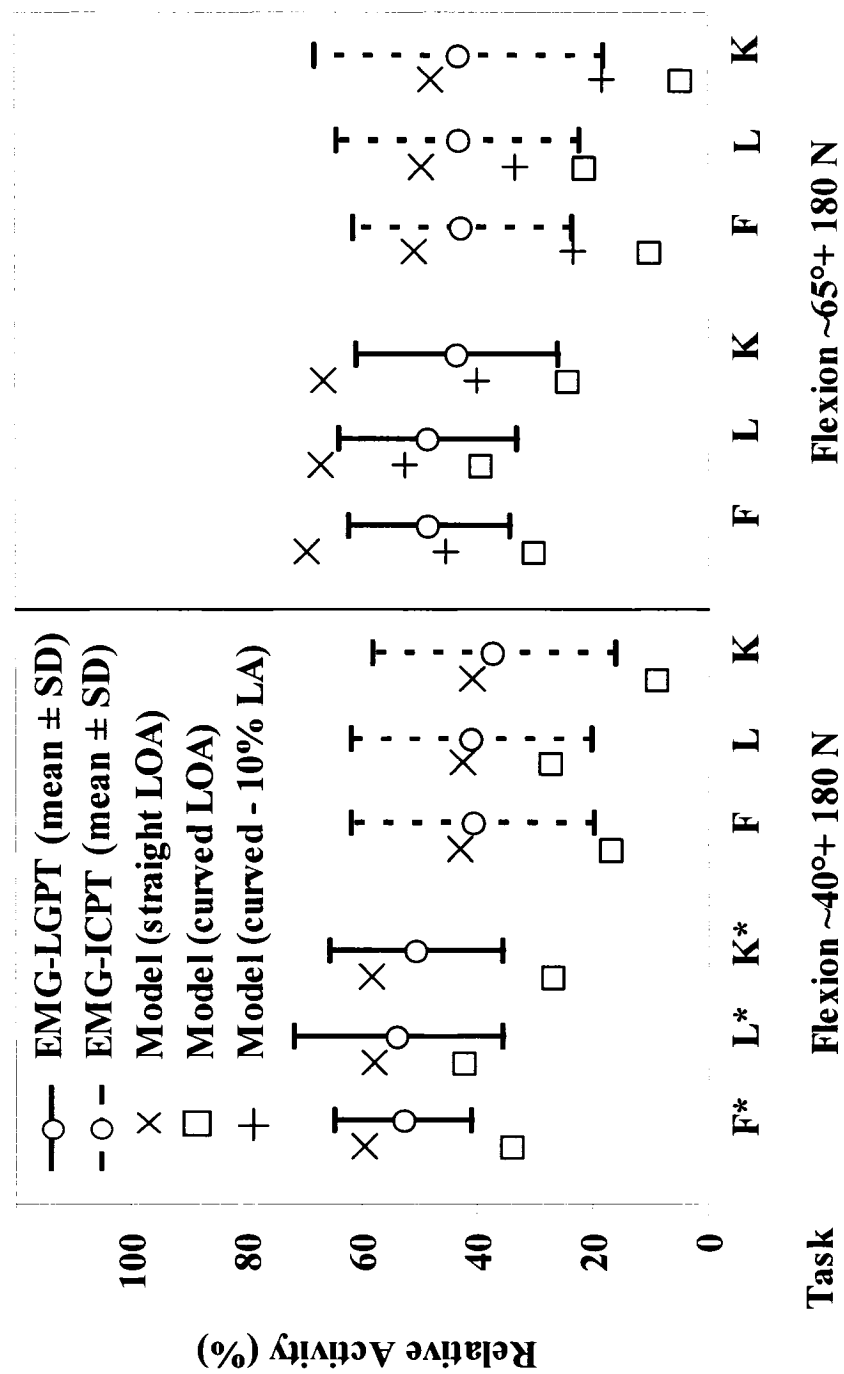


Fig. 7.3 Normalized *in vivo* measured EMG activity (mean \pm SD) of global muscles (Longissimus Thoracis pars thoracic, LGPT, and Iliocostalis Lumborum pars thoracic, ICPT) for different lifting tasks. Predictions (normalized by 0.6xPCSA) have also been shown for the cases with straight LOA, curved LOA with no reduction in LA, and curved LOA with a 10% reduction in LA for these muscles (F: free, L: lordotic, K: kypotic).

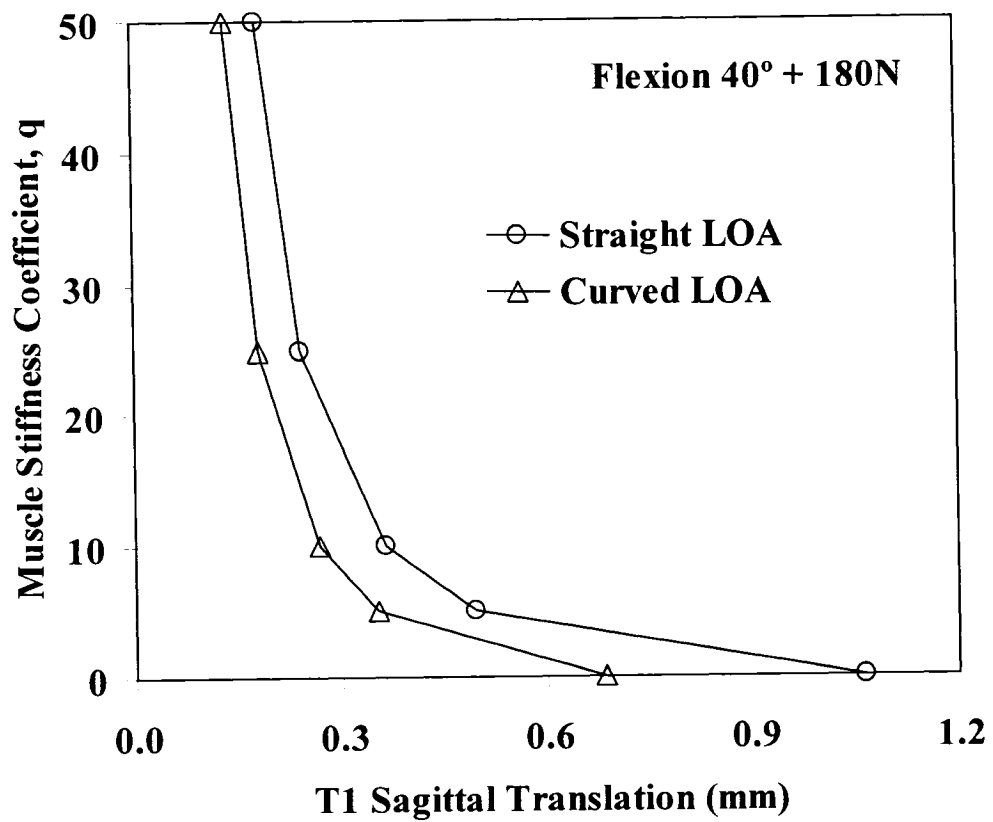


Fig. 7.4 Horizontal translation of T1 vertebra under a unit horizontal perturbation force at deformed configurations as a function of q for the flexion task (40° with 180 N in hands, free style) with straight and curved LOA.

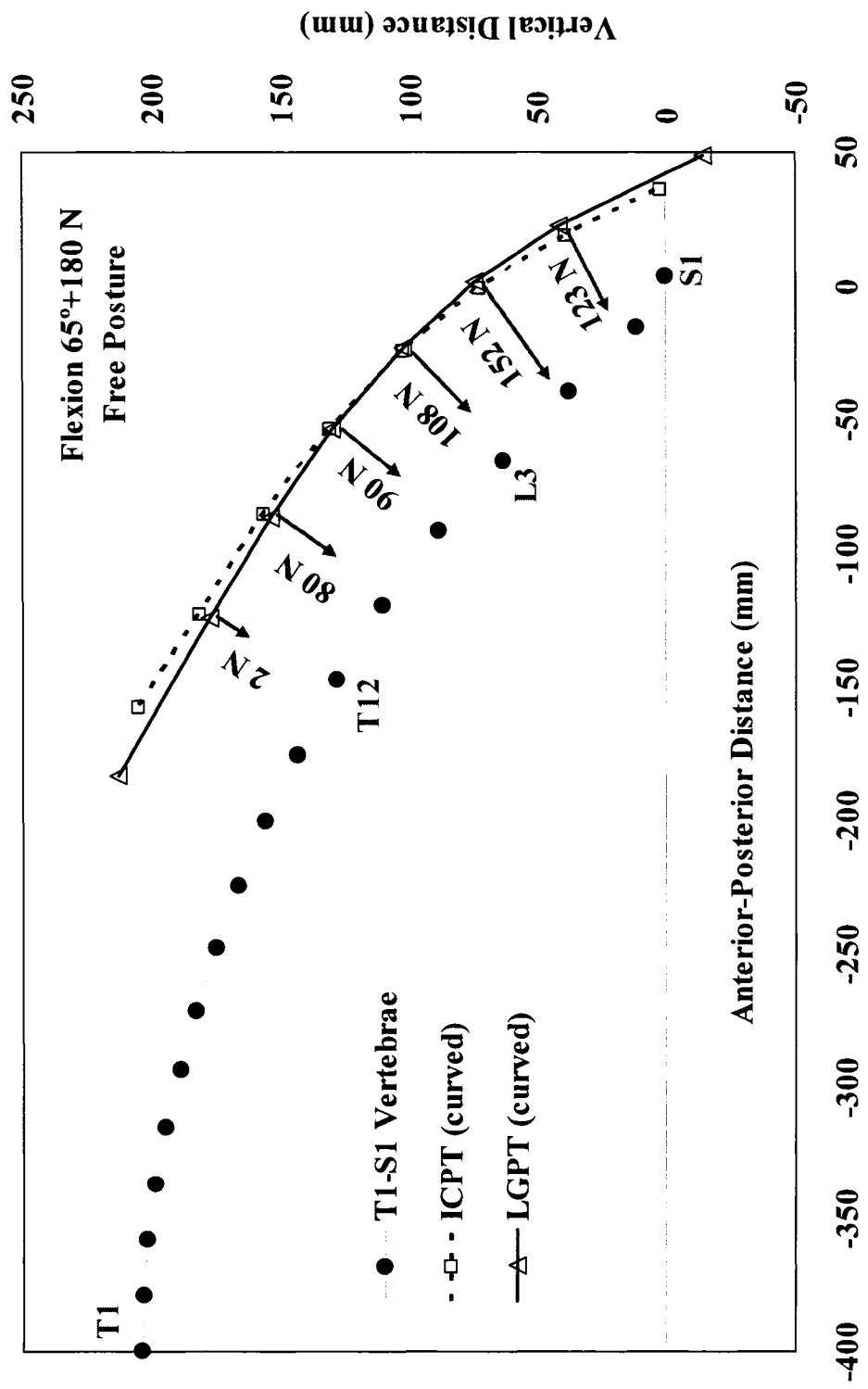


Fig. 7.5 Magnitude and direction of wrapping contact forces on the spine due to wrapping of global muscles (Longissimus Thoracis pars thoracic, LGPT, and Iliocostalis Lumborum pars thoracic, ICPT) for the case with no reduction in LAs from upright posture under trunk flexion of 65° with 180 N in hands (free style).

CHAPTER 8

TRUNK BIOMECHANICAL MODELS BASED ON EQUILIBRIUM AT A SINGLE-LEVEL VIOLATE EQUILIBRIUM AT OTHER LEVELS

N. Arjmand[†], A. Shirazi-Adl^{*†}, M. Parnianpour[‡]

[†] Division of Applied Mechanics, Department of Mechanical Engineering, École Polytechnique, Montréal, Québec, Canada

[‡] Department of Mechanical Engineering, Sharif University of Technology, Tehran, Iran

Article submitted to *Ergonomics*, March 2006

Keywords: Single-Level Free Body Diagram Model, Kinematics-Driven Model, Muscle Forces, Equilibrium, Spine, Compression

8.1 ABSTRACT

Accurate estimation of muscle forces in various occupational tasks is critical for a reliable evaluation of spinal loads and subsequent assessment of risk of injury and management of back disorders. The majority of biomechanical models of multi-segmental spine estimate muscle forces and spinal loads based on the balance of net moments at a single level with no consideration for the equilibrium at remaining levels. This work aimed to quantify the extent of equilibrium violation and alterations in estimations when such models are performed at different levels. Results are compared with those of Kinematics-driven model that satisfies equilibrium at all levels and EMG data. Regardless of the method used (optimization or EMG-assisted), single-level free body diagram models yielded estimations that substantially altered depending on the level considered. Equilibrium of net moment was also grossly violated at remaining levels with the error increasing in more demanding tasks. These models may, however, be used to estimate spinal compression forces.

8.2 INTRODUCTION

In manual material handling tasks and during movements involving relatively large trunk rotations, the trunk extensor muscles are at a clear mechanical disadvantage relative to the external and gravity loads when considering their respective lever arms. While counterbalancing the moment of external loads (including gravity and inertia loads), trunk extensor muscles exert forces substantially greater than external loads so much so that they could account for up to 90% of the total axial compression force acting on the spine during such activities (Reeves and Cholewicki 2003, Arjmand and Shirazi-Adl 2005a). Accurate prediction of muscle forces required to maintain trunk equilibrium and stability is, hence, critical for an adequate estimation of spinal loads, and thus, for the assessment of risk of injuries in passive and active tissues. Such improvements would also benefit searches for safer lifting techniques as well as more effective prevention and treatment procedures. The infeasibility in direct quantification of muscle forces and spinal loads as well as the limitations in indirect measurement methods have persuaded researchers towards the use of biomechanical modeling techniques.

Faced with the intricate anatomy, complex nonlinear properties and kinetic redundancy of the trunk musculoskeletal system, investigators have been obliged to make simplifying assumptions in order to estimate muscle forces and internal spinal loads. In doing so, anatomy/kinematics/passive properties/gravity loading have been simplified, nonlinearities were neglected, some muscles have been overlooked or grouped as synergic sets, straight lines of action (LOA) have been assumed for global trunk muscles, and finally different cost functions or limited surface EMG data along with gain factors have been introduced. The importance of adequate representation of trunk extensor muscle anatomy (McGill and Norman 1986, Bogduk et al. 1992), passive properties of the ligamentous spine (Arjmand and Shirazi-Adl 2006a) and wrapping of global muscles in large forward flexions (Arjmand and Shirazi-Adl 2006b) on model predictions have been well recognized.

Another major shortcoming in many current and earlier biomechanical model studies of multi-segment spinal structure lies in the consideration of the balance of net external moments only at a single cross section (typically at lowermost lumbar discs) rather than along the entire length of the spine (e.g., Schultz et al. 1982, McGill and Norman 1986, Cholewicki et al. 1995, Parnianpour et al. 1997, van Dieen et al. 2003, Granata et al. 2005, Marras et al. 2005). This shortcoming naturally exists in dynamic and quasi-static model studies alike while simulating either sagittally symmetric (2D) or asymmetric (3D) movements. These models have widely been employed in ergonomic applications and in injury prevention and treatment programs. It has been indicated, though with no details, that the muscle forces evaluated based on such single-level equilibrium models, once applied on the system along with external loads, may not necessarily satisfy equilibrium at remaining levels along the spine (Stokes and Gardner-Morse 1995, Arjmand and Shirazi-Adl, 2006a). The extent of violations in equilibrium at different levels and their effects on the estimated muscle forces and spinal loads, however, have not yet been quantified.

The objective of the present study is, hence, set to quantify the extent to which the muscle/spinal loads and equilibrium requirements at different levels are influenced by results of wide-spread single-level free body diagram (SLFBD) model studies. In order to do this while considering two isometric symmetric lifting tasks, the results of our Kinematics-driven (KD) model that satisfies kinematics and equilibrium requirements at all levels and directions (El-Rich et al. 2004, Arjmand and Shirazi-Adl 2005a, Arjmand and Shirazi-Adl 2006a) are compared with those based on SLFBD models. The SLFBD model is applied separately at different disc levels (from L5-S1 to T12-L1) using the deformed configuration of the spine identical to that in the reference KD model. The violation of equilibrium at remaining levels as well as muscle forces and spinal loads are subsequently quantified and compared with each other and with the results of KD model. Two isometric lifting tasks are analyzed; one in upright standing and another in

forward flexed posture of 65° while holding symmetrically in both cases 180 N load in hands. Since the net external moments, lever arm of muscles, and number of muscles that cross each level change from a level to another, it is hypothesized that SLFBD models grossly violate equilibrium at remaining levels and that the estimated muscle forces and spinal loads would alter depending on the level considered and the posture (task) simulated.

8.3 METHOD

8.3.1 Kinematics-Driven (KD) Model

For the reference cases, the nonlinear finite element model and the KD algorithm were employed to resolve redundancy in load distribution while satisfying equilibrium and kinematics conditions at all spinal levels and directions. The details of in vivo data and their model studies have been described elsewhere (El-Rich et al. 2004, Arjmand and Shirazi-Adl 2005a, Arjmand and Shirazi-Adl 2006a). In brief, a sagittally-symmetric T1-S1 beam-rigid body model consisting of 6 deformable beams with nonlinear properties to represent T12-S1 segments and 7 rigid elements to represent T1-T12 (as a single body) and lumbosacral vertebrae (L1 to S1) is used along with 46 local and 10 global muscle fascicles having straight LOAs initially in neutral standing posture (Fig. 8.1). To simulate curved paths in forward flexion tasks, global extensor muscles are assumed to wrap around vertebrae. The wrapping contact at each T12-L5 level occurs only when the instantaneous lever arm distance at that level decreases below 10% of its corresponding value in the neutral standing posture (Arjmand and Shirazi-Adl 2006b). In both cases investigated, based on the mean body weight of subjects in the in vivo study and percentage of body weight at each motion segment level reported elsewhere (Takashima et al. 1979, Pearsall 1994), a gravity load of 387 N was considered and distributed eccentrically at different levels from T1 to L5 vertebrae. The weight of 180 N was applied at the location measured in vivo via a rigid element attached to the T3 vertebra.

Mean measured rotations at pelvis and thorax obtained from our parallel in vivo studies were prescribed on the nonlinear FE model along with the gravity forces and external load carried in hands by subjects. The total lumbar rotation is calculated as the difference between preceding measured thorax and pelvis rotations and is partitioned between individual lumbar vertebrae based on earlier measurements (see Arjmand and Shirazi-Adl 2006a). Each prescribed rotation generates an equilibrium equation at its corresponding level in the form of $\Sigma r \times f = M$ where r , f , and M are lever arm of muscles with respect to the vertebra to which they are attached, unknown total forces in muscles attached to the level under consideration, and reaction moment at the vertebra under prescribed rotation, respectively. To resolve the redundancy problem, optimization algorithm with the cost function of sum of cubed muscle stresses is employed along with inequality equations of unknown muscle forces remaining positive and greater than their passive force components (calculated based on muscle strain and a tension-length relationship, Davis et al. 2003) but smaller than the sum of maximum physiological active forces (i.e., $0.6 \times$ physiological cross-sectional area, PCSA) plus the passive force components (Arjmand and Shirazi-Adl 2006a). The value of 0.6 MPa taken for the maximum allowable stress in muscles lies in the mid-range of reported values (0.3-1.0 MPa) (McGill and Norman 1986) and is an appropriate one in simulation of forward flexion tasks (Guzik et al. 1996). Axial and horizontal components of the calculated muscle forces along with the wrapping contact forces due to contact between muscles and vertebrae at wrapping points are fed back onto the FE model as updated external loads and the iteration is repeated till the convergence is reach, i.e., the calculated muscle forces remain almost identical in two successive iterations. This method satisfies equilibrium at all levels and directions while accounting for the nonlinear passive stiffness of the ligamentous spine under prescribed deformed geometry of the spine that is based on in vivo measurements.

8.3.2 Single-Level Free Body Diagram (SLFBD) Model

Under the final deformed configurations of the ligamentous spine, local and global wrapping muscles as well as gravity/external load magnitudes/locations identical to those in foregoing reference KD cases, muscle forces were re-calculated based on SLFBD equilibrium at different (L5-S1 through T12-L1) intervertebral disc mid-planes (see Fig. 8.2 as an example for the L5-S1 level under trunk flexion of 65°) expressed as follows:

$$\sum_{i=1}^n r_i \times f_i = M_{ext} - M_{passive}$$

in which n , M_{ext} , and $M_{passive}$ denote the number of all muscle fascicles crossing the cutting plane under consideration, the total net external moment due to gravity and external load carried in hands, and passive ligamentous resistant moment at that level, respectively. The passive ligamentous moments at different levels were taken exactly as those calculated in the reference KD models at the final deformed configurations. Unknown muscle forces were subsequently evaluated by the same optimization algorithm used in the reference models (i.e., sum of cubed muscle stresses). Spinal compression and shear forces at different levels were then computed by consideration of equilibrium in local axial and shear (anterior-posterior) directions.

In order to examine whether or not the muscle forces estimated based on the SLFBD model at the L5-S1 level verify the equilibrium at remaining levels, the calculated muscle forces at this level were applied onto the FBDs at each of remaining L4-L5 through T12-L1 levels. An index of equilibrium violation (IEV), defined below, was computed at each of these levels:

$$IEV \% = \frac{(M_{muscle} + M_{passive}) - M_{ext}}{M_{ext}} \times 100$$

in which M_{muscle} , $M_{passive}$, and M_{ext} denote moments at the disc level under consideration generated by muscle forces calculated based on SLFBD equilibrium at the L5-S1 level, the passive ligamentous spine, and gravity/external load carried in hands,

respectively. This index, IEV, represents, hence, an indication of the extent of moment equilibrium violation at different levels when applying the muscle forces estimated at the L5-S1 level.

Furthermore, based on the same muscle forces, axial compression force at the upper T12-L5 levels were also computed and compared at each level with their respective value estimated based on the SLFBD performed at that level rather than at the L5-S1 level. In this case, the index of error signifies the relative difference between the estimated axial compression at each level when SLFBD model is performed either at the distal L5-S1 level or at that particular level. It is to be re-iterated that the geometry of the spine and muscles for both loading cases used in the SLFBD models is taken identical to that in the final deformation of corresponding reference cases evaluated based on the KD models.

In order to investigate the relative effect of optimization cost function used in SLFBD models on predictions, the forward flexed task was also reanalyzed using the sum of either squared or linear muscle stresses instead of the sum of cubed muscle stresses. In this manner, muscle forces at the L5-S1 level were computed using either of these cost functions and the indices of error in equilibrium of moments (IEV) at upper levels (L4-L5 to T12-L1) were calculated.

Finally, for the task of upright standing posture with load in hands, the muscle forces were estimated by the SLFBD performed at the L5-S1 level using the EMG-assisted approach instead of an optimization algorithm (Marras and Granata 1997, McGill 1992). For this purpose, our measured normalized EMG data under the same task and loading were considered to drive the model (El-Rich et al., 2004). The normalized EMG activity in each abdominal muscle (Rectus Abdominus, External oblique, and Internal Oblique) was taken the same and varied from 12% (as measured) to 5% or 0% while the activity in local longissimus and iliocostalis lumbar muscles was

assumed the same as that measured in the multifidus. The activity in quadratus lumborum was taken half of this latter value. The violation of equilibrium (IEV) was, subsequently, calculated at other levels.

8.4 RESULTS

Except otherwise specified, results are obtained using the optimization-based approach with the cost function of sum of cubed muscle stresses. For the same spinal configuration, gravity/external load magnitudes/locations and passive ligamentous resistant moment as those used in the reference KD models, muscle forces at both global and local levels substantially altered when calculated based on SLFBD model applied at different levels and that regardless of the task considered (Table 8.1A, B and Fig. 8.3). Results indicate greater global thoracic muscle forces whereas generally smaller local lumbar muscle forces when comparing SLFBD models to KD reference cases. The differences in estimated forces in global muscles for the lifting task with 65° flexed posture further increased as the SLFBD equilibrium was considered at a more distal lumbar level reaching maximum values of 66% in the longissimus thoracis pars thoracic and 57% in the iliocostalis lumborum pars thoracic muscles when the SLFBD was performed at the lowermost L5-S1 level (Table 8.1A, B and Fig. 8.3). In accordance with the constraint requirements in KD model, many local muscles in the forward flexed lifting task were assigned lower-bound forces based on the muscle passive resistant force-length relationship and muscle instantaneous length (Table 8.1A, B, underlined bold).

Local compression and shear forces at different spinal levels were also influenced when calculated based on SLFBD models; the former being smaller in both lifting tasks by as much as 9% compared with the reference KD results (Table 8.2). In lifting with 65° forward flexion, the local shear force at the critical L5-S1 level, however, substantially increased by 22.4% compared to the reference case when the SLFBD was performed at this level.

When comparing the results of SLFBD models against each other, there was a marked alteration in estimated muscle forces depending on the level considered (Table 8.1A, B and Fig. 8.3). Furthermore, when applying the muscle forces initially estimated by the SLFBD at the L5-S1 level as known forces onto the SLFBD at remaining levels, the equilibrium of sagittal moment was found to be grossly violated. The extent of error in maintenance of equilibrium, identified as the index of equilibrium violation (IEV), increased as higher proximal levels were considered for this purpose and reached maximum values of 40% and 7% for the cut at the T12-L1 level under flexed and upright postures, respectively (Fig. 8.4). Similarly, axial compression forces at different levels altered substantially by as much as 51% when calculated based on SLFBD models performed either at that level itself or at the L5-S1 level (Fig. 8.5).

When cost functions of sum of squared and linear muscle stresses were used to partition moment of L5-S1 level among muscles, the violation of equilibrium at upper levels markedly exacerbated (see Fig. 8.4). In order to satisfy equilibrium at the L5-S1 level, the EMG-assisted approach predicted gains of 0.36, 0.52, and 1.32 MPa when no coactivity, coactivity of 5%, and 12% were considered for abdominal muscles, respectively. Moment equilibrium (IEV) was violated at L4-L5 through T12-L1 levels by 5.2, 12.5, 23.9, 32.5, and 24.8%, respectively, when no coactivation was considered in abdominals. These errors further increased in presence of abdominal coactivities. To simultaneously satisfy moments at different levels, one would need to alter gains for the same muscles from a level to another a remedy that would not make much sense.

8.5 DISCUSSION

This work aimed to quantify the extent to which the muscle forces, spinal loads and equilibrium requirements at different levels are influenced when considering single-level free body diagram (SLFBD) equilibrium at a specific spinal level. Such models, driven either by optimization cost functions or by EMG data, are widely employed in

biomechanical model investigations of the human spine in order to estimate muscle forces and spinal loads (Schultz et al. 1982, McGill and Norman 1986, Cholewicki et al. 1995, Parnianpour et al. 1997, van Dieen et al. 2003, Granata et al. 2005, Marras et al. 2005). For this purpose, the results of Kinematics-driven (KD) model based on in vivo measurements of two lifting tasks at upright and forward flexion postures were used as reference values to compare with those obtained by single-level cuts at different spinal levels. The SLFBD model at different disc levels (from L5-S1 to T12-L1) was carried out using the deformed configurations, external/gravity load magnitudes/positions and passive resistant moments of the reference KD cases. Results of this investigation confirmed the hypotheses of the study in that SLFBD models yield results that grossly violate the equilibrium at levels other than the one considered in the model and that the extent of such violations as well as the magnitude of muscle forces and spinal loads alter as a function of disc level considered and task simulated.

In the KD model, the optimization algorithm was employed at all levels separately one from another in order to partition the required moment calculated for a given prescribed rotation in between muscles that are attached only to the level under consideration. The remaining muscles not attached to this specific level, either crossing over or attached to lower ones, would therefore be absent in equilibrium equations under investigation. Consideration of all levels, one by one, would therefore yield all unknown muscle forces under given kinematics and external/gravity loads. On the contrary in the SLFBD model, the forces in all muscles passing through the cross-section in question, inserted or not into that specific level, were treated as the unknowns in a single equation of equilibrium. For this reason and since identical data were shared, almost the same results were obtained in both reference and single-level models for global extensor muscle forces and local spinal loads at the T12-L1 level when the FBD was considered at the T12-L1 level (Tables 8.1A, B, 8.2, and Fig. 8.3). Substantial differences in global muscle forces, especially for the forward flexion task, were however found when the lower levels were considered in SLFBD model.

The SLFBD model at the lowermost L5-S1 level dealt with all global and local muscle forces as unknowns in one single equation. The optimization algorithm at this level resulted in allocation of much greater forces in global muscles due to their relatively larger PCSAs than in local muscles as compared with the muscle forces computed in KD model (Table 8.1A, B, Fig. 8.3). For the SLFBD cut at the L5-S1 disc level and under forward flexed lifting task, global longissimus muscle activation in the optimization procedure reached 86% of its maximum force-carrying capacity far exceeding the range of normalized measured EMG data (Fig. 8.3). Similarly, very large values of 79% and 69% were computed for the global longissimus muscle when the SLFBD was performed at the upper L4-L5 and L3-L4 levels, respectively (Fig. 8.3). The KD model, on the other hand, resulted in larger forces in local muscles and, hence, a more uniform partitioning of the external moment among local and global trunk extensor muscles.

The index of violation in moment equation of equilibrium at different levels (Fig. 8.4) indicating the error in estimated muscle forces based on the SLFBD at the L5-S1 level increased proximally from the L5-S1 level to its maximum values of 7% and 40% at the T12-L1 level for the upright and forward flexed lifting postures, respectively. These errors clearly lend support to the fact that equilibrium equations at all levels and directions should be treated simultaneously as are done in KD finite element model and not in isolation one from the rest as done in SLFBD models. The substantial differences between muscle forces when calculated based on the SLFBD at different levels (Table 8.1A, B and Fig. 8.3) also suggest the major shortcoming in such model studies. It should be re-iterated that large differences predicted in this study between the results of SLFBD models both among themselves depending on the level considered and with KD results occurred despite the use of identical deformed configurations (ligamentous spine and muscles), external/gravity magnitudes/locations, passive resistant moment of the ligamentous spine, passive properties of muscles, and optimization algorithm of sum of

cubed muscle stresses. It is evident that had the muscle forces estimated from different SLFBD models been applied as additional external loads on the spine, substantially different deformed (and possibly unstable) configurations would have been generated depending on the level considered in the SLFBD. The resulting spinal configurations would also be quite different from the initial configuration considered in SLFBD calculations.

Comparison of results of KD and SLFBD models for two lifting tasks suggests that the differences increased as a function of task demand associated with the trunk forward flexion angle. In fact, the larger the net moment of external/gravity loads becomes the greater differences (Fig. 8.3) and errors in equilibrium (Fig.s 8.4 and 8.5) one should expect from SLFBD models. That is why, the indices of error in moment equilibrium (Fig. 8.4) and in axial compression (Fig. 8.5) substantially increased when the task became physically more demanding under forward flexion lifting. Such differences are expected to exist also in dynamic lifting tasks as well as those involving asymmetry in movements (e.g., asymmetric lifts). It can, hence, be argued that the heavier and more physically demanding tasks would further deteriorate the results of SLFBD models.

Regardless of the method used to resolve the redundancy problem and partition the net moment among muscles, i.e. optimization methods or EMG-assisted approach, the equilibrium was not satisfied simultaneously at levels other than the one used to estimate muscle forces. These findings further confirm the hypothesis made in this study on the shortcoming of SLFBD models. Comparison of predicted results of KD model with SLFBD models regardless of the method used to tackle the redundancy also demonstrated that the differences in computed axial compression force at different levels remained <9% (Table 8.2) being much lower than those for shear forces and muscle forces. In other words, the axial compression force appears to be less sensitive to the shortcomings in SLFBD models. Earlier investigations have also found that the effect of

different optimization cost functions (especially nonlinear ones) on the estimated axial compression in both KD models (Arjmand and Shirazi-Adl 2005b) and SLFBD ones (Parnianpour et al., 1997) is not significant. For this reason and due to the relative ease in SLFBD applications, one may argue that such SLFBD models could be carried out with the specific objective to estimate only local compression loads on the spine but not the shear forces and muscle activation levels.

8.6 ACKNOWLEDGEMENT

This research is supported by a grant from the Natural Sciences and Engineering Research Council of Canada, NSERC.

8.7 REFERENCES

ARJMAND, N. and SHIRAZI-ADL, A., 2005a, Biomechanics of lumbar posture in static lifting tasks. *Spine*, **30**, pp. 2637-48.

ARJMAND, N. and SHIRAZI-ADL, A., 2005b, Sensitivity of kinematics-based model predictions to optimization criteria in static lifting tasks. *Medical Engineering & Physics* (in press, available online).

ARJMAND, N. and SHIRAZI-ADL, A., 2006a, Model and in vivo studies on human trunk load partitioning and stability in isometric forward flexions. *Journal of Biomechanics*, **39**, pp. 510-21.

ARJMAND, N., SHIRAZI-ADL, A. and BAZRGARI, B., 2006b, Wrapping of Trunk Thoracic Extensor Muscles Influences Muscle Forces and Spinal Loads in Lifting Tasks. *Clinical Biomechanics* (in press).

BOGDUK, N., MACINTOSH, J.E. and PEARCY, M.J., 1992, A universal model of the lumbar back muscles in the upright position. *Spine*, **17**, pp. 897-913.

CHOLEWICKI, J., MCGILL, S.M. and NORMAN R.W., 1995, Comparison of muscle forces and joint load from an optimization and EMG assisted lumbar spine model: towards development of a hybrid approach. *Journal of Biomechanics*, **28**, pp. 321-31.

DAVIS, J., KAUFMAN, K.R. and LIEBER, R.L., 2003, Correlation between active and passive isometric force and intramuscular pressure in the isolated rabbit tibialis anterior muscle. *Journal of Biomechanics*, **36**, pp. 505-12.

EL-RICH, M., SHIRAZI-ADL, A. and ARJMAND, N., 2004, Muscle activity, internal loads and stability of the human spine in standing postures: combined model-in vivo studies. *Spine*, **29**, pp. 2633-42.

GRANATA, K.P., LEE, P.E. and FRANKLIN. T.C., 2005, Co-contraction recruitment and spinal load during isometric trunk flexion and extension. *Clinical Biomechanics*, **20**, pp. 1029-37.

GUZIK, D.C., KELLER, T.S., SZPALSKI, M., PARK, J.H. and SPENGLER, D.M., 1996, A biomechanical model of the lumbar spine during upright isometric flexion, extension, and lateral bending. *Spine*, **21**, pp. 427-33.

MARRAS, W.S., PARAKKAT, J., CHANY, A.M., YANG, G., BURR, D. and LAVENDER, S.A., 2005, Spine loading as a function of lift frequency, exposure duration, and work experience. *Clinical Biomechanics* (in press, available online).

MARRAS, W.S. and GRANATA. K.P., 1997, The development of an EMG-assisted model to assess spine loading during whole-body free-dynamic lifting. *Journal of Electromyography and Kinesiology*, **7**, pp. 259-268.

MCGILL, S.M., 1992, A myoelectrically based dynamic three-dimensional model to predict loads on lumbar spine tissues during lateral bending. *Journal of Biomechanics*, **25**, pp. 395-414.

MCGILL, S.M. and NORMAN, R.W., 1986, Partitioning of the L4-L5 dynamic moment into disc, ligamentous, and muscular components during lifting. *Spine*, **11**, pp. 666-78.

PARNIANPOUR, M., WANG, J.L., SHIRAZI-ADL, A., SPARTO, P. and WILKE, H.J., 1997, The effect of variations in trunk models in predicting muscle strength and spinal loads. *Journal of Musculoskeletal Research*, **1**, pp. 55-69.

PEARSALL, D.J., 1994, Segmental inertial properties of the human trunk as determined from computer tomography and magnetic resonance imagery. PhD thesis, Queen's University, Kingston, Ontario.

REEVES, N.P. and CHOLEWICKI, J., 2003, Modeling the human lumbar spine for assessing spinal loads, stability, and risk of injury. *Critical Reviews in Biomedical Engineering*, **31**, pp. 73-139.

SCHULTZ, A.B., ANDERSSON, G.B., HADERSPECK, K., ORTENGREN, R., NORDIN, M. and BJORK, R., 1982, Analysis and measurement of lumbar trunk loads in tasks involving bends and twists. *Journal of Biomechanics*, **15**, pp. 669-75.

STOKES, I.A., GARDNER-MORSE, M., 1995, Lumbar spine maximum efforts and muscle recruitment patterns predicted by a model with multijoint muscles and joints with stiffness. *Journal of Biomechanics*, **28**, pp. 173-86.

TAKASHIMA, S.T., SINGH, S.P., HADERSPECK, K.A. and SCHULTZ, A.B., 1979, A model for semi-quantitative studies of muscle actions. *Journal of Biomechanics*, **12**, pp. 929-39.

VAN DIEEN, J.H., KINGMA, I., VAN DER BUG, P., 2003, Evidence for a role of antagonistic cocontraction in controlling trunk stiffness during lifting. *Journal of Biomechanics*, **36**, pp. 1829-36.

Table 8.1A Predicted muscle forces under flexed posture using KD approach as well as SLFBD models at different disc levels from L5-S1 through T12-L1 (forces in Iliopsoas muscles are zero in all SLFBD models and are not shown for the KD model).

Muscle	Upper Attach	Muscle Forces on Each Side (N) for the Forward Flexed Posture					
		Kin. driven	L5-S1 cut	L4-L5 cut	L3-L4 cut	L2-L3 cut	L1-L2 cut
LGPI	Thorax	402	668	624	521	478	444
ICPI	Thorax	168	264	248	187	169	169
	T11	26	<u>15</u>	<u>15</u>	<u>15</u>	<u>15</u>	-
	T12	25	16	<u>16</u>	<u>16</u>	<u>16</u>	-
	L1	25	19	<u>18</u>	<u>18</u>	-	-
	L2	38	21	<u>17</u>	-	-	-
	L3	43	18	-	-	-	-
	L4	42	<u>25</u>	<u>25</u>	<u>25</u>	<u>25</u>	-
	L5	56	40	<u>39</u>	<u>39</u>	<u>39</u>	-
	TRN	60	50	<u>42</u>	<u>42</u>	-	-
	TRM	87	51	<u>36</u>	-	-	-
	T11	47	<u>34</u>	<u>34</u>	<u>34</u>	<u>34</u>	<u>34</u>
	T12	62	<u>43</u>	<u>43</u>	<u>43</u>	<u>43</u>	-
	T13	98	65	<u>49</u>	<u>49</u>	-	-
	T14	110	54	<u>37</u>	-	-	-
	T15	75	31	-	-	-	-
	T16	31	14	<u>10</u>	<u>10</u>	<u>10</u>	<u>10</u>
	T17	21	12	<u>11</u>	<u>11</u>	<u>11</u>	-
	T18	16	11	<u>10</u>	<u>10</u>	-	-
	T19	19	9	<u>9</u>	-	-	-

Table 8.1B Predicted muscle forces under upright posture using KD approach as well as SLFBD models at different disc levels from L5-S1 through T12-L1 (forces in Iliopsoas muscles are zero in all SLFBD models and are not shown for the KD model).

Muscle	Upper Vertebral Level	Kin. driven	Muscle Forces on Each Side (N) for the Standing Posture					
			L5-S1 cut	T4-T5 cut	T3-T4 cut	T2-T3 cut	T1-T2 cut	T12-L1 cut
LGPT	Thorax	161	189	190	191	197	199	162
ICPT	Thorax	68	72	74	76	80	82	68
L1	L1	15	4	4	4	3	3	-
L2	L2	1	5	4	4	4	-	-
L3	L3	2	6	5	4	-	-	-
ICPL	L4	6	6	5	-	-	-	-
L5	L5	14	5	-	-	-	-	-
L1	L1	25	7	6	6	6	5	-
ICPL	L2	3	11	10	9	8	-	-
L3	L3	5	13	12	10	-	-	-
L4	L4	13	13	10	-	-	-	-
L1	L1	27	6	5	5	5	5	-
L2	L2	3	9	9	9	9	-	-
MR	L3	7	17	16	14	-	-	-
L4	L4	17	14	12	-	-	-	-
L5	L5	24	8	-	-	-	-	-
L1	L1	18	3	3	3	3	3	-
L2	L2	1	3	3	3	3	-	-
L3	L3	1	3	3	2	-	-	-
OF	L4	3	3	2	-	-	-	-

Table 8.2 Predicted local spinal loads in both loading cases using KD model as well as SLFBD models cut at different disc levels from L5-S1 through T12-L1.

Disc Level	Spinal Loads (N)			Forward Flexed Posture			Single-Level Free Body Diagram (SLFBD) Model		
	KD Model	L5-S1	L4-L5	L3-L4	L2-L3	L1-L2	T12-L1		
	C ^a	S ^b	C	S	C	S	C	S	C
T12-L1	1398	488	-	-	-	-	-	-	-
L1-L2	1804	450	-	-	-	-	-	-	-
L2-L3	2182	236	-	-	-	-	2028	200	-
L3-L4	2592	394	-	-	2402	389	-	-	-
L4-L5	3116	264	-	2958	404	-	-	-	-
L5-S1	3247	869	3172	1064	-	-	-	-	-
Spinal Loads (N) - Upright Standing Posture									
T12-L1	925	-49	-	-	-	-	-	-	925
L1-L2	1177	-111	-	-	-	-	-	-	-
L2-L3	1207	-157	-	-	-	-	1126	-143	-
L3-L4	1263	18	-	-	1197	10	-	-	-
L4-L5	1344	131	-	1268	118	-	-	-	-
L5-S1	1338	523	1244	492	-	-	-	-	-

^a C: local axial compression (N)

^b S: local shear force (N), positive in anterior direction

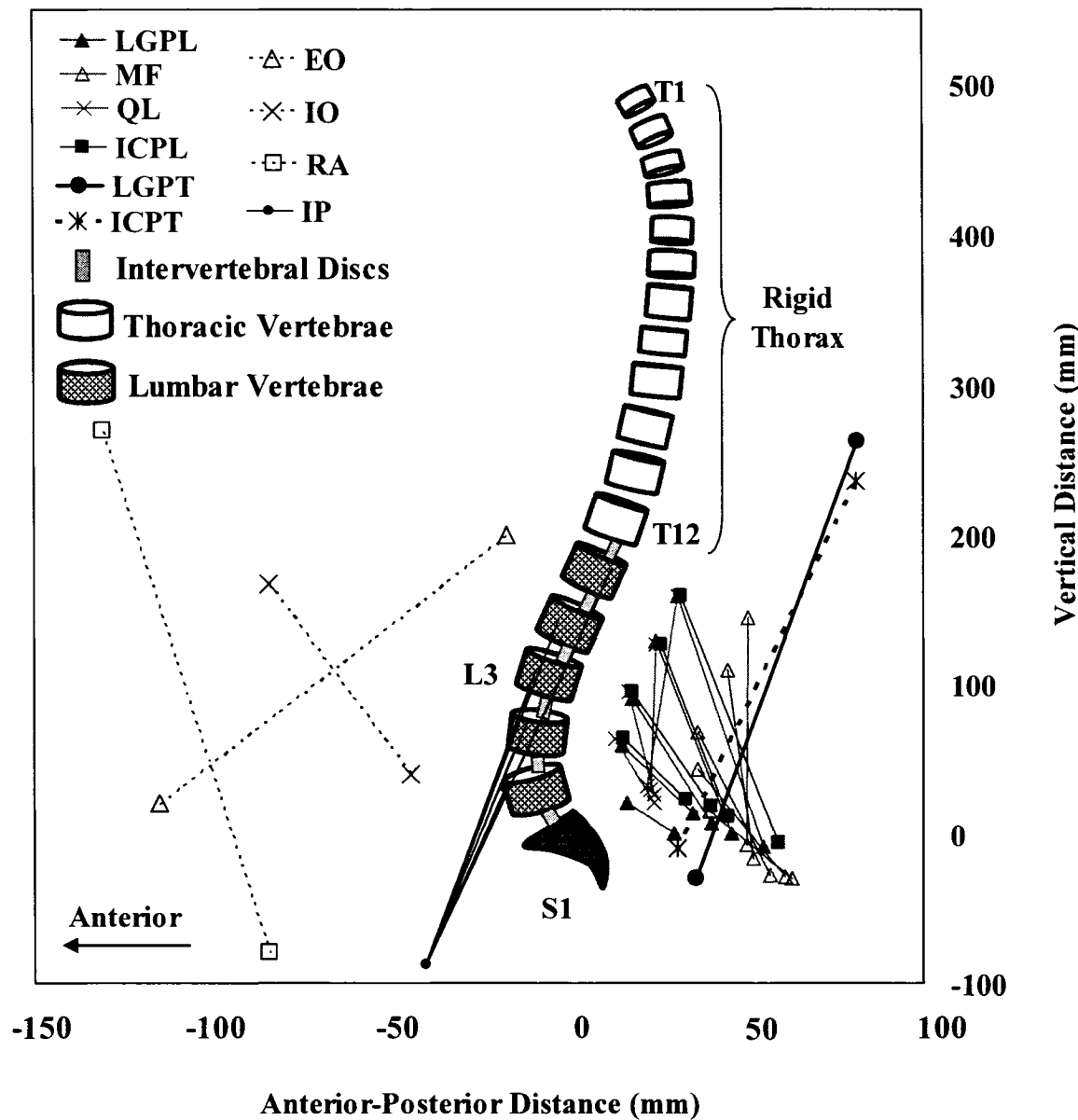


Fig. 8.1 The FE model as well as global and local musculatures in the sagittal plane (only fascicles on one side are shown) in upright standing posture at initial undeformed configuration. ICPL: Iliocostalis Lumborum pars lumborum, ICPT: Iliocostalis Lumborum pars thoracic, GPL: Longissimus Thoracis pars lumborum, LGPT: Longissimus Thoracis pars thoracic, MF: Multifidus, QL: Quadratus Lumborum, IP: Iliopsoas, IO: Internal Oblique, EO: External oblique, and RA: Rectus Abdominus (axes are not to the same scale).

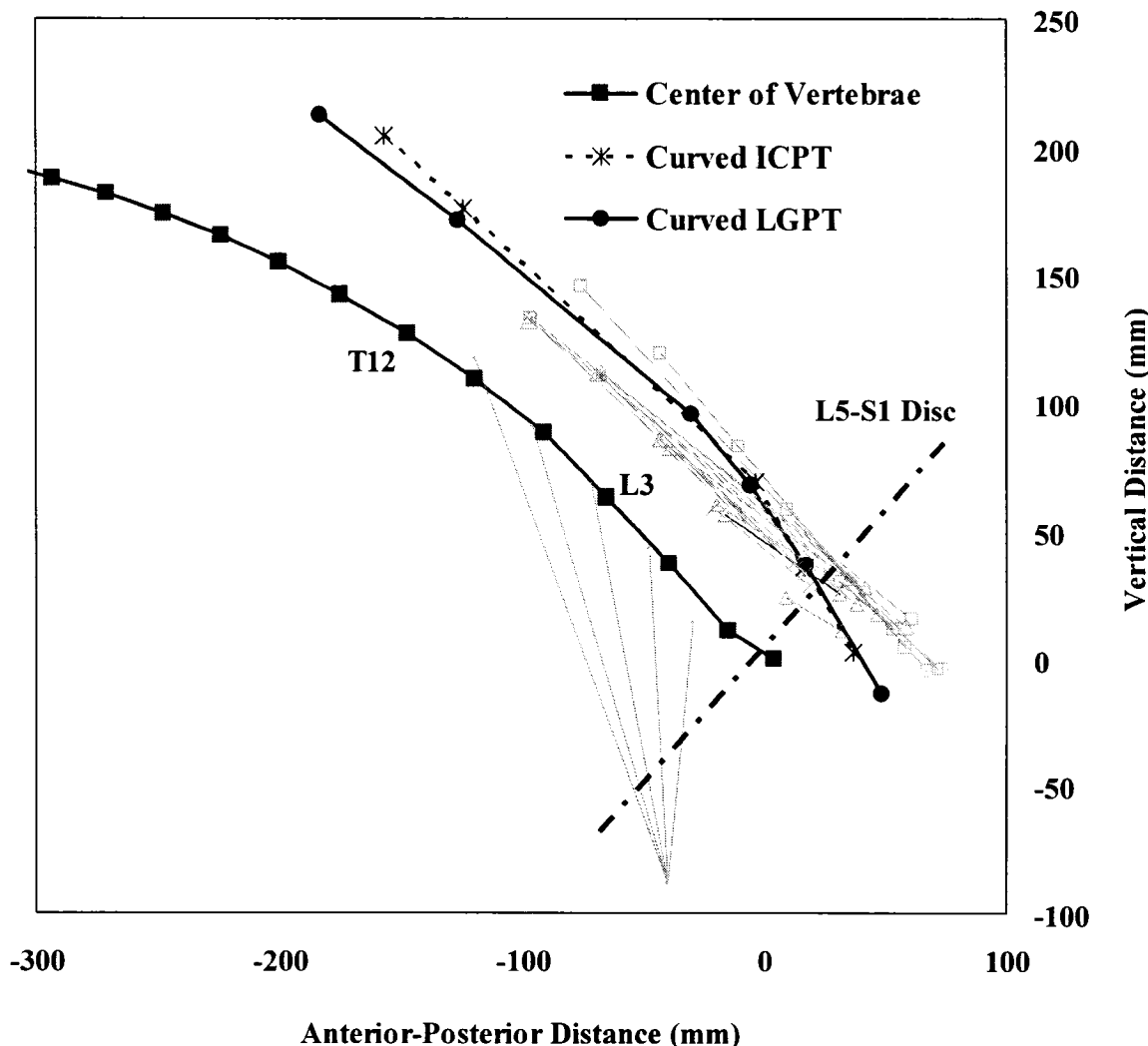


Fig. 8.2 Deformed configuration of the spine and the global muscles (Longissimus Thoracis pars thoracic, LGPT, and Iliocostalis Lumborum pars thoracic, ICPT) with curved lines of action under flexion of 65° . The cutting transverse plane for the single-level free body diagram (SLFBD) model at the L5-S1 disc level is also depicted (abdominal muscles are not shown).

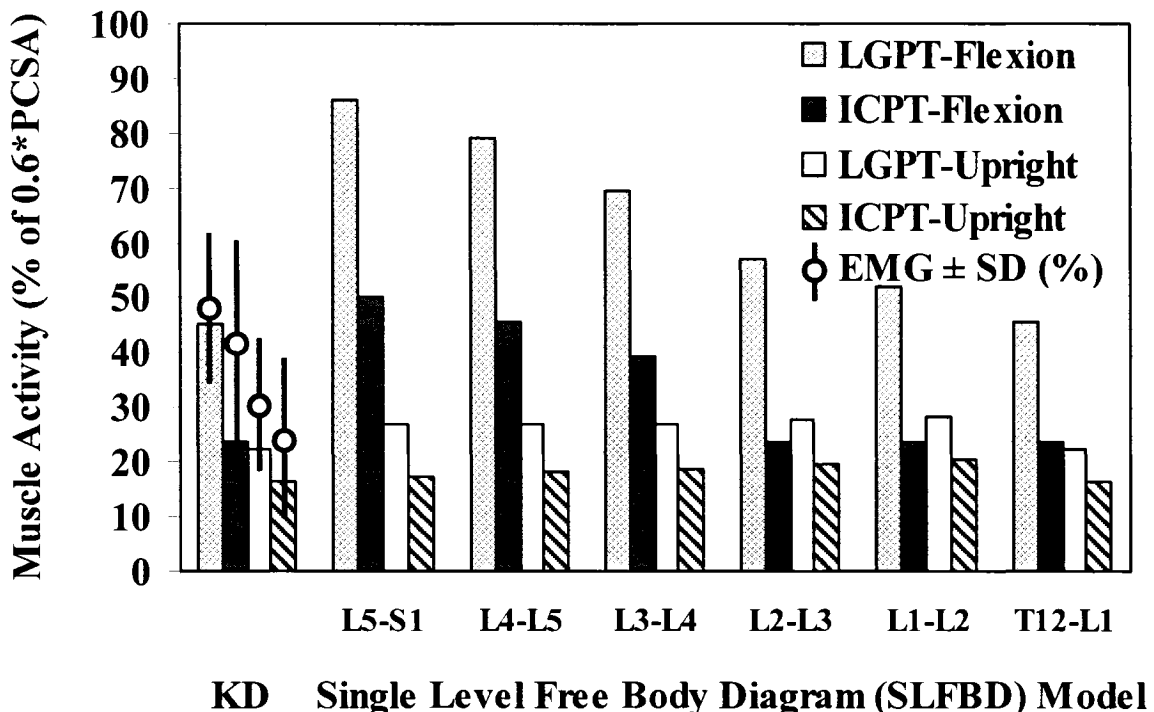


Fig. 8.3 Normalized (to 0.6 times physiological cross sectional area) activity of global muscles (Longissimus Thoracis pars thoracic, LGPT, and Iliocostalis Lumborum pars thoracic, ICPT) for both loading cases predicted using kinematics-driven (KD) approach and single-level free body diagram (SLFBD) models considered at different T12-L1 through L5-S1 levels. Normalized (to the MVC) *in vivo* measured EMG activity (mean \pm SD) of these muscles is also shown.

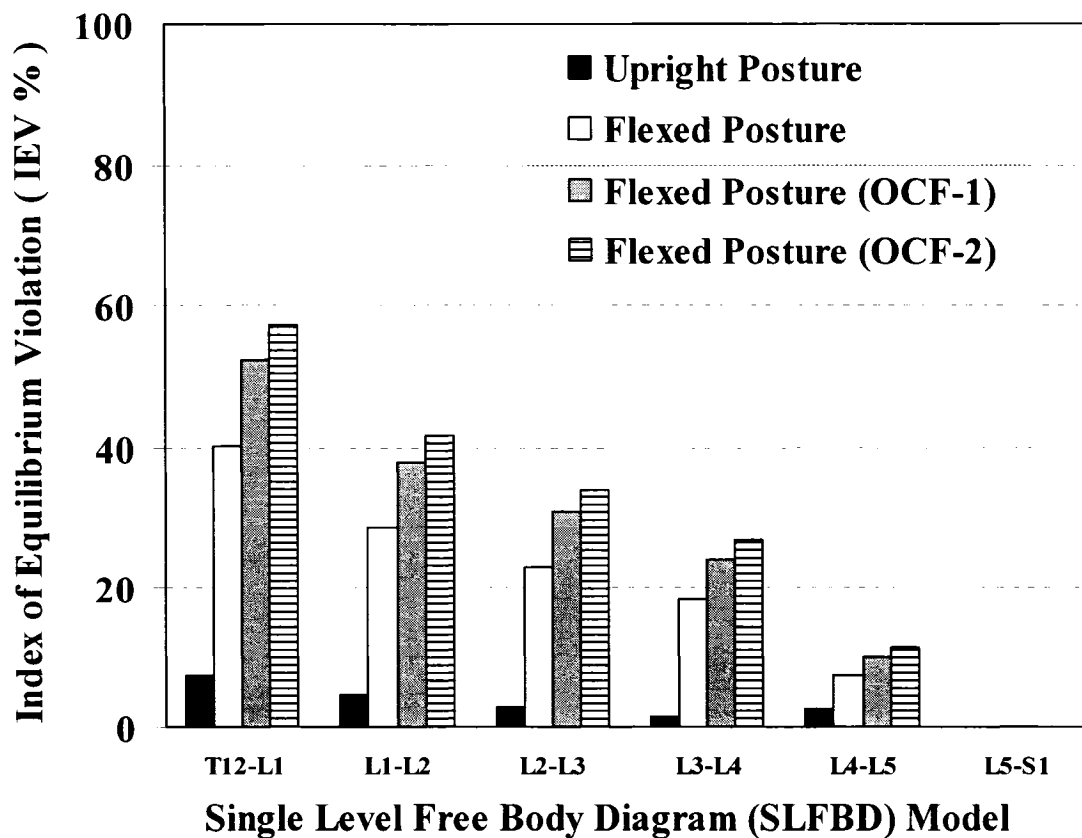


Fig. 8.4 Index of Equilibrium Violation (IEV %) at different T12-L1 through L5-S1 levels when applying muscle forces calculated based on single-level free body diagram (SLFBD) model at the L5-S1 level. OCF-1 and 2 refer to optimization cost functions of sum of squared and linear muscle stresses, respectively, used to partition net moment at the L5-S1 level between muscles.

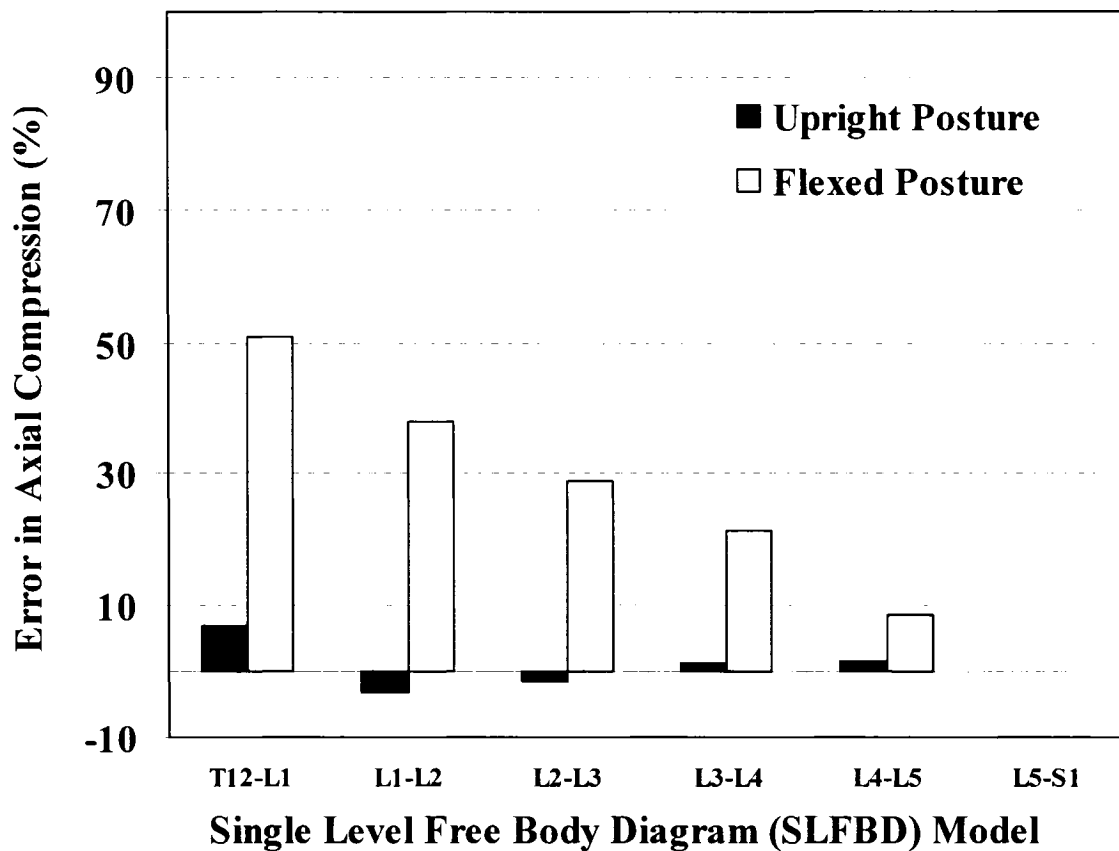


Fig. 8.5 Relative error in axial compression forces estimated at different spinal levels when applying the muscle forces calculated by the single-level free body diagram (SLFBD) model at the L5-S1 level compared to those calculated using SLFBD models directly at the level under consideration.

CHAPTER 9

DISCUSSIONS AND CONCLUSIONS

9.1 Overview

In lack of any gold-standard *in vivo* quantifications, biomechanical models of the spine to estimate spinal loads and stability are used towards design of injury prevention and rehabilitation programs. Facing with the hindrance of kinetic redundancy in spinal joints, investigators have been obliged to make simplifying assumptions in order to estimate muscle forces and internal spinal loads. Three existing modeling approaches; namely equivalent-muscle, optimization-based, and EMG-based encounter a major shortcoming in that muscle forces and spinal loads are estimated based on the satisfaction of equilibrium at one single level of the spine. This shortcoming has been found to adversely affect model predictions (Arjmand et al., 2006; see also chapter 8).

In order to tackle the redundancy problem in the system of equilibrium equations while satisfying equilibrium conditions at all spinal level, the Kinematics-based approach has been used in the present study in which *in vivo* measured kinematics of the spine are prescribed into the model as input data. Each prescribed kinematics (rotation or translation) data generates a constraint equation between external loads and muscles forces. As number of prescribed kinematics increases, degree of redundancy decreases so that if the number of prescribed kinematics reaches that of unknown muscle forces at a particular level, the equilibrium equations can be solved deterministically. Besides, this approach guarantees satisfaction of equilibrium conditions at all spinal levels and directions resulting in more realistic and reliable estimations for muscle forces, spinal load, and system stability in accordance with measured spinal kinematics and nonlinear passive properties.

The aim of this work was to develop the application of the Kinematics-based approach for static lifting tasks involving forward trunk flexion that are frequently encountered in manual material handling activities in various industrial and athletic activities. Some hypotheses were examined and two controversial issues in ergonomics regarding lumbar posture during lifting and role of intra-abdominal pressure (IAP) in unloading and stabilizing the spine during such activities were addressed. Besides, some modeling concerns, i.e. effect of optimization cost function, wrapping of trunk muscles, and use of single-level equilibrium methods on model predictions were assessed towards the improvement in mathematical representation of the spine. The understanding gained in the course of this work should help improve the prevention and treatment programs and suggest safer manual material handling techniques.

9.2 Finite Element Model

The geometry (center of vertebrae) of ligamentous thoraco-lumbar model is constructed using CT scan images of a cadaver lumbar specimen and data in the literature (Shirazi-Adl and Parnianpour, 1993, 1996). It comprises of 6 deformable beams to represent T12-S1 discs and 7 rigid elements to represent T1-T12 (as a single body) and lumbosacral vertebrae (L1 to S1). The beams modeled the overall nonlinear stiffness of T12-S1 motion segments (i.e., vertebrae, disc, facets, and ligaments) at different directions and levels.

9.2.1 Verifications of the Passive Spine Model

The nonlinear load-displacement response under single and combined axial/shear forces and sagittal/lateral/axial moments along with the flexion versus extension differences were represented in this model based on numerical and measured results of previous single- and multi-motion segment studies (Oxland et al., 1992; Pop, 2001; Shirazi-Adl et al., 2002; Shirazi-Adl, 2006; Yamamoto et al., 1989). Fig. 9.1 shows the load-displacement response of the lumbar spine model used in this study compared with that of the detailed finite element model study of Shirazi-Adl, 2006 under compressive

follower load (P) of 900 and 2700 N and that of *in vitro* study of Patwardhan et al., 2003 under compressive follower load of 1200 N. Effect of axial compressive loads on the motion segment stiffness has been found to be substantial (e.g., Broberg, 1983; Gardner-Morse and Stokes, 2003; Janevic et al., 1991; Patwardhan et al., 2003; Shirazi-Adl, 2006) and, therefore, was considered in this study.

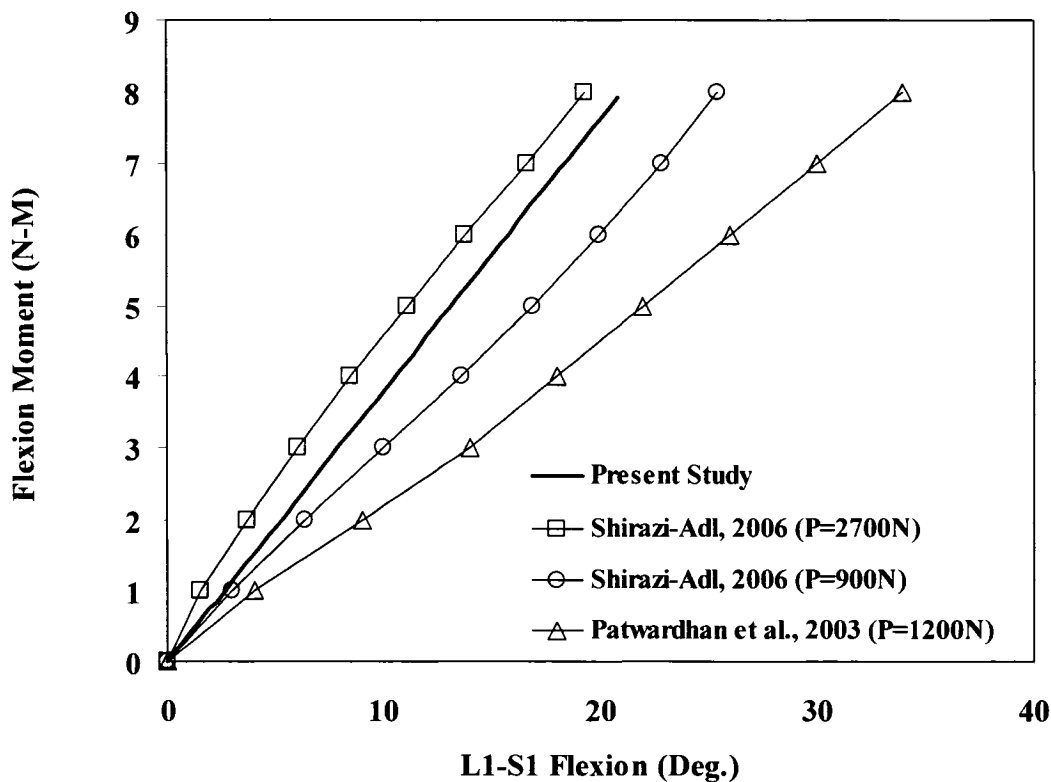


Fig. 9.1 Load-displacement response of the lumbar spine with published data of *in vitro* and finite element model studies

In vitro experimental studies on isolated osteo-ligamentous lumbar spine of cadaver specimens without muscular support have estimated an average critical buckling load of 90-120 N under vertical compressive load in the lateral plane (Crisco and Panjabi, 1992; Crisco et al., 1992; Patwardhan et al., 1992, 2001, and 2003). Besides, *in vitro* experiments have shown a buckling load of about 20 N when the whole thoraco-lumbar spine was tested (Lucas and Bresler, 1961). In comparison in the present study,

linear buckling analysis at initial un-deformed configuration of the ligamentous spine demonstrated that the lumbar spine buckled under vertical load of 103 N applied at the center of T12 vertebra. Linear perturbation analyses at deformed configurations of the structure while applying different vertical loads at the center of T12 or T1 vertebra computed a critical load of about 120 or 20 N in the sagittal plane, respectively (see Fig. 9.2 and 9.3). Lateral translations were constrained in these simulations.

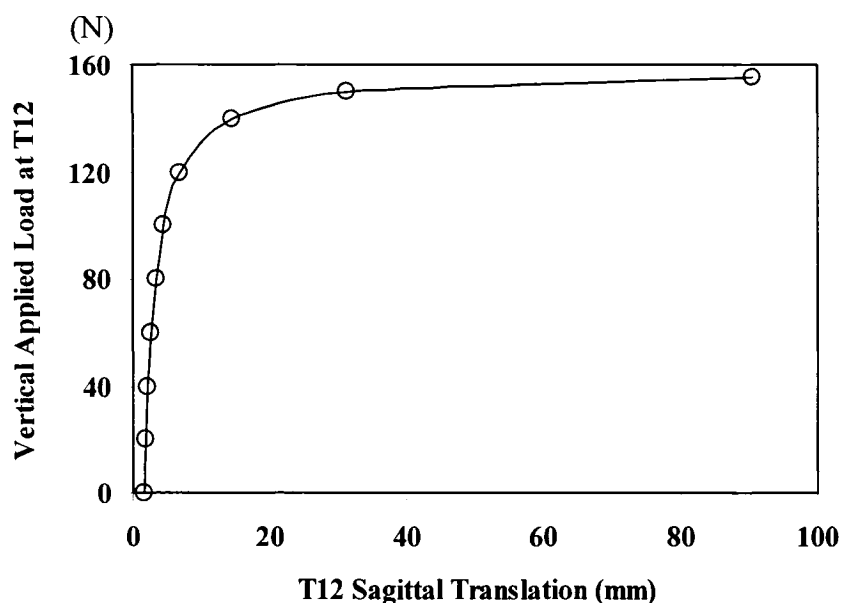


Fig. 9.2 Variation of computed T12 sagittal translation with the vertical applied load at T12 vertebra level using linear perturbation analysis at deformed configurations due to 1 N horizontal force at the T12

9.2.2 Model Loadings

Mean total body mass of the 15 subjects participated in our *in vivo* tests was measured to be about 74 kg based on which weight of trunk, head, and arms was estimated and assigned to the FE model using available anthropometric data (Zatsiorsky et al., 1990) in the literature; 256.3 N for the trunk, 58.5 N for the head, and 72.2 for the arms.

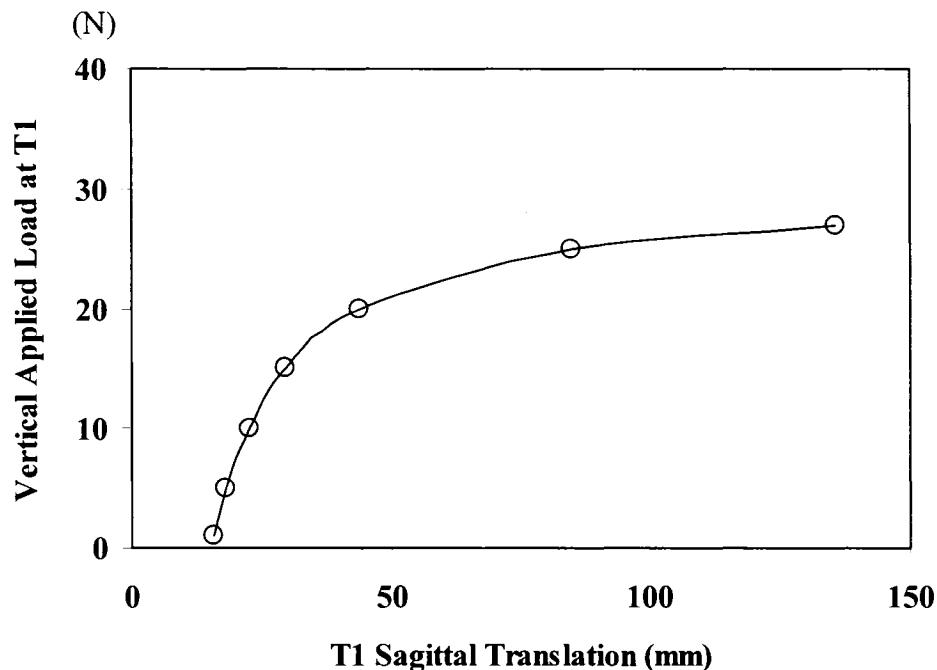


Fig. 9.3 Variation of computed T1 sagittal translation with the vertical applied load at T1 vertebra level using linear perturbation analysis at deformed configurations due to 1 N horizontal force at the T1.

A distributed loading pattern along the length of spine at different vertebral levels simulating the trunk weight (256 N) was considered based on available *in vitro* (King-Liu and Wickstrom, 1973; Takashima et al., 1979) and *in vivo* (Pearsall, 1994) studies (Fig. 9.4). The eccentricity of these loads relative to the center of vertebrae was considered based on the study of (Pearsall, 1994) (Fig. 9.5). According to the work of Takashima et al., 1979, gravity load of the head was applied 1 cm anterior to the center of T1 vertebra while that of arms was equally distributed and applied at 3 cm posterior to the center of T2, T3, and T4 vertebrae. To simulate the cases with an external load in hands, 180 N was applied via a rigid element attached to the T3 vertebra at the location measured in our *in vivo* studies.

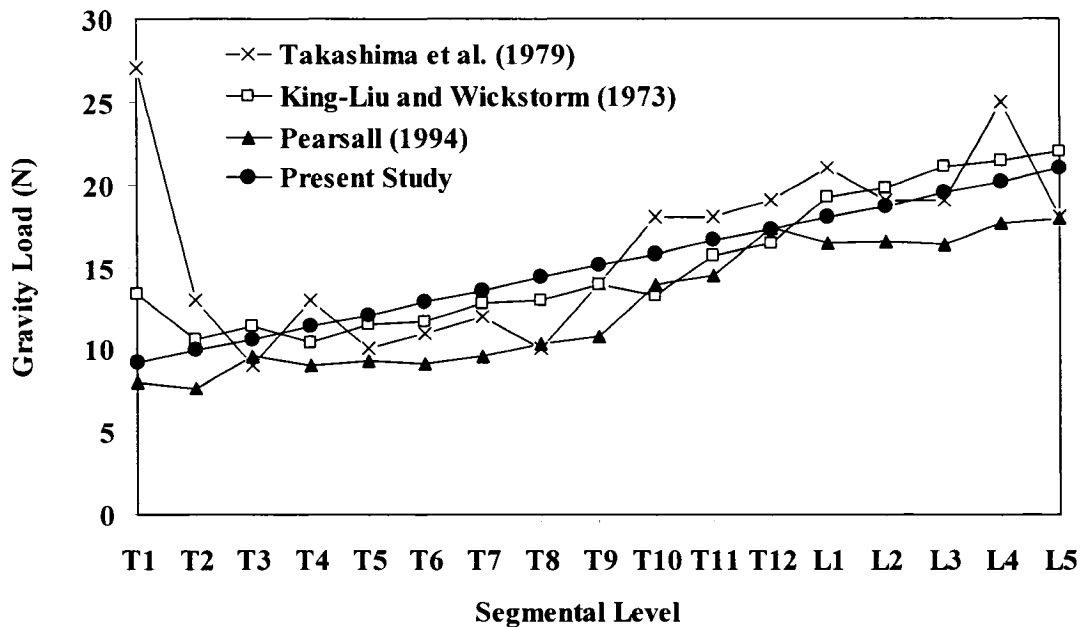


Fig. 9.4 Distribution of gravity load of the trunk applied at different spinal levels in the finite element model compared with those of other studies.

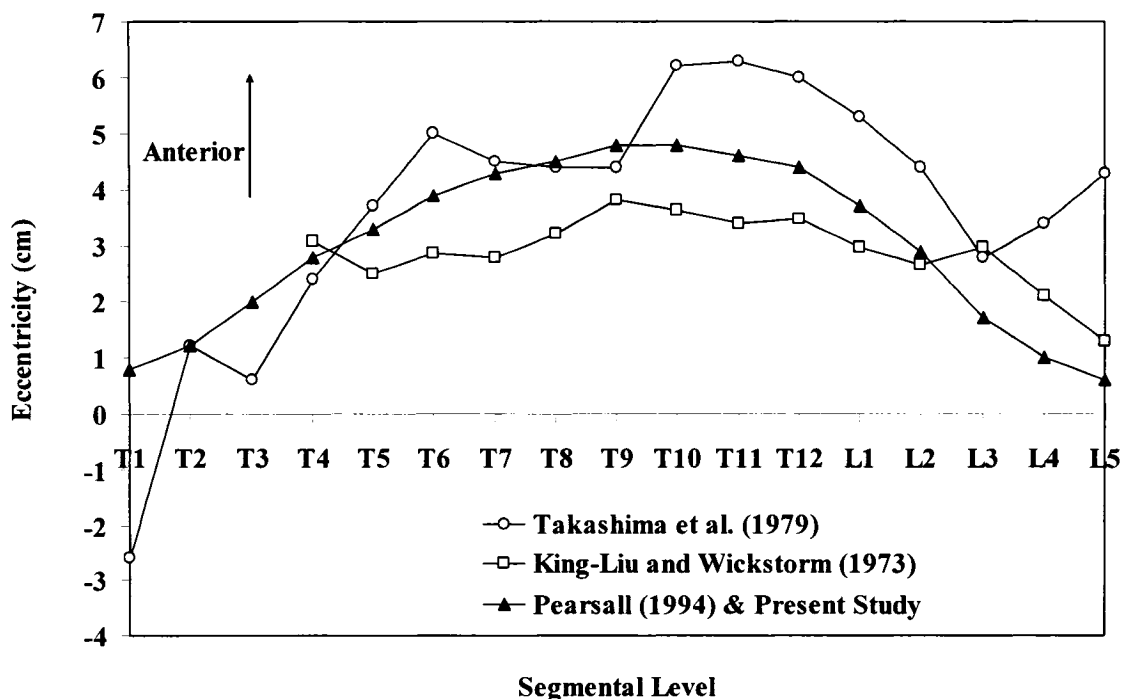


Fig. 9.5 Eccentricity of the applied gravity load of the trunk relative to the center of corresponding vertebra in the finite element model compared with those of other studies.

9.2.3 Boundary Conditions

Since simulations were done in the sagittal plane lateral translation and rotation in the frontal plane and axial rotations in the transverse plane were all fixed. The axial and sagittal translations at the base, S1, were also constrained. For each simulation case, sagittal rotations of T12 (thorax) and S1 (pelvis) was prescribed on the model according to mean values of our *in vivo* measurements (see Table 3.1 and Fig 4.4). Total lumbar rotation, calculated as the difference between the foregoing two rotations, was partitioned between lumbar vertebrae in accordance with proportions reported in earlier investigations (see Chapter 3).

The lumbar/pelvis ratio for the prescribed data into the finite element model was equal to 1.56, 1.87, 1.29, and 1.40 for flexion of 40°, flexion of 40° plus 180 N in hands, flexion of 65°, and flexion of 65° plus 180 N in hands, respectively, all for the cases with free lumbar posture. These values are well within the range of data (0.4-2.38) reported based on *in vivo* studies reporting the lumbar/pelvis ratio during lifting tasks (Esola et al., 1996; Lee and Wong, 2002; Li et al., 1996; Granata and Sanford, 2000; McClure et al., 1997; Porter and Wilkinson, 1997). Furthermore, in agreement with *in vivo* studies this ratio decreased as trunk flexion increased (Esola et al., 1996; Lee and Wong, 2002; Granata and Sanford, 2000; McClure et al., 1997; Porter and Wilkinson, 1997) and increased as magnitude of the load in hands increased (Granata and Sanford, 2000).

9.3 Muscles

9.3.1 Muscle Anatomy

Anatomy of trunk muscles including their insertion points, lever arms, and lines of action considered in the present study were mainly taken from the extensive study of Stokes and Gardner-Morse, 1998 which was, in turn, based on previous studies (e.g. Bogduk et al., 1992a, b; MacIntosh and Bogduk, 1991; Panjabi et al., 1991) as well as

the datasets of the Visible Human Project™ (National Library of Medicine, Bethesda, MD). See Appendix A for a brief description of the anatomy of trunk muscles considered in the current model.

9.3.2 Passive Property of Muscles

The total force computed by the Kinematics-based approach in each muscle was partitioned into active and passive components with the latter force evaluated based on a length-passive tension relationship. Diverse data have been reported for muscle passive force-length relationship from *in vitro* and *in vivo* experimental studies (e.g. Woittiez et al., 1984; Davis et al., 2003; Deng and Goldsmith, 1987; McCully and Faulkner, 1983) which have been used in biomechanical model studies (e.g. McGill and Kipper, 1994; Nussbaum and Chaffin, 1996; McGill and Norman, 1986; Cholewicki and McGill, 1995) (see Fig. 9.6). In the present study the relationship was defined based on a recent *in vivo* study Davis et al. (2003) whose data were fairly in between those of others.

9.4 Optimization Algorithm

The cost functions of sum of squared and cubed muscle stresses appeared most adequate with results in good agreement with measured EMG activity in global muscles (see Chapter 5). Predictions of these two cost functions remained within the lower/upper constraints on muscle forces set in the optimization approach; same results would have been obtained had limits not been introduced. Besides, force-sharing in between muscles in these cost functions accounted for both muscle lever arm and PCSA. No significant difference in spinal loads was found between predictions of these two cost functions (Table 5.3, Figs. 5.3 and 5.4). Although predictions of Σ stress³ was even less dependent on the inequality constraint equations but the criteria of Σ stress² would be easier to analytically implement especially when equilibrium is considered in more than one plane.

Optimization algorithm with the cost function of sum of cubed muscle stresses was considered in all simulations done in the current work. One of the concerns when

using a nonlinear optimization approach to solve the redundancy problem is the convergence to the global minimum. In the current study Lagrange Multiplier Method was used to analytically solve the optimization problem which guarantees the convergence of results to the global minimum. See Appendix B for a detailed description of this method.

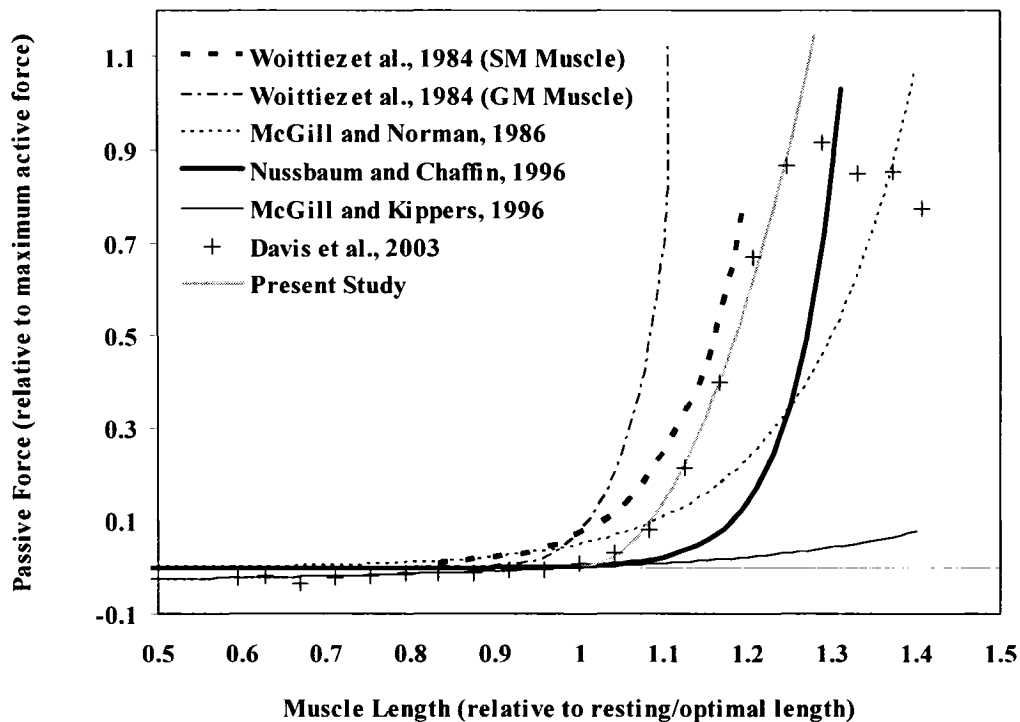


Fig. 9.6 Muscle passive force-length relationship considered in the model compared to other experimental data. Curves of McGill and Kippers (1996) and Nussbaum and Chaffin (1996) have been adapted from data of Deng and Goldsmith (1987) and McCully and Faulkner (1983), respectively. SM and GM refer to Semimembranosus and Gastrocnemius muscles respectively.

9.5 Model Validations

The models of human spine cannot be fully validated, since an adequate knowledge of the human spine loading and structure is currently not available. In other words, direct validation of the predicted tissue loads, by comparing measured and

predicted forces, is not feasible. Therefore, indirect method of model validation must be used. For instance, predicted axial compression on spinal discs may be compared with *in vivo* measured intra-discal pressure values under identical tasks, for the sake of an indirect validation.

The demonstration of agreement between the observed and predicted results, however, does not prove model validity under all circumstances (Oreskes et al., 1994). These authors suggested using the term *confirmation* to describe the single act of demonstrating the agreement between the modeled and observed phenomenon. For a modeled system that exists in the real world (e.g. human spine) but unavailable for direct experiments, Lewandowski (1982) has proposed a validation process consisting of component validation, internal validity checks, and sensitivity analysis. Cholewicki and McGill (1996) followed this process to validate their predictions obtained by a geometrically simplified model of the spine.

The component validation is based on the premise that models built of well validated sub-models will probably be valid (Lewandowski, 1982). In our study, this validation approach was applied to the passive spine in which good agreement between load-displacement and buckling behaviors of the model with *in vitro* studies was obtained (see Figs. 9.1, 9.2, and 9.3). Moreover, the passive properties of the spine have extensively been validated in earlier works under various loading conditions (El-Rich et al., 2004, El-Rich and Shirazi-Adl, 2005; Pop, 2001; Shirazi-Adl et al., 2002).

Internal validity pertains to the preservation of basic physical laws on which such a model was built. For example, one advantage of using finite element model of the spine in the current study was that equilibrium conditions were automatically satisfied at all spinal levels and in all directions. Besides, the final deformed configuration of the spine for a simulated task was in accordance with what measured *in vivo* (see Fig.3.5). Qualitative agreement between measured and predicted global muscle activities (see

Figs. 3.9, 4.5, 5.2, 6.4, and 7.3), good accordance between measured and predicted intra-discal pressure (IDP) (see below), as well as between measured and predicted intervertebral translations (see below) in different simulated tasks are indirect validations for muscles forces, spinal compression and shear forces, respectively.

In relaxed upright standing posture, the IDP of 0.43-0.50 MPa (Wilke et al., 2001), 0.56-0.97 MPa (Nachemson and Elfstrom, 1970), 0.22-0.75 MPa (mean of 0.539 MPa) (Katsuhiko et al., 1999), and 0.35 MPa (Takahashi et al., 2006) at the L4-L5 disc and of 0.33 ± 0.034 MPa (Andersson et al., 1977) and 0.27 MPa (Schultz et al., 1982) at the L3-L4 disc have been measured *in vivo*. In an *in vitro* study on seven cadaver while applying muscle forces via cables on the specimens the IDP of about 0.52 MPa was measured in standing posture (Wilke et al., 2003). For upright standing posture, our model predicted IDP of 0.51 MPa and 0.48 MPa at the L4-L5 and L3-L4 levels, respectively, while accounting for the axial compression-disc pressure relations in lumbar specimens (Shirazi-Adl and Drouin, 1988).

When flexing forward by about 36° , Wike et al., 2001 measured that IDP at the L4-L5 disc increased by 2.2 times relative to that in relaxed standing posture. For flexion of 40° , we predicted an increase by 3.48 times with straight LOA for global muscles while assuming a computed IDP-axial compression relationship (Shirazi-Adl and Drouin, 1988).

Takahashi et al. (2006) measured an increase by 4.57 times in the IDP when the lumbar spine was flexed by 30° as compared to relaxed standing posture, while for a similar task Katsuhiko et al. (1999) measured an increase by about 2.50 times. For forward flexion of 65° (lumbar flexion of 35°) we predicted a value of 4.33 times when considering straight LOA for global muscles and 3.55 times when considering wrapping of global muscles. These values have been calculated employing the results of a detailed finite element model of the lumbar spine.

Relative increase in IDP in flexed posture of about 65° with 200 N in hands with respect to the relaxed upright standing posture has been measured *in vivo* study to be by 5.1 times (Wilke et al., 2001). Our model while considering straight lines of action for global muscles and a linear relationship between spinal compression and disc pressure predicted a value of about 7.20 times that decreased to 5.82 and 5.38 times when wrapping of global muscles was considered with and without a 10% reduction in their lever arm, respectively. Unfortunately, data of Wilke et al., 2001 were based on tests on only one subject; thereby the significance of the data to the individual trends was limited.

Total relative translations in the sagittal plane between two adjacent vertebrae for the heaviest task simulated in this study, i.e. flexion of 65° plus 180 N load in hands with straight LOA for global muscles, were about 1.4, 2.9, 2.7, 2.3, 2.1, 1.45 mm for L5 to S1, L4 to L5, L3 to L4, L2 to L3, L1 to L2, and T12 to L1 vertebrae, respectively. These values are well within reported physiological limits (Hyes et al., 1989; Panjabi et al., 1989; Stokes and Gardner-Morse, 1995) and show exactly the same trends as those measured *in vivo* under forward flexion activities in which intervertebral translations decreased from their maximum value at the L4/L5 segment upward to the T12/L1 level with L5 vertebra having the minimum translation relative to the S1 (Hyes et al., 1989; Lin et al., 1994). This finding indirectly validates our predictions for anterior-posterior shear forces acting at different levels of the spine.

To further validate predictions (Oreskes et al., 1994), sensitivity analyses were conducted on one of the most important assumptions regarding distribution of total lumbar rotation between different vertebrae. Different proportions for the relative contribution of each motion segment to generate the total lumbar flexion under full trunk flexion have been reported in the literature. The most important difference exists between works of Potvin et al., 1991 (10%, 11.88%, 11.88%, 18.9%, 26.1%, and

21.24% for T12-L1, L1-L2, L2-L3, L3-L4, L4-L5, and L5-S1, respectively) and Frobin et al., 1996 (11.46%, 15.03%, 17.71%, 18.09%, 20.89%, and 16.81% respectively). The first case studies considered about 34% and 66% of the total lumbar rotation to T12/L3 and L3/S1 segments, respectively, while for the second case these values changed to 44% and 56%. In our reference case model 36% of the total lumbar rotation was assigned to T12/L3 and 64% to L3/S1 segments which are fairly similar to those of Potvin et al., 1991.

In order to study the effect of these proportions on the predicted results for muscle forces, spinal loads and stability, analyses were repeated for the case of flexion of 40° while assigning 45% and 55% to T12/L3 and L3/S1 segments, respectively, which were similar to data measured by Frobin et al., 1996. Table (9.1) and Table (9.2) compare predicted muscle forces and spinal loads with those predicted by our reference case model. Stability of the spine is even less influenced by these variations in lumbar rotations (Fig. 9.7). According to some radiological studies (Tuong et al., 1998; Woldstad and Sherman, 1998), such variations in proportions of the relative contribution of upper and lower motion segments to generate the total lumbar flexion also happen when wearing abdominal belts or lumbosacral orthoses. An orthosis, for instance, has been suggested to reduce vertebral mobility and discal deformations mainly at the upper segments (L1-L3), while increasing them at the lower levels (Tuong et al., 1998).

Table 9.1 Predicted local/global muscle forces (N) on each side for two different proportions considered to partition total lumbar rotation between lumbar vertebrae.

Level	36% to T12/L3 & 64% to L3/S1					45% to T12/L3 & 55% to L3/S1				
	ICPL	IP	LCPL	MF	QL	ICPL	IP	LCPL	MF	QL
L1	24.4	28.7	15.1	26.6	17.4	22.1	25.8	13.6	24.1	15.8
L2	38.0	-	16.9	41.3	13.8	44.2	-	19.6	48.0	16.0
L3	39.1	-	16.7	62.7	10.2	54.8	-	23.4	87.5	14.3
L4	31.4	-	13.9	40.1	7.1	31.4	-	13.9	40.0	7.1
L5	-	-	18.0	31.6	-	-	-	18.6	32.5	-
Thorax	RA	TO	EO	ICPL	LCPL	RA	TO	EO	ICPL	LCPL
	-	-	-	107.3	242.0	-	-	-	91.8	206.2

Table 9.2 Predicted spinal loads based on two different proportions considered to partition total lumbar rotation between lumbar vertebrae

Level	36% to T12/L3 & 64% to L3/S1			45% to T12/L3 & 55% to L3/S1			Differences (%)		
	M*	C*	S*	M	C	S	M	C	S
T12-L1	18.5	933	250	23.3	831	242	26.2	-11	-3
L1-L2	22.1	1171	224	27.0	1053	208	22.3	-10	-7
L2-L3	21.3	1414	111	24.2	1330	88	13.4	-6	-21
L3-L4	17.2	1669	173	15.1	1684	132	-12.1	1	-24
L4-L5	16.8	1862	95	13.3	1874	74	-20.7	1	-22
L5-S1	19.4	1912	502	15.6	1923	510	-19.5	1	1

* M: sagittal moment at mid-height, + ve in flexion (Nm); C: local axial compression at mid-height (N); S: local shear force at mid-height, +ve in anterior direction (N).

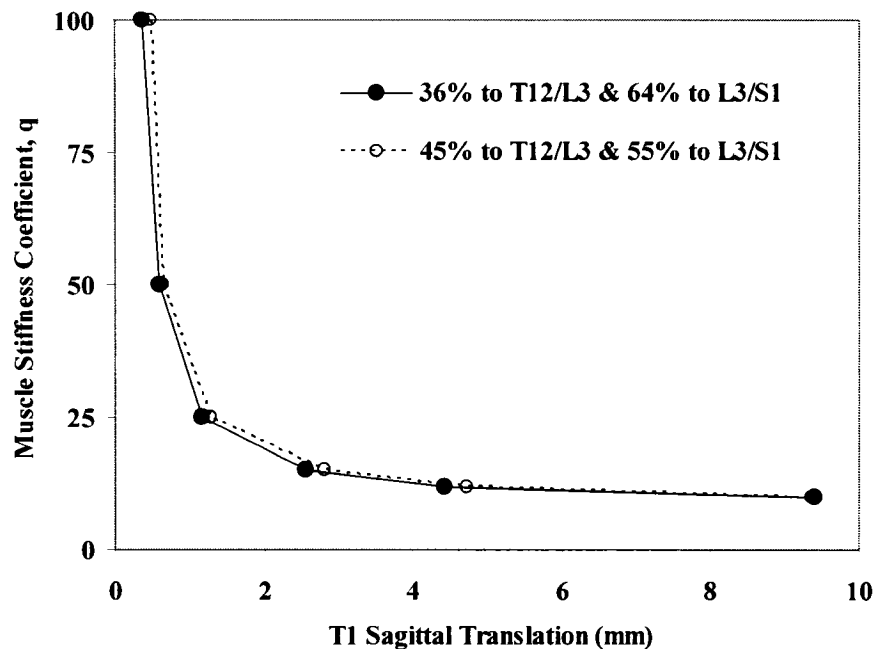


Fig. 9.7 Variation of computed T1 sagittal translation with the muscle stiffness coefficient, q , for two different lumbar rotation partitions (see text) under identical total trunk flexion of 40° using linear perturbation analysis at deformed configurations due to 1 N horizontal force at the T1. The smallest q in each case is the critical value below which the system becomes unstable.

9.6 Methodological Issues (limitations)

There are always some assumptions or limitations in both modeling and experimental studies. It is important to assess the probable effects of such assumptions and limitations on predictions, measurements and conclusions. There have been some limitations and assumptions in both experimental and modeling studies in the present work which are separately discussed in the following paragraphs.

9.6.1 Experimental Studies

Calculation of the trunk and pelvic rotations from skin markers, despite non-invasiveness and ease of measurements, is recognized to have important errors involving identification of anatomical landmarks, skin movement relative to the underlying bony landmarks, and deformability of vertebrae themselves (Lee et al., 1995; Shirazi-Adl, 1994; Zhang and Xiong, 2003). Due to inherent errors, in this work, the measurements were used only to evaluate pelvic tilt and trunk T1-T12 rotations with the intervening lumbar segmental rotations evaluated based on relative values reported in the literature. Moreover, since both the thorax and pelvis can be considered with a very good approximation as rigid bodies (see section 9.6.2), errors due to identification of anatomical landmarks or skin movement relative to the underlying bony landmarks are expected to be minimized. Tasks are designed and subjects are instructed in a manner as to minimize out-of-sagittal plane movements.

The measurement of the maximum EMG activity (MVC) in each muscle required for normalization depends amongst others on the task design, subject and electrode location (O'Sullivan et al., 2002; McGill, 1991). Since the electrodes for the multifidus at the L5 level are more likely to yield activity of adjacent longissimus (Stokes et al., 2003), comparisons between predictions and measurements were avoided for the Multifidus. The collected data for these electrodes, however, demonstrated exactly the same trends as those observed for the data of other electrodes at the L1 level

with mean normalised values being almost always greater (at most by 6%) than those measured for the LGPT markers.

9.6.2 Model Studies

Great inter-individual differences in the spinal loads and muscle activities may occur due partly to inter-subject variations in body weight, body size, posture, and tissue properties. Our predicted results, hence, represent values within the limits since mean values were used everywhere as model inputs.

The assumption of rigid body for the T1-T12 segments was confirmed by measuring nearly equal rotations from lines attaching T12 to T5 and T12 to T1, e.g., respectively $41.4 \pm 7.5^\circ$ and $41.0 \pm 7.3^\circ$ for flexion of $\sim 40^\circ$ without load in hands with free lumbar posture; an observation which is in agreement with that of others (Jager and Luttmann, 1989; Nussbaum and Chaffin, 1996; Panjabi and White, 1980) and assumed in many biomechanical model studies (e.g., Bergmark, 1989; Gardner-Morse and Stokes, 1995; Cholewicki and McGill, 1996). It has been indicated (Ashton-Miller and Schultz, 1997) that the only work investigating thorax range of motion in the early 1930s (Bakke, 1931) has found that total intersegmental flexion-extension movement does not exceed 5° . Similarly, length of thoracic spine in contrast to that of the lumbar spine has been measured to remain almost unchanged during full trunk flexion (Toussaint et al., 1995).

The thoracolumbar (or lumbodorsal) fascia (TLF or LDF) was totally neglected in the current work. The literature suggest minor role of TLF in offsetting moment of external loads during lifting activities (Bergmark, 1989; Daggfeldt and Thorstensson, 2003; Macintosh et al., 1987; McGill and Norman, 1988; Potvin et al., 1991; Tesh et al., 1987) which is in contrast to earlier suggestions by Gracovetsky and colleagues (see Gracovetsky et al., 1981; Gracovetsky, 1988). One hypothesis is that oblique abdominal and transverse abdominus (Gracovetsky et al., 1981) as well as latissimus dorsi (Bogduk

and Macintosh, 1984; McGill and Norman, 1988) muscles have potential to contribute to trunk extensor moment by transforming their tension into longitudinal tension via the TLF; i.e., it acts as both tendon and ligament. This mechanism is called active moment generation mechanism of the TLF. Another hypothesis, referred to as hydraulic amplifier mechanism, is that the contraction of erector spinae muscles contained in a thick, inelastic envelope would increase tension in TLF (Gracovetsky et al., 1985).

Anatomical, *in vitro* experimental and model studies (Bergmark, 1989; Tesh et al., 1987; Macintosh et al., 1987; McGill and Norman, 1988) have, however, all challenged the viability of the proposed mechanisms of TLF extensor moment generation and shown that the TLF forces have been overestimated and that the contribution of TLF in resisting the trunk moment is only very small. Gracovetsky (1989) himself stated that neither of two aforementioned mechanisms could be of substantial help in generating extension moment in the sagittal plane.

All trunk muscles were assumed to be bilaterally symmetric with respect to the sagittal plane having identical lines of action, lever arms, and physiological cross sectional area. Only muscles arising from pelvis (and the hip bone) and attaching to the lumbar or thoracic vertebrae or the rib cage were considered in the finite element model study while neglecting all the single joint intersegmental as well as multisegmental muscles. These neglected muscles have been reported not to play important roles in neither stabilizing the spine (Crisco and Panjabi, 1991) nor offsetting moment of external loads (Bergmark, 1989). The latissimus dorsi muscle was neglected in the model study. It has been known to produce trunk extensor moment via the lumbodorsal fascia; a contribution suggested not being sizable during lifting tasks (Bogduk et al., 1998; McGill and Norman, 1988). Its stabilizing role has also been stated to be negligible (Bergmark, 1989).

The abdominal muscles (RA, EO, and IO) were represented by single fascicles. Consideration of several fascicles instead of just one for oblique muscles (EO and IO) has influenced the estimated spinal loads significantly in asymmetric lifting tasks but only slightly in symmetric ones (Davis and Mirka, 2000) which is the case in the current study. The transverse abdominus (TA) does not play any direct role in carrying trunk moment; hence, it was neglected in the current study. It might, however, help in offsetting moment of external loads by increasing intra-abdominal pressure (Daggfeldt and Thorstensson, 2003) or play a role in controlling the spinal stability (Hodges, 1999; Hodges and Richardson, 1996; Pietrek et al., 2000). These two hypotheses were both examined in Chapter 6 while assuming fascicles of TA to be oriented in the transverse plane without having any axial compressive force penalty despite the fact that some of its fascicles especially in middle and lower regions are somewhat oblique (Urquhart et al., 2005). The values used in this study for intra-abdominal pressure (IAP), intra-abdominal area, and lever arm of intra-abdominal force all rely on the reported data in the literature for the tasks similar to the ones considered in this study.

For qualitative validation of predicted muscle activities, it was necessary to make some assumptions. First, the maximum allowable muscle stress was considered identical for all muscles (0.6 MPa). Second, the normalized passive tension-length relationship was assumed to be the same for all muscles (based on *in vivo* data of Davis et al, 2003) despite the fact that the specific architecture of each muscle could influence this relationship (Woittiez et al., 1984). Third, the effect of muscle activation level on this passive relationship (Lee and Herzog, 2002; Rassier et al., 2003) was neglected. Forth, location of muscle optimal length was assumed to be equal to their resting length in upright posture before applying gravity load. Fifth, change in muscle length was calculated with the assumption that no change occurs in length of the tendinous part of muscle and that length of this part is negligible compared with that of the active part. It must be noted that none of these assumptions have absolutely any effect on the predicted muscle forces, spinal loads and stability. In contrast, post-processing of results in order

to estimate muscle activities is influenced by each of these assumptions. It must also be emphasized that only trends of muscle activities and not their absolute magnitudes should be considered in the validation process; a fact that may further justify the fidelity of this process.

The value of 0.6 MPa taken for the maximum allowable stress in muscles lies in the mid-range of reported values (0.2-1.0 MPa) (Dagffeldt and Thorstensson, 2003; Dumas et al., 1991; Granata and Marras 1993; Guzik et al. 1996; Farfan, 1973; McGill and Norman 1986; Reid and Costigan, 1987) while a narrower range of 0.3-0.9 MPa has been estimated for trunk flexion-extension tasks (Guzik et al. 1996). This value is also used in the optimization algorithm for defining inequality conditions on the total muscle forces. However, as explained in Chapter 5 (see section 5.5.5), the used objective function in this study assigns forces to muscles which are far enough from the upper and lower limits; in other words same results would have been obtained had limits not been introduced.

The kinetic redundancy of the trunk system can be deterministically resolved if the number of prescribed kinematics data at a level reaches the number of muscles inserted into the same level. In the current study, since only sagittal rotation of vertebrae was prescribed, an optimization approach based on minimum sum of cubed muscle stresses was also used. This cost function was recognized to agree better with the EMG data (see Chapter 5). Moreover, the convergence of the nonlinear optimization solution on a global minimum was assured by solving the problem analytically using Lagrange Multiplier Method (see Appendix B).

Lines of action (LOA) of all local and global muscles were assumed to take a linear path between their insertions in upright posture with no initial strain before applying gravity load on the model. For local muscles different fascicles of ICPL, LGPL, MF, QL, IP arising from pelvis and attaching to lumbar vertebrae were

considered with distinct LOA, LA, and PCSA. For global extensor muscles i.e. ICPT and LGPT, although in reality they have several attachments to upper thorax levels (up to T2 level) but in this study since thorax is considered as a rigid body, each of global muscles was modelled with an equivalent single fascicle inserted into its attachment center at T11 (for ICPT) and T10 (for LGPT) levels.

For flexed postures, the local lumbar muscles were considered to remain straight which was in accordance with a detailed *in vivo* study suggesting these muscles not to take significantly curved orientations in flexion posture (Macintosh et al., 1993). Magnitude of the LA of local muscles under flexion tasks were in overall agreement with those reported under flexed lumbar postures (Macintosh et al., 1993). For global muscles, however, since the exact extent of reduction in LAs in flexion tasks remains unknown (Jorgensen et al., 2003; Macintosh et al., 1993; Tveit et al., 1994), an extensive investigation was carried out to study the effect of geometry of these muscles in terms of curved/straight LOA and unchanged/reduced LA with respect to the upright posture on predictions (see Chapter 7).

In the optimization algorithm, the upper limit of muscle forces was calculated using the maximum allowable active force that the muscle generates ($0.6 \times \text{PCSA}$) in its optimal length despite the fact that this maximum active force decreases as muscle elongates. It was not possible to take into account for this relationship in the optimization procedure since such relationship highly depends on the muscle activation level. It was, however, attempted to compare the predictions for muscle activities with reported data of (Davis et al., 2003) and (Nussbaum and Chaffin, 1996).

Figs. 9.8 and 9.9 show that predictions for normalized active muscle forces at different spinal levels under isometric lifting tasks while neglecting effect of IAP, abdominal coactivities, and curved LOA of muscles remain below their maximum

potential active force. One must note that these predictions are based on the five aforementioned assumptions made regarding the calculation of muscle activities.

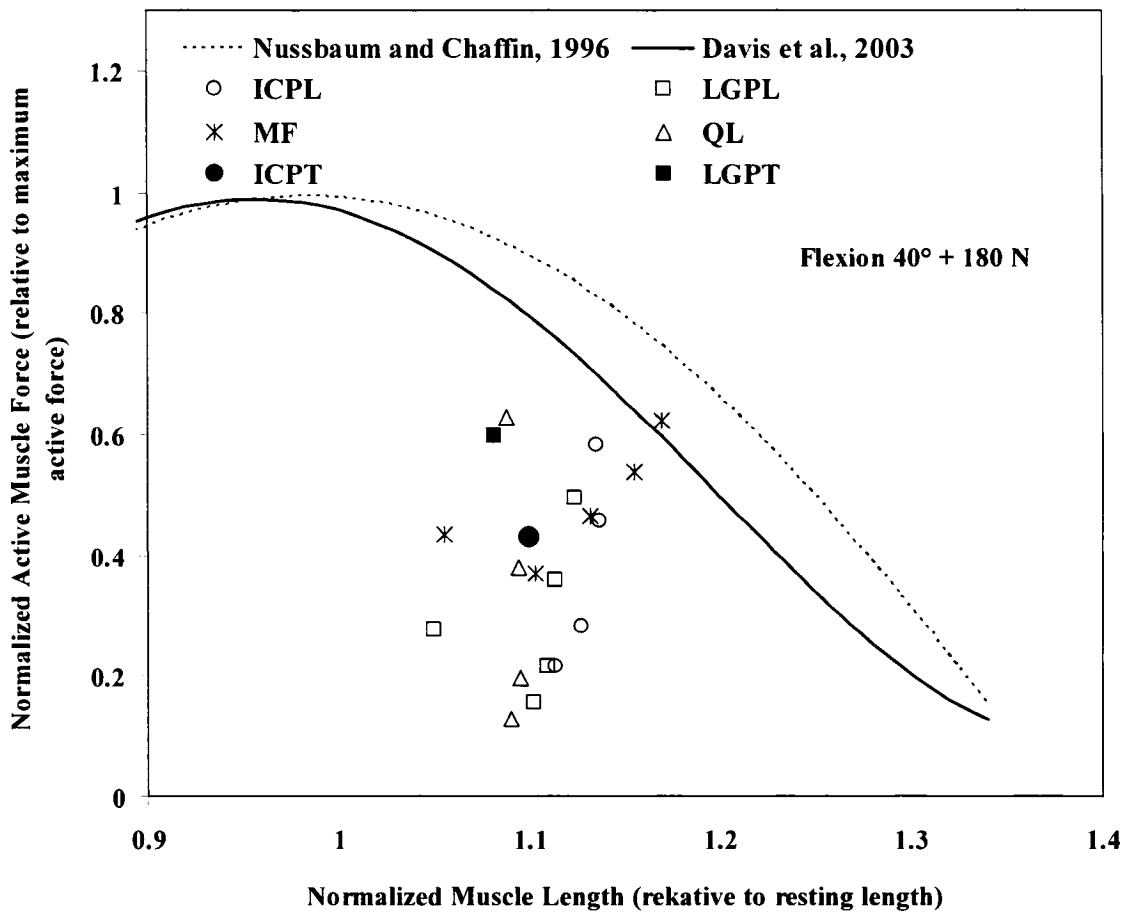


Fig. 9.8 Local and global muscle activities compared with their maximum values obtained by experimental studies under flexion of 40° plus 180 N carried in hands.

For the stability analyses, the muscle stiffness coefficient, q , was chosen the same for all muscles while a linear stiffness-force relation, rather than a nonlinear one (Cholewicki and McGill, 1995; Shadmehr and Arbib, 1992), was taken. The linear relationship between muscle stiffness and force ($K=qF/L$) was first proposed by (Bergmark, 1989) and have since been widely used by biomechanists in order to determine stability margin of the spine under different static and dynamics activities (K ,

F , L , and q in this relationship are axial muscle stiffness, active muscle force, resting length of the muscle, and a dimensionless stiffness parameter, respectively).

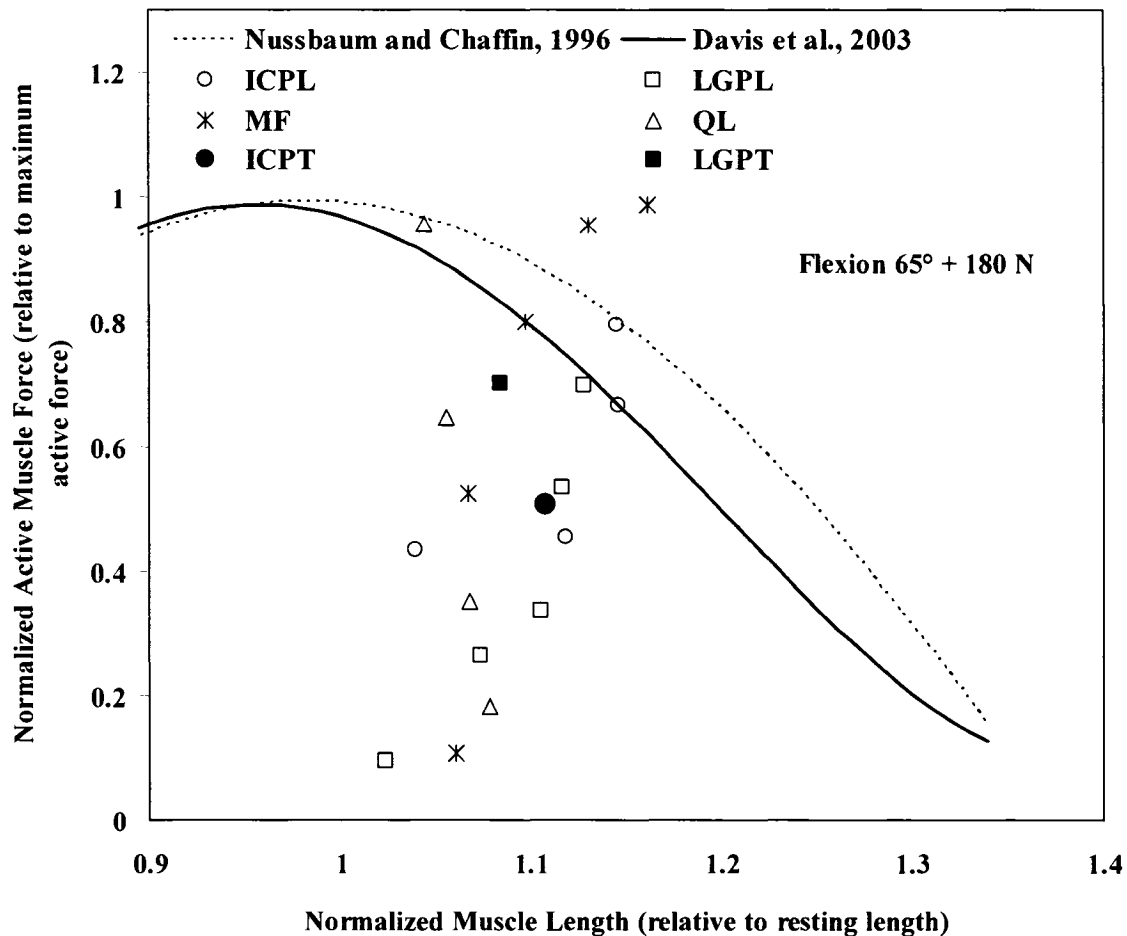


Fig. 9.9 Local and global muscle activities compared with their maximum values obtained by experimental studies under flexion of 65° plus 180 N carried in hands.

In the current study, however, F and L were considered as the total muscle force and instantaneous muscle length. In order to assess the validity of such assumption additional analyses were performed in which the muscle passive stiffness was calculated separately based directly on the slope of the passive tension-length relationship (Fig. 9.6). The total muscle stiffness was subsequently calculated as the sum of this passive stiffness and the active muscle stiffness calculated using foregoing linear relationship of

Bergmark (1989). This resulted in a more stable configuration associated with smaller q values compared with the case in which equivalent muscle stiffness for both active and passive components was considered. Due to lack of a deterministic relationship between passive tension and length of muscles, however, all stability analyses in the present study were carried out using linear relationship of Bergmark (1989). Furthermore, use of this relationship yields more conservative margin of stability for the spine.

Weight of the head and neck was considered based on anthropometric data to be 8% (58.5 N) of the total body weight (mean of ~736 N for our subjects) and was applied 1 cm anterior to the T1 level. Some anthropometric studies, however, suggest a value of as low as 6.9% of total body weight for the weight of head (Zatsiorsky et al., 1990) applied at the center of mass of head and neck. The effect of change in application point of this load from center of T1 vertebra to center of mass of head and neck on predictions for tasks performed in upright postures is negligible. For flexion tasks, however, additional analyses were run for the case with no load in hands under trunk flexion of 65° to investigate the effect of off-center application of weight of head and neck by about 14 cm (de Leva, 1996) in upward vertical direction to the center of mass of head and neck on predictions. This caused maximum axial compression and shear forces at the L5-S1 disc to increase by 4.4% and 5.9%, respectively, while maintaining the same predictions for spinal stability. Moment of gravity loads at the L5-S1 disc in upright standing posture and flexion of 65° (~9.6 Nm and 98 Nm, respectively) while weight of head and neck (58.5 N) applied at the T1 level, however, agrees with that reported in model-*in vitro* study of Serpil and Grilli (2002) (~10.2 Nm and 97.6 Nm, respectively).

9.7 Advantages of the Current Model Study

Despite earlier assumptions, the current model study offers many improvements over previous ones. One major shortcoming in many current and earlier biomechanical model studies of multi-segment spinal structure lies in the consideration of the balance of net external moments only at a single cross section (typically at lowermost lumbar

discs) rather than along the entire length of the spine (e.g., Schultz et al. 1982, McGill and Norman 1986, Cholewicki et al. 1995, Parnianpour et al. 1997, van Dieen et al. 2003, Granata et al. 2005, Marras et al. 2005). This shortcoming naturally exists in dynamic and quasi-static model studies alike while simulating either sagittally symmetric (2D) or asymmetric (3D) movements. These models have widely been employed in ergonomic applications and in injury prevention and treatment programs. It was shown in Chapter 8 of this thesis that regardless of the method used (optimization or EMG-assisted) to resolve the redundancy problem of human trunk, single-level free body diagram models yielded estimations that substantially altered depending on the level considered. Equilibrium of net moment was also grossly violated at remaining levels with the error increasing in more demanding tasks.

To overcome the foregoing shortcomings, linear finite element models along with optimization algorithms have been developed and used to evaluate muscle recruitment, internal loads, and stability margin (Dietrich et al., 1991; Gardner-Morse et al., 1995; Gardner-Morse and Stokes, 1998; Stokes and Gardner-Morse, 1995, 2001). In another study (Cholewicki and McGill, 1996), a simplified geometrical model of the spine with rotational degrees-of-freedom and nonlinear stiffness properties along with EMG-assisted optimization approach was used to evaluate muscle forces and stability margin in various tasks. The translational degrees-of-freedom at various joints and, hence, associated shear/axial equilibrium equations were totally neglected which would adversely influence predictions on muscle forces and system stability (Stokes and Gardner-Morse, 1995). Similarly, in another model (Bergmark, 1989), each vertebra was given only three degrees-of-freedom which were rotations around three axes. They also assumed that the intervertebral discs are very stiff with respect to axial and shear deformations; therefore shear/axial equilibrium equations were again totally neglected.

The effect of neglecting axial and shear deformations, i.e., neglecting translational degrees-of-freedom, at vertebral joints considered in some earlier

investigations on predictions was evaluated in our model by increasing axial and shear stiffness of all intervertebral discs by thousand times. For lifting task of 180 N with trunk flexion of 65°, both compression and shear forces increased at all levels as the discs became excessively stiff in translational degrees-of-freedom (see Table 9.3). The influence of such assumption on predicted shear forces was more significant being about 18% at the critical L5-S1 level while axial compression at different levels increased by less than 10%. Global muscle forces were also increased by nearly 10%.

Table 9.3 Predicted spinal loads while neglecting translational degrees-of-freedom (DOF) at vertebral joints compared to our reference case for lifting of 180 N with trunk flexion of 65° while considering wrapping of global muscles.

Level	Reference case		No translational DOF		Differences (%)	
	C	S*	C	S	C	S
T12-L1	1398	488	1490	524	6.6	7.4
L1-L2	1804	450	1970	502	9.2	11.6
L2-L3	2182	236	2380	280	9.1	18.7
L3-L4	2592	394	2784	475	7.4	20.4
L4-L5	3116	264	3331	357	6.9	35.1
L5-S1	3247	869	3470	1027	6.9	18.2

* M: sagittal moment at mid-height, + ve in flexion (Nm); C: local axial compression at mid-height (N); S: local shear force at disc mid-height, +ve in anterior direction (N).

The current study presented a novel kinematics-based finite element approach that simultaneously satisfies the kinematics, equilibrium and stability requirements at all levels and directions and not just the equilibrium at one level only. The proposed model allowed for the incorporation of realistic nonlinear load- and direction-dependent properties of spinal motion segments. The nonlinear stability analysis under applied forces is the gold standard in evaluating the system stability. Other complementary approaches, as used in the present study, would be the linear stability and perturbation analyses on the deformed configurations of the structure. In these latter methods, the

error involved in estimation of buckling loads is expected to diminish as the applied loads and deformed configurations approach the critical state.

Curved pathways of global muscles while taking account for the reaction forces at points of contact between muscles and vertebrae were considered for the first time in the current study. Some earlier biomechanical models (e.g. Cholewicki and McGill, 1996) report also to have considered curved pathways for extensor muscles that pass through several points at different vertebrae. These models, however, appear to have failed to account for reaction (contact) forces at these points of contact between muscles and vertebrae. These contact forces are due to changes in muscle orientation and would generate moment as well as shear/compression forces that need to be considered in associated equilibrium equations at different levels. Simulation of wrapping without the proper consideration of these contact forces at the deformed configuration of the spine is not, hence, adequate adversely affecting the accuracy of estimations.

9.8 Comparisons and Implications

9.8.1 Flexion Posture versus Upright Posture and the Effect of Load

Findings of the current study confirm suggestion of many earlier epidemiological studies in recognizing lifting as the best documented risk factor for low back disorders (Burdorf and Sorock, 1997; Damkot et al., 1984; Ferguson and Marras, 1997; Frank et al., 1996; NIOSH, 1997). When flexing forward by 65° with no load in hands axial compression and shear forces in the critical L5-S1 disc level reached 2026 N and 598 N, respectively, with wrapping of global muscles and 2332 N and 506 N, respectively, without wrapping compared to only 570 N and 190 N, respectively, in upright standing posture. This increase in axial compression and anterior-posterior shear forces by about 255% and 215%, respectively, which is solely due to upper-body gravity elucidates importance of risk of injury to the lumbar spine in such postures. The effect of optimization cost function on these relative effects is minimal since variations in

predicted axial compression and shear forces for different nonlinear cost functions whose predictions match EMG data will not be more than 11% and 9%, respectively.

When carrying 180 N in hands for flexion of 65° the predicted values for axial compression and shear forces in the critical L5-S1 disc level reached 3247 N and 869 N, respectively. These increases by about 60 % and 45 % compared to the same posture with no load in hands would decrease only by 10 % for axial compression and increase by 1.5% for shear forces had the effect of IAP (9 kPa) been introduced in calculations with no coactivity at all in abdominal muscles.

On the other hand, under 180 N load in hands, forward flexion of 65° from upright posture yields increases of more than 142% (from 1338 N to 3247 N) in axial compression and 66% (from 523 N to 869 N) in anterior-posterior shear forces. It is to be noted that considering high level of abdominal coactivities (2, 4, and 8 % in RA, EO, and IO, respectively) along with the IAP in standing posture would increase axial compression and shear forces by ~47% and 45%, respectively, while for flexion task these values would reach only 5.7% and 3%.

When flexing forward by 65° and considering wrapping of global muscles the computed total force in erector spinae (on both sides), as the sum of ICPT and LGPT muscle forces, was 716 N and 1140 N without and with 180 N in hands, respectively. This shows increases of 1332% (from 50 N) and of 149% (from 458 N) when compared to the upright standing posture, respectively. High risk of injury to extensor muscles in lifting activities involving trunk flexion, hence, becomes evident; suggesting also the vulnerability of these muscles to fatigue under similar repetitive or sustained loading conditions.

Preserving lumbar lordosis during lifting tasks would even worsen the conditions in terms of the risk of injury to the spine by increasing both spinal and muscle forces

while flexing lumbar slightly to a kyphotic posture would only slightly reduce these forces (see Table 7.1). The spinal stability is a less important issue here since the spine seems very stable under flexed postures especially if load is carried in hands. Introducing the IAP force into the model in order to consider its unloading role while assuming that the whole increase in IAP is only provided by the TA (i.e., no abdominal coactivity) would somewhat decrease axial compression; an auxiliary unloading system that is unlikely of substantial help in reducing risk of injury to the spine.

9.8.2 Comparison with Tolerant Limits

Predictions for all tasks simulated here, however, remain in the physiological limits beyond which injury may occur. Quantification of the risk of injury requires a direct comparison of the applied load on the spine with the tolerant limits of the spine. Based on *in vivo* measurements from four healthy male subjects Daggfeldt and Thorstensson (2003) proposed an average isometric maximal voluntary strength (moment about the L5-S1 disc) of about 300 Nm (± 50) under trunk flexion of 45°. The maximum sagittal moment predicted at the base of the L5-S1 disc due to external loads occurred in the current study with 180 N load in hands and 65° flexion and was about 147 Nm. For upright standing posture Daggfeldt and Thorstensson (2003) measured an average isometric maximal voluntary strength (moment about the L5-S1 disc) of about 200 Nm while our model predicted maximum value of only ~ 40 Nm at the lower node of the L5-S1 disc when carrying 180 N load (in front) in hands. Maximum isometric strength capability of the spine is a suitable factor that can provide a measure for the determination of the risk of overexertion (Parnianpour et al., 1997).

Maximum predicted axial compression occurred in flexion of 65° with 180 N load in hands with a lordotic lumbar posture at the L5-S1 disc center reaching 3943 N, 3444 N, and 3191 N with straight LOA, curved LOA with 10% reduction in LA, and curved LOA without reduction in LA, respectively (see Table 7.1). Maximum values for anterior-posterior shear force occurred with the lumbar in lordotic posture at L5/S1 disc

center being 858 N, 976 N, and 1006 N with straight LOA, curved LOA with 10% reduction in LA, and curved LOA without reduction in LA, respectively (see Table 7.1). This is consistent with findings of others that shear injury is most common at the L5-S1 joint (Mandell et al., 1989). None of these loads, however, exceeded the injury tolerant levels of lumbar segments reported in the literature (Cripton et al., 1995; McGill, 1997). Cripton et al., 1995 found the static shear tolerance of the spine to be in the neighborhood of 2000-2800 N in adult cadavers. It has been suggested by McGill (1997) that the spine is much more vulnerable to shear injury than compressive injury. The margin of safety is thought to be much larger for compressive loading since the spine may resist up to 10 kN in compression according to McGill (1997), up to 6.4 kN according to National Institute of Occupational Safety and Health (1981), and 4.4 ± 1.9 kN according to (Jager and Luttmann, 1989). These threshold values in compression and shear could, however, diminish in presence of repetitive loads and cumulative fatigue fractures of the bone (McGill, 1997). In contrast, they could be greater in professional athletes for whom shear forces of as high as 3500 N, for example, have been estimated during dead lift of 305 kg.

Maximum passive moment in the ligamentous spine occurred at L5-S1 disc level for flexion of 65° with 180 N in hands while holding a kyphotic posture; reaching about 40 Nm regardless of the LOA and LA considered for the global muscles (see Table 7.1). It has been reported that damage initiates in the ligaments when the bending moment acting on the ligamentous spine reaches 60 Nm on average (Adams et al., 1980 and Adams and Dolan, 1991; Miller et al., 1986) with the gross damage occurring at 120 Nm (Neumann et al., 1992). It has been found that ligament strains are usually within their elastic limits even for lifts involving large trunk flexion (Anderson et al., 1985).

9.8.3 Comparisons for Erector Spinae Force in Upright Posture

The predicted forces in erector spinae muscle are comparable with those of other models and *in vitro* studies. Using an *in vitro* study on seven human cadavers, Wilke at

al. (2003) predicted forces in erector spinae of 100 N in upright standing posture under gravity load of 260 N applied 200 mm cranial and 30 mm ventral to the T12-L1 disc center plus a follower load of 200 N. They included forces via cables attached into a plate fixed at the cranial end of the specimen to simulate rectus abdominus and erector spinae muscles. The muscle forces were varied until the external moment, necessary to keep the lumbar spine specimen in the desired posture, disappeared.

Using a nonlinear FE model of the lumbar spine (L1 to L5 vertebrae) while varying hip and lumbar flexion rotations in order to reach good agreement between model predictions and *in vivo* measurements for intra-discal pressure and bending moments, Rohlmann et al., 2006 found a total force of 170 N in global erector spinae muscle for upright standing postures while neglecting forces in local muscles. They approximated the stabilizing effect of local muscle forces by applying a follower load of 200 N through the lumbar spine. They considered a constant lever arm of 40 mm posterior to the center of T12-L1 disc for global extensor with straight vertical LOA while considering the gravity load as a single concentrated force of 260 N applied at 200 mm cranial and 30 mm ventral to the T12-L1 disc center (similar to that of Wilke et al., 2003). Under a constant force of 50 N in abdominal muscle (rectus abdominus, with a lever arm of 153 mm relative to the T12-L1 disc center and straight vertical LOA), total force in global erector spinae muscle increased to 310 N.

Calisse et al., 1999 using a simplified FE model of the lumbar spine in which the vertebral bodies were modeled as cuboids predicted a force in erector spinae of 250 N for upright standing posture while neglecting forces in local and abdominal muscles. Gravity load was applied at 400 mm cranial to the upper end-plate of L1 and 20 mm anterior to the center of rotation of the L2-L3 disc.

Zander et al. (2001) predicted total force of 300 N in global erector spinae when no force was considered in local muscles in upright standing posture under gravity load

of 400 N applied 400 mm cranial to the upper end-plate of L1 and 20 mm anterior to the center of rotation of the L2-L3 disc. This value, however, significantly decreased to about 40 N when a force of 5 N was considered equally in all local muscles. Our model predicted a total force of 50 N in global muscles for upright standing posture while local muscles were computed to undergo smaller forces of about 4.6 N in average. Greater force predicted in erector spinae by Wilke et al., 2003 (100 N), Calisse et al., 1999 (250 N), and Rohlmann et al., 2006 (170 N) compared to our prediction (50 N) could be due to negligence of local muscle forces in their models.

9.8.4 Comparisons for Erector Spinae Force in Flexed Posture

Calisse et al. (1999) predicted a force of 1000 N in erector spinae in forward flexion of 60° while considering an equal force of 10 N in all local muscles. Rohlmann et al. (2006) in agreement with *in vitro* study of Wilke et al. (2003) predicted a force of about 520 N in forward flexion of 30°. They did not consider local muscles in their model subjected to a follower load of 200 N passing through the lumbar spine. Depending on the assumed local muscle forces of 0, 5, and 10 N, Zander et al. (2001) predicted forces in erector spinae of about 800, 650, and 500 N, respectively, for flexion of 30°.

We predicted forces of 698 N and 949 N in global extensor muscles under flexions of 40° and 65°, respectively, while considering straight LOA for these muscles. Average force in local muscles was about 13 and 16 N in forward flexions of 40° and 65°, respectively. None of these cited previous studies have considered wrapping of global muscles. In our model and for flexion of 65° the predicted force of 949 N in global muscles decreased to 716 N (with an average force of 15 N in local muscles) when wrapping of global muscles with 10% reduction in LA was taken into account.

9.8.5 Comparisons for Predicted Spinal Compression and IDP

In section 9.5 our predictions for intra-discal pressures (IDP) as an indicator of axial compression on the disc were compared with measured *in vivo* data demonstrating a good agreement. Similarly, predictions for the axial compression acting on the lumbar discs and IDP are comparable with those of other model studies. For relaxed upright standing posture Takahashi et al. (2006), using their linear biomechanical model estimated an axial compression of 645 N at the L4-L5 disc level. This value increased to 1922 and 2305 N as lumbar spine flexed forward by 20 and 30°, respectively. Our model predicted an axial compression of 535 N at L4-L5 disc in standing posture that increased to 1862 N for lumbar flexion of 25° (trunk flexion of 40°) and further to 2319 N for lumbar flexion of 35° (trunk flexion of 65°) when straight LOA was considered for global muscles. This latest value decreased to 1900 N when considering wrapping of global muscles.

For upright standing posture Rohlmann et al., 2006 predicted an IDP of about 0.58 MPa in the L4-L5 disc using their nonlinear FE model of the lumbar spine while Calisse et al., 1999 using their simplified FE model and neglecting forces in local muscles predicted an IDP of 0.4 in the L3-L4 disc. Our model predicted IDP of 0.51 MPa and 0.48 in the L4-L5 and L3-L4 disc levels, respectively, while accounting for the axial compression-disc pressure relations in lumbar specimens (Shirazi-Adl and Drouin, 1988). When flexing forward by 60°, Calisse et al., 1999 predicted an IDP of 0.61 MPa in the L3-L4 level while assuming an equal force of 10 N in all local muscles. Our model, however, predicted a much greater value of 1.5 MPa even when wrapping of global muscles was taken into account.

9.8.6 Comparisons for Predicted Local Muscle Forces

As for the local lumbar muscles (ICPL, LGPL, QL, MF, and IP) since intra-muscular electrodes are needed to record their EMG activities, limited information is available in the literature; making comparison almost impossible. Intra-muscular EMG recordings of some of these muscles, however, have been reported by few researchers.

For instance, intra-muscular electrodes inserted into the QL muscle at the L3 vertebra level have shown an increased involvement of this muscle from upright posture to full forward flexion with no relaxation in this muscle (Andersson et al., 1996). In our model estimated average force in all four fascicles of QL muscle attached to the L1 through L4 vertebrae also increased from upright standing (~1.9 N) posture to forward flexions of 40° (~12.1 N) and 65° (~16.3 N).

Intra-muscular electrodes inserted into the ICPL muscle at the L3 vertebral level recorded greater activity in this muscle compared to the QL muscle (Andersson et al., 1996) during trunk flexion while in standing posture both ICPL and QL muscles showed very small activities; 1±1% and 1±0% of MVC for QL and ICPL, respectively. Although no relaxation was observed, activity of ICPL decreased from flexion of 90° toward full trunk flexion. Similarly, our model predicted growing activity in ICPL from upright to flexed postures. In agreement with EMG recordings (Andersson et al., 1996), greater muscle forces were predicted in all fascicles of ICPL than those in QL regardless of the task performed.

Intra-muscular electrodes inserted into the IP muscle at the L3 vertebra level recorded almost no activity regardless of the degree of lumbar flexion (Andersson et al., 1996). This observation further confirms the statement made by Bogduk et al. (1992) that only the upper fascicles of IP exerts very small moments that tend to extend the upper lumbar spine while the lower fascicles exerts very small moments that tend to flex the lower lumbar spine. In our model only the fascicle of IP which is attached to the L1 vertebra was able to generate a limited extension moment while other fascicles acted as flexor with no force assigned to them by the optimization procedure. It has been suggested that the IP muscle may play a stabilizing role rather than a moment-carrying one (Penning, 2000).

9.9 Conclusions

A novel kinematics-based finite element approach was used that simultaneously satisfied the kinematics, equilibrium and stability requirements at all levels and directions and not just the equilibrium at one level only. The proposed model allowed for the incorporation of realistic nonlinear load- and direction-dependent properties of spinal motion segments. Using single level free-body-diagram (SLFBD) models (see Chapter 8), regardless of the method used to resolve the redundancy problem and partition the net moment among muscles, i.e. optimization methods or EMG-assisted approach, the equilibrium was not satisfied simultaneously at levels other than the one used to estimate muscle forces. These findings confirmed the hypothesis made in this study on the shortcoming of SLFBD models. The heavier and more physically demanding tasks further deteriorated the results of SLFBD models. Predictions for axial compression force, however, appeared to be less sensitive to the shortcomings in SLFBD models.

9.9.1 Stabilizing Action of the Passive Spine

Ligamentous passive stiffness, which is higher during kyphotic lifts, is a very important factor in providing stability to the spine (Stokes and Gardner-Morse, 2003). Active system (Muscles) of the spine is generally considered as the main stabilizer components while our findings highlight the crucial importance of the passive components as well. When decreasing passive rotational stiffness of the spine by 10 or 30%, the stability of the spine deteriorated despite greater predicted muscle activities (see Fig. 3.7B). In contrast, increasing passive stiffness of the ligamentous spine resulted in greater stability despite smaller predicted muscle activities. The increase in stability margin despite smaller muscle activation and its deterioration despite larger muscle activation prove the important role of passive stiffness in the system stability. Reduction in passive stiffness of the ligamentous spine which can happen due to injuries and degenerations caused compensatory muscle activations which in turn could increase the risk of fatigue and injury in active/passive tissues.

9.9.2 Lumbar Posture (Lordotic vs. Kyphotic) During Lifting

The findings of the current study advocate a lumbar posture with moderate flexion (such as that in a free posture) during static lifting tasks when considering both internal spinal loads and active/passive muscle forces. This is, however, contrary to findings of some earlier studies (e.g. Delitto et al., 1987; Hart et al., 1987; McGill, 1997; McGill et al., 2000; Potvin et al., 1991; Vakos et al., 1994) while in agreement with some others (Adams and Dolan, 1995; Gracovetsky et al., 1981, 1985). From a mechanical point of view, the main argument in advocating a lordotic lumbar posture during lifting activities has been that an increase in erector spinae activities is beneficial in augmenting spinal stability and in diminishing the anterior shear force on the spine and that in lumbar kyphotic posture the subjects hang on their ligaments or the spine is without much muscular support.

Results of the present study, however, show that in lifting activities involving trunk flexion risk of injury to the spine due to system instability is of less concern compared to the risk of injury due to high muscle and spinal loads. In such tasks, due to great muscle forces and passive lumbar stiffness the spine is sufficiently stable especially when carrying load in hands. In addition, stability of the spine in kyphotic posture is as high as that in a lordotic one while imposing less axial and shear forces on the spine. Low activity of back muscles observed in kyphotic lifts does not necessarily imply that the spine is without muscular support since passive muscle forces which can not be detected by surface EMG electrodes are larger in kyphotic postures compared with lordotic ones. Besides, the ligamentous spine is much stiffer under kyphotic postures due to larger flexion of the lumbar. The beneficial role of the lumbar extensor muscles in reducing the anterior shear force in lordotic postures as suggested elsewhere (Potvin et al., 1991) does not hold true at the L5-S1 level which is subjected to the greatest shear force and, hence, risk of shear injury (see Fig. 4.8). In fact at this level, the lordotic posture, by causing much greater pelvic rotation, substantially increased the disc

inclination and, hence, the shear component of muscle forces and gravity/external loads in the anterior direction.

9.9.3 Intra-Abdominal Pressure (IAP)

As to the controversial role of IAP in unloading the spine, predictions show that the unloading action of IAP is more likely possible for lifting in forward flexed postures since not only the magnitude of IAP increases compared to the upright standing posture but the co-activity of flexor abdominal muscles decreases at the same time. Our predictions strongly suggest that in biomechanical modeling studies one should not consider IAP force while neglecting coactivity of abdominal muscles (RA, EO, and IO) (Daggfeldt and Thorstensson, 2003) or vice versa (de Looze et al., 1999). This has led one group (Daggfeldt and Thorstensson, 2003) to claim that IAP force unloads the spine by ~400 N (34-40% of total compression) during maximal back extension and another group (de Looze et al., 1999) in direct contrast to counterclaim that abdominal coactivities overload the spine by ~600 N at the L5-S1 level (12.5% of total compression) when holding 22.5 Kg at the beginning of a lift started at the knee height.

In lifting tasks while in upright standing posture, both unloading and stabilizing roles of IAP are more crucial than those in tasks involving flexed trunk postures. Given that coactivity of abdominal muscles are measured to be greater in upright standing lifting while IAP is small compared to flexed postures one can conclude that unloading role of IAP in such postures is not only almost impossible but the spine could be overloaded due to large flexor moment of abdominal muscles. It has been suggested that neglecting abdominal coactivities while predicting spinal loads in upright postures would result in an underestimation of about 47% in axial compression (Granata et al., 2005). This was in agreement with our predictions in which spinal compression increased by ~20%, 38, and 78% when considering low, intermediate, and high co-activations for abdominal muscles in presence of IAP compared to the case where no coactivity was at all considered in presence of IAP. On the other hand, the stabilizing

action of IAP, is more evident in lifting tasks in upright posture which is due to increases in both abdominal and extensor muscle activities in presence of IAP.

9.9.4 Consideration of Muscle Wrapping Phenomenon

The assumption of straight and not curved LOA for global muscles in biomechanical models simulating lifting tasks results in much greater spinal compression forces and muscle activities whereas smaller shear forces at lower levels. The spinal stability is slightly improved by the wrapping of global muscles and that despite much smaller muscle activities. The extent of reduction in the lever arm of global muscles during flexion that maybe posture dependent also influences results as such reductions substantially increase muscle forces and spinal compression. Consideration of global extensor muscles with curved paths while taking account for the wrapping contact forces and realistic lever arms is important in biomechanical analysis of lifting tasks.

9.10 Concluding Remarks

The spine and its surrounding active-passive sub-systems are much more vulnerable in lifting tasks involving trunk flexion due to substantially greater spinal and muscle forces. The stability of the trunk remains, however, of a less important concern in forward flexion tasks. Taking lordotic posture in such lifts would even worsen the conditions in terms of increasing both spinal and muscle forces; suggesting that a lift with flexed lumbar would involve less risk of injury. The IAP plays a role in unloading and stabilizing the spine in lifting tasks which are task/posture dependent. Using different nonlinear optimization cost function to share net moment of external loads would only slightly influence predictions. The presented model and methodology in this thesis guarantees satisfaction of the equilibrium equations in all directions along the entire length of the spine while yielding spinal postures in full accordance with external/gravity loads, muscle forces, and passive tissues with nonlinear properties.

9.11 Future Studies

9.11.1 Dynamics Lifting Tasks

Simulations of lifting tasks in which dynamic characteristics (inertia and damping) of the trunk are taken into account are being presently performed by our group. These studies aim to estimate muscle forces, spinal load, and system stability during various dynamic lifting tasks. In associated *in vivo* studies subjects were asked, with no instruction on lumbar posture, to perform sagittally-symmetric squat (knee bent) and stoop (knee straight) lifts with and without 180 N weight placed on a bar in front at 20 cm height from the floor. Each task lasted 4-5s and started from upright standing with no load in hands and ended again in upright standing with or without load in hands. Model predictions show that for the relatively slow lifting tasks with the lowering and lifting phases each lasting ~2s, the effect of inertia and damping was not, in general, important.

9.11.2 Relative Contribution of Individual Muscles to the Spinal Stability

In response to sudden trunk loading, patients with low back pain have shown deficiency in timing of muscle activation (Magnusson et al., 1996; Hodges and Richardson, 1999; Radebold et al., 2000). Such a corruption in motor control could lead to the loss of spine stability causing injuries to the lumbar spine (Cholewicki and McGill, 1996; Panjabi, 1992). Rehabilitation and treatment strategies are, hence, designed to improve muscles that are believed to influence spine stability (O'Sullivan, 2000; Richardson et al., 1999). One objective of future studies can, thus, be set to compare the relative contribution of various trunk muscles to lumbar spine stability during a variety of isometric/dynamic trunk activities using the Kinematics-based approach. If a muscle is found to play an important role in stabilizing the spine relative to others, rehabilitation and treatment programs needs to be so designed as to improve function of that muscle.

9.11.3 Simulation of the Flexion-Relaxation During Full Trunk Flexion

During trunk flexion from the upright posture, there is a sudden EMG silence or relaxation of the superficial erector spinae muscles, towards the end of the flexion. This phenomenon has been observed in healthy subjects and called the flexion–relaxation phenomenon (FRP). Experimental studies suggest that the FRR could clearly discriminate the patients from the healthy controls as in the subjects with low back pain the FRP is frequently absent (Kippers and Parker, 1984; Watson et al., 1997).

In order to describe the FRP several hypotheses including transfer of load from extensor muscles to passive tissues (McGill and Kipper, 1994), from superficial muscles to deeper ones (Andersson et al., 1996), or from lumbar extensors to thoracic ones (Toussaint et al., 1995) have been proposed. Manual material handling often involves full trunk flexion in which position the moment arm of upper body and carried load are maximal. Redistribution of load among active-passive components of the spine would result in changes in joint loads and alterations in the risk of injury. This underlines the necessity to improve the understanding of how the moment of external loads is offset during full trunk flexion. Undoubtedly, detailed biomechanical models of the spine such as the one used in the current work are required for more accurate prediction of spinal and muscle loads.

9.11.4 Simulation of Asymmetric Tasks

Our studies are, to date, limited to investigation of “symmetric” lifting while avoiding full trunk flexion. Combination of lifting with lateral bending and twisting (i.e., asymmetric lifting) has been identified as a frequent cause of back injury in the workplace (Hoogendoorn et al., 2000) especially when involved with full trunk flexion such as activities in construction and agriculture industries. The objective of future studies can be set, hence, to estimate muscle forces, spinal loads and system stability and, hence, risk of spinal injury under asymmetric lifts. These data are essential for improved assessment of risk of tissue injury in many industrial and athletic activities as

well as for the design of more effective prevention, treatment, and rehabilitation procedures.

9.11.5 Application of the Kinematics-Based Approach to the Cervical Spine

It would be very interesting to extend the application of the Kinematics-based approach to the human cervical spine as a frequently injured region. For this purpose, a finite element model of the whole cervical region of the spine, in which proper nonlinear properties of the passive tissues and anatomy of surrounding muscles are incorporated, must first be constructed. *In vivo* studies are required to measure kinematics of the cervical spine under different movements and head loadings such as flexion-extension and lateral bending. The same procedure, as that used in this work, would then be followed for estimation of cervical spinal loads, muscle forces, and system stability. Such knowledge is essential to assess risk of injury to the cervical spine as well as in designing effective prevention and treatment strategies.

Prevention and treatment of neck injuries due to frontal/lateral impact loading, such as those in traffic accidents, requires knowledge of neck injury mechanisms. The finite element (FE) method is suitable because it gives data on stress and strain of individual tissues that can be used to predict injuries based on tissue level criteria. The Kinematics-based approach while taking account for the dynamic characteristics of the cervical spine, loads and motions would yield accurate prediction of response and associated risk of injury.

References

Adams MA, Dolan P. 1991. A technique for quantifying bending moment acting on the lumbar spine in-vivo. *J Biomech.* 24:2. 117-26.

Adams MA, Dolan P. 1995. Recent advances in lumbar spinal mechanics and their clinical significance. *Clin Biomech.* 10:1. 3-19.

Adams MA, Dolan P, Hutton WC. 1987. Diurnal variations in the stresses on the lumbar spine. *Spine.* 12:2. 130-7.

Adams MA, Green TP, Dolan P. 1994. The strength in anterior bending of lumbar intervertebral discs. *Spine.* 19:19. 2197-203.

Adams MA, Hutton WC, Stott JRR. 1980. The resistance to flexion of the lumbar intervertebral joint. *Spine.* 5:3. 245-53.

Anderson CK, Chaffin DB, Herrin GD, Matthews LS. 1985. A biomechanical model of the lumbosacral joint during lifting activities. *J Biomech.* 18:8. 571-84.

Andersson EA, Oddsson LI, Grundstrom H, Nilsson J, Thorstensson A. 1996. EMG activities of the quadratus lumborum and erector spinae muscles during flexion-relaxation and other motor tasks. *Clin Biomech.* 11:7. 392-400.

Andersson GB. 1981. Epidemiologic aspects on low-back pain in industry. *Spine.* 6:1. 53-60.

Andersson GB, Ortengren R, Nachemson A. 1976. Quantitative studies of back loads in lifting. *Spine.* 1. 178-85.

Andersson GB, Ortengren R, Nachemson A. 1977. Intradiskal pressure, intra-abdominal pressure and myoelectric back muscle activity related to posture and loading. *Clin Orthop Relat Res.* 129. 156-64.

Arjmand N, Shirazi-Adl A., Parnianpour M. 2006. Trunk biomechanical models based on equilibrium at a single-level violate equilibrium at other levels. *Ergonomics (submitted).*

Ashton-Miller JA, Schultz AB. 1997. Biomechanics of the Human Spine. *Basic Orthopedic Biomechanics.* 2nd ed. Philadelphia: Lippincott-Raven. P. 353-393.

Bakke SN. 1931. Roentgenologische Beobachtungen über die Bewegungen der Wirbelsaule. *Acta Radiol.* 13.

Bartelink DL. 1957. The role of abdominal pressure in relieving the pressure on the lumbar intervertebral discs. *J Bone Joint Surg Br.* 39. 718-725.

Bergmark A. 1989. Stability of the lumbar spine –A study in mechanical engineering. *Acta Orthopaedica Scandinavica Supplementum.* 230. 1-54.

Bigos SJ, Spengler DM, Martin NA, Zeh J, Fisher L, Nachemson A, Wang MH. 1986. Back injuries in industry: a retrospective study. II. Injury factors. *Spine.* 11:3. 246-51.

Bogduk N, Macintosh JE. 1984 The applied anatomy of the thoracolumbar fascia. *Spine.* 9:2. 164-70.

Bogduk N, Johnson G, Spalding D. 1998. The morphology and biomechanics of latissimus dorsi. *Clin Biomech.* 13 :6. 377-385.

Bogduk N, Macintosh JE, Pearcy MJ, 1992a. A universal model of the lumbar back muscles in the upright position. *Spine.* 17:8. 897-913.

Bogduk N, Pearcy M, Hadfield G, 1992b. Anatomy and biomechanics of psoas major. *Clin Biomech.* 7. 109-119.

Bogduk, N, Twomey LT, 1987. Clinical anatomy of the lumbar spine. Churchill Livingstone, Longman Singapore Publisher, Singapore.

Bongers PM, de Winter CR, Kompier MAJ, Hildebrandt VH. 1993. Psychosocial factors at work and musculoskeletal disease. *Scand J Work Environ Health.* 19. 297-312.

Broberg KB. 1983. On the mechanical behaviour of intervertebral discs. *Spine.* 8:2.151-65.

Burdorf A, Sorock G. 1997. Positive and negative evidence of risk factors for back disorders. *Scand J Work Environ Health.* 23:4. 243-56.

Calisse J, Rohlmann A, Bergmann G. 1999. Estimation of trunk muscle forces using the finite element method and in vivo loads measured by telemeterized internal spinal fixation devices. *J Biomech.* 32:7. 727-31.

Canadian Task Force on Preventive Health Care. CMAJ. 2003 Aug 5; 169:3. 213-4.

Chaffin DB. 1969. A computerized biomechanical model-development of and use in studying gross body actions. *J Biomech.* 2:4. 429-41.

Cholewicki J, McGill SM. 1994. EMG assisted optimization: a hybrid approach for estimating muscle forces in an indeterminate biomechanical model. *J Biomech.* 27:10. 1287-9.

Cholewicki J, McGill SM. 1995. Relationship between muscle force and stiffness in the whole mammalian muscle: a simulation study. *J Biomech Eng.* 117:3. 339-42.

Cholewicki J, McGill SM, Norman RW. 1995. Comparison of muscle forces and joint load from an optimization and EMG assisted lumbar spine model: towards development of a hybrid approach. *J Biomech.* 28:3. 321-31.

Cholewicki J, McGill SM. 1996. Mechanical stability of the in vivo lumbar spine: Implications for injury and chronic low back pain. *Clin Biomech.* 11:1. 1-15.

Cholewicki J, Juluru K, McGill SM. 1999a. Intra-abdominal pressure mechanism for stabilizing the lumbar spine. *J Biomech.* 32:1. 13-7.

Cholewicki J, Juluru K, Radebold A, Panjabi MM, McGill SM. 1999b. Lumbar spine stability can be augmented with an abdominal belt and/or increased intra-abdominal pressure. *European Spine Journal.* 8:5. 388-95.

Cholewicki J, Ivancic PC, Radebold A. 2002. Can increased intra-abdominal pressure in humans be decoupled from trunk muscle co-contraction during steady state isometric exertions? *Eur J Appl Physiol.* 87:2. 127-33.

Cripton P, Berlemen U, Visarino H, Begeman PC, Nolte LP, Prasad P. 1995. Response of the lumbar spine due to shear loading. Proc. Symp. On Injury Prevention through Biomechanics. 4-5 May 1995, Wayne State University.

Crisco III JJ, Panjabi MM. 1991. The intersegmental and multisegmental muscles of the lumbar spine -A biomechanical model comparing lateral stabilizing potential. *Spine.* 16:7. 793-799.

Crisco JJ, Panjabi MM. 1992. Euler stability of the human ligamentous lumbar spine. Part I: Theory. *Clin Biomech.* 7. 19-26.

Crisco JJ, Panjabi MM, Yamamoto I, Oxland TR. 1992. Euler stability of the human ligamentous lumbar spine, Part II: Experiment. *Clin Biomech.* 7. 27-32.

Crowninshield RD, Brand RA. 1981. A physiologically based criterion of muscle force prediction in locomotion. *J Biomech.* 14:11. 793-801.

Daggfeldt K, Thorstensson A. 2003. The mechanics of back-extensor torque production about the lumbar spine. *J Biomech.* 36:6. 815-25.

Daggfeldt K, Thorstensson A. 2004. Author's response to: All abdominal muscles must be considered when evaluating the intra-abdominal pressure contribution to trunk extensor moment and spinal loading. *J Biomech.* 37:6. 955-6.

Damkot DK, Pope MH, Lord J, Frymoyer JW. 1984. The relationship between work history, work environment and low-back pain in men. *Spine.* 9:4. 395-9.

Davis PR. 1981. The use of intra-abdominal pressure in evaluating stresses on the lumbar spine. *Spine.* 6:1. 90-2.

Davis JR, Mirka GA. 2000. Transverse-contour modeling of trunk muscle-distributed forces and spinal loads during lifting and twisting. *Spine.* 25:2. 180-189.

Davis J, Kaufman KR, Lieber RL. 2003. Correlation between active and passive isometric force and intramuscular pressure in the isolated rabbit tibialis anterior muscle. *J Biomech.* 36:4. 505-12.

de Looze MP, Groen H, Horemans H, Kingma I, van Dieen JH. 1999. Abdominal muscles contribute in a minor way to peak spinal compression in lifting. *J Biomech.* 32:7. 655-62.

de Looze MP, Visser B, Houting I, van Rooy MA, van Dieen JH, Toussaint HM. 1996. Weight and frequency effect on spinal loading in a bricklaying task. *J Biomech.* 29:11. 1425-33.

de Leva P. 1996. Adjustments to Zatsiorsky-Seluyanov's segment inertia parameters. *J Biomech.* 29:9. 1223-30.

Delitto RS, Rose SJ, Apts DW. 1987. Electromyographic analysis of two techniques for squat lifting. *Phys Ther.* 67:9. 1329-34.

Deng YC, Goldsmith W. 1987. Response of a human head/neck/upper-torso replica to dynamic loading II. Analytical/numerical model. *J Biomech.* 20:5. 487-97.

Dietrich M, Kedzior K, Zagajek T. 1991. A biomechanical model of the human spinal system. *Proceedings of the Institution of Mechanical Engineers. Part H,* 205 (1), 19-26.

Dumas GA, Poulin MJ, Roy B, Gagnon M, Jovanovic M. 1991. Orientation and moment arms of some trunk muscles. *Spine.* 16:3. 293-303.

El-Rich M, Shirazi-Adl A, Arjmand N. 2004. Muscle activity, internal loads and stability of the human spine in standing postures: combined model-in vivo studies. *Spine.* 29:23. 2633-42.

El-Rich M, Shirazi-Adl A. 2005. Effect of load position on muscle forces, internal loads and stability of the human spine in upright postures. *Comput Methods Biomed Engin.* 8:6. 359-68.

Esola MA, McClure PW, Fitzgerald GK, Siegler S. 1996. Analysis of lumbar spine and hip motion during forward bending in subjects with and without a history of low back pain. *Spine.* 21:1. 71-8.

Essendrop M, Schibye B. 2004. Intra-abdominal pressure and activation of abdominal muscles in highly trained participants during sudden heavy trunk loadings. *Spine.* 29:21. 2445-51.

Essendrop M, Andersen TB, Schibye B. 2002. Increase in spinal stability obtained at levels of intra-abdominal pressure and back muscle activity realistic to work situations. *Appl Ergon.* 33:5. 471-6.

Farfan HF. 1973. Mechanical disorders of the low back. Philadelphia: Lea and Febiger. P. 182-189.

Ferguson SA, Marras WS. 1997. A literature review of low back disorder surveillance measures and risk factors. *Clin Biomech.* 12:4. 211-226.

Frank JW, Kerr MS, Brooker AS, DeMaio SE, Maetzel A, Shannon HS, Sullivan TJ, Norman RW, Wells RP. 1996. Disability resulting from occupational low back

pain. Part I: What do we know about primary prevention? A review of the scientific evidence on prevention before disability begins. *Spine*. 21:24. 2908-17.

Frobin W, Brinckmann P, Leivseth G, Biggemann M, Reikeras O. 1996. Precision measurement of segmental motion from flexion-extension radiographs of the lumbar spine. *Clin Biomech*. 11:8. 457-465.

Frymoyer J. 1996. The magnitude of the problem. In *The Lumbar Spine*. Philadelphia: WB Saunders. P. 8-15

Frymoyer JW, Pope MH, Clements JH, Wilder DG, MacPherson B, Ashikaga T. 1983. Risk factors in low-back pain. An epidemiological survey. *J Bone Joint Surg Am*. 65:2. 213-8.

Gagnon D, Lariviere C, Loisel P. 2001. Comparative ability of EMG, optimization, and hybrid modelling approaches to predict trunk muscle forces and lumbar spine loading during dynamic sagittal plane lifting. *Clin Biomech*. 16:5. 359-72.

Gardner-Morse M, Stokes IAF, Laible JP. 1995. Role of muscles in lumbar spine stability in maximum extension efforts. *Journal of Orthopaedic Research*. 13:5. 802-808.

Gardner-Morse M, Stokes IAF. 1998. The effects of abdominal muscle coactivation on lumbar spine stability. *Spine*. 23:1. 86-92.

Gardner-Morse MG, Stokes IA. 2003. Physiological axial compressive preloads increase motion segment stiffness, linearity and hysteresis in all six degrees of freedom for small displacements about the neutral posture. *J Orthop Res*. 21:3. 547-52.

Garg A, Herrin GD. 1979. Stoop or squat, a biomechanical and metabolical evaluation. *A.I.I.E. Transactions*. 11. 293-302.

Gracovetsky S. 1989. Potential of lumbodorsal fascia forces to generate back extension moments during squat lifts. *J Biomed Eng*. 11:2. 172-5.

Gracovetsky S, Farfan HF, and Lamy C. 1981. The mechanism of the lumbar spine. *Spine*. 6:3. 249-62.

Gracovetsky S. 1988. *The Spinal Engine*. New York: Springer-Verlag.

Gracovetsky S, Farfan H, Helleur C. 1985. The abdominal mechanism. *Spine*. 10:4. 317-24.

Granata KP, Lee PE, Franklin TC. 2005. Co-contraction recruitment and spinal load during isometric trunk flexion and extension. *Clin Biomech*. 20:10. 1029-37.

Granata KP, Marras WS. 1993. An EMG-assisted model of loads on the lumbar spine during asymmetric trunk extensions. *J Biomech*. 26:12. 1429-38.

Granata KP, Orishimo KF. 2001. Response of trunk muscle coactivation to changes in spinal stability. *J Biomech*. 34:9. 1117-23.

Granata KP, Sanford AH. 2000. Lumbar-pelvic coordination is influenced by lifting task parameters. *Spine*. 25:11. 1413-8.

Guzik DC, Keller TS, Szpalski M, Park JH, Spengler DM. 1996. A biomechanical model of the lumbar spine during upright isometric flexion, extension, and lateral bending. *Spine*. 21:4. 427-33.

Hagen KB, Hallen J, Harms-Ringdahl K. 1993. Physiological and subjective responses to maximal repetitive lifting employing stoop and squat technique. *Eur J Appl Physiol Occup Physiol*. 67:4. 291-7.

Hagins M, Pietrek M, Sheikhzadeh A, Nordin M, Axen K. 2004. The effects of breath control on intra-abdominal pressure during lifting tasks. *Spine*. 29:4. 464-9.

Han JS, Ahn JY, Goel VK, Takeuchi R, McGowan D. 1992. CT-based geometric data of human spine musculature. Part I. Japanese patients with chronic low back pain. *J Spinal Disord*. 5:4. 448-58.

Harman EA, Rosenstein RM, Frykman PN, Nigro GA. 1989. Effects of a belt on intra-abdominal pressure during weight lifting. *Med Sci Sports Exerc*. 21:2. 186-90.

Hart DL, Stobbe TJ, Jaraiedi M. 1987. Effect of lumbar posture on lifting. *Spine*. 12:2. 138-45.

Hayes MA, Howard TC, Gruel CR, Kopta JA. 1989. Roentgenographic evaluation of lumbar spine flexion-extension in asymptomatic individuals. *Spine*. 14:3. 327-31.

Herzog W. 1992. Sensitivity of muscle force estimations to changes in muscle input parameters using nonlinear optimization approaches. *J Biomech Eng.* 114:2. 267-8.

Herzog W, Leonard TR. 1991. Validation of optimization models that estimate the forces exerted by synergistic muscles. *J Biomech.* 24:1. 31-9.

Hodges PW. 1999. Is there a role for transversus abdominis in lumbo-pelvic stability? *Manual Therapy.* 4:2. 74-86.

Hodges P, Cresswell A, Thorstensson A. 1999. Preparatory trunk motion accompanies rapid upper limb movement. *Exp. Brain Res.* 124:1. 69-79.

Hodges PW, Cresswell AG, Daggfeldt K, Thorstensson A. 2001. In vivo measurement of the effect of intra-abdominal pressure on the human spine. *J Biomech.* 34:3. 347-53.

Hodges PW, Richardson CA. 1996. Inefficient muscular stabilization of the lumbar spine associated with low back pain. A motor control evaluation of transversus abdominis. *Spine.* 21:22. 2640-50.

Hodges PW, Richardson CA. 1999. Altered trunk muscle recruitment in people with low back pain with upper limb movement at different speeds. *Arch Phys Med Rehabil.* 80:9. 1005-12.

Hoogendoorn WE, Bongers PM, de Vet HC, Douwes M, Koes BW, Miedema MC, Ariens GA, Bouter LM. 2000. Flexion and rotation of the trunk and lifting at work are risk factors for low back pain: results of a prospective cohort study. *Spine.* 25:23. 3087-92.

Hsiang SM, Brogmus GE, Courtney TK. 1997. Low Back Pain (LBP) and Lifting Technique: A Review. *Int J Ind Ergonomics.* 19. 59-74.

Hughes RE. 1995. Choice of optimization models for predicting spinal forces in a three-dimensional analysis of heavy work. *Ergonomics.* 38. 2476-2484.

Hughes RE, Bean JC, Chaffin DB. 1995. Evaluating the effect of co-contraction in optimization models. *J Biomech.* 28:7. 875-8.

Hughes RE, Chaffin DB, Lavender SA, Andersson GB. 1994. Evaluation of muscle force prediction models of the lumbar trunk using surface electromyography. *J Orthop Res.* 12:5. 689-98.

Jager M, Luttmann A. 1989. Biomechanical analysis and assessment of lumbar stress during load lifting using a dynamic 19-segment human model. *Ergonomics.* 32:1. 93-112.

Janovic J, Ashton-Miller JA, Schultz AB. 1991. Large compressive preloads decrease lumbar motion segment flexibility. *J Orthop Res.* 9:2. 228-36.

Jorgensen MJ, Marras WS, Granata KP, Wiand JW. 2001. MRI-derived moment-arms of the female and male spine loading muscles. *Clin Biomech.* 16:3. 182-93.

Jorgensen MJ, Marras WS, Gupta P, Waters TR. 2003. Effect of torso flexion on the lumbar torso extensor muscle sagittal plane moment arms. *The Spine J.* 3:5. 363-9.

Kelsey JL, Githens PB, White AA 3rd, Holford TR, Walter SD, O'Connor T, Ostfeld AM, Weil U, Southwick WO, Calogero JA. 1984. An epidemiologic study of lifting and twisting on the job and risk for acute prolapsed lumbar intervertebral disc. *J Orthop Res.* 2:1. 61-6.

Kerr MS, Frank JW, Shannon HS, Norman RW, Wells RP, Neumann WP, Bombardier C. 2001. Ontario Universities Back Pain Study Group. Biomechanical and psychosocial risk factors for low back pain at work. *Am J Public Health.* 91:7. 1069-75.

Kiefer A, Shirazi-Adl A, Parnianpour M. 1997. Stability of the human spine in neutral postures. *Eur Spine J.* 6:1. 45-53.

King-liu YK, Wickstrom JK. 1973. Estimation of the inertia property distribution of the human torso from segmented cadaveric data. In *Perspectives Biomed Eng.* McMillan New York, 203-213.

Kippers V, Parker AW. 1984. Posture related to myoelectric silence of erector spinae during trunk flexion. *Spine.* 9. 740-745.

Krag MH, Byrne KB, Gilbertson LG, Haugh LD. 1986. Failure of intra-abdominal pressurization to reduce erector spinae loads during lifting tasks. *Proceedings of the*

10th Annual Congress of the North American Society of Biomechanics. Montreal, Canada.

Lander JE, Hundley JR, Simonton RL. 1992. The effectiveness of weight-belts during multiple repetitions of the squat exercise. *Med Sci Sports Exerc.* 24:5. 603-9.

Lee YH, Chiou WK, Chen WJ, Lee MY, Lin YH. 1995. Predictive model of intersegmental mobility of lumbar spine in the sagittal plane from skin markers. *Clin Biomech.* 10:8. 413-420.

Lee HD, Herzog W. 2002. Force enhancement following muscle stretch of electrically stimulated and voluntarily activated human adductor pollicis. *Journal of Physiology.* 545. 321-30.

Lee RY, Wong TK. 2002. Relationship between the movements of the lumbar spine and hip. *Hum Mov Sci.* 21:4. 481-94.

Leskinen TP, Stalhammar HR, Kuorinka IA, Troup JD. 1983. The effect of inertial factors on spinal stress when lifting. *Eng Med.* 12:2. 87-9.

Lewandowski A. 1982. Issues in model validation, *Angewandte Systemanalyse* 3: 2-11.

Li Y, McClure PW, Pratt N. 1996 The effect of hamstring muscle stretching on standing posture and on lumbar and hip motions during forward bending. *Phys Ther.* 76:8, 836-49.

Lin RM, Yu CY, Chang ZJ, Lee CC, Su FC. 1994. Flexion-extension rhythm in the lumbosacral spine. *Spine.* 19:19. 2204-9.

Lucas D, Bresler B. 1961. Stability of the ligamentous spine. In: Technical report no. 40. Biomechanics Laboratory, University of California, Berkeley.

Macintosh JE, Bogduk N, Gracovetsky S. 1987. The biomechanics of the thoracolumbar fascia. *Clin Biomech.* 2. 78-83.

Macintosh JE, Bogduk N. 1991. The attachments of the lumbar erector spinae. *Spine.* 16. 783-792.

Macintosh JE, Bogduk N, Pearcy MJ. 1993. The effects of flexion on the geometry and actions of the lumbar erector spinae. *Spine.* 18. 884-93.

Magnusson ML, Aleksiev A, Wilder DG, Pope MH, Spratt K, Lee SH, et al. 1996. Unexpected load and asymmetric posture as etiologic factors in low back pain. *Eur Spine J.* 5:1. 23–35.

Mandell P, Lipton MH, Bernstein J, et al. 1989. Low back pain. An Historical and Contemporary Overview of the Occupational, Medical, and Psychological Issues of Chronic Pain. Thorofare, New Jersey: SLACK, Inc. P. 219.

Marras WS, King AI, Joynt RL. 1984. Measurements of loads on the lumbar spine under isometric and isokinetic conditions. *Spine.* 9. 176–88.

Marras WS, Granata KP. 1997. The development of an EMG-assisted model to assess spine loading during whole-body free-dynamic lifting. *Journal of Electromyography and Kinesiology.* 7. 259-268.

Marras WS, Lavender SA, Leurgans SE, Fathallah FA, Ferguson SA, Allread WG, Rajulu SL. 1995. Biomechanical risk factors for occupationally related low back disorders. *Ergonomics.* 38:2. 377-410.

Marras WS, Mirka GA. 1996 Intra-abdominal pressure during trunk extension motions. *Clin Biomech.* 11. 267–74.

Marras WS, Parakkat J, Chany AM, Yang G, Burr D, Lavender SA. 2005. Spine loading as a function of lift frequency, exposure duration, and work experience. *Clin Biomech.* (in press).

McClure PW, Esola M, Schreier R, Siegler S. 1997. Kinematic analysis of lumbar and hip motion while rising from a forward, flexed position in patients with and without a history of low back pain. *Spine.* 22:5. 552-8.

McCowin PR, Borenstein D, Wiesel SW. 1991. The current approach to the medical diagnosis of low back pain. *Orthop Clin North Am.* 22:2. 315-25.

McCully KK, Faulkner JA. 1983. Length-tension relationship of mammalian diaphragm muscles. *J Appl Physiol.* 54:6. 1681-6.

McGill SM. 1991. Electromyographic activity of the abdominal and low back musculature during the generation of isometric and dynamic axial trunk torque: Implications for lumbar mechanics. *Journal of Orthopaedic Research.* 9. 91-103.

McGill SM. 1997. The biomechanics of low back injury: implications on current practice in industry and the clinic. *J Biomech.* 30. 465-75.

McGill SM. 2002. Low Back Disorders, Evidence-Based Prevention and Rehabilitation. 1st ed. Human Kinetics Publishers.

McGill SM, Hughson RL, Parks K. 2000. Changes in lumbar lordosis modify the role of the extensor muscles. *Clin Biomech.* 15. 777-80.

McGill SM, Kippers V. 1994. Transfer of loads between lumbar tissues during the flexion-relaxation phenomenon. *Spine.* 19. 2190-96.

McGill SM, Norman RW. 1986. Partitioning of the L4-L5 dynamic moment into disc, ligamentous, and muscular components during lifting. *Spine.* 11. 666-78.

McGill SM, van Wijk MJ, Axler CT, Gletsu M. 1996a. Studies of spinal shrinkage to evaluate low-back loading in the workplace. *Ergonomics.* 39. 92-102.

McGill S, Juker D, Kropf P. 1996b. Appropriately placed surface EMG electrodes reflect deep muscle activity (psoas, quadratus lumborum, abdominal wall) in the lumbar spine. *J Biomech.* 29:11. 1503-7.

McGill SM, Norman RW. 1987. Reassessment of the role of intra-abdominal pressure in spinal compression. *Ergonomics.* 30. 1565-88.

McGill SM, Norman RW. 1988. Potential of lumbodorsal fascia forces to generate back extension moments during squat lifts. *J Biomed Eng.* 10:4. 312-8.

McGill SM, Sharratt MT. 1990. Relationship between intra-abdominal pressure and trunk EMG. *Clin Biomech.* 5. 59-67.

McGill SM, Norman RW, Sharratt MT. 1990. The effect of an abdominal belt on trunk muscle activity and intra-abdominal pressure during squat lifts. *Ergonomics.* 33. 147-60.

Miller JA, Schultz AB, Warwick DN, Spencer DL. 1986. Mechanical properties of lumbar spine motion segments under large loads. *J Biomech.* 19:1. 79-84.

Mirka G, Kelaher D, Baker A, Harrison A, Davis J. 1997. Selective activation of the external oblique musculature during axial torque production. *Clin. Biomech.* 12. 172-180.

Morris J, Lucas DB, Bresler B. 1961. Role of the trunk in stability of the spine. *J Bone Joint Surg.* 43A. 327-351

Moseley GL, Hodges PW, Gandevia SC. 2002. Deep and superficial fibers of the lumbar multifidus muscle are differentially active during voluntary arm movements. *Spine.* 27:2. E29-36.

Nachemson A. 1981. Disc pressure measurements. *Spine* 6. 93-97.

Nachemson AL. 1992. Newest knowledge of low back pain. A critical look. *Clin Orthop Relat Res.* 279. 8-20.

Nachemson AL, Andersson GBJ, Schultz AB. 1986. Valsalva maneuver biomechanics. Effects on lumbar trunk loads of elevated intraabdominal pressures. *Spine.* 11. 476-479.

Nachemson A, Elfstrom G. 1970. Intravital dynamic pressure measurements in lumbar discs. A study of common movements, maneuvers and exercises. *Scand J Rehabil Med Suppl.* 1. 1-40.

National Institute for Occupational Safety and Health (NIOSH) 1981. A work practices guide for manual lifting. Cincinnati, Ohio, U.S. Department of Health and Human Services, P. 30-43 (Technical report no. 81-122).

National Institute for Occupational Safety and Health (NIOSH) 1997. Musculoskeletal disorders and workplace factors. U.S. Dept. of Health and Human Services.

Neumann P, Osvalder AL, Nordwall A, Lovsund P, Hansson T. 1992. The mechanism of initial flexion-distraction injury in the lumbar spine. *Spine.* 17:9. 1083-90.

Nussbaum MA, Chaffin DB. 1996. Development and evaluation of a scalable and deformable geometric model of the human torso. *Clin Biomech.* 11:1. 25-34.

Nussbaum MA, Chaffin DB, Rechtien CJ. 1995. Muscle lines-of-action affect predicted forces in optimization-based spine muscle modeling. *J Biomech.* 28:4. 401-9.

Oreskes N, Shrader-Frechette K, Belitz K. 1994. Verification, validation, and confirmation of numerical models in the earth sciences. *Science.* 263. 641-646.

O'Sullivan PB. 2000. Lumbar segmental instability: clinical presentation and specific stabilizing exercise management. *Man Ther.* 5. 2-12.

O'Sullivan PB, Grahamslaw KM, Kendell M, Lapenskie SC, Moller NE, Richards KV. 2002. The effect of different standing and sitting postures on trunk muscle activity in a pain-free population. *Spine*. 27. 1238-1244.

Oxland T, Lin RM, Panjabi M. 1992. Three-dimensional mechanical properties of the thoracolumbar junction. *Journal of Orthopaedic Research*. 10. 573-580.

Panjabi MM. 1992a. The stabilizing system of the spine. Part I. Function, dysfunction, adaptation, and enhancement. *J Spinal Disord*. 5:4. 383-9.

Panjabi MM. 1992b. The stabilizing system of the spine. Part II. Neutral zone and instability hypothesis. *J Spinal Disord*. 5:4. 390-6.

Panjabi MM. 2003. Clinical spinal instability and low back pain. *J Electromyogr Kinesiol*. 13:4. 371-9.

Panjabi M, Abumi K, Duranceau J, Oxland T. 1989. Spinal stability and intersegmental muscle forces. A biomechanical model. *Spine*. 14:2. 194-200.

Panjabi MM, Takata K, Goel V, Federico D, Oxland T, Duranceau J, Krag M. 1991. Thoracic human vertebrae. Quantitative three-dimensional anatomy. *Spine*. 16. 888-901.

Panjabi MM, White AA 3rd. 1980. Basic biomechanics of the spine. *Neurosurgery*. 7:1. 76-93.

Parnianpour M, Wang JL, Shirazi-Adl A, Sparto P, Wilke HJ. 1997. The effect of variations in trunk models in predicting muscle strength and spinal loads. *Journal of Musculoskeletal Research*. 1. 55-69.

Patwardhan AG, Havey RM, Meade KP, Lee B, Dunlap B. 1999. A follower load increases the load-carrying capacity of the lumbar spine in compression. *Spine*. 24:10. 1003-9.

Patwardhan AG, Lee B, Meade KP. 2001. Frontal plane response of the lumbar spine subjected to a follower load- role of muscles. *J Biomech Eng*. 123. 212-7.

Patwardhan AG, Havey RM, Carandang G, Simonds J, Voronov LI, Ghanayem AJ, Meade KP, Gavin TM, Paxinos O. 2003. Effect of compressive follower preload on

the flexion-extension response of the human lumbar spine. *Journal of Orthopaedic Research*. 21:3. 540-6.

Pearsall DJ. 1994. Segmental inertial properties of the human trunk as determined from computer tomography and magnetic resonance imagery. PhD thesis. Queen's University, Kingston, Ontario.

Penning L. 2000. Psoas muscle and lumbar spine stability: a concept uniting existing controversies. Critical review and hypothesis. *Eur Spine J*. 9:6. 577-85.

Pietrek M, Sheikhzadeh A, Nordin M, Hagins M. 2000. Biomechanical modeling of intra-abdominal pressure generation should include the transversus abdominis. *J Biomech*. 33: 787-790.

Pop DG. 2001. Analyse non linéaire par éléments finis du système actif passif de la colonne vertébrale humaine. M.Sc.A. Dissertation. Génie mécanique, École Polytechnique, Montréal, Québec.

Porter JL, Wilkinson A. 1997. Lumbar-Hip Flexion Motion: A Comparative Study Between Asymptomatic and Chronic Low Back Pain in 18- to 36-year-old Men. *Spine*. 22:13. 1508-1514.

Porterfield, JA, DeRosa, C, 1998. Mechanical low back pain. 2nd edition, W.B. Saunders Company, Philadelphia.

Potvin JR, McGill SM, Norman RW. 1991. Trunk muscle and lumbar ligament contributions to dynamic lifts with varying degrees of trunk flexion. *Spine*. 16. 1099-107.

Praemer A, Furner S, Rice DP. 1992. Musculoskeletal Conditions in the United States. Park Ridge, III: American Academy of Orthopaedic Surgeons, 23-33

Prilutsky BI, Isaka T, Albrecht AM, Gregor RJ. 1998. Is coordination of two-joint leg muscles during load lifting consistent with the strategy of minimum fatigue? *J Biomech*. 31. 1025-34.

Radebold A, Cholewicki J, Panjabi MM, Patel TC. 2000. Muscle response pattern to sudden trunk loading in healthy individuals and in patients with chronic low back pain. *Spine*. 25. 947-54.

Rassier DE, Herzog W, Wakeling J, Syme DA. 2003. Stretch-induced, steady-state force enhancement in single skeletal muscle fibers exceeds the isometric force at optimum fiber length. *J Biomech.* 36:9. 1309-16.

Reeves NP, Cholewicki J. 2003. Modeling the human lumbar spine for assessing spinal loads, stability, and risk of injury. *Crit Rev Biomed Eng.* 31. 73-139.

Reid JG, Costigan PA. 1987. Trunk muscle balance and muscular force. *Spine.* 12:8. 783-6.

Richardson C, Jull G, Hodges P, Hides J. 1999. Therapeutic exercise for spinal segmental stabilization in low back pain. Scientific basis and clinical approach. London: Churchill Livingstone.

Rohlmann A, Bauer L, Zander T, Bergmann G, Wilke HJ. 2006. Determination of trunk muscle forces for flexion and extension by using a validated finite element model of the lumbar spine and measured in vivo data. *J Biomech.* 39:6. 981-9.

Sato K, Kikuchi S, Yonezawa T. 1999. In vivo intradiscal pressure measurement in healthy individuals and in patients with ongoing back problems. *Spine.* 24:23. 2468-74.

Schultz A, Andersson G, Ortengren R, Haderspeck K, Nachemson A. 1982. Loads on the lumbar spine. Validation of a biomechanical analysis by measurements of intradiscal pressures and myoelectric signals. *J Bone Joint Surg Am.* 64:5. 713-20.

Schultz A, Andersson G, Ortengren R, Haderspeck K., Ortengren, R., Nordin, M. and Bjork, R. 1982, Analysis and measurement of lumbar trunk loads in tasks involving bends and twists. *J Biomech.* 15. 669-75.

Seireg A, Arvikar RJ. 1973. A mathematical model for evaluation of forces in lower extremities of the musculo-skeletal system. *J Biomech.* 6:3. 313-26.

Serpil Acar B, Grilli SL. 2002. Distributed body weight over the whole spine for improved inference in spine modelling. *Comput Methods Biomed Engin.* 5:1. 81-9.

Shadmehr R, Arbib MA. 1992. A mathematical analysis of the force-stiffness characteristics of muscles in control of a single joint system. *Biological Cybernetics*. 66. 463-477.

Shirazi-Adl A. 1994. Analysis of the role of bone compliance on mechanics of a lumbar motion segment. *Journal of Biomechanical Engineering*. 116. 408-412.

Shirazi-Adl A, Drouin G. 1988. Nonlinear gross response analysis of a lumbar motion segment in combined sagittal loadings. *Journal of Biomechanical Engineering*. 110. 216-222.

Shirazi-Adl A, Parnianpour M. 1993. Nonlinear response analysis of the human ligamentous lumbar spine in compression. On mechanisms affecting the postural stability. *Spine*. 18:1. 147-58.

Shirazi-Adl A, Parnianpour M. 1996. Stabilizing role of moments and pelvic rotation on the human spine in compression. *J Biomech Eng*. 118:1. 26-31.

Shirazi-Adl A, Parnianpour M. 2001. Finite element model studies in lumbar spine biomechanics. *Computer Techniques and Computational Methods in Biomechanics*. New York: CRC press. P. 1-36.

Shirazi-Adl A, Sadouk S, Parnianpour M, Pop D, El-Rich M. 2002. Muscle force evaluation and the role of posture in human lumbar spine under compression. *European Spine Journal*. 11. 519-526.

Shirazi-Adl A, El-Rich M, Pop DG, Parnianpour M. 2005. Spinal Muscle forces, internal loads and stability in standing under various postures and loads: applications of kinematics-based algorithm. *Eur Spine J*. 14:4. 381-92.

Shirazi-Adl A. 2006. Analysis of large compression loads on lumbar spine in flexion and in torsion using a novel wrapping element. *J Biomech*. 39:2. 267-75.

Stokes IA, Gardner-Morse M. 1995. Lumbar spine maximum efforts and muscle recruitment patterns predicted by a model with multijoint muscles and joints with stiffness. *J Biomech*. 28. 173-86.

Stokes IA, Gardner-Morse M. 1999. Quantitative anatomy of the lumbar musculature. *J Biomech*. 32. 311-6.

Stokes IA, Gardner-Morse M. 2001. Lumbar spinal muscle activation synergies predicted by multi-criteria cost function. *J Biomech.* 34. 733-740.

Stokes IA, Gardner-Morse M. 2003. Spinal stiffness increases with axial load: another stabilizing consequence of muscle action. *J Electromyogr Kinesiol.* 13:4. 397-402.

Stokes IA, Henry SM, Single RM. 2003. Surface EMG electrodes do not accurately record from lumbar multifidus muscles. *Clin Biomech.* 18. 9-13.

Stokes IA, Gardner-Morse M. 2001. Lumbar spinal muscle activation synergies predicted by multi-criteria cost function. *J Biomech.* 34:6. 733-40.

Strohl KP, Mead J, Banzett RB, Loring SH, Kosch PC. 1981. Regional differences in abdominal muscle activity during various maneuvers in humans. *J. Appl. Physiol.* 51. 1471-1476.

Takahashi I, Kikuchi S, Sato K, Sato N. Mechanical load of the lumbar spine during forward bending motion of the trunk-a biomechanical study. *Spine.* 2006. 31:1. 18-23.

Takashima ST, Singh SP, Haderspeck KA, Schultz AB. 1979. A model for semi-quantitative studies of muscle actions. *J Biomech.* 12. 929-939.

Tesh KM, Dunn JS, Evans JH. 1987. The abdominal muscles and vertebral stability. *Spine.* 12:5. 501-8.

Toussaint HM, de Winter AF, de Haas Y, de Looze MP, Van Dieen JH, Kingma I. 1995. Flexion relaxation during lifting: implications for torque production by muscle activity and tissue strain at the lumbo-sacral joint. *J Biomech.* 28:2. 199-210.

Troup JD, Martin JW, Lloyd DC. 1981. Back pain in industry. A prospective survey. *Spine.* 6:1. 61-9.

Tuong NH, Dansereau J, Maurais G, Herrera R. 1988. Three-dimensional evaluation of lumbar orthosis effects on spinal behavior. *J Rehabil Res Dev.* 35:1. 34-42.

Tveit P, Daggfeldt K, Hetland S, Thorstensson A. 1994. Erector spinae lever arm length variations with changes in spinal curvature. *Spine.* 19. 199-204.

Urquhart DM, Barker PJ, Hodges PW, Story IH, Briggs CA. 2005. Regional morphology of the transversus abdominis and obliquus internus and externus abdominis muscles. *Clin Biomech.* 20. 233-41.

Vakos JP, Nitz AJ, Threlkeld AJ, Shapiro R, Horn T. 1994. Electromyographic activity of selected trunk and hip muscles during a squat lift: Effect of varying the lumbar posture. *Spine.* 19. 687-95.

van Bolhuis BM, Gielen CC. 1999. A comparison of models explaining muscle activation patterns for isometric contractions. *Biol Cybern.* 81. 249-61.

van Dieen JH, Toussaint HM. 1993. Spinal shrinkage as a parameter of functional load. *Spine* 18. 1504-14.

van Dieen JH, Hoozemans MJ, Toussaint HM. 1999. Stoop or squat: a review of biomechanical studies on lifting technique. *Clin Biomech.* 14. 685-96.

van Dieen JH, de Looze MP. 1999. Sensitivity of single-equivalent trunk extensor muscle models to anatomical and functional assumptions. *J Biomech.* 32. 195-8.

van Dieen JH, Kingma I. 2005. Effects of antagonistic co-contraction on differences between electromyography based and optimization based estimates of spinal forces. *Ergonomics.* 48:4. 411-26.

van Dieen JH, Kingma I, van Der Burg P. 2003. Evidence for a role of antagonistic cocontraction in controlling trunk stiffness during lifting. *J Biomech.* 36. 1829-36.

Varma KM, Porter RW. 1995. Sudden onset of back pain. *Eur Spine J.* 4:3. 145-7.

Watson PJ, Booker CK, Main CJ, Chen AC. 1997. Surface electromyography in the identification of chronic low back pain patients: the development of the flexion relaxation ratio. *Clin Biomech.* 12:3. 165-171.

Webster BS, Snook SH. 1994. The cost of 1989 workers' compensation low back pain claims. *Spine.* 19:10. 1111-5

Wilke HJ, Neef P, Caimi M, Hoogland T, Claes LE. 1999. New in vivo measurements of pressures in the intervertebral disc in daily life. *Spine.* 24. 755-763.

Wilke HJ, Neef P, Hinz B, Seidel H, Claes L. 2001. Intradiscal pressure together with anthropometric data –A data set for the validation of models. *Clin Biomech.* 6. S111-S126.

Wilke HJ, Rohlmann A, Neller S, Graichen F, Claes L, Bergmann G. 2003. ISSLS prize winner: A novel approach to determine trunk muscle forces during flexion and extension: a comparison of data from an in vitro experiment and in vivo measurements. *Spine.* 28:23. 2585-93.

Woittiez RD, Huijing PA, Boom HB, Rozendal RH. 1984. A three-dimensional muscle model: a quantified relation between form and function of skeletal muscles. *J Morphol.* 182:1. 95-113.

Woldstad JC, Sherman BR. 1998. The effects of a back belt on posture, strength, and spinal compressive force during static lift exertions. *Int J Ind Ergonom.* 22. 409-16.

Wood S, Pearsall DJ, Ross R, Reid JG. 1996. Trunk muscle parameters determined from MRI for lean to obese males. *Clin Biomech.* 11. 139-144.

Yamamoto I, Panjabi M, Crisco T, Oxland T. 1989. Three-dimensional movements of the whole lumbar spine and lumbosacral joint. *Spine.* 14. 1256-1260.

Yettram AL, Jackman MJ. 1982. Structural analysis for the forces in the human spinal column and its musculature. *J Biomed Eng.* 4:2. 118-24.

Zander T, Rohlmann A, Calisse J, Bergmann G. 2001. Estimation of muscle forces in the lumbar spine during upper-body inclination. *Clin Biomech.* 16:1. S73-80.

Zatsiorsky V, Seluyanov V, Chugunova L. 1990. In vivo body segment inertial parameters determination using a gamma-scanner method. In *Biomechanics of Human Movement: Applications in Rehabilitation, Sports and Ergonomics* (Edited by Berme, N. and Cappozzo, A.), Ohio: Bertec. P. 186-202.

Zetterberg C, Andersson GB, Schultz AB. 1987. The activity of individual trunk muscles during heavy physical loading. *Spine.* 12:10. 1035-40.

Zhang X, Xiong J. 2003. Model-guided derivation of lumbar vertebral kinematics in vivo reveals the difference between external marker-defined and internal segmental rotations. *J Biomech.* 36:1. 9-17.

APPENDIX A:

THE LIGAMENTOUS SPINE AND TRUNK MUSCLE ARCHITECTURE

A.1. Introduction

The trunk musculoskeletal system consists of the spine, rib cage, pelvis as well as associated fascia and musculature. In this appendix we will focus on the functional anatomy of the spine and its surrounding muscles which have been considered in our finite element (FE) model studies.

A.2. The Passive Ligamentous Spine

The spine consists of 24 semi-rigid vertebrae that are separated by flexible intervertebral discs. It is divided into four regions of cervical, thoracic, lumbar, and sacral spine. Our focus here would be more on the lumbar region since the thoracic part is considered as a rigid body in our FE model while the cervical part is not directly considered.

The principal movements exhibited by the lumbar spine and its individual joints are axial compression, flexion/extension rotation, lateral rotation and axial rotation. Axial compression is the main load that occurs during weight lifting in the upright posture. During forward flexion, at each intervertebral segment, flexion involves a combination of anterior sagittal rotation and anterior translation. Under gravity-directed compression and in forward flexion, due to local shear forces, there will be a tendency for the vertebrae to slide anteriorly on top of lower vertebrae.

Trunk flexion is provided by both anterior pelvis rotation and lumbar flexion. It is well known that in the initial phase of trunk flexion the flexion of lumbar segments is dominant over that of pelvis while in the final stage of trunk flexion the rotation of pelvis is dominant over lumbar flexion. An important portion of the lumbar flexion (up

to 65% of total) is provided by relative rotation of the lower intersegmental vertebrae (L3/S1) while the upper intersegmental vertebrae (T12/L3) provide the remaining smaller portion.

A. 3. Vertebrae

The anatomy of a typical lumbar vertebra is shown in Fig. A.1 while a brief explanation on various anatomical parts of it is provided in the figure caption.

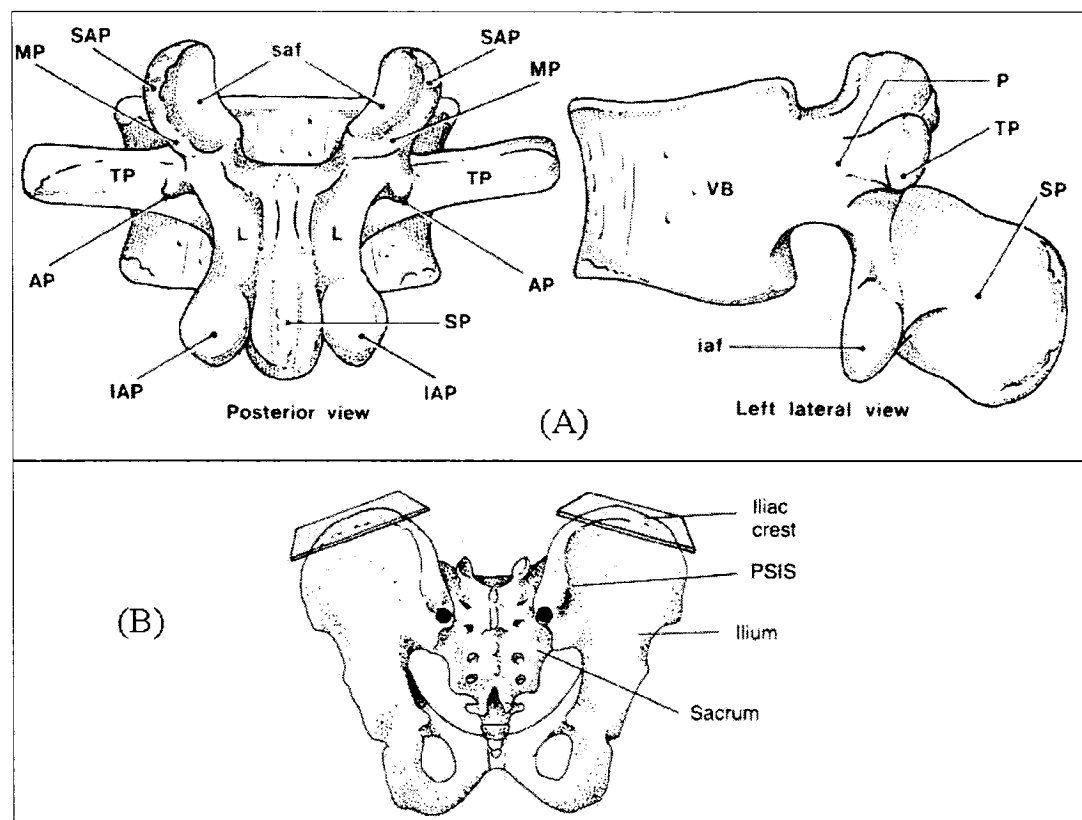


Fig A.1 (A): The parts of a typical lumbar vertebra. SP: spinous process. TP: transverse process. AP: accessory process. MP: mamillary process, (B): The anterior posterior iliac spine, iliac crest and posterir superior iliac spine (reproduced from the book of *Clinical Anatomy of the Lumbar Spine, 1987*).

A.4 Discs and ligaments

An intervertebral disc consists of a strong layer, but deformable, soft tissue that separates two vertebral bodies. The space between vertebral bodies allows the upper vertebra to tilt forward without its lower edge coming into contact with the lower vertebral body. Each intervertebral disc consists of two basic components: a central *nucleus pulposus*, surrounded by a peripheral *annulus fibrosus*. A third component of the intervertebral disc are two layer of cartilage which cover the top and bottom aspects of each disc; *the vertebral end-plate*. The principle functions of the disc are to allow movement between vertebral bodies and to transmit loads from one vertebral body to the next.

Ligaments that interconnect the vertebral bodies are the anterior and posterior longitudinal ligaments. The anterior longitudinal ligament is a long band which covers the anterior aspects of the spine. Because of strictly longitudinal disposition, the anterior longitudinal ligament serves principally to resist vertical separation of the anterior ends of the vertebral bodies. In doing do, it functions during extension movements and resists forward or backward sliding movements of the vertebral bodies. Like the anterior longitudinal ligament, the posterior longitudinal ligament is represented throughout the vertebral column. Its fibers mesh with those of the *annulus fibrosus*. The posterior longitudinal ligament serves to resist separation of the posterior ends of the vertebral bodies.

A.5. Extensor Trunk Muscles

A brief functional anatomy of all extensor trunk muscles used in the finite element model study is given here. Except otherwise cited all figures have been reproduced from the book of *Clinical Anatomy of the Lumbar Spine* by Bogduk and Twomey (1987).

A.5.1 Iliocostalis Lumborum Pars Lumborum (ICPL)

The lumbar components of Iliocostalis arise from L1 through to L4 vertebrae and each fascicle attaches to the tip of the transverse process and to an area extending 2-3 cm laterally onto the middle layer of the thoracolumbar fascia (Fig A.2). The fascicle from L4 is the deepest, and caudally it is attached directly to the iliac crest just lateral to the posterior superior iliac spine. This fascicle is covered by the fascicle from L3 that has a similar but more dorsolaterally located attachment on the iliac crest. In sequence, L2 covers L3 and L1 covers L2 with insertion on the iliac crest becoming successively more dorsal and lateral.

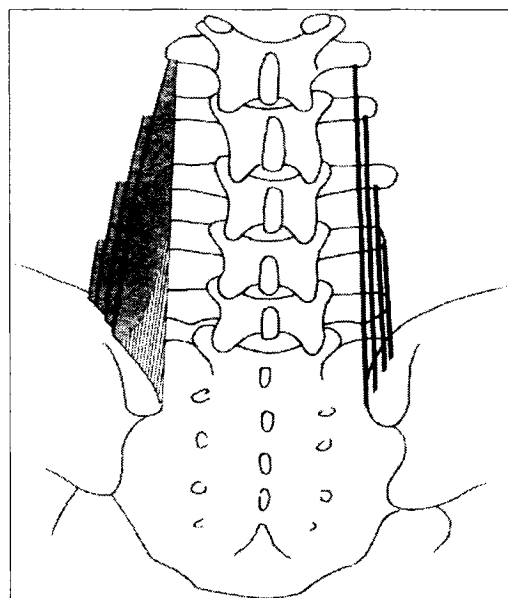


Fig. A.2 The lumbar fibres of iliocostalis. On the left, the four lumbar fascicles of iliocostalis are shown. On the right, their span and attachments are indicated by the lines

Action of lumbar iliocostalis can be resolved into horizontal and vertical vectors (Fig A.3). The vertical vector is predominant, and therefore, the lumbar fascicles of iliocostalis contracting bilaterally can act as posterior sagittal rotators.

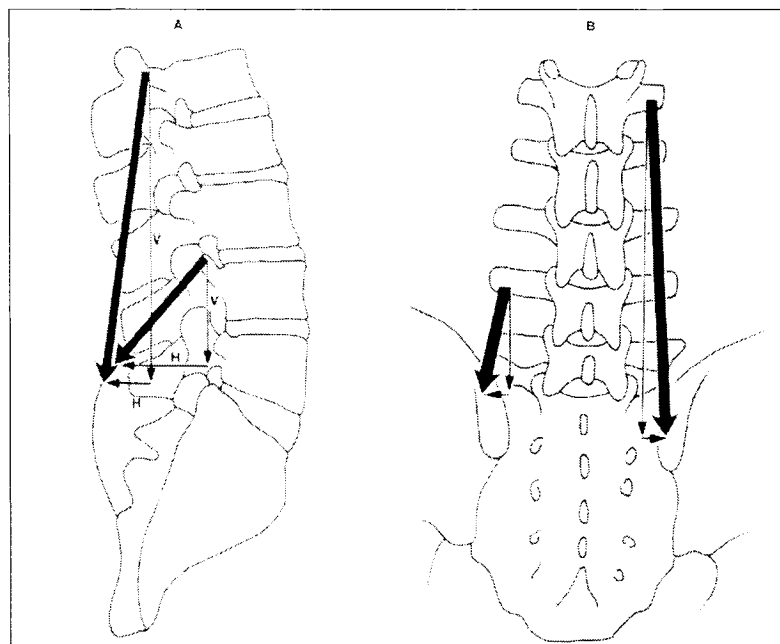


Fig. A.3 The force vector of the lumbar iliocostalis. (A) In a lateral view, the line of action of the fascicles can be resolved into vertical (V) and horizontal (H) vectors. The horizontal vectors are larger at lower lumbar levels. (B) In a postero-anterior view, the line of action is resolved into a vertical vector and a very small horizontal vector.

A.5.2 Longissimus Thoracis Pars Lumborum (LGPL)

Lumbar longissimus arises from the accessory process and the adjacent medial end of the dorsal surface of the transverse process of the lumbar vertebra (Fig A.4 and A.5). The fascicles of L5 vertebra is the deepest and shortest. Its fibers insert directly into the medial aspect of the posterior superior iliac spine. The fascicle from L4 also lies deeply, but lateral to that from L5. Succeeding fascicles lie progressively more dorsally so that L3 fascicle covers those from L4 and L5, but is itself covered by the L2 fascicle, while the L1 fascicle lies most superficially. Each fascicle of the lumbar longissimus has both a dorsoventral and a rostrocaudal orientation. Therefore, the action of each fascicle can be resolved into a vertical and horizontal vector, the relative sizes of which differ from L1 to L5. Consequently, the relative actions of longissimus differ at each segmental level.

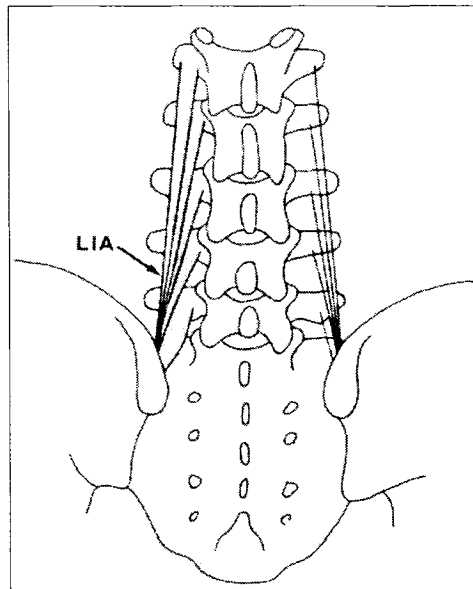


Fig. A.4 The lumbar fibers of longissimus. On the left, the five fascicles of the intact muscle are drawn. The formation of the lumbar intermuscular aponeurosis (LIA) by the lumbar fascicles of longissimus is depicted. On the right, the lines indicate the attachments and span of the fascicles.

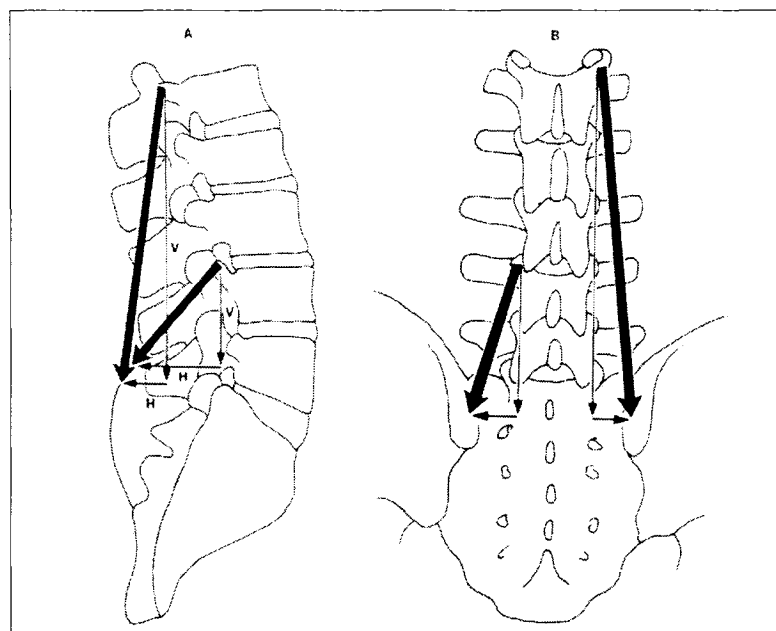


Fig A.5 The force vectors of the lumbar longissimus. (A) lateral view, (B) in a postero-anterior view.

A.5.3 Lumbar Multifidus (MF)

Lumbar multifidus arises from the dorsal surface of the sacrum. It originates from the mammillary processes of the lumbar vertebra. The muscle has a slight anterior inclination as it travels to attach to the lumbar spinous processes at the apex of the lordosis (Fig. A.6). The attachment of the multifidus muscles to the spinous processes results in an effective lever arm for lumbar extension. In a posterior view, the fascicles of multifidus are seen to have an oblique, caudolateral orientation. Their line of action, therefore, can be resolved into two vectors: a large vertical vector and a considerably smaller horizontal vector (Fig A.6). The principal action of multifidus is expressed by its vertical vector, and further insight is gained when this vector is viewed in a lateral projection (Fig A.6). Each fascicle of multifidus, at every level, acts virtually at right angles to its spinous process of origin. This, using the spinous process as a lever, every fascicle is ideally disposed to produce posterior sagittal rotation of its vertebra.

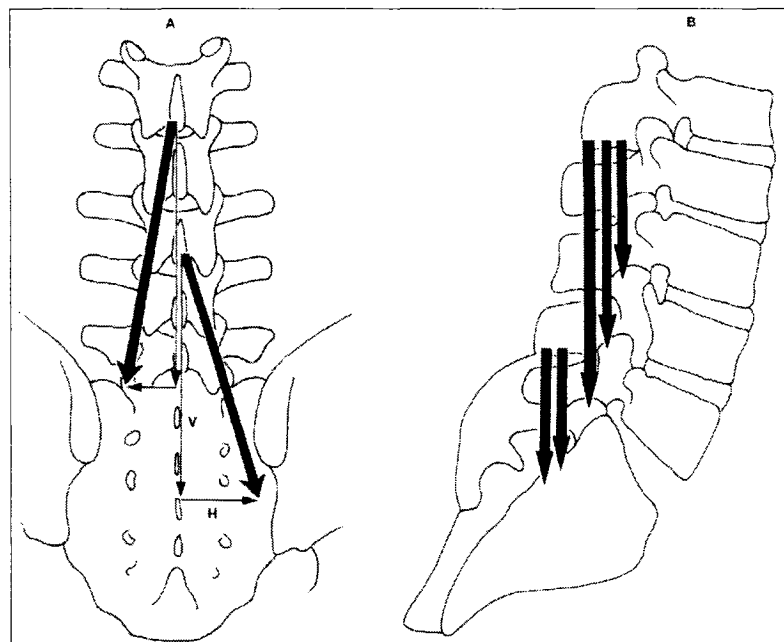


Fig A.6 (A) Postero-anterior and (B) sagittal view revealing the vector or line of pull of the multifidus muscle that makes it strong spinal extensor.

A.5.4 Quadratus Lumborum (QL)

The Quadratus Lumborum is a wide, more or less rectangular muscle that covers the lateral two third or so of the anterior surfaces of the L1 to L4 transverse processes and extends laterally a few centimetres beyond the tips of the transverse process (Fig A.7 and A.8). The majority of the fibers of the quadratus lumborum are connected to the 12th rib. The remaining fibers of quadratus lumborum connect the ilium to the upper four lumbar transverse processes.

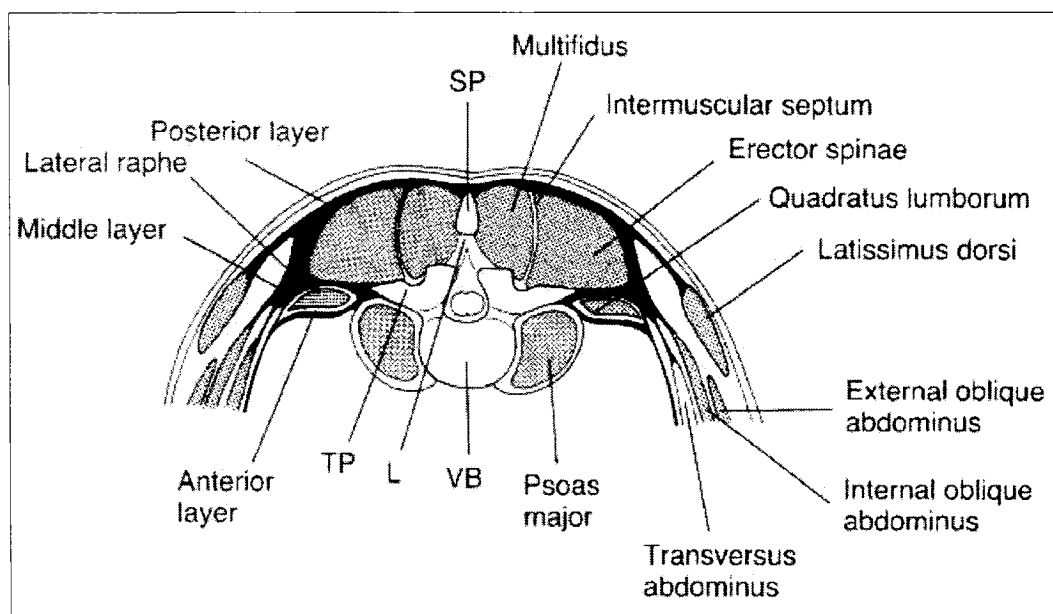


Fig A.7 Transverse section of the lumbar spine showing the layers of thoracolumbar fascia and the muscles attached to it. SP: spinous process, TP: transverse process, VB: vertebra body and L: lamina. The figure has been scanned from the book of *Mechanical Low Back Pain* authored by Porterfield and DeRosa (1998).

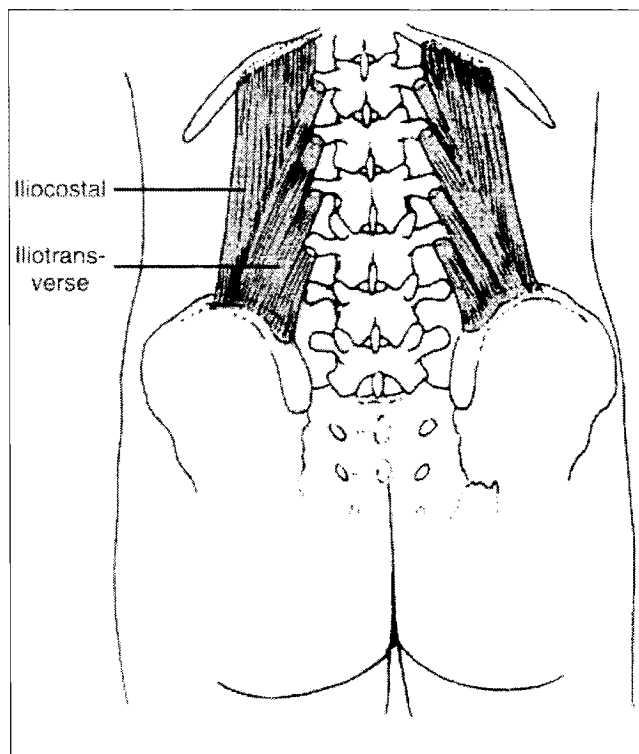


Fig A.8 Posterior view showing the quadratus lumborum muscle. This muscle has three portions, iliocostal, iliotransverse and costotransverse. This figure does not show the costo-transverse portion because it is often insignificant in its size and function. The figure has been scanned from the book of *Mechanical Low Back Pain* authored by Porterfield and DeRosa (1998).

A.5.5 Iliocostalis Lumborum Pars Thoracic (ICPT)

The thoracic iliocostalis consists of fascicles from the lower seven or eight ribs (5th –12th) that attach caudally to the ilium and sacrum (Fig. A.9). This muscle is a major extensor as well as stabilizer of the trunk.

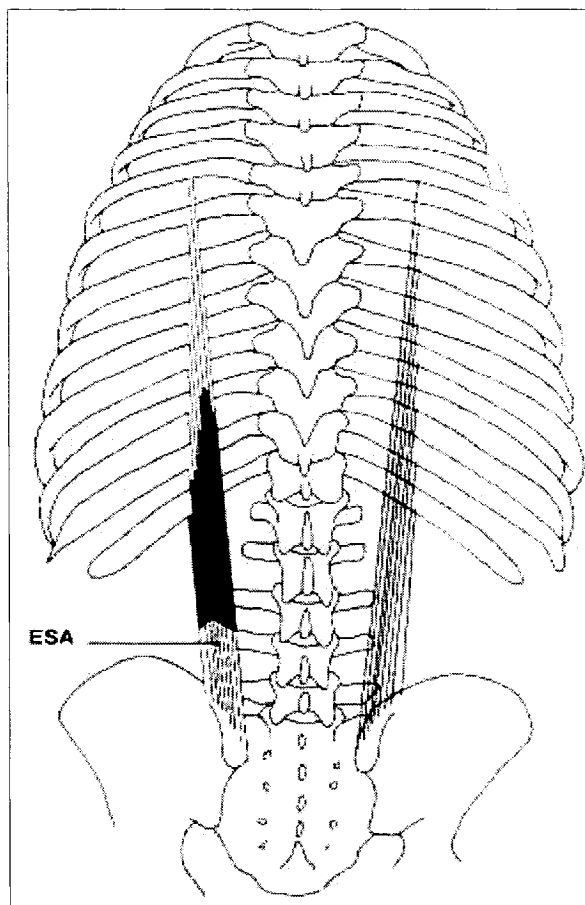


Fig A.9 The thoracic fibers of iliocostalis lumborum

A.5.6 Longissimus Thoracis Pars Thoracic (LGPT)

The thoracic longissimus arises from ribs and transverse process of T1 or 2 down to T12 (Fig A.10). The fascicles from T2 level attach to the L3 spinous process, while the fascicles from the remaining levels insert into spinous process at progressively lower levels. For example, those from T5 attach to L5 and those from T7 attach to S2 or S3. Those from T8 to T12 diverge from the midline to find attachment to the sacrum along a line extending from S3 spinous process to the caudal extent of the posterior superior iliac spine. This muscle is a major extensor as well as stabilizer of the trunk.

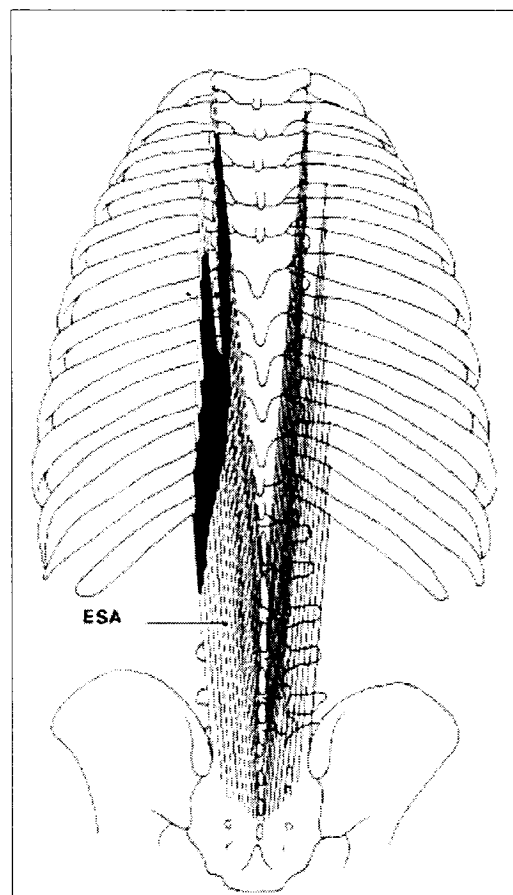


Fig A.10 The thoracic fibers of longissimus.

APPENDIX B:

OPTIMIZATION: LAGRANGE MULTIPLIERS METHOD

In this study an in-house program was used to solve the redundancy in equilibrium equations. This program is able to analytically solve an optimization problem using different objective functions such as cubed sum of muscle stresses, squared sum of muscle stress, sum of muscle stress, sum of muscle forces, and a double linear approach (see Chapter 5). All optimization problems except the one based on cubed sum of muscle stresses approach were solved using Matlab Optimization Toolbox (The MathWorks Inc., Natick, MA). Matlab Optimization Toolbox nevertheless failed to find the global minimum of this cost function (i.e., cubed sum of muscle stresses) since initial starting values for muscle forces were required that affect the final results for predicted muscle forces. Actually, based on this procedure a local minimum of the objective function was calculated.

Therefore, the in-house program was modified in order to find the global minimum of the objective function analytically by using Lagrange Multipliers Method. The goal of this optimization procedure is to determine the individual muscle forces that equilibrate a given joint moment equation by solving the following static optimization:

$$\text{Minimize } \text{Objective Function} = \sum_{i=1}^m \left(\frac{x_i}{d_i}\right)^3 = OF$$

subject to the equality constrain:

$$f = \sum_{i=1}^m r_i x_i - M = 0$$

and inequality constrain:

$$0 \leq \frac{x_i}{d_i} \leq 0.6 \text{ MPa}$$

where x_i denotes unknown force in muscle i , d_i denotes physiological cross sectional area (PCSA) of i th muscle, m denotes number of muscles spanning a vertebral level, r_i is the moment arm of the i th muscle and M is the resultant moment in sagittal plane at the spinal level under consideration. Resultant moment at the joint, muscle moment arm and PCSAs are a priori known. The equality constraint equation requires the optimal muscle forces to produce the known joint moment while the inequality constraint equation requires muscles to produce tensile stress that are smaller than maximum stress of 0.6 MPa. The Lagrange function is defined as follow:

$$L = OF - \lambda f$$

where λ is unknown Lagrange multiplier. The necessary conditions for the existence of an extremum of the Lagrange function, and hence of the objective function OF is that first partial derivative of L with respect to the design variables x_i becomes zero at the optimal point:

$$\frac{\partial L}{\partial x_i} = \frac{3}{d_i^3} (x_i)^2 - \lambda(r_i) = 0 \rightarrow x_i = \sqrt{\frac{\lambda r_i d_i^3}{3}}$$

There are $m+1$ unknowns (x_i and λ) and $m+1$ equations (the above equation plus equality constraint equation) and the problem can be solved analytically for muscle forces. The obtained muscle forces from this algorithm were entered as starting guess for muscle forces in the routine *fmincon* of the Matlab Optimization Toolbox to verify the results.